NASA Tech Briefs

Official Publication of
National Aeronautics and
Space Administration
Volume 14 Number 12

Transferring Technology
to American Industry
and Government

December 1990

Advanced Software Simulates Space

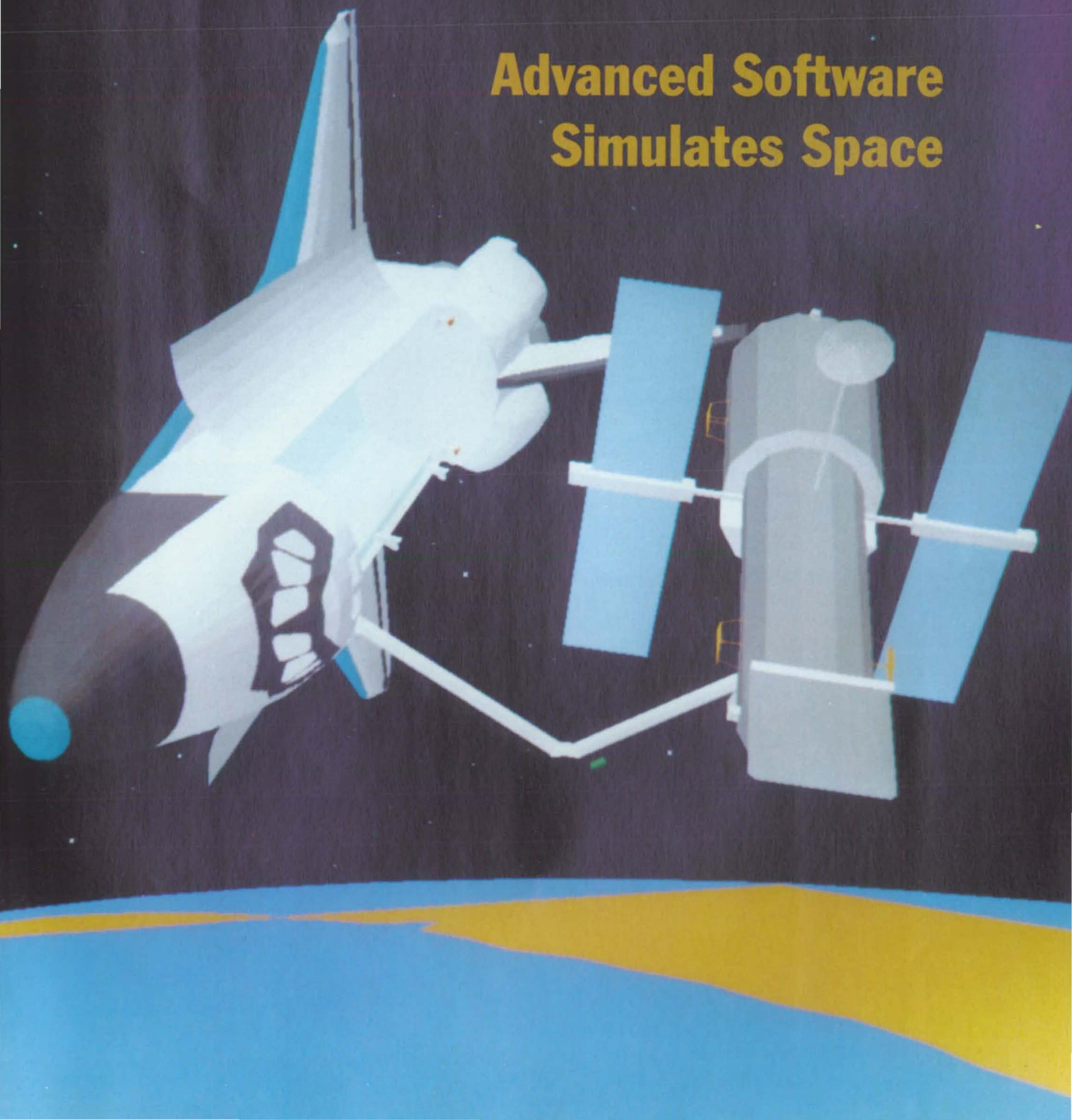

Clean, lean vacuum machine.

The Balzers Wide-Range Turbopump

The wide-range turbopump lets you produce clean high and ultrahigh vacuum and keep your operating costs lean. How? You can back your wide-range turbopump with an oil-free diaphragm pump to avoid process contamination. Or, you can use a backing pump that's 10 to 50 times smaller than needed with a conventional high-vacuum pump — cutting energy, fluid and space requirements.

Only the Balzers wide-range turbopump, with permanent magnetic upper bearing, incorporates a turbopump and a two-stage drag pump, for a compression ratio of 10^{12} for N_2 and an exhaust pressure to 10 Torr. Speeds from 180-450 liters/second, including corrosive-gas models, accommodate virtually any semiconductor, high-energy physics or clean HV or UHV application.

Contact Balzers for more details on the clean, lean vacuum machine that can streamline your process.

BALZERS

Reader Service No. 402
To Receive Literature

Reader Service No. 405
To Have A Sales Representative Contact You

Balzers • 8 Sagamore Park Road • Hudson, NH 03051
TEL (603) 889-6888 • FAX (603) 889-8573

Pfeiffer Vakuumtechnik • Postfach 1280 • D-6334 Asslar
TEL (06441) 802-0 • FAX (06441) 802-202

The Sensible Solution

Circle Reader Action No. 364

"Before humans become long-range spacefarers, we must design our spacecraft to provide conditions necessary for human life on earth. That includes a breathable atmosphere, agreeable temperatures, water, and three square meals a day.

"Boeing is working with the NASA Marshall Space Flight Center to develop Environmental Control and Life Support Systems for spacecraft. In addition to this contracted work, Boeing has invested its own funds to speed progress.

"The task of my group is to design systems to maintain a suitable atmosphere for astronauts and air cooling for machinery (avionics air), plus automatic fire detection and suppression for both.

"The first use for this technology is Space Station Freedom.

"The avionics air will be very dry and isolated from the air the astronauts breathe. This is because dry air requires less energy to cool, and power

is a premium in space.

"The air people breathe will have about 50% humidity, and will recycle continuously. The system will filter out dust and other particles automatically, add oxygen, adjust gas mixture and temperature.

"The technical challenge is great, but if we all work together, we can make the atmosphere aboard the spacecraft what you'd expect on a typical spring morning: clean, fresh air."

Tamra Ozbolt
Mechanical Design Engineer
Environmental Control and
Life Support Systems
Boeing Defense & Space Group

WE'RE WITH YOU

Boeing has been a partner in America's space programs for more than 30 years.

BOEING

NASA Tech Briefs

Transferring Technology to American Industry and Government

December 1990
Volume 14 Number 12

ABP BPA

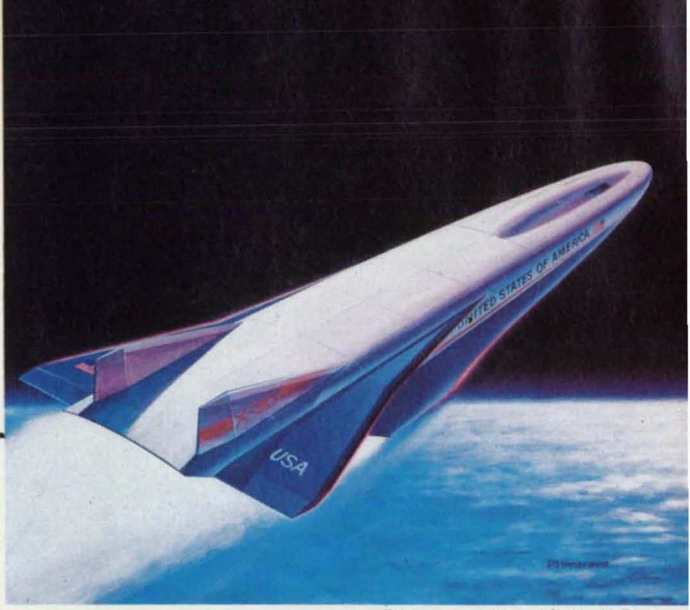

Photo courtesy United States Air Force

The National Aero-Space Plane (NASP) contractor team — consisting of Rockwell North American Aircraft, McDonnell Douglas, General Dynamics, Pratt and Whitney, and Rocketdyne —has unveiled a new design concept for the X-30 technology flight demonstrator. The twin-tailed lifting body will use between three and five connected propulsion modules that integrate ramjet/scramjet engines along with small rocket motors. A joint NASA and Department of Defense effort, NASP is developing technologies to enable flexible, controlled hypersonic flight within the atmosphere and into space. In addition to propulsion advances, NASA expects the NASP program to drive technology in computational fluid dynamics, materials, structures, and flight controls. ***See page 10.***

SPECIAL FEATURES

Future Paths: An Interview With NASA Deputy Administrator James R. Thompson 10
NASA Software Update 44

TECHNICAL SECTION

New Product Ideas 14
NASA TU Services 16
Electronic Components and Circuits 18
Electronic Systems 22
Physical Sciences 28
Materials 32
Computer Programs 38
Mechanics 45
Machinery 52
Fabrication Technology 57
Mathematics and Information Sciences.......... 64
Life Sciences 67
Subject Index...................... 70

DEPARTMENTS

On The Cover: Researchers at NASA's Goddard Space Flight Center have created a real-time mission monitoring software tool that computes and displays a realistic three-dimensional solid model image of the space shuttle, its remote-manipulator system, its payload, and its surroundings from telemetry data. It enables the user to change the viewpoint to anywhere in the universe, to query an object for information, or to toggle the image of a celestial object or spacecraft on and off. ***Turn to page 38.***

(Photo courtesy NASA)

New on the Market...........68
New Literature.......69
Advertisers Index............100

Annual Subject Index
This issue contains an expanded subject index beginning on page 70 which features cross-referenced listings for all technical reports appearing in NASA Tech Briefs during 1990.

NASA Tech Briefs, ISSN 0145-319X, USPS 750-070, copyright © 1990 in U.S., is published monthly by Associated Business Publications Co., Ltd., 41 E. 42nd St., New York, NY 10017-5391. The copyrighted information does not include the individual tech briefs which are supplied by NASA. Editorial, sales, production and circulation offices at 41 East 42nd Street, New York, NY 10017-5391. Subscription for non-qualified subscribers in the U.S. , Panama Canal Zone, and Puerto Rico, $75.00 for 1 year; $125.00 for 2 years; $200.00 for 3 years. Single copies $10.00. Remit by check, draft, postal or express orders. Other remittances at sender's risk. Address all communications for subscriptions or circulation to NASA Tech Briefs, 41 East 42nd Street, New York, NY 10017-5391. Second-class postage paid at New York, NY and additional mailing offices.

POSTMASTER: please send address changes to NASA Tech Briefs, 41 E. 42nd Street, Suite 921, New York, NY 10017-5391.

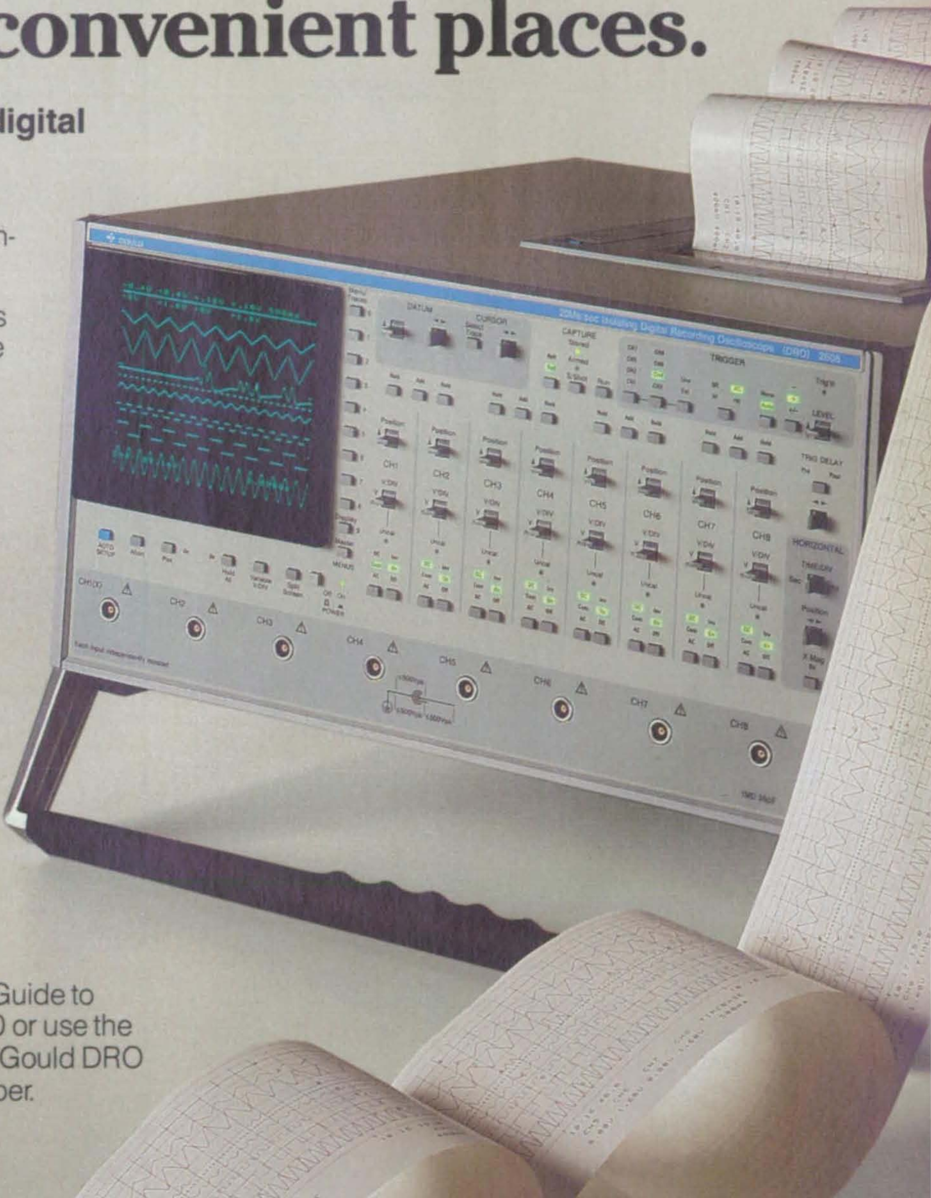

NASA Tech Briefs

Official Publication of
National Aeronautics and
Space Administration

NASA Tech Briefs:

Published by .... **Associated Business Publications**
Editor-in-Chief/Publisher .... **Bill Schnirring**
Associate Publisher .... **Frank Nothaft**
Editor .... **Joseph T. Pramberger**
Managing Editor .... **R.J Laer**
Assistant Editor .... **Theresa M. Detko**
Assistant Editor .... **Kathleen Carrea**
Assistant Editor .... **Justina Cardillo**
Assistant Editor .... **Patrick Corbett**
Technical Advisor .... **Dr. Robert E. Waterman**
Production Manager .... **Rita Nothaft**
Traffic Manager .... **James E. Cobb**
Art Director .... **Pierre Granier**
Circulation Manager .... **Cheryl Cohen**
Advertising Coordinator .... **Daniel Murphy**
Telecommunications Specialist .... **Evelyn Mars**
Reader Service Manager .... **Sylvia Valentin**

Briefs & Supporting Literature:
Provided to National Aeronautics and Space Administration by
International Computers & Telecommunications, Inc.,
NY, NY with assistance from **Logical Technical Services**, NY, NY
Technical/Managing Editor .... **Ted Selinsky**
Art Director .... **Luis Martinez**
Administrator .... **Elizabeth Texeira**
Chief Copy Editor .... **Lorne Bullen**
Staff Writers/Editors .... **Dr. James Boyd, Dr. Larry Grunberger, Dr. Theron Cole, Jordan Randjelovich, George Watson, Oden Browne**
Graphics .... **Vernald Gillman, Pamela Baynham, Charles Sammartano**
Editorial & Production .... **Bill Little, Ivonnne Valdes, Frank Ponce**

NASA:
NASA Tech Briefs are provided by the National Aeronautics and Space Administration, Technology Utilization Division, Washington, DC:
Administrator .... **Richard H. Truly**
Assistant Administrator for Commercial Programs .... **James T. Rose**
Deputy Assistant Administrator(Programs) .... **Henry J. Clarks**
Acting Director TU Division(Publications Manager) .... **Leonard A. Ault**
Manager, Technology Utilization Office, NASA Scientific and Technology Information Facility .... **Walter M. Heiland**

Associated Business Publications
41 East 42nd Street, Suite 921, New York, NY 10017-5391
(212) 490-3999 FAX (212) 986-7864
President .... **Bill Schnirring**
Executive Vice President .... **Frank Nothaft**
Vice President .... **Domenic A. Mucchetti**
Operations Manager .... **Rita Nothaft**
Controller .... **Felecia Lahey**

Advertising:
New York Office:(212) 490-3999 FAX (212) 986-7864
Director of Advertising Sales .... **Domenic A. Mucchetti**
Account Executive (NY,NJ) .... **Brian Clerkin** at (201) 366-2751
Account Executive (VA,DC,MD,DE,WV) .... **John D. Floyd, CBC** at (215) 399-3265
Account Executive .... **Debby Crane** at (201) 967-9838
Account Executive (Midwest) .... **Paul Lesher,CBC** at (708) 501-4140
Account Executive (Northwest) .... **Bill Hague** at (206) 858-7575
Regional Sales Manager (South) .... **Douglas Shaller** at (212) 490-3999
Account Executives (Eastern MA,NH,ME,RI) .... **Paul Gillespie** at (508) 429-8907;**Bill Doucette** at (508) 429-9861
Account Executives (Western MA,CT,VT) .... **George Watts** or **David Haggett** at (413) 253-9881
Account Executives (Calif.,AZ,NV,NM)
for Area Codes 818/213/805 **Robert D'Alexander**
for Area Codes 408/415/916/209/707) **Elizabeth Cooper**
and for Area Codes 619/714 - **Karen Mock** (213) 372-2744

NTBM-Research Center
Account Supervisor .... **Lourdes Del Valle**

The best way to appreciate our new thermal array?

Inch by inch.

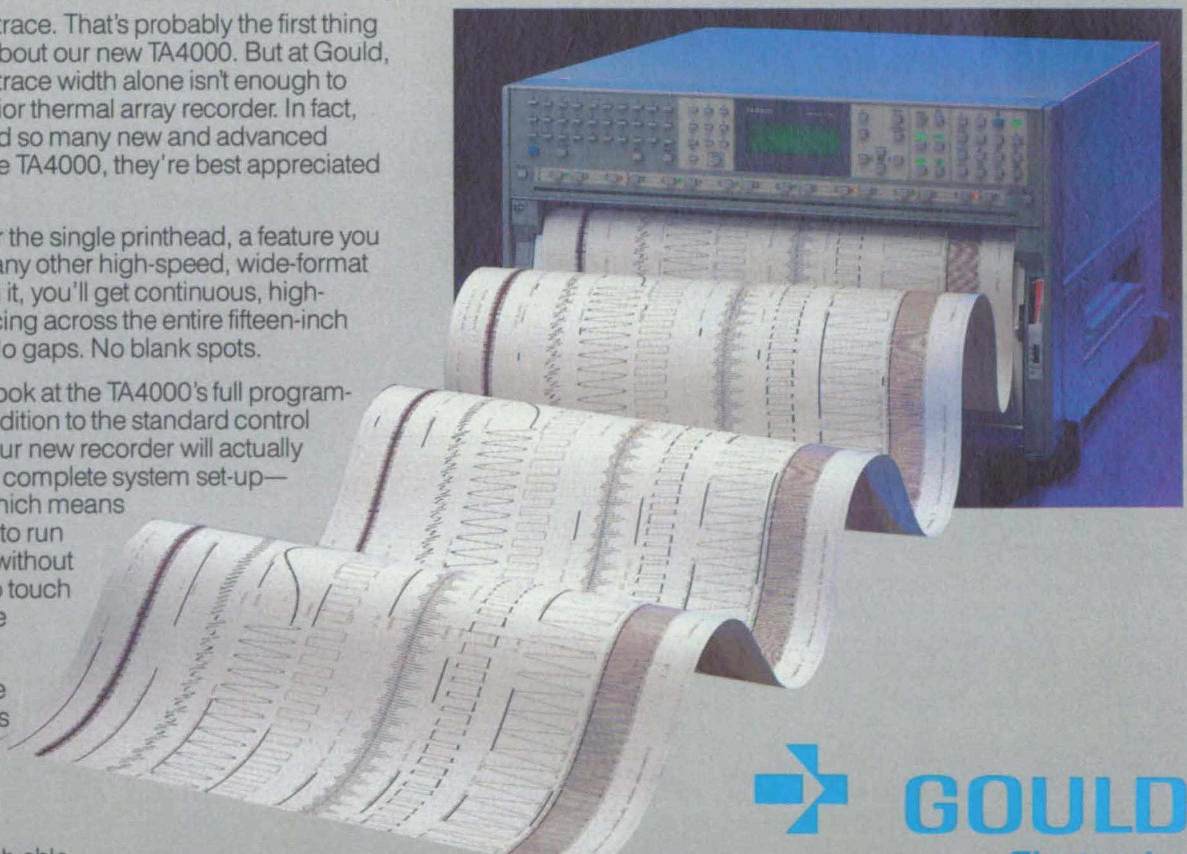

A fifteen-inch trace. That's probably the first thing you'll notice about our new TA4000. But at Gould, we know that trace width alone isn't enough to make a superior thermal array recorder. In fact, we've included so many new and advanced features on the TA4000, they're best appreciated one by one.

First, consider the single printhead, a feature you won't find on any other high-speed, wide-format recorder. With it, you'll get continuous, high-resolution tracing across the entire fifteen-inch chart width. No gaps. No blank spots.

Then have a look at the TA4000's full programmability. In addition to the standard control capabilities, our new recorder will actually calibrate your complete system set-up—all by itself. Which means you'll be able to run an entire test without ever having to touch or readjust the instrument.

And if multiple measurements are what you're after, the TA4000 has up to 24 channels, each able to handle either analog signals or digitized data. What's more, our new recorder will simultaneously record analog and digitized inputs, giving you maximum measurement flexibility.

Of course, the TA4000 is push-button simple. It's designed for maintenance efficiency. And it features Micropulsing™, a new technology that extends thermal array head life and increases contrast quality.

But why measure the TA4000 by words alone?

Call your Gould representative today to schedule your own demonstration. They'll answer any questions you may have. They'll provide you with product specifications. And together, you'll cover all the benefits of the TA4000. Inch by inch.

GOULD
Electronics

Yes! I want to see how Gould measures up! Please send me more information about the TA4000.

NTB 12/90 (please print)

NAME: ____________________

TITLE: ____________________

COMPANY: ____________________

STREET: ____________________

CITY: ____________ STATE: ______ ZIP: ________

TELEPHONE: (   ) ____________________

Send to: Gould, Inc., Test and Measurement Group, 8333 Rockside Road, Valley View, Ohio 44125 or call (216) 328-7000, Fax: (216) 328-7400

Future Paths:

An Interview with NASA Deputy Administrator James R. Thompson

In an interview with *NASA Tech Briefs'* editors, NASA deputy administrator James R. Thompson, Jr. discussed the agency's future direction and goals, and his ideas on technology transfer.

Prior to being named deputy administrator in July 1989, Thompson served for approximately three years as head of the Marshall Space Flight Center in Huntsville, AL. During that period, he oversaw the redesign and testing of the space shuttle's solid rocket boosters. The success of that effort was a prerequisite to NASA's "return to flight" on Sept. 29, 1988, when Discovery was launched on the first shuttle mission since the Challenger accident.

Before heading Marshall, Thompson was deputy director for technical operations at Princeton University's Plasma Physics Laboratory. From March to June 1986, he served as the vice chairman of the NASA task force inquiring into the cause of the Challenger accident, leading the team that collected and analyzed information for the Rogers Commission.

Previously, Thompson spent 20 years with NASA Marshall in various positions, including associate director for engineering and manager of the space shuttle main engine project, where he oversaw development and operation of the shuttle's advanced liquid propulsion rocket engine.

A native of Greenville, SC, Thompson received a bachelor's degree in aeronautical engineering from the Georgia Institute of Technology in 1958 and a master's degree in mechanical engineering from the University of Florida in 1963. He began his professional career in 1960 as a development engineer with Pratt and Whitney Aircraft.

Thompson was awarded the NASA Medal for Exceptional Service in 1973 and NASA Medals for Distinguished Service in 1981 and 1988. He was one of five members of NASA's Return to Flight Team awarded the Goddard Memorial Trophy for 1989.

***NASA Tech Briefs*:** *You are chairman of the recently established Space Commerce Steering Group. What is this group's purpose?*

Thompson: It's to look for opportunities within NASA where the private sector can use NASA technology and convert it into commercial enterprises.

***NTB*:** *Will this group set policy?*

Thompson: When we have policy issues, we'll try to deal with them. Where we can act as an internal stimulus, by thinking, 'Are there more opportunities for the private sector in a real commercial way?' then we'll try to do that as well.

***NTB*:** *In what areas or ways would you like to see NASA increase its technology transfer efforts?*

Thompson: I would like to see the space side of NASA be as productive as the aeronautics side has been. The way to do that is to strengthen the ties between industry and the NASA centers that do this research, to get more input from industry in terms of where we need to divert our technology and research dollars in order to make the U.S. more competitive.

Our aeronautics program is a part of NASA where you don't normally think of technology transfer. But really, that is what the program has been all about. There's an excellent relationship with industry, and as a result of that technology transfer the U.S. is without question the world's leader in aeronautics. We have a positive trade balance in the range of 20 billion dollars, which we got with a very modest aeronautics program, in the range of about half a billion dollars annually. So I think that's a good model.

***NTB*:** *You've stated previously that you want NASA to reach out more to states that are not presently working with the agency.*

Thompson: If you look at where the NASA money goes, there's a natural tendency, just because of the locale and the close working relationship that's been established, for it to be clustered around our NASA centers. But the whole country supports NASA, so I would like to see other states, other locations that have nothing to do with our NASA centers, get more actively involved in the space program.

***NTB*:** *Who must take the initiative to accomplish this?*

Thompson: It's a two-way street, but I think NASA ought to take the lead role. I think our centers need to reach out more, not just in their immediate areas and in their own states, but even in the surrounding states. I think Lewis has got to do more business with Montana, for example, and Goddard with New Hampshire, and Marshall with Kansas.

***NTB*:** *Some groups have proposed establishing a new government agency to oversee the transfer of federal technology to industry. Do you see a need for such an agency?*

Thompson: I think it's too bureaucratic. It's best to get the technology transfer ingrained in the agencies that are already doing the research work.

***NTB*:** *So the technology management should come from within.*

Thompson: That's where the strength is. If somehow we could get all 24,000 people inside of NASA thinking about technology transfer, as it applies to projects they're working on, then that's the way to work it. To have us thinking about our aeronautics and space programs and some other agency worrying about technology transfer is not the right way to go about this problem.

***NTB*:** *NASA recently announced plans to develop a system for launching and recovering commercial space-borne experiments. What do you see as the near-term opportunities for the commercial development of space?*

Thompson: There are a lot of opportunities, but it's a fairly new field and for some time it's still going to be expensive to go to space and for the private sector to make a buck. We're working on lowering those costs, but it's still expensive.

It's getting and using in a commercial way the data that comes from space that is going to have the high-gain, near-term potential, because the risk is low and you don't have to go to space to do it. You just have to capitalize on all the data that's being sent down. I've seen good examples in the fishing industry, forestry, land resource management, not to mention the whole communications industry. Projects like EOS—the Earth Observing System—are going to be transmitting a lot of data down to the ground and I think we've just started to tap in an innovative way how that data can be applied not only to better understand the Earth, but also how it can be used by the commercial sector to improve daily life.

NTB: *EOS data is expected to accumulate at approximately a terabit a day. How does NASA plan to handle this massive amount of information?*

Thompson: We recognize that it's going to be a tremendous job, and that's one of the major emphases early on in the EOS program. Approximately half of the program dollars are going into determining the architecture: how we're going to manage, distribute, and use the data.

NTB: *Besides EOS, what future NASA missions are you especially excited about?*

Thompson: One is NASP, the National Aero-Space Plane, a hybrid between our aeronautics and space programs. It's going to drive technology in computational fluid dynamics, in new materials, and in how we handle propellants. It's going to drive technology in avionics, propulsion, and hypersonic flight, and a lot of that is going to spill over into the commercial aircraft fleet that will be flying by the year 2010 or 2020. Not that you will be flying on a NASP commercially; but the technology that comes out of the NASP program is going to find its way into our commercial aircraft industry.

NTB: *Can NASP answer the need for low-cost access to space? Could it reduce our dependence on the space shuttle by rapidly and inexpensively carrying payloads into orbit, as some technologists have suggested?*

Thompson: I don't believe a single-stage-to-orbit experimental vehicle like NASP is going to carry much cargo to space. It can eventually be a carrier of people, but I think expendable rockets are going to carry the mass to low-Earth-orbit for a long time to come.

NTB: *NASA recently awarded a major contract for the development of the Advanced Solid Rocket Motor. How is this going to enhance the nation's capabilities in space?*

Thompson: It's going to give us more payload capabilities—in the range of 12,000 pounds. The single biggest advantage is that it is going to allow us to make these big solid rocket motors more repeatable, with fewer people involved, which is more reliable, because robotics will be used.

NTB: *If and when the Advanced Launch System program comes to fruition, what will it mean to America's space efforts?*

Thompson: The ALS is going through some rocky times right now, but it's really to give the country heavy lift launch capabilities. It could complement the space shuttle, and at the same time allow the Department of Defense to handle larger payloads.

NASA Deputy Administrator James R. Thompson

***NTB**: Last summer, President Bush announced a major new initiative that would send man back to the moon and then on to Mars. What are some of the key technologies NASA must concentrate on to bring this Space Exploration Initiative to reality?*

Thompson: Space power, for example, nuclear power; the life sciences, learning to live and work in space for prolonged periods of time; technologies in environmental control and life support systems; communications; and packaging—the smaller the systems you have to send, the cheaper it will be to send them.

***NTB**: There appears to be a consensus in the scientific community that the Space Exploration Initiative will require an international effort. If so, who are likely partners for the U.S.?*

Thompson: Making the SEI program an international endeavor has got to be the president's call. You've got to make that policy at the top and he has not yet done that. I think it's too early in the process; until you know the scope of the program and at what pace you're going to do it, you can't start striking agreements. But however we do it, even if it's just a sharing of data or ideas, then I think a number of our partners on space station Freedom would be obvious participants.

***NTB**: Have the delays and much-publicized problems with the Freedom station hurt future opportunities for international cooperation?*

Thompson: No, I think it will work out, but it's a caution signal that when you enter into these agreements it's got to be a strong tie. It's got to be assured. A lot of countries have five-year budgets. In this country we budget every year and so our budgeting is less stable and less assured. As a result, there's always the danger, as we've seen somewhat with space station, of not being able to fulfill our end of the bargain.

***NTB**: In your view, is space station integral to the success of SEI?*

Thompson: I think it is, not because space station would be a launch port, but if you're going to take a trip to Mars and be productive once you get there you need to first go 300 miles up into orbit and learn to live in space. The life sciences knowledge to come out of the space station program is, I believe, fundamental to the success of SEI.

***NTB**: What technology spinoff do you anticipate from the space station program?*

Thompson: A space station is going to drive technology in power systems, robotics, and materials research. But frankly, it's hard to say. In the 1960s, if you had asked me what spinoffs I expected from the Apollo program, I perhaps could have made up a list, but I would have been far off the mark. And it would have been far too short a list.

***NTB**: What would you like to accomplish as deputy administrator that you have not yet done?*

Thompson: I'd like to see NASA achieve a good balance between aeronautics, our space sciences, our Earth sciences, manned programs, and unmanned robotic programs to the planets. I'd also like to make sure that, whatever resources the country devotes to the space program, NASA does a good job of planning its programs and then executing them. And we've got some room there to improve. ❑

New Product Ideas

New Product Ideas are just a few of the many innovatrions described in this issue of *NASA Tech Briefs* and having promising commercial applications. Each is discussed further on the referenced page in the appropriate section in this issue. If you are interested in developing a product from these or other NASA innovations, you can receive further technical information by requesting the TSP referenced at the end of the full-length article or by writing the Technology Utilization Office of the sponsoring NASA center (see page 16). NASA's patent-licensing program to encourage commercial development is described on page 16.

TAZ-8A Alloy Increases the Thermal Endurance of Steel

A high-strength, nickel-based alloy called TAZ-8A can be used as an overlay to protect steel in long-term, cyclic, high-temperature applications. This alloy exhibits high strength at temperatures as high as 1,400 °F (760 °C), resistance to oxidation, excellent cyclic shock resistance between 600 and 2,000 °F (316 and 1,093 °C), and superplasticity at 1,800 °C. (See page 32)

Improved Voice-Coil Actuators Have Lower Copper Losses

A proposed design for electromagnetic linear-motion actuators of the loudspeaker-voice-coil type reduces copper losses and magnetic interference with other equipment. The new actuators are intended for use where power supplies are limited, heating must be minimized, and/or adequate performance at temperatures far below ambient is required.
(See page 18)

Heat- and Oxidation-Resistant Electrodes

Alloys coated with electrically conductive ceramics can be used to make strong, oxidation-resistant electrodes for electrochemical cells operating at temperatures of 1,000 to 1,300 °C. Coated electrodes are more resistant to chemical attack than an all-metal electrode, less brittle than an all-ceramic electrode, and less costly than either alternative.
(See page 34)

Sintered Fiber Electrodes

Improved porous electrodes for oxygen pumps, oxygen sensors, high-temperature solid-electrolyte fuel cells, and high-temperature solid-electrolyte electrolysis cells would be made of sintered fibers to increase porosity without sacrificing strength or conductivity.
(See page 32)

Beam Stop for High-Power Lasers

A graphite/aluminum beam stop absorbs most of the radiation in the beam from an excimer or other high-power laser. It can withstand pulsed ultraviolet peak power of greater than 100 MW/cm^2 and continuous power of more than 100 W/cm^2 without damage.
(See page 28)

Simple Regulator for Positive-Pressure Glove Box

A capacious inflated bag absorbs transient pressure changes in a positive-pressure glove box. Such a regulator can replace an elaborate system of pressure-activated valves. (See page 62)

HOW YOU CAN BENEFIT FROM NASA's TECHNOLOGY UTILIZATION SERVICES

If you're a regular reader of TECH BRIEFS, then you're already making use of one of the low-and no-cost services provided by NASA's Technology Utilization (TU) Network. But a TECH BRIEFS subscription represents only a fraction of the technical information and applications/engineering services offered by the TU Network as a whole. In fact, when all of the components of NASA's Technology Utilization Network are considered, TECH BRIEFS represents the proverbial tip of the iceberg.

We've outlined below NASA's TU Network—named the participants, described their services, and listed the individuals you can contact for more information relating to your specific needs. We encourage you to make use of the information, access, and applications services offered by NASA's Technology Utilization Network.

How You Can Utilize **NASA's Industrial Applications Centers**—A nationwide network offering a broad range of technical services, including computerized access to over 100 million documents worldwide.

You can contact NASA's network of Industrial Applications Centers (IACs) for assistance in solving a specific technical problem or meeting your information needs. The "user friendly" IACs are staffed by technology transfer experts who provide computerized information retrieval from one of the world's largest banks of technical data. Nearly 500 computerized data bases, ranging from NASA's own data base to Chemical Abstracts and INSPEC, are accessible through the ten IACs located throughout the nation. The IACs also offer technical consultation services and/or linkage with other experts in the field. You can obtain more information about these services by calling or writing the nearest IAC. User fees are charged for IAC information services.

Aerospace Research Center (ARAC)
Indianapolis Center for Advanced Research
611 N. Capitol Avenue
Indianapolis, IN 46204
Dr. F. Timothy Janis, Director
(317) 262-5036

Central Industrial Applications Center/NASA (CIAC)
Rural Enterprises, Inc.
P.O. Box 1335
Durant, OK 74702
Dr. Dickie Deel, Director
(405) 924-5094
(800) 658-2823 (toll-free U.S.)

Science and Technology Research Center (STRC)
Post Office Box 12235
Research Triangle Park, NC 27709-2235
H.L. (Lynn) Reese, Director
(919) 549-0671

NASA Industrial Applications Ctr. 823 William Pitt Union
University of Pittsburgh
Pittsburgh, PA 15260
Lani Hummel
Acting Director
(412) 648-7000

Southern Technology Applications Center (STAC)
Box 24
Progress Ctr., One Progress Blvd
Alachua, FL 32615
J. Ronald Thornton, Director
(904) 462-3913
(800) 354-4832 (FL only)
(800) 225-0308 (toll-free US)

NASA/UK Technology Applications Program
University of Kentucky
109 Kinkead Hall
Lexington, KY 40506-0057
William R. Strong, Director
(606) 257-6322

NERAC, Inc.
One Technology Drive
Tolland, CT 06084
Dr. Daniel U. Wilde, President
(203) 872-7000

Technology Application Center (TAC)
University of New Mexico
Albuquerque, NM 87131
Dr. Stanley A. Morain, Director
(505) 277-3622

NASA Industrial Applications Center
University of Southern California
Research Annex
3716 South Hope Street
Los Angeles, CA 90007-4344
Robert Stark, Director
(213) 743-6132
(800) 642-2872 (CA only)
(800) 872-7477 (toll-free US)

NASA/SU Industrial Applications Center
Southern University Department of Computer Science
P.O. Box 9737
Baton Rouge, LA 70813-9737
Dr. John Hubbell, Director
(504) 771-6272
(504) 771-4950

If you represent a public sector organization with a particular need, you can contact NASA's Application Team for technology matching and problem solving assistance. Staffed by professional engineers from a variety of disciplines, the Application Team works with public sector organizations to identify and solve critical problems with existing NASA technology. **Technology Application Team, Research Triangle Institute, P.O. Box 12194, Research Triangle Park, NC 27709; *Doris Rouse, Director,* (919) 541-6980**

How You Can Access Technology Transfer Services At NASA Field Centers: **Technology Utilization Officers & Patent Counsels**—Each NASA Field Center has a Technology Utilization Officer (TUO) and a Patent Counsel to facilitate technology transfer between NASA and the private sector.

If you need further information about new technologies presented in NASA Tech Briefs, request the Technical Support Package (TSP). If a TSP is not available, you can contact the Technology Utilization Officer at the NASA Field Center that sponsored the research. He can arrange for assistance in applying the technology by putting you in touch with the people who developed it. If you want information about the patent status of a technology or are interested in licensing a NASA invention, contact the Patent Counsel at the NASA Field Center that sponsored the research. Refer to the NASA reference number at the end of the Tech Brief.

Ames Research Ctr.
Technology Utilization Officer: Laurance Milov
Mail Code 223-3
Moffett Field, CA 94035
(415) 604-4044
Patent Counsel:
Darrell G. Brekke
Mail Code 200-11
Moffett Field, CA 94035
(415) 604-5104

Lewis Research Center
Technology Utilization Officer: Anthony F. Ratajczak
Mail Stop 7-3
21000 Brookpark Road
Cleveland, OH 44135
(216) 433-2225
Patent Counsel:
Gene E. Shook
Mail Code LE-LAW
21000 Brookpark Road
Cleveland, OH 44135
(216) 433-5753

John C. Stennis Space Center
Technology Utilization Officer: Richard A. Galle (acting)
Code HA-32
Stennis Space Center, MS 39529
(601) 688-1929

John F. Kennedy Space Center
Technology Utilization Officer: Thomas M. Hammond
Mail Stop PT-PMO-A
Kennedy Space Center, FL 32899
(407) 867-3017
Patent Counsel:
James D. Harrell
Mail Code PT-PAT
Kennedy Space Center, FL 32899
(407) 867-2544

Langley Research Ctr.
Technology Utilization Officer: John Samos
Mail Stop 139A
Hampton, VA 23665
(804) 864-2484
Patent Counsel:
George F. Helfrich
Mail Code 279
Hampton, VA 23665
(804) 864-3523

Goddard Space Flight Center
Technology Utilization Officer: Donald S. Friedman
Mail Code 702.1
Greenbelt, MD 20771
(301) 286-6242
Patent Counsel:
R. Dennis Marchant
Mail Code 204
Greenbelt, MD 20771
(301) 286-7351

Jet Propulsion Lab.
NASA Resident Office
Technology Utilization Officer: Arif Husain
Mail Stop 180-801
4800 Oak Grove Drive
Pasadena, CA 91109
(818) 354-4862
Patent Counsel:
Thomas H. Jones
Mail Code 180-801
4800 Oak Grove Drive
Pasadena, CA 91109
(818) 354-5179
Technology Utilization Mgr. for JPL: Dr. Norman L. Chalfin
Mail Stop 156-211
4800 Oak Grove Drive
Pasadena, CA 91109
(818) 354-2240

George C. Marshall Space Flight Center
Technology Utilization Officer: Ismail Akbay
Code AT01
Marshall Space Flight Center, AL 35812
(205) 544-2223
Fax (205) 544-3151
Patent Counsel:
Bill Sheehan
Mail Code CC01
Marshall Space Flight Center, AL 35812
(205) 544-0021

Lyndon B. Johnson Space Center
Lyndon B. Johnson
Technology Utilization Officer: Dean C. Glenn
Mail Code IC-4
Houston, TX 77058
(713) 483-3809
Patent Counsel:
Edward K. Fein
Mail Code AL3
Houston, TX 77058
(713) 483-4871

NASA Headquarters
Technology Utilization Officer: Leonard A. Ault
Code CU
Washington, DC 20546
(202) 557-5598
Assistant General Counsel for Patent Matters: Robert F. Kempf, Code GP
Washington, DC 20546
(202) 453-2424

A Shortcut To Software: **COSMIC®**

—For software developed with NASA funding, contact COSMIC, NASA's Computer Software Management and Information Center. New and updated programs are announced in the Computer Programs section. COSMIC publishes an annual software catalog. For more information call or write: **COSMIC®**, 382 East Broad Street, Athens, GA 30602 *John A. Gibson, Dir.,* (404) 542-3265.

If You Have a Question..**NASA Scientific & Technical Information Facility**

NASA Scientific & Technical Information Facility can answer questions about NASA's Technology Utilization Network and its services and documents. The STI staff supplies documents and provides referrals. Call, write or use the feedback card in this issue to contact: **NASA Scientific and Technical Information Facility,** Technology Utilization Office, P.O. Box 8757, Baltimore, MD 21240-0757. *Walter M. Heiland, Manager,* (301) 859-5300, Ext. 242,243.

Electronic Components and Circuits

Hardware, Techniques, and Processes

18 Improved Voice-Coil Actuators Have Lower Copper Losses

20 Charging/Safety-Interlock Connection for Capacitor Bank

Improved Voice-Coil Actuators Have Lower Copper Losses

Pr/Fe/B permanent magnets yield better performance at lower temperatures.

Marshall Space Flight Center, Alabama

An improved design concept for electromagnetic linear-motion actuators of the loudspeaker-voice-coil type reduces both copper losses (dissipation of power in the electrical resistances of the windings) and magnetic interference with other equipment. The new actuators are intended for use where power supplies are limited, heating must be minimized, and/or adequate performance at temperatures far below ambient is required.

In a loudspeaker-voice-coil actuator, a coil of roughly cylindrical shape moves in a radial magnetic field set up by permanent magnets, exerting an axial force proportional to the driving electrical current and to this field. To increase the force obtainable from a given current, reduce the current needed to obtain a given driving force, and/or reduce the copper loss at a given current or force, one has to use a permanent magnet of greater energy product (the energy product is a measure of the strength of the permanent magnetic field and the ability of the permanent magnets to retain the field). However, two major design issues arise when attempting to improve an actuator in this way: (1) the permanent-magnet material of choice — Nd/Fe/B — has the highest known energy product at room temperature, but the reorientation of electron spins causes the energy product to decrease at temperatures below 140 K; (2) the simple magnetic circuits of the traditional voice-coil design (see Figure 1) are not appropriate for high-energy-product magnets.

The first issue is addressed by the use of Pr/Fe/B magnets, which have energy products nearly equivalent to those of Nd/Fe/B magnets at room temperature but do not exhibit reorientation of spins. The second issue is addressed by use of a new magnetic circuit (see Figure 2) that both increases the energy efficiency and enhances the useful magnetic flux density. Unlike the traditional voice-coil magnetic circuit, which is open at one end, this circuit is closed. This feature removes most of the fringing flux from the airgap, concentrating it in the coil. In so doing it also contains the magnetic field more nearly completely within the device, thereby reducing magnetic interference with nearby equipment.

This work was done by Satoru Simizu, Faiz Pourarian, Edwin B. Boltich, and Suryanarayan G. Sankar of Advanced Materials Corp. for **Marshall Space Flight Center**. *For further information, Circle 19 on the TSP Request Card.*

Inquiries concerning rights for the commercial use of this invention should be addressed to the Patent Counsel, Marshall Space Flight Center [see page 16]. Refer to MFS-26111.

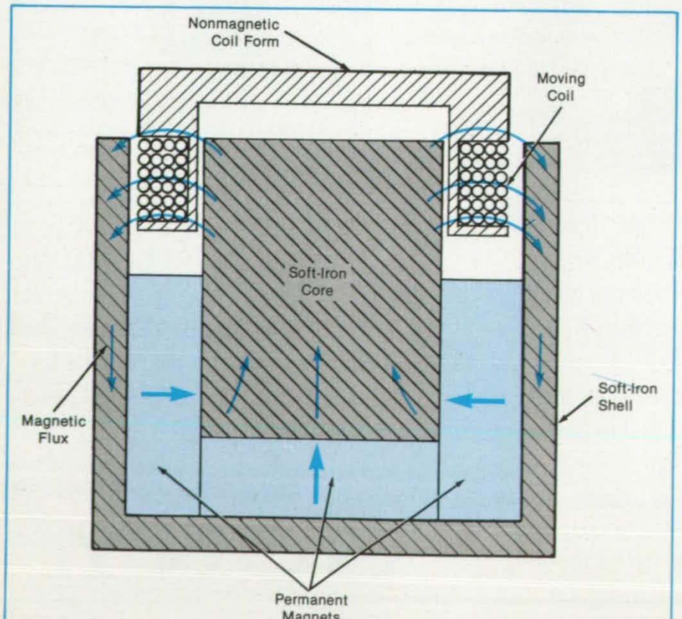

Figure 1. A **Voice Coil** of the type used traditionally in loudspeakers has an open end, which gives rise to some fringing flux.

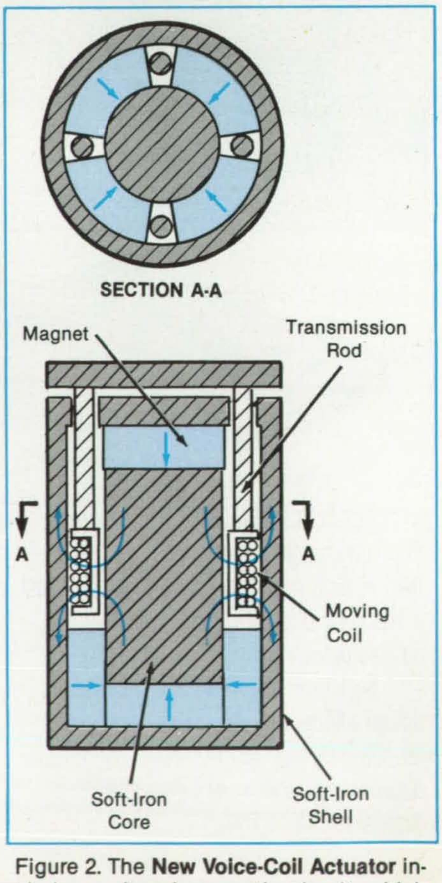

Figure 2. The **New Voice-Coil Actuator** includes a closed magnetic circuit, which suppresses the fringing flux.

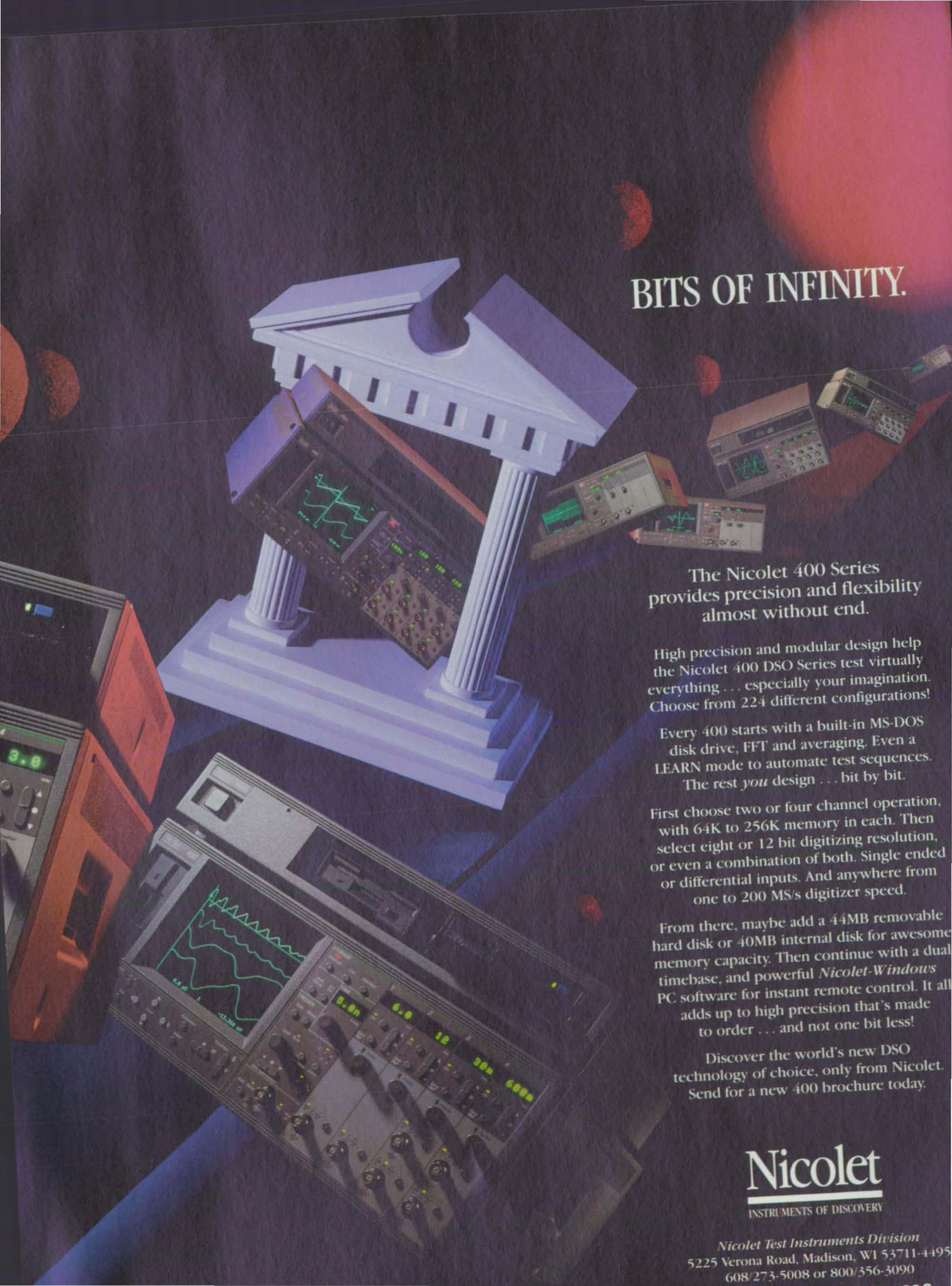

BITS OF INFINITY.
The Nicolet 400 Series provides precision and flexibility almost without end.
High precision and modular design help the Nicolet 400 DSO Series test virtually everything . . . especially your imagination. Choose from 224 different configurations!
Every 400 starts with a built-in MS-DOS disk drive, FFT and averaging. Even a LEARN mode to automate test sequences. The rest *you* design . . . bit by bit.
First choose two or four channel operation, with 64K to 256K memory in each. Then select eight or 12 bit digitizing resolution, or even a combination of both. Single ended or differential inputs. And anywhere from one to 200 MS/s digitizer speed.
From there, maybe add a 44MB removable hard disk or 40MB internal disk for awesome memory capacity. Then continue with a dual timebase, and powerful *Nicolet-Windows* PC software for instant remote control. It all adds up to high precision that's made to order . . . and not one bit less!
Discover the world's new DSO technology of choice, only from Nicolet. Send for a new 400 brochure today.
Nicolet
INSTRUMENTS OF DISCOVERY
Nicolet Test Instruments Division
5225 Verona Road, Madison, WI 53711-4495
608/273-5008 or 800/356-3090

Charging/Safety-Interlock Connection for Capacitor Bank

Precharge before connection and discharge before disconnection are assured.

NASA's Jet Propulsion Laboratory, Pasadena, California

An electrically controlled mechanical interlock apparatus prevents the connection of a bank of capacitors to a battery or other dc power supply until the capacitors are precharged to nearly the full supply voltage. The precharge eliminates excessive inrush current, which can damage the capacitors, wires, or connectors. The circuit in the apparatus also discharges the capacitors after power is turned off or the capacitors are disconnected from the power supply.

Figure 1 shows the charging and interlock-controlling circuit. The main connection between the capacitors and the power supply is made through the plug and socket designated collectively as J_1 (see Figure 2). The auxiliary connection for precharging is made through J_2. The socket part of J_1 is equipped with a spring-loaded blocking pin, which prevents the insertion of the plug part of J_1 unless the plunger is withdrawn by activation of solenoid S.

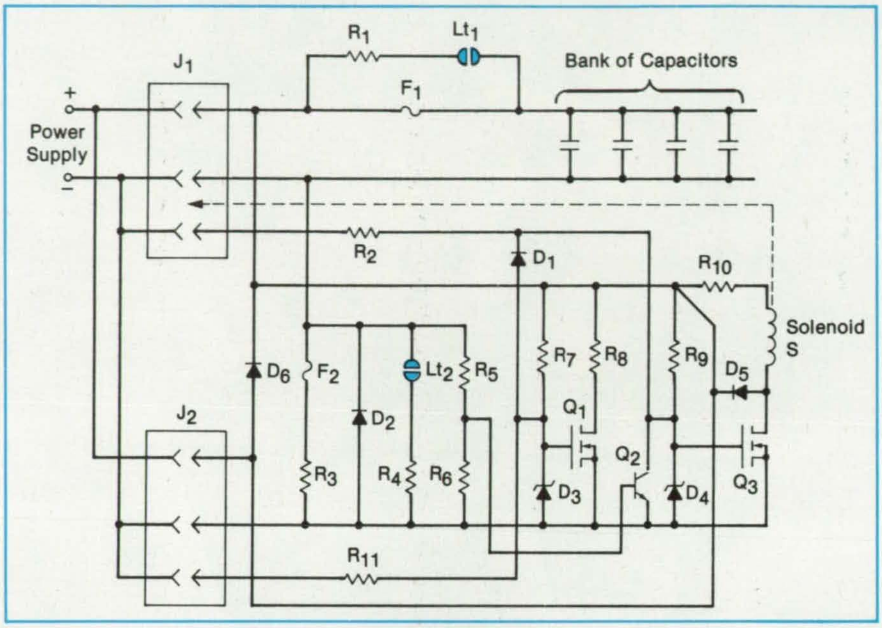

Figure 1. The **Safety-Interlock Circuit** prevents the connection of the capacitors to the power supply through main connector J_1 until the capacitors have been precharged gently through J_2. The circuit also discharges the capacitors after power is turned off.

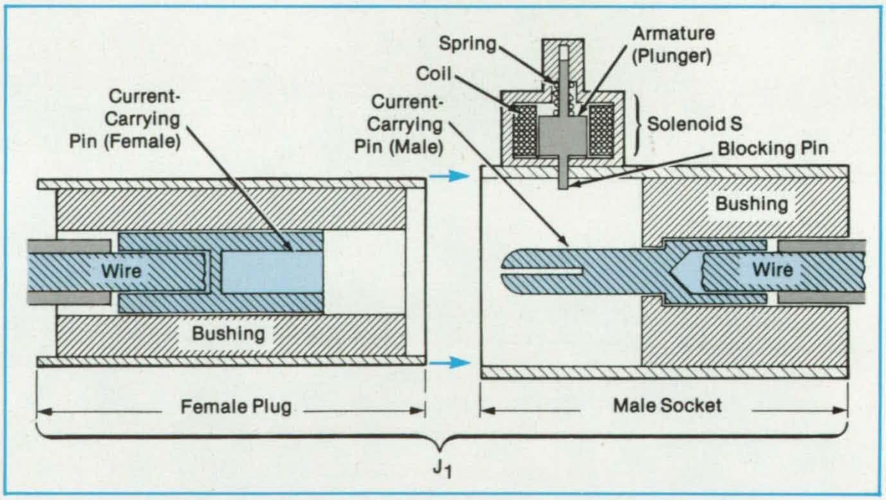

Figure 2. This **Detail of Part of Main Connector** J_1 shows how the blocking pin prevents the connection of the mating parts of J_1 until the blocking pin is withdrawn by actuation of the solenoid.

To activate the solenoid and thereby enable the main connection, it is necessary to precharge the capacitor bank first. To begin charging, one connects J_2. This causes limited charging current to flow from the positive terminal of the power supply through diode D_6, into the capacitors through main fuse F_1, then from the capacitors through charging fuse F_2 and current-limiting resistor R_3, then back to the power supply through its negative terminal. The charging time constant is the product of R_3 and the total capacitance of the bank.

During precharging, a portion of the voltage appearing across R_3 is put on the base of transistor Q_2 by the voltage divider R_5 and R_6. This turns on Q_2, thereby holding Q_3 off and keeping current from flowing through the solenoid S. The plunger of S remains inserted through the shell of J_1, preventing the connection of main power during precharging.

When the capacitor bank is charged almost to the full power-supply voltage, Q_2 is turned off. The voltage for this transition is set by the ratio of R_5 and R_6. The turning off of Q_2 allows Q_3 to turn on, thus activating solenoid S. The plunger is withdrawn, and the plug and socket of J_1 can be connected.

After power is turned off, J_1 and J_2 can be disconnected in any order, because the voltage on the capacitors holds Q_3 on. Even if solenoid S is inactivated, the parts of J_1 can be separated against the slight friction imposed by the plunger against the shell of the plug. The voltage on the capacitors holds on transistor Q_1, via pullup resistor R_7 and Zener diode D_3. This allows current to flow through dissipative power resistor R_8, transistor Q_1, and diode D_2, thus discharging the capacitors.

The circuit provides other safety and convenience features. If the main fuse F_1 is blown, the full power-supply voltage appears across it, and lamp Lt_1 lights up at any attempt to connect J_2 and/or J_1. If a fault or overload occurs across the input bus and F_1 does not blow, the mating of J_2 causes a constant current to flow through charging fuse F_2. Proper sizing of this fuse allows the ordinary short-term charging currents to flow, even in excess of its rating, but the prolonged constant current due to a fault melts the fuse, and lamp Lt_2 then lights up to provide an indication of trouble. The solenoid can also be used to prevent the actuation of other electrical contactors or the closure of manually actuated switches.

This work was done by Wally E. Rippel of Caltech for **NASA's Jet Propulsion Laboratory**. *For further information, Circle 89 on the TSP Request Card.*
NPO-17519

The Solution Is At Your Fingertip...

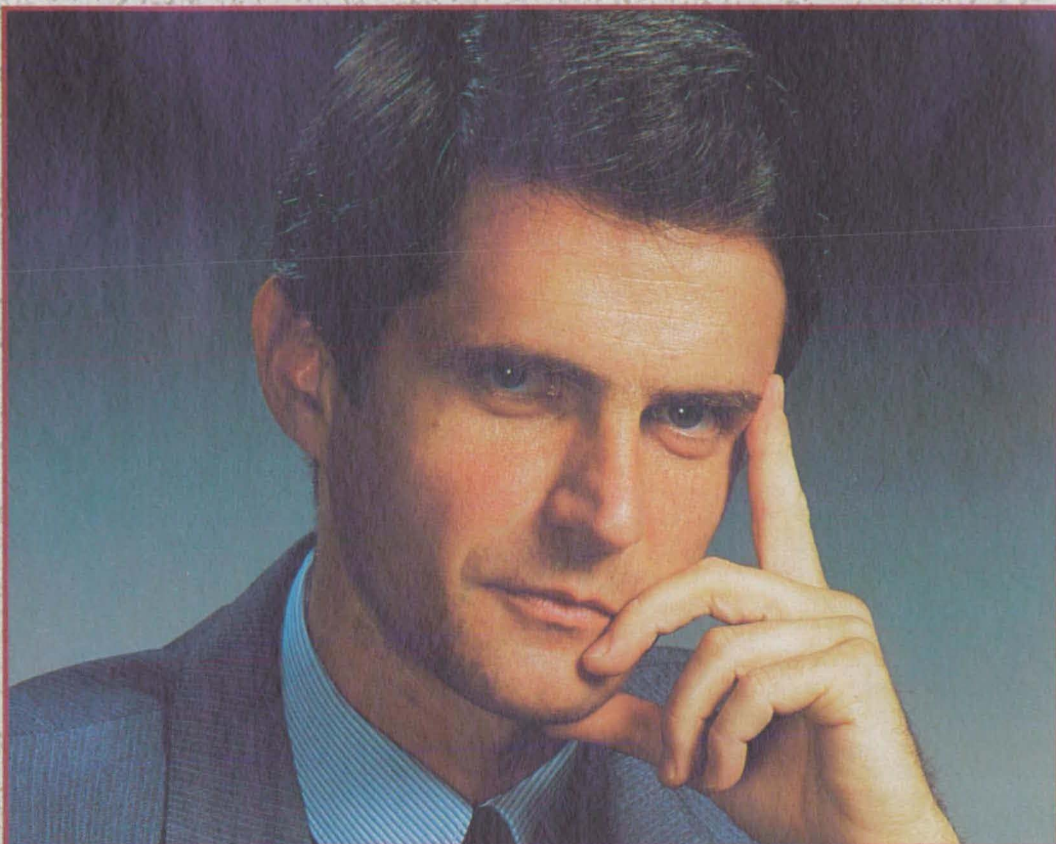

...With A Custom Touch Panel From EMS.

Why Didn't I Think Of This Before?

Still struggling to incorporate a standard touch product when your application begs for a custom solution? If so, consider a custom touch panel from Electro Mechanical Systems (EMS).

EMS touch panels are designed with solid-state components and use a matrix of pulsed infrared (IR) light beams in front of the display to implement a touch function.

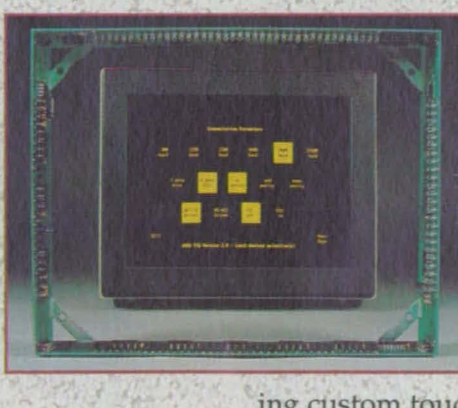

The performance of every EMS touch panel is further enhanced by our patented circuit, which gives our touch panels additional resiliency in tough industrial applications.

Because each custom application requires special attention to every detail, EMS engineers work closely with our customers to provide a timely, cost-effective solution.

Call EMS today to discuss your specific application. Our engineers have been designing custom touch panels since 1975. Isn't it time we designed one for you?

EMS TOUCH

Electro Mechanical Systems 801 W. Bradley Avenue/Champaign IL 61820/U.S.A./(217) 359-7125/FAX 217-359-2075

Circle Reader Action No. 518

Hardware, Techniques, and Processes

22 Neural Network Solves "Traveling-Salesman" Problem

24 Adaptive Neurons for Artificial Neural Networks

25 SCSI Communication Test Bus

26 Controlling Gas-Flow Mass Ratios

27 Simplified Learning Scheme for Analog Neural Network

Computer Programs

38 Analyzing Distributed Processing for Electric Utilities

38 Local-Area-Network Simulator

38 Software for Three-Dimensional Space-Shuttle Imagery

39 Data-Management Software for PiFEx

Neural Network Solves "Traveling-Salesman" Problem

Optimization problems could be solved faster and more cheaply.

NASA's Jet Propulsion Laboratory, Pasadena, California

An experimental electronic neural network solves the "traveling-salesman" problem, which is to plan a round trip of minimum distance among *N* cities, visiting every city once and only once (without backtracking). This problem is a paradigm of many problems of global optimization (e.g., routing or the allocation of resources) that occur in industry, business, and government. When fully developed and applied to a large number of cities (or resources), circuits of this kind are expected to solve the problem faster and more cheaply than can digital computers that compare all $N!/2N$ possible routes (or allocations) to find the optimum one. Furthermore, whereas the complexities of typical prior electronic neural networks conceived for this purpose are approximately proportional to N^3 or more, the complexities of circuits of the new type are approximately proportional to N^2.

The neural network includes an inhibitory binary synaptic feedback matrix that enforces two of the binary constraints: (1) visit each city only once and (2) do not backtrack. The neurons are amplifiers or other sources through which signals representative of the intercity distances (or the costs of allocation of resources) are fed into the network. In the simplified four-city example of Figure 1, turning neuron AB "on" signifies travel from city A to city B. This precludes travel from A to C or D; and, by application of the no-backtracking rule to this and the next leg of the journey, it also precludes travel from B, C, or D to A, or from C or D to B. To enforce these preclusions, the binary synaptic connections in the top row of the network cause neurons AC, AD, BA, CB, and DB to turn off when AB is turned on.

The intercity distances are used to generate the analog excitatory prompts to all the neurons (proportional to the corresponding distances or other costs subtracted from a fixed, preselected excitation level). When the neurons are prompted initially with the analog values, the network generates a tour that goes through all the cities, visiting every city once and only once. However, in an attempt to minimize the distance or cost as much as possible, the network in the form shown in Figure 1 often tends to generate disjointed, closed loops that connect smaller groups of cities, rather than making a single closed loop. Therefore, to enforce the binary condition that there should be only one closed-loop tour, an auxiliary circuit is necessary.

In this auxiliary circuit (see Figure 2), a 4 × 4 array of binary switches, except for the diagonal, is directly connected with a fixed threshold, to the outputs of the neurons of the network of Figure 1. In this circuit, each voltage source represents a city. When a solution starts emerging from the network of Figure 1, the switches in this auxiliary network close and the signals from the various city (voltage) sources start to become connected in a series, adding to a signal that comes from the network of Figure 1. In one scenario, this auxiliary circuit can be used to inhibit several of the neurons that are "on" in a multiloop solution. This prevents the multiloop solution from being a stable state of the network. On the other hand, if all cities are connected in a single tour as desired, the auxiliary circuit "approves" by sending no inhibitory signal to the winning set of neurons.

This work was done by Anilkumar P. Thakoor and Alexander W. Moopenn of Caltech for **NASA's Jet Propulsion Laboratory.** *For further information, Circle 110 on the TSP Request Card.*

This invention is owned by NASA, and a patent application has been filed. Inquiries concerning nonexclusive or exclusive license for its commercial development should be addressed to the Patent Counsel, NASA Resident Office — JPL *[see page 16].* *Refer to NPO-17807.*

Figure 1. The **Analog/Binary Feedback Network** represented by this simplified schematic diagram solves the "traveling-salesman" problem for four cities.

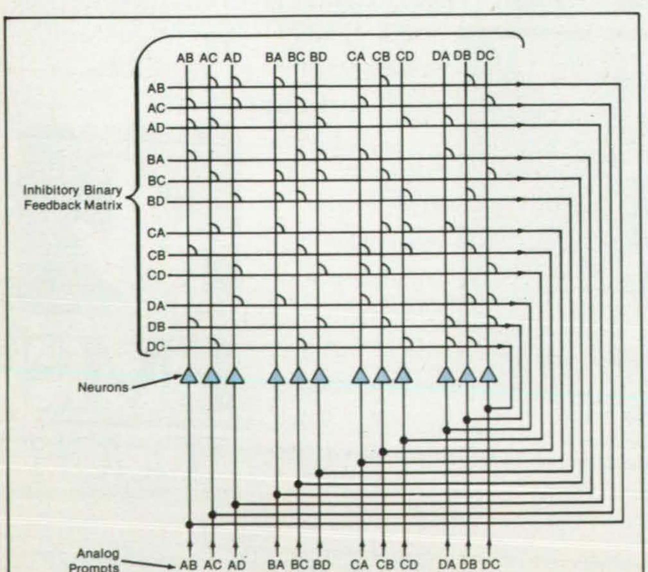

Figure 2. This **Auxiliary Circuit**, when connected to the network illustrated in Figure 1, prevents the solution reached by that network from breaking down into separate small, closed loops.

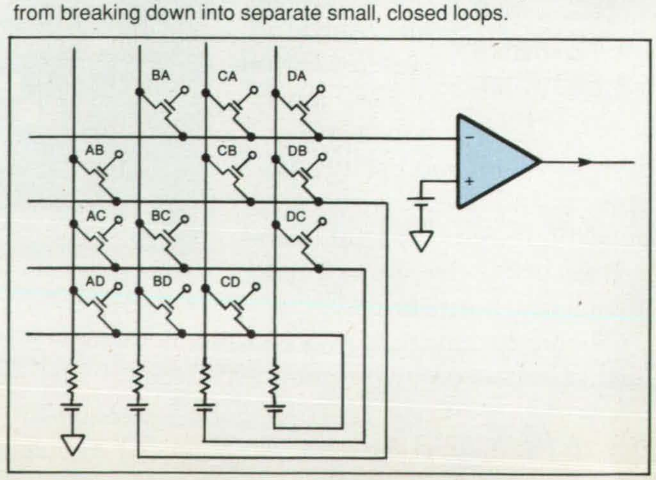

Implement Digital Signal Processing Without A/D Conversion

The ACT Signal MicroProcessor brings programmability to high-speed analog processing.

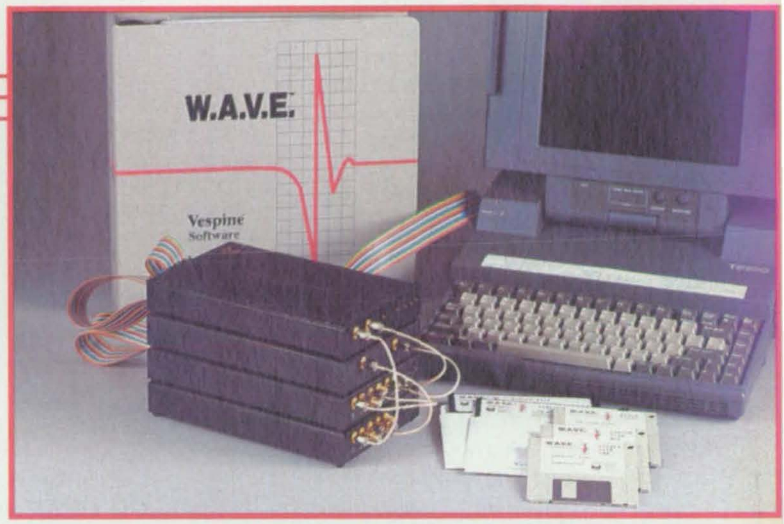

Acoustic Charge Transport (ACT) technology has enabled the development of revolutionary Signal MicroProcessors capable of performing over 45 billion multiply-and-accumulate operations per second.

The Signal MicroProcessor (SMP) is a software-programmable chip which processes RF and video analog signals with the same versatility and ease that the digital microprocessor processes data. The SMP Development Station is an evolving system of PC-based instrumentation modules that use the SMP as a massively parallel processing engine capable of handling RF and video signals with bandwidths up to 150 MHz. User interface and control of the SMP is provided through powerful and easy-to-use W.A.V.E.® data aquisition and analysis software. W.A.V.E.® runs on any IBM-PC/AT or 100% compatible personal computer.

The first SMP Development Station module is a 128-tap programmable transversal filter (PTF) which is useful for signal generation, extraction, modification and characterization. It has been used to verify the design of an LPI radar system, built-in network analyzers, multipath equalizers, pulse-shaping equalizers, magnetic read-head equalizers, programmable bandpass filters, smart scope triggers, anti-aliasing filters, synthesizers, waveform generators, spread-spectrum matched filters, interference cancellers, target simulators, and pattern matchers for signals and images.

Users can expect to have the SMP Development Station up and running in less than 1 hour.

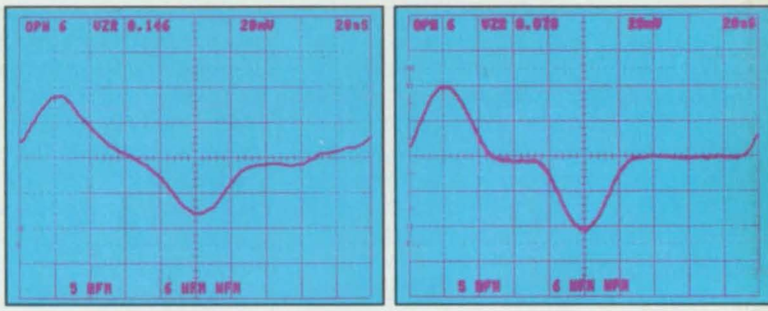

Pre-equalization Post-equalization

Pulse shaping / equalization

Unparalleled ability to shape wideband waveforms and equalize channels.

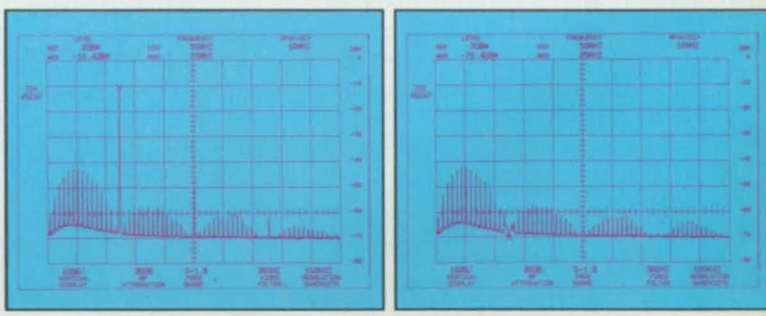

Pre-cancellation Post-cancellation

Interference cancellation

Measurement and cancellation of single or multiple interference sources.

ELECTRONIC DECISIONS INCORPORATED

1776 East Washington Street Urbana, Illinois 61801

(800) 373-3628

Adaptive Neurons for Artificial Neural Networks

Training time decreases dramatically.

NASA's Jet Propulsion Laboratory, Pasadena, California

In an improved mathematical model of a neural-network processor, the temperature of the neurons (in addition to the connection strengths, also called the weights, of the synapses) is varied during the supervised-learning phase of operation according to a mathematical formalism and not a heuristic rule. In previous mathematical models of neural networks, neurons were treated as passive nonlinear elements, and only the connection strengths of the synapses were varied during learning. The improved model may be more realistic in that there is evidence that biological neural networks also process information at the neuronal level.

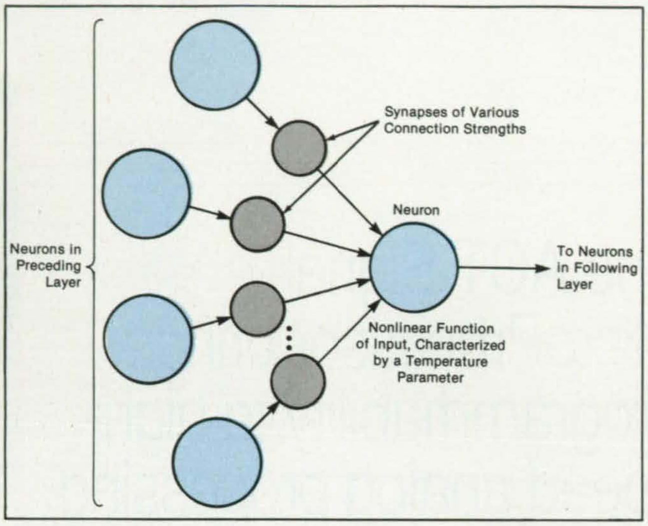

Figure 1. The **Output of a Neuron** in the nth layer is a nonlinear function of the **synaptically** weighted outputs of the neurons in the previous layer.

In this as in previous models, a neural network consists of layers of neurons. Each neuron in each layer (except the input and output layers) is connected to some or all neurons in the preceding and following layers via the synapses. The response of each neuron is specified by an activation function — a nonlinear function of the sum of the synaptically weighted responses of the neurons of the preceding layer to which it is connected (see Figure 1). Often, the activation function is taken to be a sigmoid function of a type that appears in Fermi–Dirac statistical mechanics and in which the sum of the synaptically weighted responses is analogous to activation energy and is divided by a parameter analogous to temperature. The function could also include an amplitude factor peculiar to each neuron, but here this factor is set equal to 1.

In the adaptive-neuron model as in many previous models, supervised learning is a repetitive feed-forward/back-propagation process. During the feed-forward phase, the network is stimulated by an input vector, causing it to respond with an output vector. This output vector is compared with the target output vector (the "correct" response) via an error function defined as the sum-square difference between these two vectors. During the back-propagation phase, a gradient-descent algorithm reduces this error by adjusting synaptic weights and neuronal temperatures. This algorithm can be given an additional degree of freedom by specifying different synaptic and neuronal learning rates. The algorithm is applied, layer by layer, proceeding from the output layer back toward the input layer. The feed-forward/back-propagation cycle can be repeated as many times as necessary to bring the error below a specified level.

The adaptive-neuron model was tested in the numerical simulation of a simple neural network that was to be trained to perform the exclusive-OR operation. The performance of the new model was compared with that of a conventional back-propagation (synaptic weights only) model. As shown in Figure 2, the new model learned the exclusive-OR function with a mean-square error of $<10^{-5}$ in fewer than 10^3 iterations, while the conventional model still produced an error about 10^3 times as large after 10^6 iterations.

This work was done by Raoul Tawel of Caltech for **NASA's Jet Propulsion Laboratory**. *For further information, Circle 130 on the TSP Request Card.*

This invention is owned by NASA, and a patent application has been filed. Inquiries concerning nonexclusive or exclusive license for its commercial development should be addressed to the Patent Counsel, NASA Resident Office-JPL [see page 16]. Refer to NPO-17803.

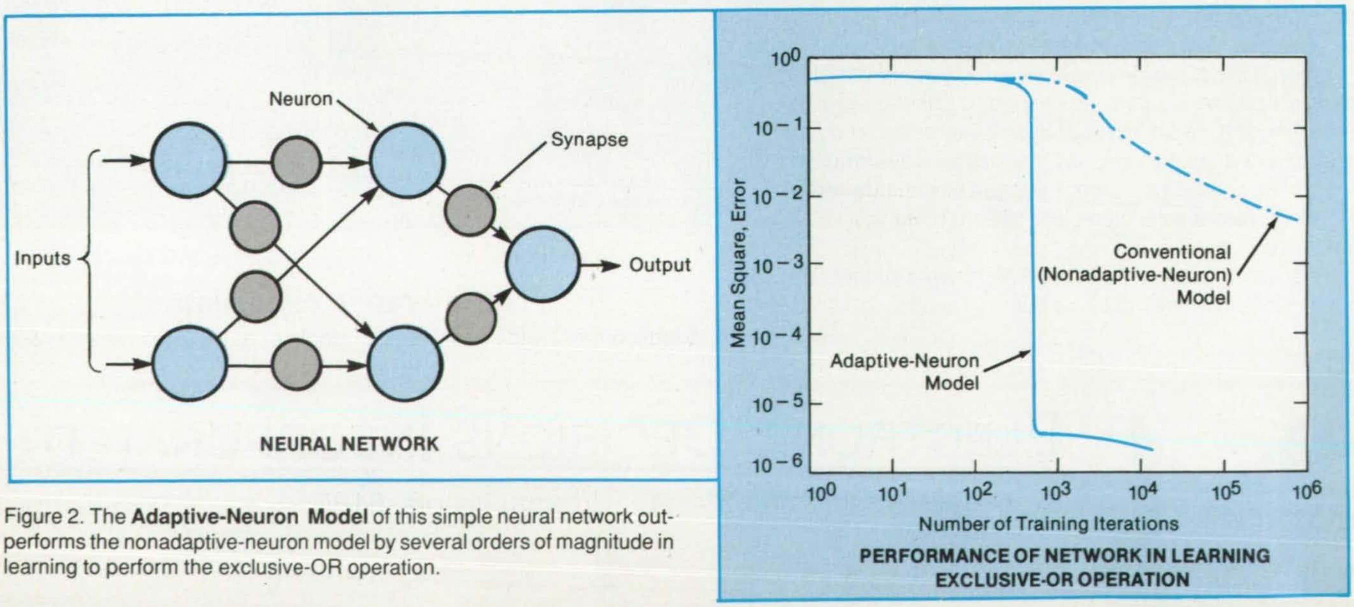

Figure 2. The **Adaptive-Neuron Model** of this simple neural network outperforms the nonadaptive-neuron model by several orders of magnitude in learning to perform the exclusive-OR operation.

SCSI Communication Test Bus

The SCSI connection sustains the transfer of data at a greater rate.

Lyndon B. Johnson Space Center, Houston, Texas

The Small Computer System Interface (SCSI) communication test bus provides a high-data-rate, standard interconnection that enables communication among an International Business Machines (IBM) Personal System/2 Micro Channel, other devices connected to the Micro Channel, test equipment, and a host computer. Previously, slower and less-intelligent interface buses have been used for testing: these include the IEEE-488 [general-purpose interface bus (GPIB)], the RS-232, and the RS-422. The SCSI communication test bus is implemented by use of the SCSI bus (see figure), which, heretofore, has been used primarily commercially as a communication channel between a host computer and a direct-access storage device.

One requirement that motivated this application of the SCSI is the need for a "debugger" that can monitor activities on the Micro Channel nonintrusively. The debugger must also enable test equipment to communicate with an 80386 microprocessor on the Micro Channel. The debugger operates in two modes: nonintrusive and interfacing. In the nonintrusive mode, the debugger behaves as a passive monitoring device that does not affect any activities on the Micro Channel. In the interfacing mode, it enables test equipment to communicate with the 80386 microprocessor through the Micro Channel. The debugger also enables the host computer to read from, and write to, the memory or input/output ports of the Micro Channel. This interfacing mode is also known as the "bus master" mode of the Micro Channel.

The data-transfer rate of the SCSI — 4 MB/s — meets the high-speed-communication requirement for the debugger, and upgrades to higher speeds are under consideration. The maximum attainable speeds of previous test buses (e.g., 1 MB/s in the IEEE-488) were insufficient for sending data back to host computers while continuously acquiring more data. Usually, to hold large traces of collected test data, previous debuggers included large and costly high-speed memories. The collected data were transferred back to the host computer only after the traces had been stopped. The data could be used for monitoring only; real-time processing and other actions were not possible.

With the high speed of the SCSI bus and the intelligence of the SCSI controller, data from the debugger can be sent back to the controlling host computer continuously while the debugger collects more data from the Micro Channel. The number of data that can be collected by the debugger is limited only by the storage capacity of the controlling host computer. This opens up the possibility of using the debugger in real-time applications that were impossible with older test buses.

This work was done by Chanh V. Hua, John J. D'Ambrose, Richard C. Jaworski, Elaine M. Halula, David N. Thornton, Robert L. Heligman, and Michael R. Turner of International Business Machines Corp. for **Johnson Space Center.** *For further information, Circle 17 on the TSP Request Card. MSC-21704*

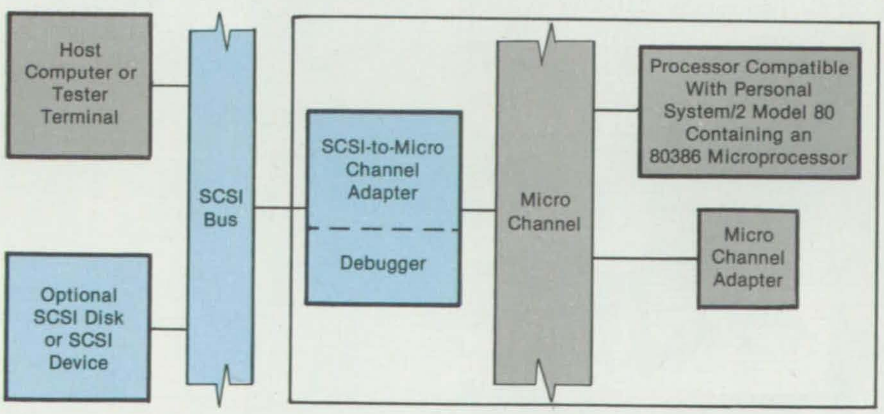

The **SCSI Communication Test Bus** serves primarily as a nonintrusive input/output attachment to the PS/2 Micro Channel bus, providing rapid communication for the debugger.

Controlling Gas-Flow Mass Ratios

Stoichiometric proportions of reacting gases would be supplied.

Lyndon B. Johnson Space Center, Houston, Texas

A proposed system would automatically control the proportions of gases flowing in supply lines. The system was conceived for control of the oxidizer-to-fuel ratio in new gaseous-propellant rocket engines. The concept is also applicable to the control of mass ratios in such gaseous industrial processes as chemical-vapor deposition of semiconductor materials and in automotive engines operating on compressed natural gas.

In the rocket engine, oxygen and hydrogen would be fed simultaneously to a combustion chamber, where they would be burned to provide thrust. The gases should be supplied in the mass ratio of eight parts oxygen to one part hydrogen to ensure that they burn completely, that their chemical energy is fully extracted, and that energy is not wasted in the form of unused gas when one propellant is consumed before the other.

The proposed system would maintain the stoichiometric mass ratio in the combustion chamber despite changes in temperature and density in the supply tanks and in pressure in the combustion chamber. Unlike in a liquid system, the temperature, pressure, and density in a gas system vary significantly because the gases expand in their supply tanks as they are consumed. Moreover, the variations are different for different gases; even though oxygen and hydrogen may start out at the same temperature and pressure in their respective tanks, the conditions in the two gases change at different rates.

The system (see figure) would control the individual mass flows with electronically controlled variable-pressure regulators, which are available commercially. It would set target values for the parameters of the gas system, monitor the parameters by measurement and calculation, and adjust control parameters to assure that the target parameters are met.

The preset target parameters would be the oxygen/hydrogen mass ratio supplied to the chamber, the pressure in the engine chamber, and the set-point voltages of the oxygen and hydrogen regulators. The control system would include sensors that would measure pressures in the engine chamber, in the inlets of the hydrogen and oxygen venturis, and in the hydrogen and oxygen tanks. It would also include sensors to measure the temperatures in the hydrogen and oxygen tanks.

From these measurements, the control system would calculate the mass-flow rates of oxygen and hydrogen, the actual oxygen/hydrogen mass ratio in the gas flowing to the chamber, and new set-point voltages for the oxygen and hydrogen regulators. The control system would adjust the regulator set-point voltages from the preset values to the newly calculated values and thus change the mass ratio in the gas flowing to chamber.

The control computer would execute adjustments according to three goals listed in order of descending priority:

- Maintain the pressure in the engine chamber within the proper range.
- Balance the gases remaining in the tanks according to the stoichiometric mass ratio.
- Control the oxygen/fuel ratio supplied to the chamber.

This work was done by Brian G. Morris of **Johnson Space Center**. *For further information, Circle 117 on the TSP Request Card.*

This invention is owned by NASA, and a patent application has been filed. Inquiries concerning nonexclusive or exclusive license for its commercial development should be addressed to the Patent Counsel, Johnson Space Center [see page 16]. Refer to MSC-21542.

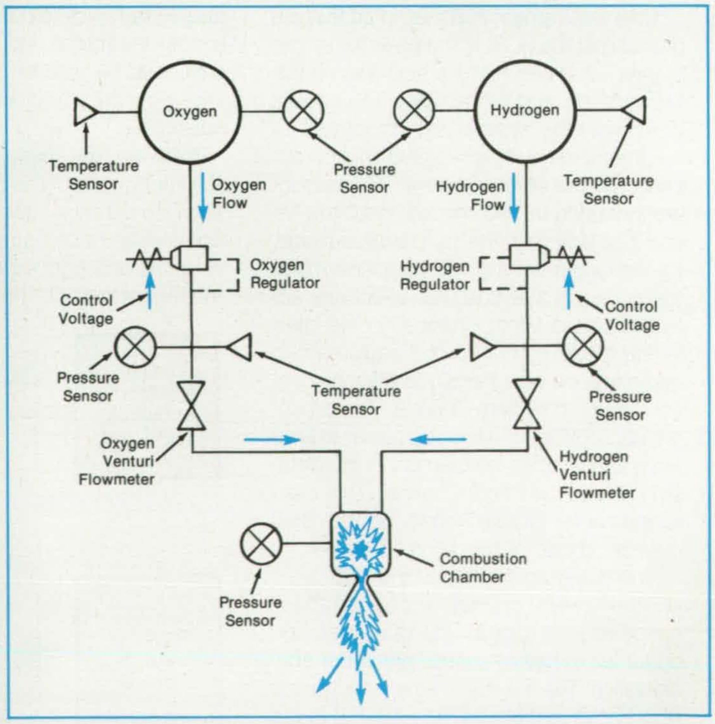

The **Gas-Flow Control System** would measure temperatures and pressures at various points. From these data, it would calculate control voltages for electronic pressure regulators for oxygen and hydrogen. The system would include commercially available components.

Not for every vacuum application

... only the tough ones.

Balzers Roughing Pumps

Rotary vane pumps from 1.2 - 320 cfm

Balzers pumps are designed for applications as tough as yours. Whether you're pumping helium or tritium gas, working with aggressive, explosive or toxic gases or need a pump you can install right in your cleanroom—Balzers can provide the solution.

How do we do it? Foremost, we've developed the design technologies that meet the toughest application challenges. For example, the Balzers B Series is the only rotary vane system in which the motor is enclosed within the pump housing, eliminating the particulate-generating radial shaft seal.

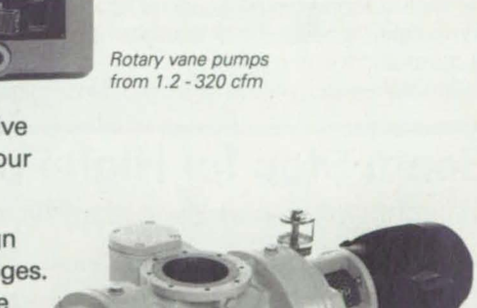

Roots pumps from 190 - 15,000 cfm

Bring us your tough application. We'll provide the rotary vane or roots pump you need, along with the benefits all Balzers pumps have in common: low maintenance, long service life, reliable performance, clean vacuum pumping.

Reader Service No. 403
To Receive Literature

Reader Service No. 404
To Have A Sales Representative Contact You

BALZERS

Balzers • 8 Sagamore Park Road • Hudson, NH 03051
TEL (603) 889-6888 • FAX (603) 889-8573

Pfeiffer Vakuumtechnik • Postfach 1280 • D-6334 Asslar
TEL (06441) 802-0 • FAX (06441) 802-202

The Sensible Solution

Physical Sciences

Hardware, Techniques, and Processes
28 Flux Jacobian Matrices for Equilibrium Real Gases
28 Beam Stop for High-Power Lasers

Books and Reports
30 Numerical Methods for Chemically Reacting Flows
30 Analysis of Used Arc-Jet Electrodes
31 Further Studies of Hot-Wire Anemometry
31 Optimization of Array of Laser Retroreflectors

Flux Jacobian Matrices for Equilibrium Real Gases

An improved formulation includes a generalized Roe average and extension to three dimensions.

Ames Research Center, Moffett Field, California

Flux Jacobian matrices derived previously for use in numerical solutions of conservation-law differential equations of inviscid flows of ideal gases have been extended to real gases. The real-gas formulation of these matrices retains the simplifying assumptions of thermodynamic and chemical equilibrium, but adds the effects of vibrational excitation, dissociation, and ionization of gas molecules via a general equation of state.

For a one-dimensional flow, the flux Jacobian matrix $\bar{A}$ is defined by the differential equation $d\mathbf{F} = Ad\mathbf{U}$, where $\mathbf{U}$ is the column vector composed of the densities of mass, momentum, and total energy (which are conservative variables) and $\mathbf{F}$ is the column vector composed of the mass-flux density, the pressure plus the momentum-flux density, and the total energy-flux density plus the product of pressure and velocity. In this formulation, the pressure is expressed by a general equation of state as a function of the densities of mass and internal energy.

Some previous methods for the solution of conservation laws have involved local linearization, in which the flux at a point that separates two states $\mathbf{U}_L$ and $\mathbf{U}_R$ is based on the eigenvalues and eigenvectors of some average flux Jacobian matrix $\bar{A}$. The optimum choice for $\bar{A}$ is one that satisfies $\mathbf{F}_R - \mathbf{F}_L = \bar{A}(\mathbf{U}_R - \mathbf{U}_L)$. One way to obtain $\bar{A}$ is to seek an average state $\bar{\mathbf{U}}$ that satisfies $\bar{A} = A(\bar{\mathbf{U}})$. Such a state is called a Roe-averaged state, having been derived by Roe for a perfect gas. In previous efforts to generalize the Roe average to a real gas, it was established that such a state exists but is not uniquely defined. In the present formulation, the Roe-averaged state of a real gas in the one-dimensional case is uniquely defined in terms of the thermodynamic states L and R in a manner consistent with that for a perfect gas.

To begin the generalization to the three dimensional case, one expands $\mathbf{U}$ to include the two additional vector components of the momentum density. Next, one expands $\mathbf{F}$ to $\mathbf{F}_n$ by changing the pressure-plus-momentum-flux-density term in $\mathbf{F}$ to the component of momentum flux perpendicular to a possibly moving coordinate surface or surface of a cell in a finite-volume computational grid, plus the pressure multiplied by a unit vector perpendicular to that surface. The generalized flux Jacobian matrix is then defined by expressing $d\mathbf{F}_n$ in terms of the expanded $d\mathbf{U}$. Finally, performing calculations guided by the reasoning in the one-dimensional case, one obtains the generalized Roe average for the three-dimensional case.

This work was done by Marcel Vinokur of Sterling Federal Systems, Inc., for **Ames Research Center**. *Further information may be found in NASA CR-177512 [N89-17445], "Flux Jacobian Matrices and Generalized Roe Average for an Equilibrium Real Gas."*

Copies may be purchased [prepayment required] from the National Technical Information Service, Springfield, Virginia 22161, Telephone No. (703) 487-4650. Rush orders may be placed for an extra fee by calling (800) 336-4700.
ARC-12409

Beam Stop for High-Power Lasers

A graphite/aluminum plate absorbs most of the light.

NASA's Jet Propulsion Laboratory, Pasadena, California

A beam stop absorbs most of the radiation in the beam from an excimer or other high-power laser. It can withstand pulsed ultraviolet peak power of greater than 100 MW/cm^2 and continuous power of more than 100 W/cm^2 without damage. Beams of such high powers can burn or shatter ordinary beam stops. The device can be used for a variety of blocking purposes. For example, it can block a laser beam after it has passed through an experimental setup, or at each stage of a setup so stages can be checked and tested in sequence. In such service, the negligible reflectance of the device is a valuable safety feature, inasmuch as it protects both users and equipment from reflections.

The new stop consists of a graphite plate bonded to a finned aluminum heat sink with a thermally conductive silicone compound. A laser beam impinging on the graphite quickly forms a layer of carbon black on it. The layer readily absorbs the light with negligible reflection. The heat generated by the absorbed light energy is quickly removed through the graphite and silicon to the heat sink.

The stop has been used in experiments with ultraviolet laser light at a wavelength of 308 nanometers. It was not damaged even when exposed to beams with peak pulsed power densities greater than 1 GW/cm^2. It is expected to be equally effective at other ultraviolet wavelengths and perhaps at visible and infrared wavelengths as well.

This work was done by Iain S. McDermid and William B. Williamson of Caltech for **NASA's Jet Propulsion Laboratory**. *For further information, Circle 138 on the TSP Request Card.*
NPO-17465

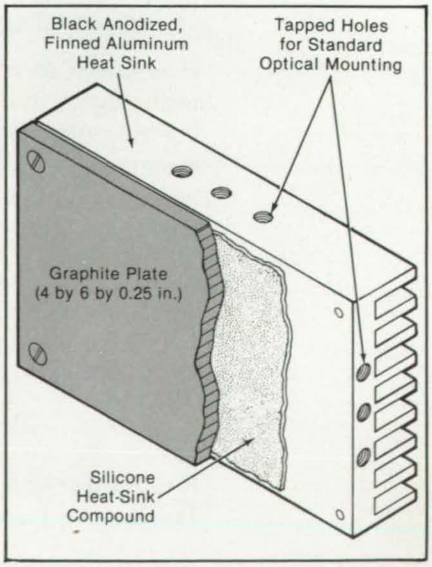

The Beam Stop fits on a standard optical mounting fixture. The graphite plate is thick enough to absorb the incident laser beam but thin enough to transfer heat quickly to the heat sink.

Books and Reports

These reports, studies, handbooks are available from NASA as Technical Support Packages (TSP's) when a Request Card number is cited; otherwise they are available from the National Technical Information Service.

Numerical Methods for Chemically Reacting Flows

Issues related to numerical stability, accuracy, and resolution are discussed.

A technical memorandum presents issues in the numerical solution of hyperbolic conservation laws that contain "stiff" (relatively large and rapidly changing) source terms. Such equations are often used to represent chemically reacting flows. The equations are usually solved by finite-difference numerical methods. The source terms generally necessitate the use of small time and/or space steps to obtain sufficient resolution, especially at discontinuities, where incorrect mathematical modeling can result in unphysical solutions.

The question of numerical stability also arises, but the authors dismiss it summarily on the ground that it can be addressed adequately by the use of implicit numerical methods. The discussion proceeds immediately to the strengths and weaknesses of two approaches to numerical solution, with a view toward obtaining the requisite accuracy and correct placement of discontinuities while using time and space grids that may be relatively coarse. The methods are tested by applying them to the one-dimensional model problem

$$\frac{\partial u}{\partial t}+\frac{\partial u}{\partial x} = \psi(u) = \mu u(u-1)(u-½)$$

where $u(x, t)$ is the dependent variable sought, t is time, x is a spatial coordinate, ψ is the source term, and μ is a parameter that represents the strength of the source term.

The first approach is based on MacCormack's predictor/corrector method — a second-order-accurate method for conservation laws that can be modified to include the source terms, which appear at every space and time step. Stiff source terms are usually handled in a semi-implicit manner to obtain stability with reasonable time steps. To avoid oscillations near discontinuities, MacCormack's method can be modified by the addition of a flux-correction step motivated by the theory of total-variation-diminishing methods. Two different forms of this correction are compared.

The second approach is based on the time-splitting method, in which one alternates between solving the conservation laws (flow only) in one step and solving the stiff differential equations (chemical reactions only; no flow) in the next step. One advantage of this approach is that numerical methods of high quality have already been developed for each subproblem. It is shown that the combination of these numerical methods via time splitting can yield stable, second-order-accurate methods for the solution of the full problem.

Numerical tests on the model problem show that both approaches yield stable, second-order-accurate solutions. However, in the present of shock waves and when the stiff parameter increases, the solutions show such unphysical behavior as reaction waves propagating one mesh cell per time step, regardless of the true speeds. Methods to overcome this deficiency are suggested. These include some form of refinement of meshes, tracking of shocks, and mathematically modeling the integral of ψ by use of subcell resolution.

This work was done by R. J. LeVeque of the University of Washington and H. C. Yee of **Ames Research Center**. *Further information may be found in NASA TM-100075 [N88-18343], "A Study of Numerical Methods for Hyperbolic Conservation Laws with Stiff Source Terms."*

Copies may be purchased [prepayment required] from the National Technical Information Service, Springfield, Virginia 22161, Telephone No. (703) 487-4650. Rush orders may be placed for an extra fee by calling (800) 336-4700.
ARC-12282

Analysis of Used Arc-Jet Electrodes

Whiskers grow out from the cathode toward the anode, eventually causing failure.

A report discusses the conditions of electrodes that were used in an arc-jet engine. The electrodes were examined in the effort to determine the causes of erosion and to develop recommendations for improved electrode designs that would yield longer operating lives.

The arc-jet engine had a coaxial-electrode configuration. The anode and cathode were both made of thoriated tungsten. The anode was the outer electrode, in the form of a plenum chamber, constrictor, and expansion nozzle. The cathode, located on the axis, was a rod with a rounded conical tip that protruded slightly into the upstream orifice of the constrictor section of the outer electrode. The electrodes were insulated from each other by boron nitride spacers equipped with grooves and holes to admit the propellent gas, which was ammonia.

The engine was operated in a vacuum chamber for several intervals that amounted to a total of 573 h, at power levels slightly less than the rated level of 30 kW and with ammonia flowing into the engine at rates of 0.25 to 0.27 g/s. The test was ended when a sudden decrease of voltage and increase of current signaled a failure. The accumulated operating time was sufficient to clearly establish the patterns and causes of erosion.

"Before" and "after" pictures of the tip of the cathode were taken, and both electrodes were sectioned after the engine test to get a better visual indication of erosion patterns. A scanning electron microscope was used to study the effects of the emission of electrons and the consequent pattern of erosion by arcs on the surface of the cathode and to study recrystallization on the hot surface of the anode.

The tip of the cathode was found to be eroded into an almost perfectly hemispherical crater covered with pits caused by microarcs. Whiskers of electrode material had grown radially outward from the rim of the crater. Apparently, the failure that made it necessary to stop the engine test was either a short circuit or a diversion of a large portion of the arc current into a high-current arc, between a whisker and the anode, which was established when one of the whiskers grew close to, or touched, the anode.

The whiskers are believed to grow from tungsten vapor created inside the hemispherical crater and pumped out to the rim by a pressure gradient induced by electromagnetic forces. To diminish the growth of whiskers, it might help to machine a cavity into the tip of the cathode to reduce the amount of vapor available. It has also been suggested that ripple in the arc voltage and current might influence the growth of whiskers and that a ripple-free power supply might reduce such growth.

The downstream portion of the constrictor in the anode was found to be eroded, probably by evaporation at high temperature. To reduce this kind of erosion, one would have to provide better cooling; for example, by increasing the emissivity of the radiation-cooled surface, by cooling regeneratively, and/or by embedding heat pipes in the anode.

This work was done by Thomas J. Pivirotto and William D. Deininger of Caltech for **NASA's Jet Propulsion Laboratory**. *To obtain a copy of the report, "Analysis of Thoriated Tungsten Arcjet Engine Electrodes," Circle 99 on the TSP Request Card.*
NPO-17575

Further Studies of Hot-Wire Anemometry

Measurements of fluctuations of temperature and density are complicated by spurious effects.

A report discusses the factors that affect the readings of a hot-wire anemometer in a turbulent supersonic boundary layer. This represents an extension of the work described in "Hot-Wire Anemometry Versus Laser-Induced Fluorescence" (ARC-11802), *NASA Tech Briefs*, Vol. 13, No. 6, page 60. The report presents a theoretical analysis of the responses of a hot-wire probe to changes in the flow; it also compares measurements by a hot-wire probe with measurements of the same flows by laser-induced fluorescence (LIF). Because LIF provides spatially and temporally resolved data on temperature, density, and pressure, it provides independent means to determine the responses of hot-wire anemometers to these quantities.

The usual objective of hot-wire anemometry is to measure the fluctuations in the speed of flow. In this study, the objective is to measure the amplitudes of fluctuations of static temperature and density. However, hot-wire anemometry is not always adequate for either purpose because a hot wire responds to a combination of speed, density, and total temperature, the total temperature being the temperature at a stagnation point in the flow. While comparisons of hot-wire anemometry with laser Doppler velocimetry can provide partial speed calibrations, they provide no information on responses to fluctuations in density and temperature.

The basic equation of hot-wire anemometry is a linearized expression for the fluctuation in the voltage across a hot wire immersed in a flow:

$$(\Delta E/E) = S_\varrho(\Delta\varrho/\varrho) + S_U(\Delta U/U) + S_T(\Delta T/T)$$

where E = the voltage, ϱ = the density, U = the speed, T = the total temperature, S = the sensitivity to the subscripted quantity, and Δ denotes the fluctuation in the associated quantity. For mach numbers above 1.2 and Reynolds numbers above 20 (based on wire diameter), $S_\varrho \approx S_U = S_m$, where $m = \varrho U$ = mass flux. The theoretical analysis explores the mathematical consequences of these equations under various assumed flow conditions to derive equations for three different calibration methods.

The first two methods are based on the concept of "single high overheat": the wire is operated at such a high temperature that it is sensitive only to mass flux and not to fluctuations of temperature in the flow. In the first method (the centerline method), S_m is determined from measurements that are made at the centerline of a blowdown wind tunnel, where the flow is relatively free of disturbances. The stagnation pressure, and consequently the mass flux (but not the mach number), is varied from run to run. The second method (boundary-layer method), which is less vulnerable to certain calibration errors, involves the determination of S_m from measurements of the boundary-layer flow with mass flow estimated from pitot-static measurements by the standard equations of compressible flow. The third method is more complicated: through measurements at various wire temperatures (multiple overheats) and statistical analysis, it provides for the determination of both S_m and S_T.

The three methods were applied to a mach 2.06 flow of nitrogen in a blowdown wind tunnel and compared with LIF measurements. As a result, the following conclusions were drawn:

- A hot wire obtains the same measurements of amplitudes of fluctuation of mass flux when operated at a single high-overheat ratio or at multiple overheat ratios.
- The boundary-layer and centerline methods give the same measurements of mass flux. In flows where the mean mass flux can be measured consistently, the boundary-layer method minimizes errors.
- If a high overheat is used to measure only fluctuations in mass flux, then the amplitudes of fluctuations of temperature and density cannot be determined accurately.
- If multiple-overheat measurements are taken of the mass flux, the total temperature, and the correlation between them, and if there are no unsteady shocks or other sources of pressure fluctuations, then the amplitudes of fluctuations of temperature and density can be determined accurately.

This work was done by Robert McKenzie of **Ames Research Center** *and Pamela Logan and Daniel Bershader of Stanford University. To obtain a copy of the report, "Accuracy of Hot-Wire Measurements in Supersonic Turbulence From Comparisons With Laser-Induced Fluorescence," Circle 60 on the TSP Request Card.*
ARC-12104

Optimization of Array of Laser Retroreflectors

Adjustments of design parameters reduce mass by almost 10 percent.

A report discusses the analysis and optimization of the design of an array of corner-cube prism retroreflectors for use on the TOPEX satellite. The analysis builds on a methodology developed for array antennas where the far-field pattern-shape requirements dictate the optimum orientation and location of the antenna elements, in this case laser retroreflectors. The array reflects laser pulses emitted from the baseline MOBLAS ground tracking stations back to the stations. The return pulses must produce photoelectron counts in the detector sufficient to enable determination of the height of an orbit at zenith or of the distance to the satellite at elevations above 20° to an accuracy of 5 cm or better, the design goal being 2 cm. A 100-electron signal is required for 2-cm accuracy.

The report reviews the design requirements for the array and describes signal-attenuation effects that must be considered, including laser-pointing error, weather, atmospheric scintillations and scatter, deterioration of the reflectors, manufacturing errors in the dihedral angles of the cubes, the use of weaker lasers, changes in the output powers of lasers during operation, and background noise. A design margin of 7 dB is allocated to allow for these losses. Thus, the basic signal requirement for ranging at satellite elevations between 20° and 30° is raised from 100 to 500 electrons. At elevations from 30° to 75°, the signal requirement is set 10 dB higher (5,000 electrons) to provide higher reliability in ranging. Accurate orbit-height calibration at zenith can be done only once every 10 days as the satellite passes overhead at Bermuda; to provide an additional margin for weather for that critical calibration, the signal requirement has been set an additional 3 dB higher (10,000 electrons) for elevations above 75°.

The performance of the array was evaluated as a function of the angle of orientation of the cube with respect to the nadir, the number of prisms, and the geometrical layout of the array. The report includes graphs of the expected detector photoelectron count vs. zenith angle for various values of these parameters. Also included are graphs of the detector-performance margins at selected pairs of zenith angles, with cube orientation angle as the independent parameter.

The analysis showed that the size and mass of the array could be reduced, while improving performance at low satellite elevations. The number of retroreflector cubes was reduced from 216 to 192; the diameter of the ring of retroreflector cubes, from 78.2 in. (1.99 m) to 70.4 in. (1.79 m); and the mass, from 46.4 to 41.9 kg. The orientation angle of the cubes with respect to the nadir was increased from 33° to 40° to increase the intensity of the return signal at low elevation at the expense of a small reduction at high elevations.

This work was done by Shlomo Dolinsky of Caltech for **NASA's Jet Propulsion Laboratory**. *For further information, Circle 109 on the TSP Request Card.*
NPO-17778

Materials

Hardware, Techniques, and Processes
32 Sintered Fiber Electrodes
32 TAZ-8A Alloy Increases the Thermal Endurance of Steel
34 Heat- and Oxidation-Resistant Electrodes
34 Cheaper Hydride-Forming Cathodes
35 Polyimides Containing Carbonyl and Ether Connecting Groups

Books and Reports
36 Optical Properties of Ceramic Fabrics
36 New Materials and Treatments for Turbopump Bearings
37 Mechanical Properties of SiC/Si_3N_4 Laminates

Sintered Fiber Electrodes

Porosity would be increased without sacrificing strength or conductivity.

NASA's Jet Propulsion Laboratory, Pasadena, California

A method has been proposed to make improved porous electrodes for oxygen pumps, oxygen sensors, high-temperature solid-electrolyte fuel cells, and high-temperature solid-electrolyte electrolysis cells. The electrodes would be made of sintered fibers rather than sintered powder, which is the conventional method.

The relative advantages and disadvantages of the two kinds of materials are illustrated schematically in the figure. Powders consist of roughly spherical particles. When they are sintered, electrical conduction is limited by the numbers and cross-sectional areas of the bonds between them. If the porosity is made high to facilitate the desirable passage of gas, the bonds tend to be fewer and smaller, resulting in low electrical conductivity and strength. If the particles are bonded more tightly into a low-porosity structure, the flow of gas is impeded. In the proposed method, an electrode would be made by sintering a mat of conducting fibers. The many sintered bonds between intersecting fibers would increase electrical conductivity and provide strength, yet allow the mat to remain highly porous.

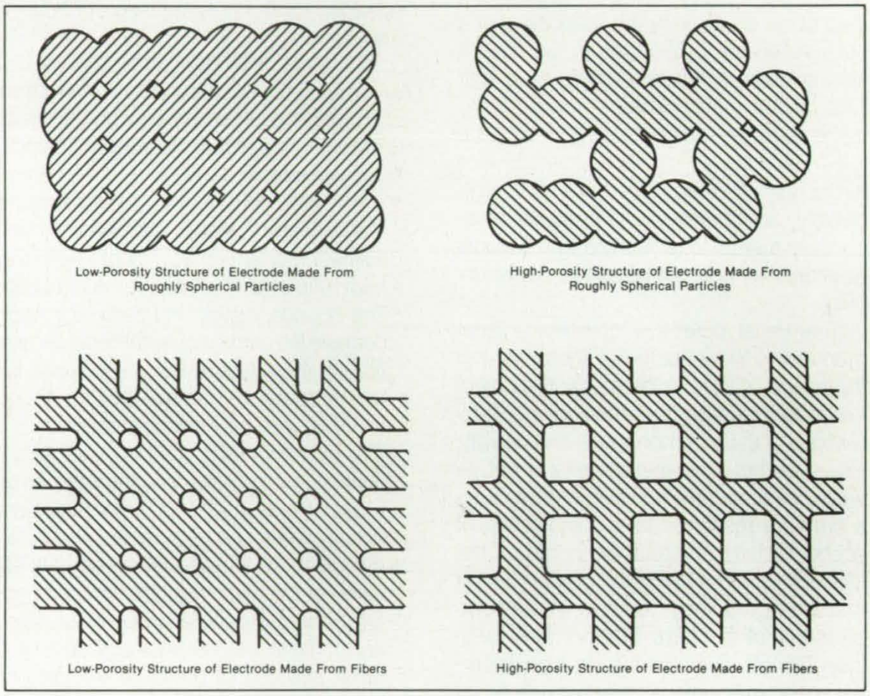

Electrode Structures of Low and High Porosity are conventionally made from roughly spherical particles (above) but would be made from fibers (below) in the proposed method.

Fabrication would begin with the suspension of very-finely-powdered electrode material in a rapidly drying liquid consisting of binder, plasticizer, and solvent. The resulting mixture would be forced through fine nozzles to make fibers, as in making cotton candy from molten sugar.

The fibers could then be pyrolized to drive off the volatiles, leaving pure electrode material behind. The fibers would be broken into short lengths, sized, and incorporated in a ceramic slip that could be tape-cast into thin sheets. Alternatively, the fibers could be added to another binder/plasticizer/solvent liquid and be tape-cast into thin sheets, as is now done with electrode powder. A sandwich would then be made of a tape-cast ceramic electrolyte sheet between two electrode sheets. The sandwich would be pyrolized to form the fibrous-electrode/electrolyte/fibrous-electrode structure.

This work was done by James E. Schroeder of Caltech for **NASA's Jet Propulsion Laboratory**. *For further information, Circle 24 on the TSP Request Card.*

Inquiries concerning rights for the commercial use of this invention should be addressed to the Patent Counsel, NASA Resident Office-JPL [see page 16]. Refer to NPO-17213.

TAZ-8A Alloy Increases the Thermal Endurance of Steel

Surface treatment with this alloy prolongs service life and reduces costs.

Lewis Research Center, Cleveland, Ohio

The use of steel in long-term, cyclic, high-temperature applications is very limited. Iron-based alloys and nickel-based alloys that are most commonly employed do not provide long-term service either. Iron-based alloys are unable to withstand thermal shock when subjected to prolonged rapid cyclical heating and cooling. Nickel-based alloys not only have a similar deficiency but are extremely costly. One way to obtain a metal capable of surviving these severe conditions would be to bond a suitably resistant material securely to the substrate alloy.

The answer lies in high-strength, nickel-based alloy called TAZ-8A. Not only does this material exhibit high strength at temperatures as high as 1,400 °F (760 °C) and resistance to oxidation; it also exhibits excellent cyclic shock resistance between 600 and 2,000 °F (316 and 1,093 °C) and

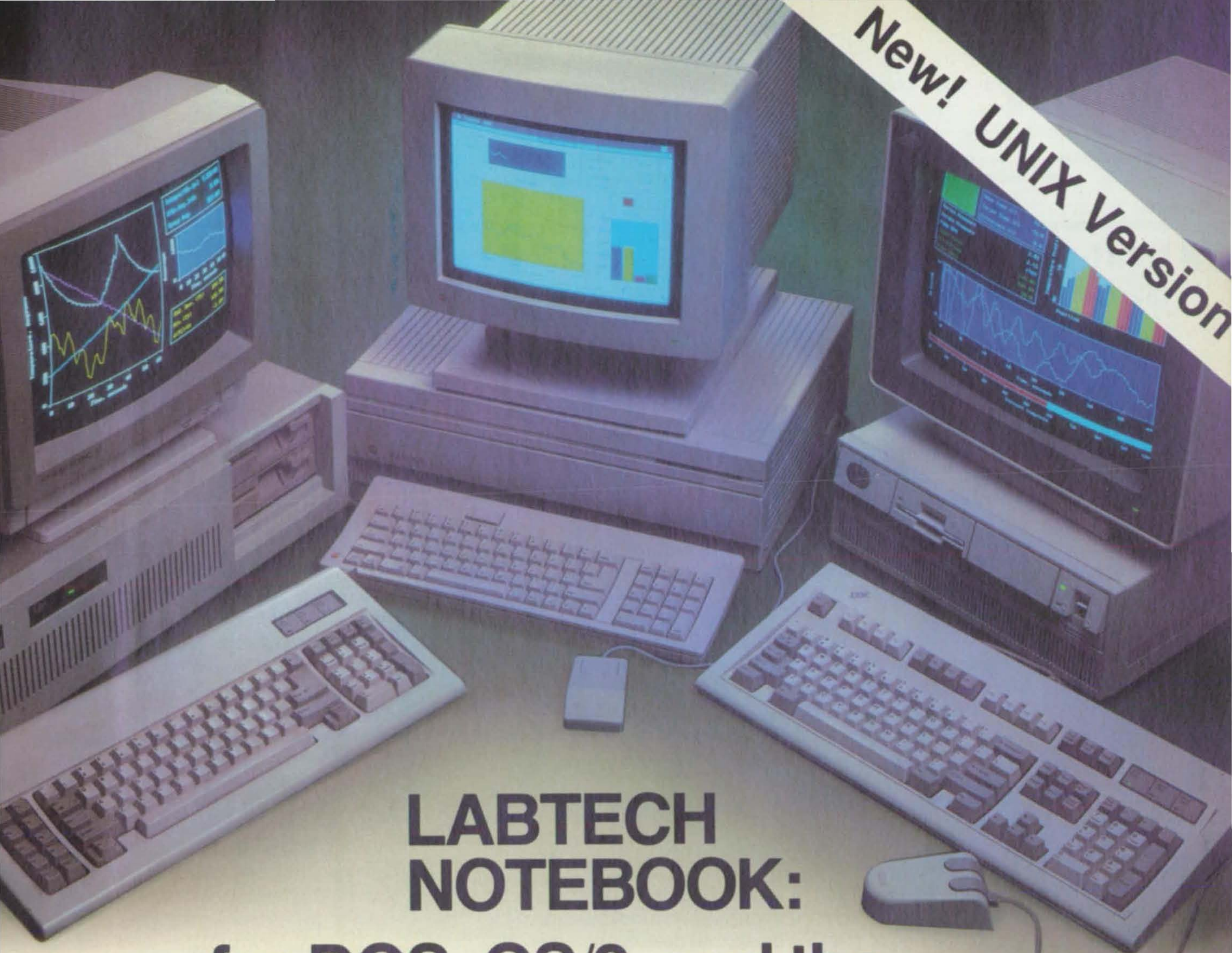

LABTECH NOTEBOOK:

for DOS, OS/2, and the Macintosh

LABTECH NOTEBOOK has been the accepted standard for data acquisition and control software since we introduced NOTEBOOK for MS-DOS. Now, we've taken the next step into the future with NOTEBOOK for OS/2 and the Macintosh.

LABTECH NOTEBOOK now gives you a choice of platforms — The IBM® PC/XT/AT, PS/2, compatibles, and the Apple® Macintosh. Setups and configurations are compatible — configure your system on one platform and run the same setup on another.

LABTECH NOTEBOOK collects data from multiple channels, displays the data graphically and stores it to disk in real-time. It features user defined acquisition, control and display setups; real-time mathematical, statistical and signal processing; sophisticated triggering; data replay; and continuous data collection while you work in other programs. Many input types, including analog, digital, thermocouple, RTD, strain and pressure gages, resistance, counters and frequency, are supported by NOTEBOOK.

The DOS version supports foreground/background operation and, as an option, expanded memory. The OS/2 version takes advantage of OS/2's multitasking capability and protected memory support. NOTEBOOK for the Macintosh works under Multifinder and follows the Macintosh menu and icon conventions.

LABTECH NOTEBOOK, with an installed base of 10,000 systems, supports hundreds of board-level data acquisition interfaces and distributed I/O systems from more than 30 manufacturers. NOTEBOOK can be found in most Fortune 500 companies, as well as in smaller enterprises.

New improved GPIB support

LABTECH

Laboratory Technologies Corporation • 400 Research Drive • Wilmington, MA 01887 • 508-657-5400 • FAX 508-658-9972

Circle Reader Action No. 423

superplasticity at 1,800 °F (982 °C).

TAZ-8A can be converted into a fine powder and then flame-, plasma-, arc-, or wire-sprayed onto inexpensive steel substrate. The use of the TAZ-8A material as an overlay on the steel will impart the necessary thermal endurance and significantly reduce the cost of manufacture of such an item.

This work was done by William J. Waters of **Lewis Research Center**. *No further documentation is available.*

Inquiries concerning rights for the commercial use of this invention should be addressed to the Patent Counsel, Lewis Research Center [see page 16]. Refer to LEW-14280.

Heat- and Oxidation-Resistant Electrodes

Thin layers of electrically conductive ceramic help Fe_3Al and Ni_3Al alloys survive.

NASA's Jet Propulsion Laboratory, Pasadena, California

Alloys coated with electrically conductive ceramics can be used to make strong, oxidation-resistant electrodes for electrochemical cells operating at temperatures of 1,000 to 1,300 °C. In particular, Fe_3Al or Ni_3Al coated with strontium-doped lanthanum manganite ($La_{0.8}Sr_{0.2}{\bullet}MnO_3$) is more resistant to chemical attack than an all-metal electrode, less brittle than an all-ceramic electrode, and less costly than either alternative.

First, the nonconductive aluminum oxide that forms spontaneously on the surface of the alloy is removed chemically. A film of an inert metal like platinum can be applied to the alloy to prevent reoxidation. The coat can be applied to the alloy as a powder or liquid suspension of the ceramic. The coated alloy is then sintered at 1,000 to 1,300 °C to form the hard, impermeable, conductive coat.

The coat can also be applied in precursor form. Water-soluble compounds of lanthanum, strontium, and manganese are mixed in water with citrate ions and ethylene glycol, then heated until the mixture polymerizes. The resulting gel is dried and applied to the alloy, either directly or suspended in a suitable liquid vehicle. Baking converts the precursor to ceramic. Whether applied directly or as a precursor, the ceramic coat has a thickness of about 0.001 in. (0.025 mm).

This work was done by James E. Schroeder of Caltech for **NASA's Jet Propulsion Laboratory**. *For further information, Circle 22 on the TSP Request Card.*

Inquiries concerning rights for the commercial use of this invention should be addressed to the Patent Counsel, NASA Resident Office-JPL [see page 16]. Refer to NPO-17156.

Cheaper Hydride-Forming Cathodes

Plated titanium or other powder might replace scarce solid palladium.

NASA's Jet Propulsion Laboratory, Pasadena, California

Hydride-forming cathodes for electrochemical experiments might be made out of materials or combinations of materials that are cheaper and more abundant than pure palladium, according to a proposal. Although the concept of the new cathodes was prompted by the needs of experimenters in the now-discredited concept of electrochemical nuclear fusion, the cathodes may also be useful in other electrochemical applications involving the generation or storage of hydrogen, deuterium, or tritium.

The palladium cathodes that are to be replaced form interstitial hydrides (Pd_2H, Pd_2D, or Pd_2T) under appropriate electrochemical conditions. In general, such a hydride reverts to metallic Pd when the electrochemical cell is run in reverse. Palladium resists attack by typical electrolytes, but it is costly and the supply is very limited.

The new cathode could be made of titanium powder plated with palladium and pressed between conductive end plates in a nonconductive housing. The thin coat of palladium would protect the titanium from the electrolyte but would allow the isotope of hydrogen in question to pass through to the underlying particle, where the hydride would be formed. The plating of a powder cathode would require far less palladium than does a solid cathode.

Most hydride compounds break down into small particles during repeated electrochemical charge/discharge cycles. The breakdown does not continue indefinitely, however. The size of the particles stabilizes at a few micrometers after about 5,000 cycles. Therefore, the cathode material would be subjected to at least that number of cycles before being plated.

Other candidate cathode materials include Zr, Mg_2Ni, ZrNi, and possibly $LaNi_5$. Like Ti, these materials react readily with hydrogen and form powders that can be expected to stabilize after about 5,000 reaction cycles (see figure). They are also attacked by electrolytes and would, therefore, have to be similarly plated and packaged.

This work was done by Jack A. Jones and Gary Blue of Caltech for **NASA's Jet Propulsion Laboratory**. *For further information, Circle 54 on the TSP Request Card.* *NPO-17927*

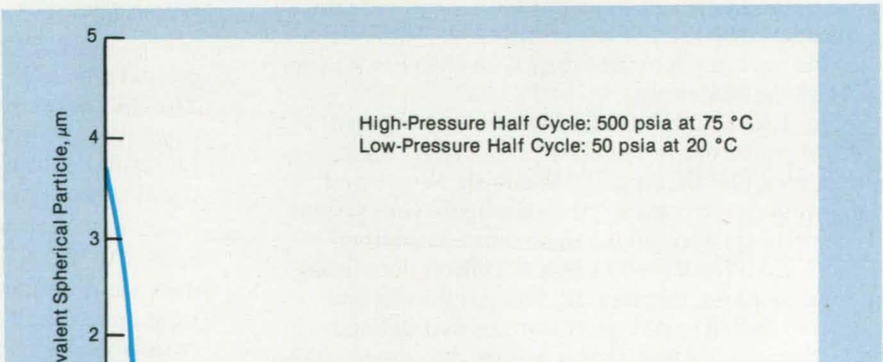

Decrepitation of $LaNi_5$ Stops after about 5,000 cycles of hydrogenation and dehydrogenation.

Polyimides Containing Carbonyl and Ether Connecting Groups

The introduction of crystallinity increases moduli of elasticity and resistances to solvents.

Langley Research Center, Hampton, Virginia

Polyimides of a new class are made from the chemical reactions of aromatic dianhydrides with novel aromatic diamines in which carbonyl and ether groups connect the aromatic rings. The new polyimides are melt-processable, strong, resistant to impacts, and resistant to solvents and other chemicals. These polymers are useful as adhesives, coatings, films, membranes, and composite matrices.

It has long been known that the introduction of some crystallinity into a polymer can increase its tensile strength and its resistance to solvents. If, in addition, the crystallinity is of the proper type and degree, the polymer can also exhibit extremely high toughness. The carbonyl and ether connecting groups between aromatic rings allow portions of the molecule to order or crystallize. The ratio of the number of carbonyl linkages to the number of ether linkages is critical in determining the properties that make these polymers thermally processable.

The carbonyl and ether linkages could be incorporated into either the dianhydride or the diamine portions of the repeating polymer units. Experience has shown that the modifications of the diamine portions are easier because they involve fewer steps than do the synthesis of the new dianhydrides. Novel diamines that contain various ratios of numbers of carbonyl groups to numbers of ether groups can be synthesized by the general sequence of reactions illustrated in figure 1 or by catalytic hydrogenation of the corresponding dinitro compounds.

Figure 2 illustrates the synthesis of a polyimide of the new type. As in the synthesis of a conventional polyimide, the aromatic dianhydride and the diamine react to form an intermediate polyamide acid. The intermediate product is cyclodehydrated, either chemically or by heating to a temperature above 150 °C. In the manufacture of a composite or laminate, the polyamide acid can be applied to the fibers while it is still dissolved in the reaction solvent. Thus, the fibers can be thoroughly wetted before thermal cyclodehydration forms the insoluble polyimide.

Mechanical properties of the polyimides are highly dependent upon the diamine structure. For example, the polyimide from 3,3′,4,4′-benzophenonetetracarboxylic dianhydride and bis(4-aminophenoxy-4′-phenyl) phenyl phosphine oxide formed a tough amorphous film that had a glass transition temperature of 258 °C. Tensile strength, tensile modulus, and elongation at break of this polyimide were determined to be 14,600 psi (101 MPa), 453,000 psi (3,126 MPa), and 6.1 percent, respectively, at 25 °C. The polyimide from 3,3′,4,4′-benzophenonetetracarboxylic dianhydride and 1,6-bis(4-aminophenoxy-4′-benzoyl) hexane formed a brittle semicrystalline film that had a glass transition temperature of 172 °C and a crystalline melt transition at 332 °C. This material was readily compression molded at 380 °C under 1,000 psi (6.9 MPa) to give a molding that was not affected by solvents and strong bases, such as 30 percent sodium hydroxide solution.

This work was done by Paul M. Hergenrother of **Langley Research Center** *and Stephen J. Havens of Planning Research Corp. For further information, Circle 157 on the TSP Request Card.*
LAR-14001

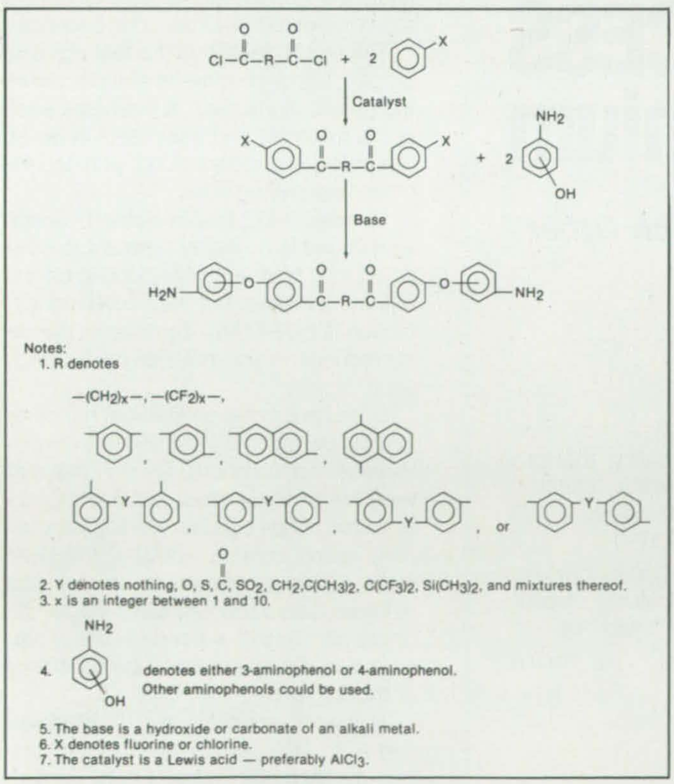

Figure 1. A **Variety of Diamines Containing Carbonyl and Ether Linkages** between aromatic rings can be synthesized readily from commercially available materials.

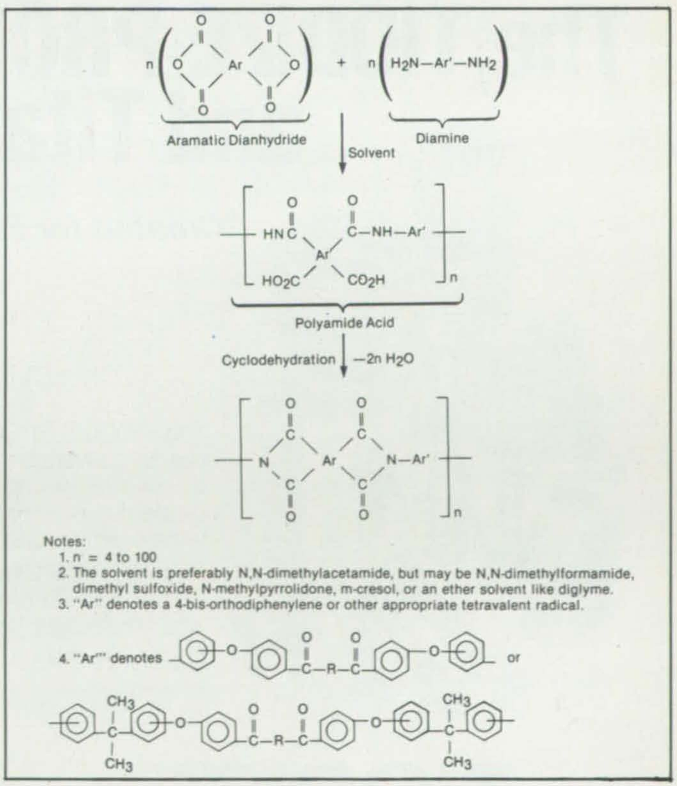

Figure 2. **Polyimides Containing Carbonyl and Ether Linkages** are synthesized from aromatic dianhydrides and novel diamines that incorporate these linkages.

Books and Reports

These reports, studies, handbooks are available from NASA as Technical Support Packages (TSP's) when a Request Card number is cited; otherwise they are available from the National Technical Information Service.

Optical Properties of Ceramic Fabrics

Theory and measurements of reflectance and transmittance are presented.

A report discusses the optical properties of ceramic fabrics woven from silica, aluminoborosilicate, and silicon carbide yarns. Directional hemispheric reflectance and transmittance data are given for several different weave patterns, yarn constructions, and fabric weights. Measurements were made over the spectral range from 250 to 2,500 nm.

The section weights of the fabrics, which ranged from about 100 to 700 g/m^2, had the greatest effect on the optical properties, regardless of the material. The weave patterns also affected optical properties, although to a lesser extent.

The reflectances of silica and aluminoborosilicate fabrics increase with increasing weight per unit area over the wavelength range, but the reflectance of silicon carbide fabric decreases with increasing weight per unit area for wavelengths greater than about 500 nm. The reflectances of silica and aluminoborosilicate fabric are greater than that of black silicon carbide by a factor of 10. The absorptance of the silica fabric as well as of the aluminoborosilicate fabric increases rapidly with decreasing wavelength below 500 nm; values for the heaviest aluminoborosilicate fabrics tested approach 0.9 at 250 nm.

The lighter-weight, more-loosely-woven fabrics have spaces between yarns that allow some radiation to pass through without being scattered or refracted. However, this "see-through" component of transmittance is only 0.08 or less. Interestingly, the heaviest fabrics, even through they have no transmittance in the normal direction, have increased transmission because of between-yarn open areas that appear at off-normal angles about the warp direction. The transmission increases to a maximum at an angle of 65° but drops rapidly at larger angles.

A two-flux model for radiation transfer was used to derive spectral hemispherical bulk absorption and scattering coefficients from the silica and aluminoborosilicate data. The coefficients, the report notes, compare well with available data at visible wavelengths for a polycrystalline ceramic.

This work was done by M. A. Covington and P. M. Sawko of **Ames Research Center**. *To obtain a copy of the report, "Optical Properties of Woven Ceramic Fabrics for Flexible Heat Shields," Circle 102 on the TSP Request Card.*

Inquiries concerning rights for the commercial use of this invention should be addressed to the Patent Counsel, Ames Research Center [see page 16]. Refer to ARC-11739.

New Materials and Treatments for Turbopump Bearings

Tests of friction and durability are documented and evaluated.

A report evaluates materials and surface treatments for bearings for liquid-oxygen turbopumps. Key properties sought for this application are low friction, low wear, and resistance to corrosion and rolling-contact fatigue. The evaluation is based on tests of specimens in a traction rig and a rolling-contact rig. This equipment simulated the normal stress and tangential strain expected in turbopump bearings.

The report describes the test rigs and preparation of specimens and discusses the results of the tests. It evaluates each of the materials and treatments in detail, illustrating the conclusions with tables, plots, and photographs.

Standard 440C stainless-steel bearings were found to be highly resistant to wear when they have an oxide coating on the bearing surfaces, but their coefficient of friction is high (0.55). Removal of the oxide reduces friction, but then the bearings wear rapidly.

Such hard coats as titanium nitride or thin, dense chrome (Armoloy) and ceramic-metal combinations greatly reduced wear but had little effect on friction. Coats of silicon nitride on stainless steel and on thin, dense chrome exhibited the least wear. Silicon nitride coats on stainless steel increased rolling-contact fatigue life under pure rolling. A bonded coat of molybdenum disulfide reduced the coefficient of friction to less than 0.15.

This work was done by L. D. Wedeven and N. C. Miller of Wedeven Associates, Inc., for **Marshall Space Flight Center**. *To obtain a copy of the report, "Development of New Materials for Turbopump Bearings — Phase II," Circle 120 on the TSP Request Card.*
MFS-27238

Mechanical Properties of SiC/Si_3N_4 Laminates

Specimens are evaluated at ambient and high temperatures.

Two reports describe tests to determine the mechanical properties of laminates made of reaction-bonded silicon nitride matrices reinforced with 30 volume percent of aligned silicon carbide fibers. The two reports emphasize different aspects of the topic. One focuses on behavior related to strength at ambient temperature; the other focuses on the strength after exposure to high temperatures.

The room-temperature study involved three types of unidirectional laminates, one type of cross-plied laminate, and an angle-plied laminate. The objectives of this study were the following:

- To determine the effects of the orientations of the fibers, of the gauge (unsupported) lengths of the specimens, and of machined notches on mechanical properties;
- To study the deformation and fracture behavior of the various types of laminates; and
- To determine the applicability of constitutive equations and the theory of laminates for the prediction of the elastic properties of these composite materials.

The results for the unidirectional laminates tested at various angles to the direction of reinforcement indicate large anisotropy in in-plane properties. The strength properties along the fibers were independent of gauge length and unaffected by notches perpendicular to the fibers. Splitting parallel to the fibers at the tips of the notches appears to be the dominant crack-blunting mechanism responsible for the insensitivity to notches. The results of tests of the cross- and angle-ply laminates showed that their matrix-failure strains were similar to those of the unidirectional laminates loaded along the fibers, but their primary elastic moduli, matrix-cracking strengths, and ultimate composite strengths were lower. The results for all three types of laminates show that their elastic properties can be predicted from modified constitutive equations and the theory of laminates.

The high-temperature study involved only unidirectional laminates. The major issue in this study was whether the metallike stress-versus-strain behavior and excellent properties of the laminates as fabricated could survive exposure to environmental and thermal conditions similar to those of high-performance engines. The high-temperature strengths of specimens were measured after 15 min of exposure in air at temperatures up to 1,400 °C. Specimens were also tested at room temperature after a thermal shock treatment that consisted of heating for 15 min at temperatures up to 1,200 °C followed by quenching in water at 25 °C.

The results indicate no significant loss in strength at high temperature and no loss in matrix-fracture strength after quenching. However, some ultimate flexural strength was lost after quenching from temperatures above 600 °C. Overall, the results indicate that SiC-reinforced Si_3N_4 composites have superior properties, which, when coupled with their low densities, make them candidates for use at high temperatures; for example, as components of heat engines.

This work was done by R. T. Bhatt of the U.S. Army Aviation Research and Technology Activity (AVSCOM) and R. E. Philips of Sverdrup Technology, Inc., for **Lewis Research Center**. *Further information may be found in*

NASA TM-101350 [N89-10952], "Laminate Behavior for SiC Fiber-Reinforced Reaction-Bonded Silicon Nitride Matrix Composites" and

NASA TM-101348 [N89-10134] "Thermal Effects on the Mechanical Properties of SiC Fiber Reinforced Reaction Bonded Silicon Nitride Matrix (SiC/RBSN) Composites."

Copies may be purchased [prepayment required] from the National Technical Information Service, Springfield, Virginia 22161, Telephone No. (703) 487-4650. Rush orders may be placed for an extra fee by calling (800) 336-4700.

LEW-14896

Circle Reader Action No. 320

Computer Programs

38 Analyzing Distributed Processing for Electric Utilities
38 Local-Area-Network Simulator
38 Software for Three-Dimensional Space-Shuttle Imagery
39 Data-Management Software for PiFEx
40 Software for Least-Squares and Robust Estimation
41 Design-Tradeoff Model for Space Station
42 An Ada Linear-Algebra Software Package Modeled After HAL/S
44 CYBER-205 Devectorizer

COSMIC: Transferring NASA Software

COSMIC, NASA's Computer Software Management and information Center, distributes software developed with NASA funding to industry, other government agencies and academia.

COSMIC's inventory is updated regularly; new programs are reported in *Tech Briefs*. For additional information on any of the programs described here, circle the appropriate TSP number.

If you don't find a program in this issue that meets your needs, call COSMIC directly for a free review of programs in your area of interest. You can also purchase the annual *COSMIC Software Catalog*, containing descriptions and ordering information for available software.

COSMIC is part of NASA's Technology Utilization Network

COSMIC® — *John A. Gibson, Director,*
(404) 542-3265
The University of Georgia, 382 East Broad Street, Athens, Georgia 30602

Computer Programs

These programs may be obtained at a very reasonable cost from COSMIC, a facility sponsored by NASA to make computer programs available to the public. For information on program price, size, and availability, circle the reference number on the TSP and COSMIC Request Card in this issue.

Electronic Systems

Analyzing Distributed Processing for Electric Utilities

A quantitative assessment model helps to determine tradeoffs between communication and computation.

The Distributed Processing Trade-off Model for Electric Utility Operation computer program is based upon a study performed at the California Institute of Technology for NASA's Jet Propulsion Laboratory. This study presented a technique that addresses the question of tradeoffs between expanding a communications network or expanding the capacity of distributed computers in the energy-management system (EMS) of an electric utility. The technique resulted in the development of a quantitative assessment mathematical model that is presented in a Lotus 1-2-3 worksheet environment. The model gives EMS planners a macroscopic tool for the evaluation of architectures of distributed-processing systems and the major technical and economic tradeoffs as well as interactions within systems.

The inputs to the model (which may be varied according to application and need) include geographic parameters, data-flow and -processing workload parameters, operator-staffing parameters, and technology/economic parameters. The outputs of the model are total costs in various categories, a number of intermediate cost and technical calculation results, and graphical presentation of costs vs. percent distribution for various parameters.

The model has been implemented on an IBM personal computer using the LOTUS 1-2-3 spreadsheet software and was developed in 1986. Also included with the spreadsheet model are a number of representative but hypothetical examples of utilities.

This program was written by Stanley A. Klein, Harold Kirkham, and Julie A. Beardmore of Caltech for **NASA's Jet Propulsion Laboratory**. *For further information, Circle 13 on the TSP Request Card. NPO-17710*

Local-Area-Network Simulator

This program provides simulations for use in analysis and design.

The Local Area Network Extensible Simulator (LANES) computer program provides a method for simulating the performance of high-speed local-area-network (LAN) technology. LANES was developed as a design and analysis software tool for networking computers on board the proposed Space Station. The load, network, link, and physical layers of a layered network architecture are all modeled. LANES mathematically models according to different lower-layer protocols: the Fiber Distributed Data Interface (FDDI) and the Star*Bus. The load and network layers are included in the mathematical model as a means of introducing upper-layer processing delays associated with the transmission of messages; they do not model any particular protocols.

FDDI is an American National Standard and an International Organization for Standardization (ISO) draft standard for a 100 megabit-per-second fiber-optic token ring. Specifications for the LANES model of FDDI are taken from the Draft Proposed American National Standard FDDI Token Ring Media Access Control (MAC), document number X3T9.5/83-16 Rev. 10, February 28, 1986. This is a mature document describing the FDDI media-access-control protocol. Star*Bus, also known as the Fiber Optic Demonstration System, is a protocol for a 100 megabit-per-second fiber-optic star-topology LAN. This protocol, along with a hardware prototype, was developed by Sperry Corporation under contract to NASA Goddard Space Flight Center as a candidate LAN protocol for the Space Station.

LANES can be used to analyze the performance of a networking computing system based on either FDDI or Star*Bus under a variety of loading conditions. Delays due to upper-layer processing can easily be nullified, enabling analysis of FDDI or Star*Bus as stand-alone protocols. LANES performs a parameter-driven simulation; it provides considerable flexibility in specifying both protocol and run-time parameters. Code has been optimized for fast execution, and detailed tracing facilities have been included.

LANES was written in FORTRAN 77 for implementation on a DEC VAX computer under VMS 4.6. It consists of two programs: a simulation program and a user-interface program. The simulation program requires the SLAM II simulation library from Pritsker and Associates, W. Lafayette IN; the user interface is implemented by use of the Ingres data base manager from Relational Technology, Inc. Information about running the simulation program without the user-interface program is contained in the documentation. The memory requirement is 129,024 bytes. LANES was developed in 1988.

This program was developed by Jim Gibson, Joe Jordan, and Terry Grant of **Ames Research Center**. *For further information, Circle 163 on the TSP Request Card. ARC-12168*

Software for Three-Dimensional Space-Shuttle Imagery

The display can show almost any desired perspective.

The Flight Dynamics/Space Transportation System Three-Dimensional Monitor System (3-D Mon) is a real-time graphical mission-monitoring software tool developed and used by the Flight Dynamics Division of NASA/Goddard Space Flight Center. The main objective of 3-D Mon is to compute and display a realistic three-dimensional solid model image of the Space Shuttle, its remote-manipulator system, its payload, and its surroundings from real-time Space Shuttle telemetry data (received at intervals of 2 to 10 seconds). The ability to support spacecraft other than the Space Shuttle has also been incorporated.

Along with generation of images in nearly real time, the system provides for interaction with the user to enable the user to change the viewpoint to anywhere in the universe, to query an object for information, or to toggle the image of a celestial object or spacecraft (e.g., the Moon, Earth, and other satellites) on and off. A user can also review a given scenario in a playback mode in which the image/record update rate is controlled interactively.

The 3-D Mon is part of a distributed-processing software system, because of its reliance on externally provided, real-time data. Telemetry data are received and processed on a National Advanced Systems (NAS) 8063 mainframe computer. The processed data are then transmitted over an asynchronous 2,400-baud serial communications line to a Silicon Graphics IRIS 4D/60T graphics workstation running the 3-D Mon software. The 3-D Mon then converts the processed data into three-dimensional images on the IRIS high-resolution graphics monitor.

The NAS-computer section of this distributed-processing software system is specific to the hardware, software, and telemetry streams available in the Flight Dynamics Facility. Therefore, only the 3-D Mon IRIS workstation portion of the software system is available from COSMIC. However, the stand-alone system test version of the IRIS software has been included along with a system test data file that simulates the distributed-processing environment.

Developed over four years beginning in 1985, the software is written in the C programming language specifically for the graphics environment provided by the Silicon Graphics IRIS 4D/60 Turbo workstation running the UNIX-based IRIX 3.147 operating system.

This program was written by Ernest J. Pittarelli, Michele Langrehr, Glenn Tamkin, Gary Hunt, Robert Durbeck, and David Green of Computer Sciences Corp., and James Jeletic of **Goddard Space Flight Center.** *For further information, Circle 118 on the TSP Request Card. GSC-13246*

Data-Management Software for PiFEx

This UNIX-based software processes data from a mobile/satellite signal-propagation experiment.

The UNIX Based Data Management System is a collection of computer programs for use in the Pilot Field Experiment (PiFEx), which is an attempt to mimic the mobile/satellite-communications (MSAT) scenario. The major purposes of PiFEx are to define the mobile-communications channels and test the workability of new concepts used to design various components of the receiver system. The results of the PiFEx experiment are large amounts of raw data that must be retrieved according to a researcher's needs. This software system is intended to manage the PiFEx data in an interactive way. The system not only handles files as necessary to retrieve the desired data but also provides several FORTRAN programs to generate some standard results that pertain to data on the propagation of signals. This package is based on the assumption that the file of the data initially generated in the experiment has already been converted from binary to ASCII format.

The data-management system consists of programs divided into two categories: those programs that handle the files generated by the PiFEx and those that are used for "number-crunching" of these files. Five FORTRAN programs and one UNIX shell script file are used to manipulate the files. These manipulations include calibration of the acquired data and parsing of the large data file into sets of data concerned with different aspects of the experiment; for example, the specific calibrated propagation data, dynamic- and static-loop-error data, statistical data, and temperature and spatial data on the equipment used in the experiment.

The five remaining FORTRAN programs generate usable information about the data. Signal-level probabilities, probability densities of signals fitting the Rician density function, frequencies of data fades of various durations, and Fourier transforms of the data can all be generated from these data-manipulation programs. In addition, one program generates a downloadable file from the signal-levels and signal-phases files for use with the plotting routine AKPLOT (NPO-16931).

All programs in this software package are written in either FORTRAN-77 or UNIX shell-scripts. The package does not include test data. The programs were developed in 1987 for use with a UNIX operating system on a DEC MicroVAX computer.

This program was written by Anil V. Kantak of Caltech for **NASA's Jet Propulsion Laboratory**. *For further information, Circle 142 on the TSP Request Card.*
NPO-17463

Mathematics and Information Sciences

Software for Least-Squares and Robust Estimation

The GAUSSFIT language is easy to use.

The GAUSSFIT computer program includes a full-featured programming language that facilitates the creation of mathematical models that solve least-squares and robust-estimation problems. The programming language is especially designed to make it easy to specify complex reduction models. The GAUSSFIT language provides an easy and natural way to formulate: (1) problems in nonlinear estimation and problems in which an equation of condition can contain more than one observation, (2) problems with correlated observations, (3) problems involving exact constraints among the parameters, and (4) problems in which the mathematical models can be expressed only algorithmically and not in closed form.

GAUSSFIT consists of a number of parts. The compiler takes the user's model, written in the GAUSSFIT programming language, and converts it into an assembly-language program for an abstract computer whereby the program is then interpreted. The data obtained from the user's data and parameter files form the equations of condition and constraint. (The Marquard-Levenburg method of nonlinear estimation of parameters is implemented.) The interpreter relies on a built-in algebraic manipulator to calculate the value of every arithmetic operation as well as the required derivative information. The resulting matrix is sent to the solution algorithm, which has been chosen by the user.

For the least-squares estimation, the algorithm is a Householder orthogonal-transformation method; for median-type estimators, it is based on the Barrodale and Roberts implementation of the Simplex algorithm; and for other robust methods, Householder transformations are used together with either Newton's method or the method of iteratively-reweighted least squares. The data files are then updated to reflect the results of the calculation, and the process is iterated until some iteration criterion has been satisfied.

GAUSSFIT was written in 100 percent C language and requires 143k bytes of memory. The present version runs under Berkeley UNIX v.4.3, on Digital VAX computers under

VMS, on Intel and Hewlett-Packard, and on The Apple Macintosh Plus and Macintosh II computers. GAUSSFIT was developed in April of 1989.

This program was written by William H. Jeffreys, Michael J. Fitzpatrick, Barbara E. McArthur, and James McCartney of University of Texas for **Marshall Space Flight Center**. *For further information, Circle 70 on the TSP Request Card.*
MFS-26108

Design-Tradeoff Model for Space Station

This program helps to enforce consistency of design objectives throughout the system.

Although extensive knowledge of the design of space stations exists, the information is widely dispersed. The Space Station Freedom Program needs policies and procedures that ensure the use of consistent design objectives throughout its organizational hierarchy. The System Design Tradeoff Model (SDTM) computer program produces information that can be used for this purpose. SDTM is a mathematical model of a set of possible designs for Space Station Freedom.

By use of the SDTM program, one can find the particular design that enables the station to provide specified amounts of resources to users at the lowest total (or life-cycle) cost. One can also compare alternative design concepts by changing the set of possible designs, while holding the specified services to the users constant, and then comparing costs. Finally, both costs and services can be varied simultaneously when comparing different designs.

SDTM selects its solution from a set of feasible designs. Feasibility constraints include safety considerations, minimum levels of resources required for station users, budget allocation requirements, time limitations, and Congressional mandates. The total, or life-cycle, cost includes all of the U.S. costs of the station: design and development, purchase of hardware and software, assembly, and operations throughout its lifetime.

The SDTM development team has identified, for a variety of possible space-station designs, the subsystems that produce the resources to be modeled. The team has also developed formulas for the cross-consumption of resources by other resources, as functions of the amounts of resources produced. SDTM can find the values of station resources, so that designers of subsystems can choose new design concepts that further reduce the life-cycle cost of the station.

The fundamental input to SDTM is a set of formulas that describe the subsystems that constitute a reference design. Most of the formulas identify how the resources required by each subsystem depend upon the size of the subsystem. Some of the formulas describe how the costs of subsystems depend on their sizes. The formulas can be complicated and nonlinear (if nonlinearity is needed to describe how designs change with size). The outputs of SDTM are amounts of resources, life-cycle costs, and marginal costs.

SDTM 1.1 runs on IBM XT and AT personal computers and on computers that are 100 percent compatible with them. It requires 640K of random-access memory and at least 3 Mb of fixed-disk storage. A printer that can print in 132-column mode is also required, and a mathematics coprocessor chip is highly recommended. This code is written in Turbo C 2.0. However, since the developers used a modified version of the proprietary Vitamin C source-code library, the complete source code is not available. The executable code is provided, along with all nonproprietary source code. This program was released in 1989.

This program was written by Robert G. Chamberlain, Jeffrey L. Smith, Chester S. Borden, Govind K. Deshpande, George Fox, William H. Duquette, Larry A. DiLullo, Larry Seeley, and Robert Shishko of Caltech for **NASA's Jet Propulsion Laboratory**. *For further information, Circle 139 on the TSP Request Card.* NPO-17878

An Ada Linear-Algebra Software Package Modeled After HAL/S

New avionics software can be written more easily.

This software package extends the Ada programming language to include linear-algebra capabilities similar to those of the HAL/S programming language. The package is designed for such avionics applications as Space Station flight software. In addition to the built-in functions of HAL/S, the package incorporates the quaternion functions used in the Space Shuttle and Galileo projects and routines from LINPAK that solve systems of equations that involve general square matrices. Language conventions in this package follow those of HAL/S to the maximum extent practical and minimize the effort required for writing new avionics software and translating existent software into Ada.

Valid numeric types in this package include scalar, vector, matrix, and quaternion declarations. (Quaternions are four-component vectors used in representing motion between two coordinate frames.) Single-precision and double-precision floating-point arithmetic is available in addition to the standard double-precision integer manipulation. Infix operators are used instead of function calls to define dot products, cross products, quaternion products, and mixed scalar•vector, scalar•matrix, and vector•matrix products. The package contains two generic programs: one for floating-point computations and one for integer computations. The actual component type is passed as a formal parameter to the generic linear-algebra package. The procedures for solving systems of linear equations defined by general matrices include GEFA, GECO, GESL, and GIDI. The HAL/S functions include ABVAL, UNIT, TRACE, DET, INVERSE, TRANSPOSE, GET, PUT, FETCH, PLACE, and IDENTITY.

The source code is available as ASCII text files on two 360K, 5.25-in. (13.3-cm) floppy disks written on an IBM/AT personal computer running under PC DOS, v. 3.1. The size of the largest file is 74,141 bytes. The software was developed using VAX Ada, v. 1.5 under DEC VMS, v. 4.5. It uses nothing outside the Ada language except a square-root function for floating-point scalars (such as SQRT in the DEC VAX MATHLIB software package). It should be portable to any validated Ada compiler, and it should be executable either interactively or in batch. The software was developed in 1989.

This program was written by Allan R. Klumpp and Charles L. Lawson of Caltech for **NASA's Jet Propulsion Laboratory**. *For further information, Circle 143 on the TSP Request Card.*
NPO-17985

All the features of HP BASIC, and more.

For less.

HTBasic	BASIC FEATURES:	HP BASIC
YES	IEEE-488 GPIB (HP-IB), RS-232 Instrument Control	YES
YES	Integrated Environment: Mouse, Editor, Debugger, Calculator	YES
YES	Supports 16 Megabytes of Memory (breaks DOS 640K barrier)	YES
YES	Engineering Math: Matrix Math, Complex Numbers	YES
YES	High Level Graphics: Screen, Plotter, Printer	YES
YES	Structured Programming with Independent Subprograms	YES
YES	Runs on Industry Standard Personal Computers	NO*
YES	Industry Standard Graphic Printer Support: Epson, IBM, lasers, etc.	NO
YES	Industry Standard Network Support: Novell, IBM, Microsoft, NFS, etc.	NO
YES	Industry Standard IEEE-488 Support: National Instruments, IOtech, etc.	NO
YES	Exchange data files with Industry Standard PC applications	NO*
YES	No-charge Telephone Technical Support	NO
YES	Instant on-line HELP system	NO

A Costly Situation. Every engineer needs the power and features of a "Rocky Mountain" BASIC workstation, but not everyone can have one. They simply cost too much. Fewer workstations, less productivity. **The Best Way.** TransEra HTBasic software provides the *only* way for serious technical computer users to turn their PC into a workstation without having to add costly hardware. Powerful workstations for everyone means greater productivity. **Extraordinary Versatility.** In addition, TransEra HTBasic works with the Industry Standard Personal Computer hardware, software, and networks. It even allows you to easily exchange data between your favorite DOS programs and the files you create in the BASIC workstation environment. All at a fraction of the cost of other solutions.

More compatibility. More versatility. More possibilities. Less expense. Less hassle.

To find out more, call 1-801-224-6550.

Circle Reader Action No. 473

TransEra

Engineering Excellence for 15 Years™

CYBER-205 Devectorizer

Explicit vector-notation syntax is converted to standard FORTRAN.

DEVECT (CYBER-205 Devectorizer) is a CYBER-205 FORTRAN source-language-preprocessor computer program that reduces vector statements to standard FORTRAN. It is sometimes desirable to run programs developed for a CDC CYBER 200 vector-processor computer on a different computer. However, such programs use special FORTRAN source statements that contain explicit vector (semicolon) notation syntax and require a large amount of code to convert them to American National Standards Institute (ANSI) standard FORTRAN. DEVECT performs this time-consuming and extremely-labor-intensive conversion process without requiring large computational resources. It is estimated that on one of the larger codes, this program could result in labor savings of the order of several weeks to months. The low utilization of resources by DEVECT encourages interactive execution of the program.

In general, FORTRAN for a CDC CYBER 200 vector processor allows the programmer to express vector (from 1 to 65,535 elements in an array) operations many different ways. The vast majority of vector-related operations in a typical vectorized program involves the vector-arithmetic-assignment statement. The left side of this replacement statement is a vector reference, and its right side is a vector expression. DEVECT recognizes this explicit vector-notation syntax and generates exclusive, analogous scalar DO loops in place of the vector-referencing semicolon notation.

In addition, DEVECT has many other standard and optional features that simplify the conversion of vector-processor programs for the CYBER 200 to other computers. Sixty different vector intrinsic functions, specific and generic, are handled by conversion to the analogous scalar intrinsic reference. Default processing compacts consecutively generated scalar DO's to minimize DO-loop overhead, although it can be selectively inhibited under control by the user. All of the generated code is highlighted by appropriate indentation. DEVECT can also generate code compatible with the CRAY 2 computer.

This program is written in FORTRAN IV and was implemented on a CYBER 170/850 computer with a CDC NOS 2.7.1 operating system. It requires a memory of about 21,500 CYBER words. DEVECT was developed in 1989.

This program was written by Christopher D. Lakeotes of Computer Sciences Corp. for **Langley Research Center**. *For further information, Circle 78 on the TSP Request Card.* *LAR-13810*

NASA Software Update

Each month NASA Tech Briefs features new computer programs available through COSMIC, NASA's Computer Software and Information Center in Athens, GA. In addition to creating new programs, NASA continually updates and enhances existing software. Programs updated in the past year include:

An Engineer's Tool for Prediction of Airframe Integrated Scramjet Performance (SCRAM) This program was developed to support research on the National Aero-Space Plane, which will take off horizontally and fly into orbit. SCRAM performs nose-to-tail simulation of real gas flow with equilibrium thermodynamic characteristics such as will be encountered in a hydrogen-fueled ramjet/scramjet engine. Although written for supersonic flows, the code has been modified to handle subsonic flows and dual-mode combustor operation. SCRAM is written in FORTRAN 77 and is machine independent. *Circle 1 on the TSP Request Card. ARC-12338*

Information System Life-Cycle and Documentation Standards (SMAP DIDS) Although not a computer program, the SMAP DIDS were written to provide systematic, NASA-wide structure for documenting information system development projects. Each DID (data item description) outlines a document required for top-quality software development. When combined with management, assurance, and life cycle standards, the Standards protect all parties who participate in the design and operation of a new information system. The SMAP DIDS are delivered in five volumes and as a set of diskettes. *Circle 2 on the TSP Request Card. COS-10300*

Integrated Analysis Capability (IAC) The IAC system is an interactive tool for robotics design, integrating a common database with programs from the fields of structures, thermodynamics, controls, and system dynamics. The program is written in FORTRAN 77 for a DEC VAX. *Circle 3 on the TSP Request Card. GSC-13341*

Optimal Regulator Algorithms for the Control of Linear Systems (ORACLS) This control theory design package offers the engineer a full range of subroutines to manipulate and solve Linear-Quadratic-Gaussian types of problems. ORACLS is a rigorous tool, intended for multi-input and multi-ouput dynamic systems in both continuous and discrete form. The program is written in FORTRAN and has been implemented on DEC VAX, CDC, and IBM mainframe computers. *Circle 4 on the TSP Request Card. GCS-13067*

Goddard Mission Analysis System (GMAS) Written to simulate complex satellite orbits including attitude control and orbital maneuvers, GMAS can also perform shadow and station coverage studies and graph-selected orbital parameters for two satellites. It is written in FORTRAN and ASSEMBLER for the IBM mainframe. *Circle 5 on the TSP Reader Request Card. GSC-13292*

Thermal Radiation Analysis System (TRASYS II) This program solves thermal heating problems such as the effect of sunlight on a satellite. Surface geometry features include a complete shadowing ability, including shadowing by semi-transparent surfaces. TRASYS II was written for the DEC VAX and has been ported for the CONVEX. *Circle 6 on the TSP Request Card. MSC-21030*

C Language Integrated Production System (CLIPS) Ideal for developing expert systems, the CLIPS language is easy to use and can be called from or make calls to other programs. Advanced features include a cross-reference, style, and verification facility that catches logic errors in large systems. Versions of CLIPS are available for the IBM PC, Macintosh, and other platforms, but the program is machine independent. *Circle 7 on the TSP Request Card. MSC-21208*

Space Systems Integrated Simulation (SPASIS) This complex program models everything on a user-defined space station, from the control gyros to the mass effect of an astronaut moving along a strut. Other features include plume impingement, attitude control, propellant slosh, docking, and gravity. The program runs on a DEC VAX. *Circle 8 on the TSP Request Card. MSC-21462*

Neural Network Development Tool (NETS) Artificial neural networks are formed from hundreds or thousands of simulated neurons, connected in a manner similar to that in the human brain. Such a network can model learning behavior. Using NETS involves translating the problem to be solved into input/output pairs, designing a network configuration, and training the network. NETS is written in C and is machine independent. *Circle 9 on the TSP Request Card. MSC-21588*

Artificial Satellite Analysis Program (ASAP) This program is suited for studying planetary orbit missions that include mapping and flyby components. Sample data is included for a geosynchronous station drift cycle study, a Venus radar mapping strategy, a frozen orbit about Mars, and a repeat ground trace orbit. ASAP is written in FORTRAN for use on the IBM PC series. *Circle 10 on the TSP Request Card. NPO-17522*

45 Measuring Monodisperse Small Particles En Masse
46 O-Ring-Testing Fixture
46 Corrosion-Resistant Ball Bearings
47 Spring-Loaded-Bolt Locking Device
47 Atomized Water as Couplant for Ultrasonic Inspection
48 Trap for Noncondensable Gas in Heat-Transfer Fluid

Measuring Monodisperse Small Particles En Masse

Arrays of the particles act as diffraction gratings.

Langley Research Center, Hampton, Virginia

A new optical method enables the determination of the sizes of approximately-micron-sized particles. Previously, a microscope with a magnification of 2,000 was used to determine the diameters of the particles. The new technique could replace measurements made with high-magnification microscopes.

When a suspension of solid particles of the same size is spread in a thin layer on a microscope slide, the surface tension of the evaporating liquid draws the particles into regions of planar close-packed hexagonal array. The distance, S, between parallel rows of particles in such an array is related to the particle diameter, D, by

$$S = D \cos 30°$$

These rows of particles can act as a diffraction grating, and reflected light is visible to an observer when the light waves reflected from successive lines of particles are in phase. This situation occurs when the distance, d, between the wavefronts reflected from successive rows is an integral number of half-wavelengths ($\lambda/2$) of the light, which is reflected at an angle of θ from the perpendicular to the plane of the particles.

$$d = \frac{n\lambda}{2}$$

$$\text{but } d = S \sin \theta$$
$$\text{and } S = D \cos 30°$$

$$\text{Therefore, } (D \cos 30°) \sin \theta = \frac{n\lambda}{2}$$

$$\text{and } D = \frac{n\lambda}{2 \cos 30° \sin \theta}$$

For first order spectra, $n = 1$, and

$$D = \frac{0.577\lambda}{\sin \theta}$$

The figure shows schematically a device for measuring the sizes of particles in this way. White light from a lamp is collimated by a lens and partially reflected from a mirror, which is either half-silvered or has a hole in the reflecting surface to enable the observer to view the reflected light along the same path as that of the incident light. This device is adjusted with the sample slide perpendicular to the beam of light (indicator at ∞ on the particle-size scale) so that the bright reflection of the beam of light is seen by the observer.

The turntable is then rotated until light of the selected color is seen. The size of the particles is then read on the scale. When white light is used, the green portion of the spectrum gives good results. A typical wavelength for green light is 0.52 μm. The use of this value in the equation for D yields a scale on which 3-μm particles are equivalent to an angle of 5.7°, 1-μm particles to 17.5°, and 0.5-μm particles to 36.9°.

The theoretical limit for measurements of particles under these conditions would be 0.3 μm, but because the angle of incidence becomes very small near the limit, it is not feasible to measure sizes near the limit. The use of a monochromatic light source like a low-power laser or a color-filtered lamp would increase precision by eliminating color judgement and would enable measurements by use of a phototube instead of the human eye.

This device is being used regularly at the NASA Langley Research Center to determine monodispersity and diameters of polystyrene latex microspheres that are used as seeding material for laser-velocimetry flow measurements in NASA's wind tunnels. The characterization of particle sizes is important in a wide range of fields, including the manufacture of plastics and ceramics, biochemistry, and medicine.

This work was done by Robert A. Bruce and Cecil E. Nichols, Jr., of **Langley Research Center**. *For further information, Circle 45 on the TSP Request Card.*
LAR-14152

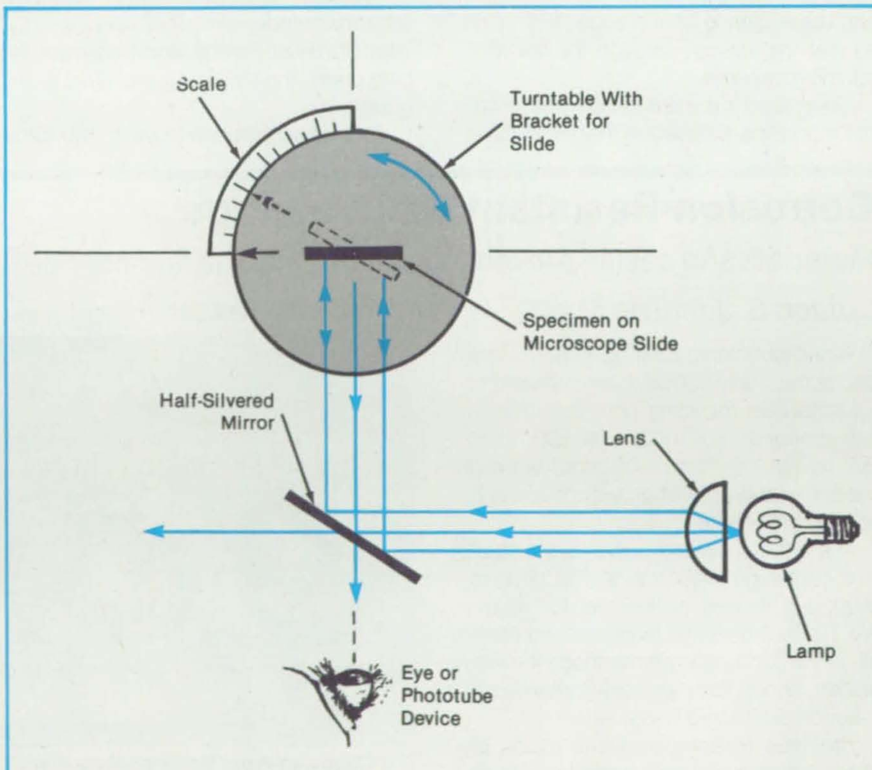

This **Simple and Inexpensive Apparatus** has replaced high-magnification microscopes in measurements of the diameters of small polystyrene latex spheres.

O-Ring-Testing Fixture

An apparatus exposes O-rings to a variety of dynamic conditions.

Marshall Space Flight Center, Alabama

A fixture is used to evaluate the properties of O-rings of various materials. The fixture creates controlled axial and radial gaps between the sealing surfaces around the ring so that the effectiveness of the material in maintaining a seal can be determined under dynamic conditions.

The ability to seal can be studied under a wide range of conditions of temperature, pressure, rate of pressurization, time of the start of pressurization relative to the initiation of the opening of the radial gap, change in the radial gap, speed of change of the radial gap, and position of the O-ring in its gland before pressurization. Test temperatures range from 10 to 130 °F (−12 to +54 °C). The maximum pressure is 1,000 lb/in.^{2} (6.9 MPa), the maximum rate of pressurization is 11,500 lb/in.^{2}•s (79.3 MPa/s), and the maximum rate of radial-gap movement is 20 in./min (8.47 mm/s).

A conical plug holds O-rings in grooves and fits in a conical hole in a housing (see figure). The half cone angle of both the plug and the hole is 15°. A hydraulic cylinder adjusts the vertical position of the plug and thereby controls the sizes of the axial and radial gaps between the plug and the inner wall of the housing. The bottom gland holds the O-ring being tested. O-rings in middle and upper glands create secondary seals so that the leakage through the test ring can be measured.

Several ports are drilled through the wall of the housing. One allows the pressurizing gas to be introduced to the lower side of the test ring. The others provide for measurement of leakage past the test ring and of the pressures on each of the other two rings. Thermocouples monitor the temperatures of the plug and the housing. The assembly is preheated by resistance-heating strips or precooled with liquid nitrogen.

A profile generator controls the hydraulic cylinder. It is programmed to adjust the time, magnitude, and rate of opening of the gap. Shims at the top and bottom of the plug preset the initial and final sizes of the gaps.

The fixture has been built in two sizes. The larger unit measures 16.25 in. (41.3 cm) across the housing. The smaller unit is 8.75 in. (22.2 cm) in diameter.

This work was done by James E. Turner and D. Scott McCluney of **Marshall Space Flight Center**. *For further information, Circle 18 on the TSP Request Card.*

This invention is owned by NASA, and a patent application has been filed. Inquiries concerning nonexclusive or exclusive license for its commercial development should be addressed to the Patent Counsel, Marshall Space Flight Center [see page 16]. Refer to MFS-28376.

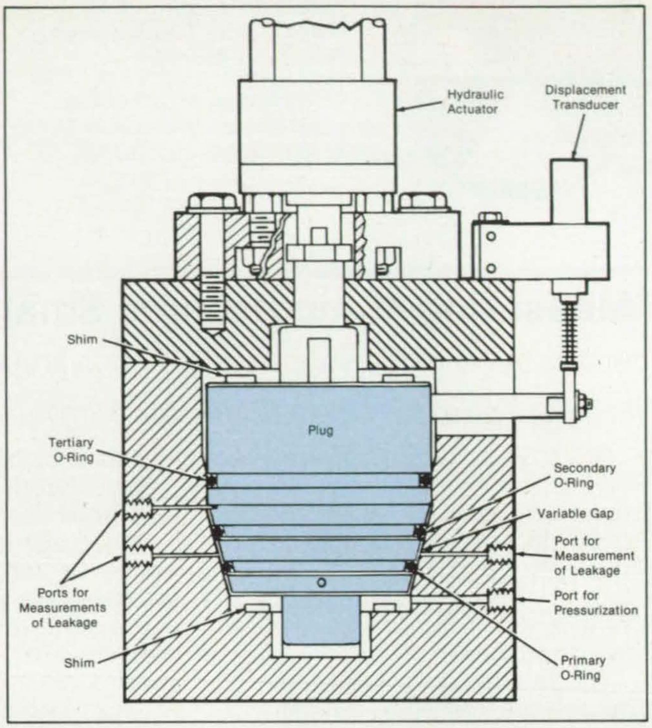

The **Hydraulic Actuator Positions the Plug** in the housing, creating a controlled, variable gap in the O-ring glands formed by grooves in the plug and by the inner wall of housing.

Corrosion-Resistant Ball Bearings

Materials and design prevent corrosion by acids and provide lubrication.

Lyndon B. Johnson Space Center, Houston, Texas

A self-lubricating bearing system withstands the highly corrosive environment of a wastewater-recycling unit. The system has operated continuously for 500 hours (8.1 million bearing revolutions) without corroding and without growth of bacteria on its components.

The bearing system supports the shaft of a centrifuge that turns at 230 r/min to evaporate treated wastewater for recovery. The two bearings in the system operate at the partial vacuum needed for evaporation, one of them partially immersed in sulfuric-acid-treated wastewater.

Previous bearing systems made of bearing steel or stainless steel corroded so severely that they could not function after a few hundred hours. The bearing races and balls became fouled by corrosion prod-

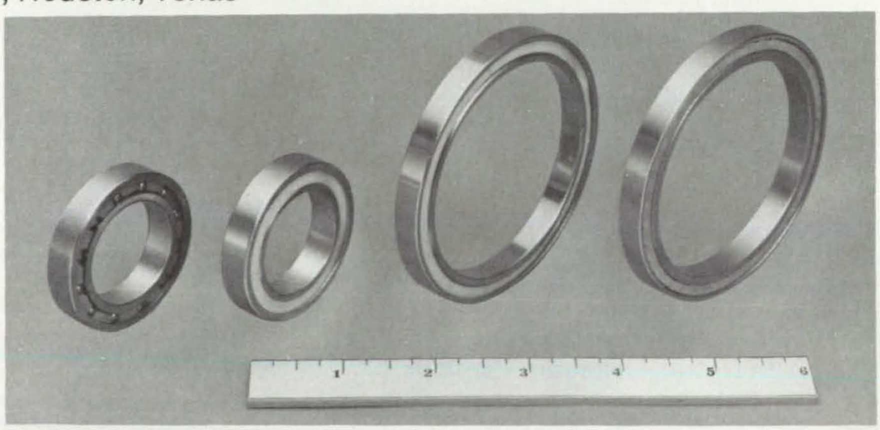

The **Corrosion-Proof Bearings** were made in two sizes, each for use at one end of the centrifuge shaft of a wastewater-recovery unit. The bearing at left is turned to show the balls and self-lubricating cage between the inner and outer races. The other bearings are turned to show the polytetrafluoroethylene seals that prevent wastewater from splashing on the inner parts.

ucts. In addition, the bearing grease dried out in the partial vacuum, forming a residue that contributed to fouling. To make matters worse, raw wastewater splashed into the relatively warm bearings and evaporated, leaving a precipitate that caused more fouling.

The new bearings contain cobalt-based-alloy balls and races, graphite/polyimide polymer ball cages, and single integral polytetrafluoroethylene seals on the wet sides (see figure). The materials were chosen to resist attack by the sulfuric acid. The ball cages lubricate themselves, thus eliminating the need for grease and the grease-evaporation problem. The integral seal prevents gross fouling by splashed wastewater.

Initially, the cobalt-alloy races had a hardness of 35 on the Rockwell C scale, whereas a hardness of at least 48 is needed for use in bearings. Unlike conventional bearing materials, the cobalt alloy could not be heat-treated or nitrided to increase hardness. Instead, the cobalt-alloy races were cold-worked during manufacturing to raise the Rockwell C hardness above 45, then aged to bring their final hardness to about 50. Low hardness was not a problem with the cobalt-alloy balls because they were made by powder-metallurgy techniques that yielded a hardness of more than 55.

This work was done by E. M. Zdankiewicz and E. L. Linaburg of Life Systems, Inc., and L. J. Lytle of Quality Bearing, Inc., for **Johnson Space Center**. *For further information, Circle 41 on the TSP Request Card.* MSC-21319

Spring-Loaded-Bolt Locking Device

Moderate vibrations do not cause accidental unlocking.

Lewis Research Center, Cleveland, Ohio

A locking device is designed to clamp small objects temporarily onto an object or vehicle that may accelerate. The device is intended to be used in place of a toggle clamp, which can snap out of lock during excessive shock or vibration or because of accidental contact of a person or object with the toggle locking handle.

The device somewhat resembles a door bolt, both in appearance and operation. Like a door bolt, it includes a handle attached to a shaft that is free to rotate through part of a circle and to slide a short distance along its length. Unlike a conventional door bolt, the device includes a spring that pushes against a collar on the shaft (see figure).

To prepare to lock, the operator pushes the handle and bolt to the left (1), then pushes the handle down (2) and (3) until it lies parallel with a slot in the locking block (4). The operator then allows the device to lock by releasing the handle, letting the spring push the handle to the right and into the slot. When shocks, vibrations, and gentle accidental contacts with the handle push the handle part away out of the slot, the spring pushes it back in, maintaining lock. Under most conditions, the device remains in lock unless the operator deliberately pushes the handle out of the slot against the force of the spring and turns the handle outward.

Curved cam surfaces on the locking block facilitate locking and unlocking by reducing the range of necessary movements and applied forces. (The cam surfaces could be eliminated. This would make operation more difficult but could increase resistance to accidental unlocking.) It should also be possible to make electrically actuated versions by inclusion of suitable solenoids, gears, and/or levers.

This work was done by Frank S. Calco of **Lewis Research Center**. *For further information, Circle 39 on the TSP Request Card.*

Inquiries concerning rights for the commercial use of this invention should be addressed to the Patent Counsel, Lewis Research Center [see page 16]. Refer to LEW-14887.

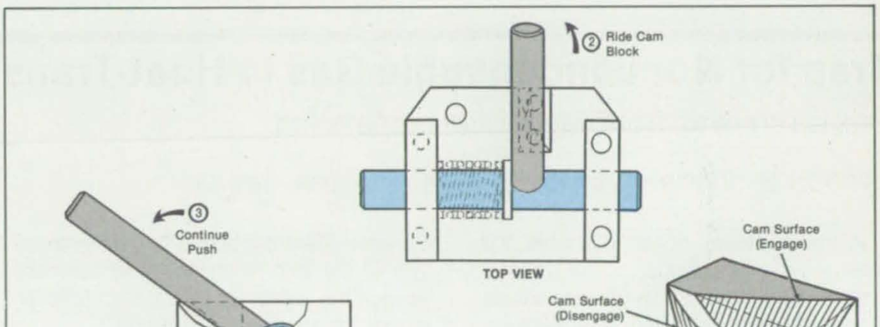

The **Locking Device** looks and operates somewhat like a spring-loaded door bolt. Shown here in lock position, it can clamp an object between the handle and the base.

Atomized Water as Couplant for Ultrasonic Inspection

Droplets coalesce into a film under the transducer.

Marshall Space Flight Center, Alabama

A simple technique makes it possible to use demineralized water as a coupling fluid for the manual-scan ultrasonic inspection of convex objects. In addition to having the required coupling properties, demineralized water is preferred over other couplants because it leaves little or no residue on the inspected parts. Previously, it was necessary to perform such inspections with thick gel couplants, which adhered to the inspected parts and had to be cleaned off after inspection. When demineralized water is used, it is necessary only to dry the part after inspection.

In the new technique, a fine mist of demineralized water is sprayed onto the part to be inspected, by use of a simple pump spray bottle equipped with an atomizing nozzle. (A commercial detergent or window-cleaner bottle could be used.) The surface tension in the sprayed droplets keeps them intact when they strike the object, and the friction between the droplets and the surface exceeds their weight, so that the droplets remain where they strike the surface instead of running off. The result is a fairly uniform coat of droplets on the surface.

Where the ultrasonic transducer is brought into contact with the droplets on the surface, the droplets coalesce into a film between the transducer and the surface. This film serves as the coupling medium. As the transducer is scanned across the part, it leaves the film behind. The excess water in the film coalesces into larger drops, which run off the part (see figure). This wiping action confers an additional advantage: one can distinguish visually between areas that have been inspected ultrasonically (they are free of droplets) and those that have not been inspected ultrasonically (they are still covered with droplets). Thus, it is easy to assure the complete inspection of the part.

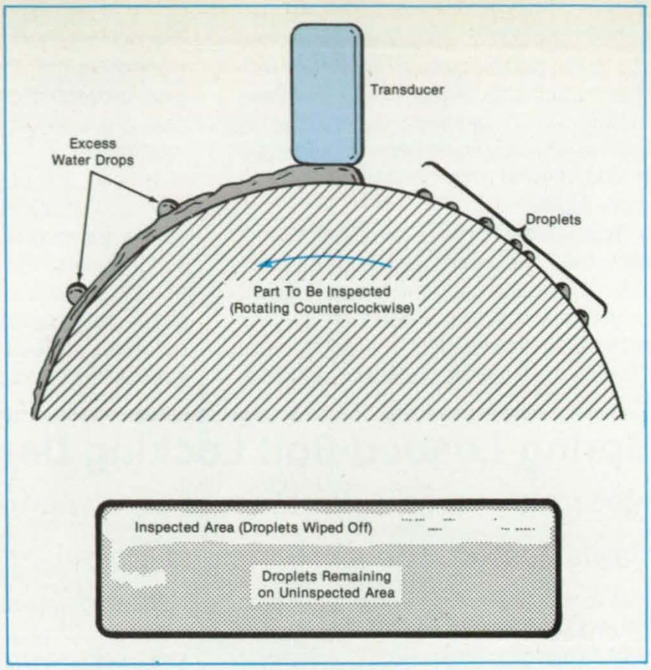

As the Transducer Scans Across the Surface, the droplets feed the film of water under the transducer. The excess water runs off the part. The inspected areas can then be distinguished visually from the uninspected areas by absence or presence of droplets, respectively.

This work was done by Carl G. Bouvier of Martin Marietta Corp. for **Marshall Space Flight Center**. *No further documentation is available.*

Inquiries concerning rights for the commercial use of this invention should be addressed to the Patent Counsel, Marshal Space Flight Center [see page 16]. Refer to MFS-28442.

Trap for Noncondensable Gas in Heat-Transfer Fluid

Gas is removed from vapor during operation.

Lyndon B. Johnson Space Center, Houston, Texas

A trap removes noncondensable gas from a vapor/liquid-phase heat-transfer system. Noncondensable gas can impair the operation of the system by accumulating in the condenser, blocking access of the heat-transfer fluid (e.g., one of the chlorofluoromethanes) to the heat-transfer surface of the condenser. Noncondensable gas can be present as a contaminant or can be generated slowly by the system.

The trap (see figure) includes a tube of stainless steel or other poorly thermally conductive material that is attached to a tap on top of the main vapor line where the vapor flows toward the condenser. Subcooled liquid from the outlet of the condenser cools the upper end of the tube below the vapor temperature.

A small fraction of the flow in the main vapor line enters the trap and travels to the upper end. There, the vapor condenses, and the liquid is returned to the main line by gravity. (In the absence of gravity, it could be returned by the capillary action of a wick.) Noncondensable gas that was entrained in the upward flow of vapor accumulates gradually, thereby increasing the effective thermal conductance of the upper end of the trap and decreasing the temperature T_1 measured by a thermocouple near the upper end. When T_1 decreases to a preset differential above T_2, the temperature of the incoming coolant, a solenoid valve at the upper end opens momentarily to vent the noncondensable gas.

This work was done by Fred Edelstein, Bruce Cordes, and Richard F. Brown of Grumman Aerospace Corp. for **Johnson Space Center**. *No further documentation is available.*
MSC-21389

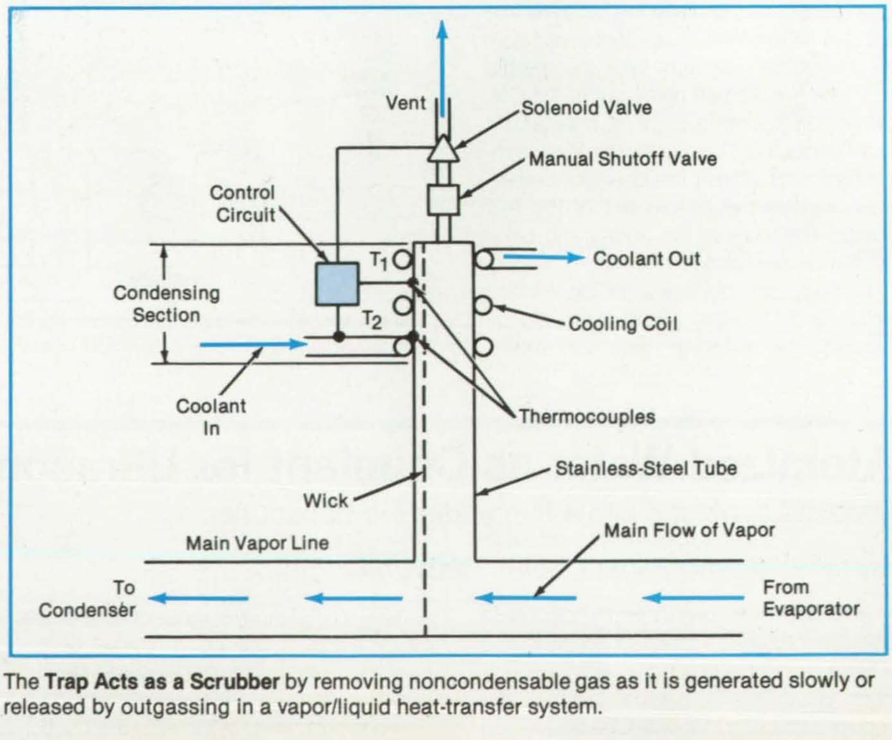

The **Trap Acts as a Scrubber** by removing noncondensable gas as it is generated slowly or released by outgassing in a vapor/liquid heat-transfer system.

Hardware, Techniques, and Processes

52 Agile Walking Robot
52 Rolling Robot
53 Rugged Walking Robot
53 Heat Shield and Axial Retainer for Turbopump Blade
54 Computing Flows in Turbine End Bearings
56 Rotary Ball Locking Mechanism

Agile Walking Robot

A six-legged unit would travel over rough terrain.

NASA's Jet Propulsion Laboratory, Pasadena, California

A proposed agile walking robot would operate over rocky, sandy, and sloping terrain. It would offer stability and climbing ability superior to those of other conceptual mobile robots.

Equipped with six articulated legs like those of an insect (see figure), the agile walker would continually feel the ground under a leg before applying weight to it. If a leg sensed an unexpected object or failed to make contact with the ground at the expected point, it would seek an alternative position within a radius of 20 cm. Failing that, the robot would halt, examine the area around the foot in detail with a laser ranging imager, and replan the entire cycle of steps for all legs before proceeding.

With its legs bent at right angles at the knees — the most stable configuration — the walker would clear objects as high as 0.85 m. However, it would be able to change the knee angle as necessary to lower its body to the ground or raise it 1.65 m above the ground.

The walker could climb steps as high as 2.6 m and would negotiate ditches 3 m wide. It would ascend or descend grades greater than 100 percent on hard surfaces and up to 70 percent on loose sand. Placing three legs at a time in front of the other three, the walker would travel at an average speed of 100 m/h.

The walker would navigate semiautonomously along a corridor specified from a remote control point. It would examine the terrain along its path with the ranging laser imager and video cameras and plot a route that would avoid insurmountable obstacles. As it proceeded along the route, it would select the placement of its feet from video data and adjust the placement as necessary according to locally monitored tactile data. The walker would stop briefly every 10 meters to review the terrain ahead and modify its planned route if necessary.

Its computation load would be somewhat greater than those of the other conceptual robots. Nine processors, each operating at about 1 million instructions per second, would be required for the navigation and control calculations.

A six-leg configuration was chosen because it offers much greater speed and stability than does the four-leg configuration. (Increasing the number of legs to eight would increase speed and stability only slightly, while adding substantially to the complexity and weight.) The legs would rotate horizontally and vertically at hip joints and vertically at knee joints. The ankle joints would flex compliantly. Footpads 0.5 m in diameter would distribute the weight of the walker over large contact areas.

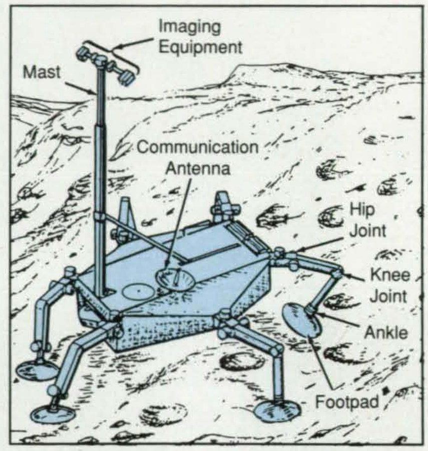

Six Legs would carry the walker over terrain that may be rocky, pitted, steep, and soft.

This work was done by Stanley J. Larimer, Thomas R. Lisec, Andrew J. Spiessbach, and Kenneth J. Waldron of Martin Marietta Corp. for **NASA's Jet Propulsion Laboratory**. *For further information, Circle 134 on the TSP Request Card.* *NPO-17874*

Rolling Robot

A simple but rugged semiautonomous rover would have large wheels and an articulated body.

NASA's Jet Propulsion Laboratory, Pasadena, California

A proposed rolling robot would routinely traverse rough terrain, clearing rocks as high as 1 m. It would climb steps 1 m high and span ditches 2.3 m wide.

The drive system would be simple, consisting of four powered wheels and an articulated chassis for steering (see figure). Ordinarily, only two-wheel drive would be used. For negotiating obstacles, soft soil, and loose sand grades, four-wheel drive would be used in combination with yawing and rolling about the axes of the chassis. The rolling and yawing motions would ensure that all wheels make contact with the surface at all times for maximum traction.

Like other conceptual robot vehicles, the rolling robot would navigate semiautonomously along a corridor specified from a remote control site. The robot would sense the terrain along the corridor, choose a path to avoid insurmountable obstacles, and monitor the state of the vehicle for unexpected hazards.

The robot would be equipped with large wheels 3.25 m in diameter to help it clear large obstacles and to ensure ample traction. The compliant spokes of the wheels would absorb shocks and provide a relatively smooth ride for the body of the vehicle, which would contain navigation and communication equipment. The wheels could be compressed like scrolls to 21 percent of their full volumes for compactness in storage and shipment. When bands

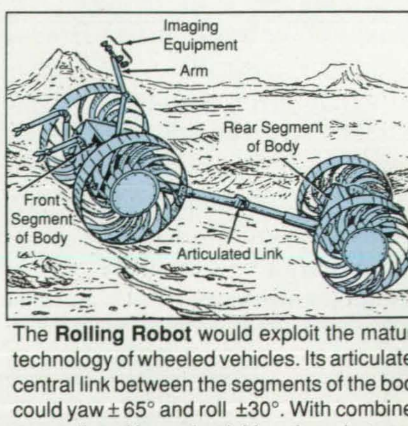

The **Rolling Robot** would exploit the mature technology of wheeled vehicles. Its articulated central link between the segments of the body could yaw ± 65° and roll ±30°. With combined yaw, roll, and four-wheel drive, the robot could crawl slowly to pass over soft or sandy terrain.

holding the stowed wheels were released, the compressed spokes would unfold and expand the wheels to their full diameters.

With laser ranging imagers on its mast, the robot would scan the terrain over the next 30 m before it and select a path. After traveling only 10 m along the path, the robot would plan for another 30-m path. This would ensure that the vehicle would travel only on a path that has been mapped from three different perspectives — from 30, 20, and 10 m away, reducing the incidence of backtracking by making available a path 3 times longer than will be used.

Each time it would plan a path, the robot would select local landmarks 1 m apart along the path, for example, rocks 20 to 200 cm high. As the vehicle traveled, it would note its position with respect to the landmarks and adjust its direction to stay on course. It would also note the time at which it passes a landmark and adjust its speed to stay on schedule.

To detect hazards en route, the robot would view the ground below it with two laser scanners, one directed at a line 2 m in front of the wheels and the other directed at a line where the wheels first touch the ground. The difference between the heights of the vehicle above ground determined by these two scans would serve as an estimate of the compression of the ground by the wheels. If the compression were found to be excessive, the robot would stop and replan its path. It might decide, for example, to lock the rear wheels and fold the link between the segments of the body while driving the front wheels in reverse. This maneuver would generate more than twice the traction of ordinary wheel rolling and could extricate the vehicle from exceptionally difficult situations.

The maximum speed would be limited by the speed with which the robot could handle navigation calculations. For an average speed of 100 m/h, five processors, each operating at 1 million instructions per second, would be needed.

This work was done by Stanley J. Larimer, Thomas R. Lisec, and Andrew J. Spiessbach of Martin Marietta Corp. for **NASA's Jet Propulsion Laboratory**. *For further information, Circle 136 on the TSP Request Card. NPO-17842*

Rugged Walking Robot

A conceptual unit features relative simplicity in construction and data processing.

NASA's Jet Propulsion Laboratory, Pasadena, California

A proposed walking-beam robot would be simpler and more rugged than articulated-leg walkers are, would require less data processing, and would use power more efficiently. The robot would pass over rocks or climb steps 1.7 m high and straddle ditches 1.8 m wide. It would walk at an average speed of 100 m per hour.

The robot would include a pair of tripods, one nested in the other (see figure). It would propel itself by raising, translating, and lowering the tripods in alternation. It would steer itself by rotating the raised tripod on a turntable.

Each of the six legs would include a three-segment telescoping tube with its own geared motor and brakes. An internal cable would drive each telescoping segment. Made of aromatic polyamid, the cables would stay flexible even at extremely low temperatures. The cables would be sheathed, and the segment joints would be equipped with wiping seals to protect parts from dust.

The footpad on each leg would be shaped like an inverted saucer, much like a camel's foot. This shape would compress loose material underneath, thereby aiding locomotion. it would also shed material that fell on the top of the footpad during walking.

The legs would move only vertically and thus would not kick the ground as articulated legs tend to do. They would, therefore, disturb the soil minimally. The footpads would tilt at ball-and-socket joints to accommodate uneven terrain. The extensions of the legs could be varied independently by the control system either to keep the chassis truly horizontal on a grade for maximum stability or to orient the chassis parallel to the grade to obtain the maximum step size.

The chassis would consist of two beams in a T configuration. The stem of the T would be a track on which the inner tripod would translate with respect to the outer tripod. The translation — on roller bearings — would be nearly frictionless.

The horizontal translation of the tripods would be independent of the vertical motion of the legs. There would, therefore, be no occasion for one actuator to oppose the movement of another — a common phenomenon that wastes power in articulated walkers.

The inner tripod would hold power supplies, communication equipment, computers, instrumentation, sampling arms, and articulated sensor turrets. The outer tripod would hold a mast on which antennas for communication with a remote control site and video cameras for viewing local and distant terrain would be mounted.

Routes would be planned at the remote site. Steps would be planned by the computers on the walker. After human operators at the remote site gain experience with the terrain, they could turn over route-planning authority to the walker over a corridor of limited width and length — say 10 m by 1 km. Five processors, some of which would be redundant at least some of the time, operating at a peak load of a total of 2 million instructions per second, would be needed for navigation.

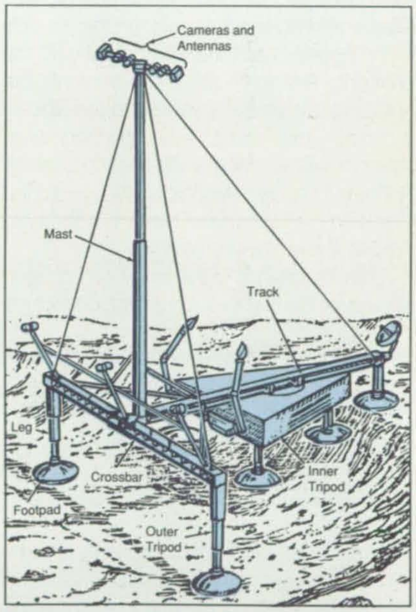

Members of a Pair of Tripods would alternately raise their legs, slide on horizontal track, and lower their legs. The robot would thus walk across terrain.

This work was done by Stanley J. Larimer, Thomas R. Lisec, and Andrew J. Spiessbach of Martin Marietta Corp. for **NASA's Jet Propulsion Laboratory**. *For further information, Circle 30 on the TSP Request Card. NPO-17825*

Heat Shield and Axial Retainer for Turbopump Blade

Operating life is expected to be increased.

Marshall Space Flight Center, Alabama

A modified configuration for the axial retention of the blades of a cryogenic turbopump is expected to reduce dynamic and thermal stresses, thereby increasing operating life. The modification is expected to overcome some of the structural limitations of the previous configuration, in which various components of the "fir-tree" blade/disk attachments are shaped in such a way as to concentrate the stresses.

In the modified configuration (see figure), the blade is restrained against rearward motion by placing a split ring in a slot cut in an extension of the disk so that the blade presses on the extension of the disk through the split ring. A seal/ring holder provides a sealing surface and restrains the split ring against outward radial motion under centrifugal loading. The seal/ring holder is held in place by a tang that interlocks with the split ring.

During assembly, the split ring is compressed into a slot in the extension of the disk while the seal/ring holder is slid into position along disk/seal attachment grooves in the extension of the disk (shown in cross section on the left side of the figure). Once the seal/ring holder is in position, the split ring is allowed to expand outward to make contact with it. The blade can then slide rearward along the disk/blade attachment grooves (also shown in cross section on the left side of the figure) until it makes contact with the split ring. A tang on the blade prevents the split ring from moving inward in the slot — a motion that would cause the undesired loss of axial retention of the seal/ring holder. A low-overhung-mass side plate is added to shield the face of the disk from the cold fluid in the adjacent cavity.

The advantages of the modified configuration over the previous configuration include the following:

- There is no overhung loading on the attachment faces of the disk or blades;
- No additional stress concentrators are added to the attachment faces of the disk or blades; and
- There are no large axial thermal gradients on the edges of the disk and blades.

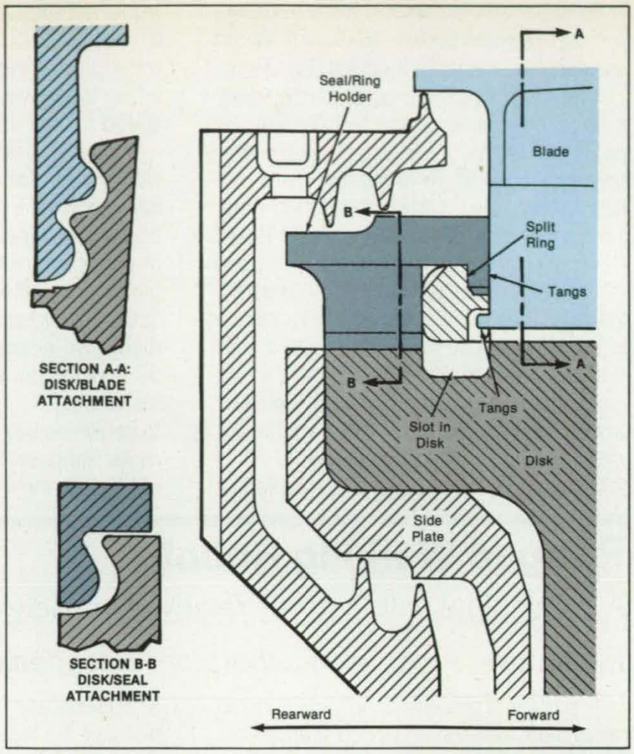

The **Modified Configuration** for axial retention of a turbopump blade in the turbopump disk reduces dynamic and thermal stress.

This work was done by Jerry H. Moore of United Technologies Corp. for **Marshall Space Flight Center**. *For further information, Circle 36 on the TSP Request Card.*

Inquiries concerning rights for the commercial use of this invention should be addressed to the Patent Counsel, Marshal Space Flight Center [see page 16]. Refer to MFS-28417.

Computing Flows in Turbine End Bearings

The effects of a hydrostatic damper and/or back-pressure seal are included.

Marshall Space Flight Center, Alabama

A computer program implements a mathematical model of the flow through the turbine end bearings of the high-pressure-oxygen turbopump of the Space Shuttle main engine. It is intended to determine the rate of flow and the margin before vaporization in these bearings for various types of geometries. Presumably, it could be modified for application to other turbomachines and fluids other than oxygen. The program differentiates between static and total pressures and fits the geometry of the pump more realistically than did a previous mathematical model. It represents the properties of the fluid on the basis of static quantities, thereby providing for improved mathematical modeling of the margin before vaporization within the bearings.

The boundary conditions of the mathematical model include the pressure and temperature at the inlet and outlet of the pump, the drain discharge pressure, and the heat added to the bearings; these must all be supplied by the user as input data. Coefficients of loss and of "pumping" are determined by computational fluid dynamics, experiments, or analytical correlations.

The drops in pressure through resistances to flow are treated as drops in total pressure with a constant enthalpy. The velocity head is "backed out" to determine the static pressure for updating the density. Because average densities are used in calculating the drops in pressure, iterations are performed on the rate of flow and the density until the solution converges. An algorithm for the solution of nonlinear equations is used to obtain convergence of the rates of flow. The effects of mixing are modeled on the basis of enthalpy, but perfect mixing is assumed. "Pumping" effects caused by rotating walls are modeled as increases in static pressure at constant entropy. The model includes the hydrodynamic effects of a hydrostatic damper and/or a back-pressure seal upon the bearings. The computer program also includes a mathematical model of the primary liquid-oxygen/gaseous-oxygen seal to determine rates of overboard leakage.

One likely modification of the program would be to treat the "pumping" effects as increases in enthalpy instead of increases in static pressure. The program should also be modified to differentiate between static enthalpy on the one hand and total enthalpy and total temperature on the other hand to improve the calculation of the properties of the fluid and of the margin before vaporization within the bearings (at least in a gross-flow sense). Effects of heat transfer should also be included throughout the model.

This work was done by Tyn S. Smith of Rockwell International Corp. for **Marshall Space Flight Center**. *No further documentation is available.*

Inquiries concerning rights for the commercial use of this invention should be addressed to the Patent Counsel, Marshall Space Flight Center [see page 16]. Refer to MFS-29681.

Rotary Ball Locking Mechanism

The output shaft can be locked in, and turned between, two fixed positions.

Lyndon B. Johnson Space Center, Houston, Texas

A ball locking mechanism links an input drive shaft to an output shaft and disengages the two shafts from each other when it locks the output shaft at either of two fixed angular positions. The mechanism is part of a drive system that turns a microwave antenna 143.5° between stowage and deployment orientations and holds it at either orientation without back-loading the drive motor and gears. The angular interval and dimensions could be modified for use in robotic or other actuators in which it may be desirable to "rest" the drive trains while locking the actuators at fixed positions.

The input shaft is a camshaft with 10 hemispherical recesses (ball detents) at 1 axial station and 4 cylindrical recesses (roller detents) at another axial station. The housing has similar recesses. The figure shows an operating sequence. In step 1, the input shaft holds the balls in a position that prevents the output shaft from turning in the housing, as shown at the left. The output shaft is thus locked in position, and the load (if any) is evenly distributed around the circumference to the 10 ball detents. However, as shown at the left and right, the input shaft is free to begin rotating counterclockwise by itself.

In step 2, the input shaft rotates until its ball detents become aligned with the slip-through holes for the balls in the output shaft. Because the balls are now free to slide through the holes to the detents in the input shaft, the output shaft is no longer locked to the housing. At this point, the input shaft begins to turn the output shaft because the sides of two recesses in the input shaft make contact with rollers 1 and 3.

In step 3, the rotation continues and forces the outer ball of each pair out of its detent in the housing. The rotation also forces rollers 4 and 2 out of their detents in the housing. All four rollers are now restrained in positions to lock the input and output shafts together and remain this way throughout the 143° angular travel.

In step 4, the shafts approach the end of travel, and the output shaft is released from the input shaft as rollers 1 and 3 are pushed into detents. The input shaft is now free to rotate a little farther by itself until the sides of two recesses make contact with rollers 2 and 4. The input shaft rotates, pushing the balls into the recesses in the housing and thus locking the output shaft in position at step 5.

The motor of the input drive is equipped with limit switches to turn it off as the mechanism approaches either end of travel. As a precaution to prevent the motor from driving the input shaft against the mechanical stops of rollers 2 and 4, the design allows the input shaft to travel 3.5° beyond the position where the output shaft becomes locked to the housing.

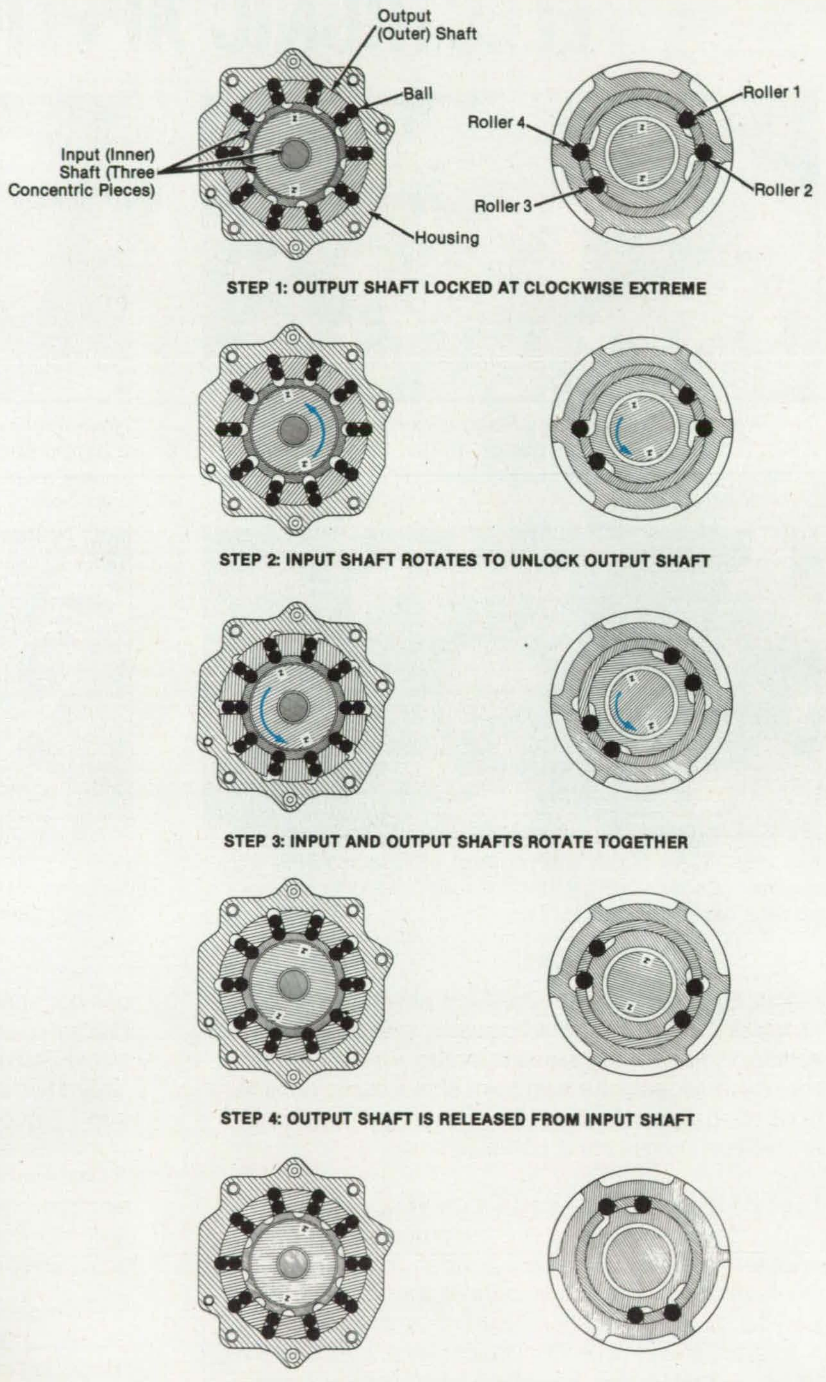

STEP 1: OUTPUT SHAFT LOCKED AT CLOCKWISE EXTREME

STEP 2: INPUT SHAFT ROTATES TO UNLOCK OUTPUT SHAFT

STEP 3: INPUT AND OUTPUT SHAFTS ROTATE TOGETHER

STEP 4: OUTPUT SHAFT IS RELEASED FROM INPUT SHAFT

STEP 5: OUTPUT SHAFT LOCKED AT COUNTERCLOCKWISE EXTREME

The **Input and Output Shafts** are engaged and disengaged by the movements of the rollers, as shown on the right side. The output shaft is locked to, or unlocked from, the housing by the movements of the balls, as shown on the left side. Z-Z′ is a reference axis attached to the input shaft to illustrate its rotation.

This work was done by Earl V. Holman of Rockwell International Corp. for **Johnson Space Center**. *For further information, Circle 113 on the TSP Request Card.*
MSC-21396

Fabrication Technology

Hardware, Techniques, and Processes

57 Software for Drawing Design Details Concurrently
57 Computer Program Re-layers Engineering Drawings
58 Numerically Controlled Machining of Wind-Tunnel Models
58 Cleaning With Supercritical CO_2
59 Transducer-Mounting Fixture
59 Washing off Polyurethene Foam Insulation
60 Measuring Weld Profiles by Computer Tomography
61 Positioning X-Ray Film Inside a Flow Splitter
62 Simple Regulator for Positive-Pressure Glove Box
62 FTIR Monitoring of Curing of Composites
63 Polishing Difficult-to-Reach Cavities

Software for Drawing Design Details Concurrently

More than one designer can work on the same part at the same time.

Marshall Space Flight Center, Alabama

A software system that contains five computer-aided-design programs enables more than one designer to work on the same part or assembly at the same time. The system reduces the time necessary to produce the design by implementing the concept of parallel or concurrent detailing, in which all the detail drawings that document a three-dimensional model of the part or assembly can be produced simultaneously, rather than sequentially as in conventional practice. The system keeps the various detail drawings consistent with each other and with the overall design by distributing the changes in each detail to all other affected details.

To use the software system, the design team follows a sequence of eight steps, each of which includes a number of substeps. In step 1, one designer, called the "modeler," completes a set of graphical constructions in a "model mode" to define the part or assembly, then prepares the detailing environment by activating all proposed drawings and defining all views necessary to describe the portion of the model represented by each drawing.

In step 2, which is called "baselining," each graphical entity defined in the model mode is provided with a "fingerprint" or "stamp" that serves as an accurate means of identification during parallel detailing. For each part defined in the model mode, the baseline-model program adds or updates a special property (called the "baseline-property") with the current value of that property. During this step, the computer video terminal displays the total number of entities within the part that were processed and the total number of entities that were baselined. After the computer executes the "baseline model" command, the revised drawing of the part is saved in the computer storage along with all affected "fingerprinted" model-mode entities.

In step 3, the information on each part is copied, checked, and distributed to provide for parallel detailing. In step 4, a designer prepares a file on a part about to be detailed. The designer gives the "detail part" command and the "purge detail" command, which causes the removal of any "model-mode" and "draw-mode" entities not associated with the selected detail drawing. In step 5, the system operates in the "draw mode," and the designer works on a particular drawing for which he or she is reponsible. In step 6, the designer issues the "put detail" command, which sends the detail drawing in its current state to the computer storage. This command can be issued repeatedly during work on the detail to update the external file so that any possible loss of detailing through error or malfunction is minimized.

In step 7, the model is prepared for incorporation of the results of a detailing session. The "purge model" command deletes any "draw-mode" entities associated with the drawing in question. In step 8, the "get detail" command incorporates the results of a detailing session via the external file that was created via the "put detail" command.

This work was done by Dewey C. Crosby III of Martin Marietta Corp. for **Marshall Space Flight Center**. *For further information, Circle 115 on the TSP Request Card.*

Inquiries concerning rights for the commercial use of this invention should be addressed to the Patent Counsel, Marshall Space Flight Center [see page 16].Refer to MFS-28444.

Computer Program Re-layers Engineering Drawings

Drawings are examined for conformity to standards.

Marshall Space Flight Center, Alabama

The RULCHK computer program aids in structuring the layers of information pertaining to a part or assembly designed with the software described in the preceding article, "Software for Drawing Design Details Concurrently." Layers are used to discriminate among the various attributes of a model and its associated documentation. The layering of the information pertaining to a part according to standards promotes the subsequent use of this information by other designers as they make changes and engage in other design activities.

Heretofore, designers have structured layers manually by placing the attributes of parts on standard layers. This practice consumes much time, is prone to errors, and does not contribute to the construction of a computer model of the part(s) or assembly or to its associated documentation.

RULCHK checks and optionally updates the structure of the layers for a part. It enables the designer to construct the model and annotate its documentation without the burden of manually layering the part to conform to standards at design time. Instead, the standards can be applied at a more opportune time. The benefits of RULCHK include the following:

1. The information pertaining to the part is layered automatically.
2. The program is controlled by design rules defined by the user.
3. The program maintains a consistent layered structure.
4. The designer is freed of activity not related to design.

This work was done by Dewey C. Crosby III of Martin Marietta Corp. for **Marshall Space Flight Center**. *For further information, Circle 87 on the TSP Request Card.*

Inquiries concerning rights for the commercial use of this invention should be addressed to the Patent Counsel, Marshall Space Flight Center [see page 16].Refer to MFS-28445.

Numerically Controlled Machining of Wind-Tunnel Models

Lightweight composite models are constructed quickly and accurately.

Langley Research Center, Hampton, Virginia

Typically, dynamic models and parts for wind-tunnel tests or radio-controlled flight tests are constructed by use of wooden patterns and handlaid molds. With these manual techniques, accuracy and symmetry are sometimes difficult to achieve. A new procedure involves the use of a single-phase numerical control (NC) technique to produce highly-accurate, symmetrical models in less time.

In the development of a fuselage, fabrication begins with a rough-cut blank of commercial polyurethane foam (see step 1 in the figure) large enough to encompass half of the fuselage structure: right, left, top, or bottom. The blank is bolted to the NC machine table. A computer-generated program is operated to rough-cut the blank to a given exterior fuselage surface, usually undersize by an amount equal to the thickness of the skin (see step 2).

Next, fiberglass and resin are applied to furnish a surface slightly oversized (step 3). Then another computer-generated program is used to machine the exact exterior fuselage shape, leaving a fiberglass skin of specified thickness (step 4). Extra machining is then done to create slots for wing spars or stabilizers and pockets for hardware or any other needed items (step 5).

After one side of the half of the fuselage is completed, a jig is constructed (step 6) to rotate the workpiece 180° and locate it precisely on the NC table. Then the core of the workpiece is excavated to produce a shell (step 7). The thickness of the shell is chosen in advance for compatibility with the fiberglass skin to furnish the required strength, weight, and internal volume. Also, during operations from this side, slots and pockets are machined for bulkheads, firewalls, sting or balance attachment mounts, hard points for locating pins, or other hardware (step 8).

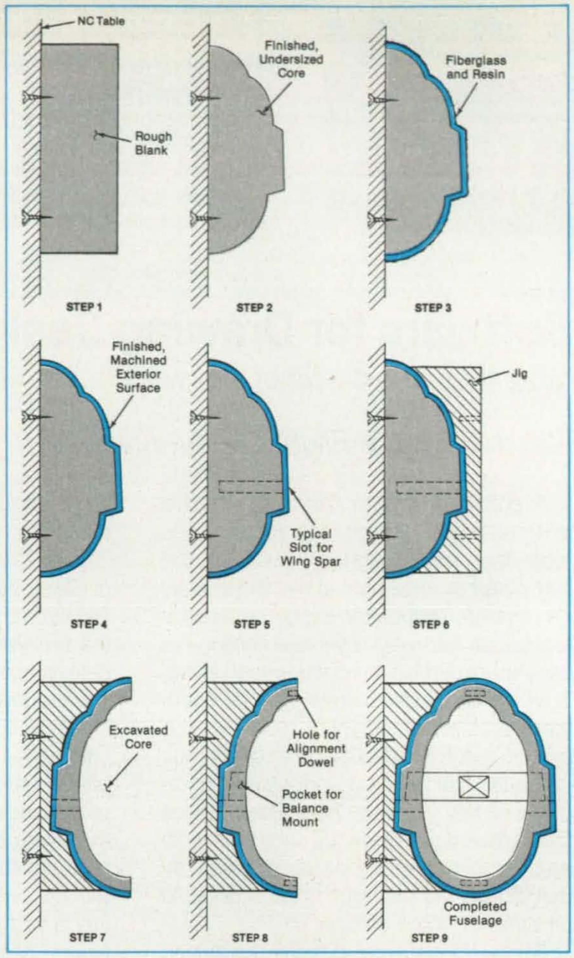

These are **The Steps of the Numerically Controlled Machining** in fabrication of a model fuselage (or other part). Numerically controlled fabrication is faster than manual fabrication and yield models of greater accuracy and symmetry.

The process is inverted and repeated to fabricate the other half of the fuselage. All hardware, stiffeners, and internal structures are fitted and installed in one half of the core, and then the two halves are located and bonded together (step 9). The fuselage is then sanded and painted and ready for installation of wings, stabilizers, canards, landing gear, or other attachments. Such other components as wings, canards, and tails can be fabricated by the same technique.

This work was done by John B. Kovtun of **Langley Research Center**. *No further documentation is available.*

This invention is owned by NASA, and a patent application has been filed. Inquiries concerning nonexclusive or exclusive license for its commercial development should be addressed to the Patent Counsel, Langley Research Center [see page 16]. Refer to LAR-14004

Cleaning With Supercritical CO_2

Quasi-liquid carbon dioxide can substitute effectively for harmful halocarbons.

Marshall Space Flight Center, Alabama

Supercritical carbon dioxide is an effective industrial cleaning agent. It can replace conventional halocarbon solvents for degreasing parts that have become coated with oil during such manufacturing procedures as forming and machining. Carbon dioxide presents none of the environmental threats and occupational hazards associated with halocarbon solvents. It spontaneously evaporates after use and thus leaves no waste to be disposed of as conventional solvents do. Moreover, the evaporated gas can readily be collected and recycled.

A supercritical gas is one that has been compressed at a temperature slightly above its critical (liquefaction) temperature. It is almost as dense as a liquid but still retains such gaslike properties as low viscosity and high diffusivity.

Carbon dioxide becomes supercritical at temperatures above 31 °C and pressures above 74 bars (7.4 MPa). In this state, it quickly dissolves many materials, including non-hydrogen-bonding organic materials. Its ability to dissolve increases with pressure; at pressures less than 350 bars (35 MPa), its solubilizing properties resemble those of carbon tetrachloride.

Carbon dioxide is attractive for many reasons. It is plentiful and can easily be extracted from the atmosphere. It is nontoxic, relatively unreactive, nonflammable, and environmentally safe. It contains no hydrogen or halogen and, therefore, does not corrode metal parts. It evaporates so quickly that there is no need to allow drying time.

In the cleaning process, supercritical carbon dioxide flows over a part, washing contaminants from its surface. Away from the part, the pressure of the gas is reduced drastically. The solubility of the dissolved contaminants decreases accordingly, and the contaminants precipitate from the carbon dioxide.

The process has been demonstrated in a small-scale laboratory system (see figure). It was used to clean steel bars that had been dipped in oil and drained; the amount of oil residue on the bars after cleaning was quite low — about the same as for halogen solvents, as measured by extremely sensitive Auger electron spectroscopy. The system was also used to clean oil-laden steel wool; it removed 95.5 percent of the oil.

The laboratory system can operate at pressures up to 5,000 psi (34 MPa), temperatures up to 60 °C, and rates of flow up to 20 standard ft^3/h (1.6×10^{-4} standard m^3/s). Its sample holder has a volume of 16 mL and can accommodate samples up to 0.4 in. (10.2 mm) in diameter and 8 in. (203.2 mm) long. Typical experimental cleaning times are 10 or 30 min.

The system was used to study the relationships among pressure, temperature, rate of flow, and cleaning time. The results are being used to build a full-scale system for cleaning parts and machining chips. The new system will feature rapid loading and unloading, remote process control, recycling of carbon dioxide, and ease of disassembly for inspection and maintenance.

This work was done by James J. Herzstock of Rockwell International Corp. for **Marshall Space Flight Center**. *For further information, Circle 74 on the TSP Request Card.*

Inquiries concerning rights for the commercial use of this invention should be addressed to the Patent Counsel, Marshall Space Flight Center [see page 16]. Refer to MFS-29611.

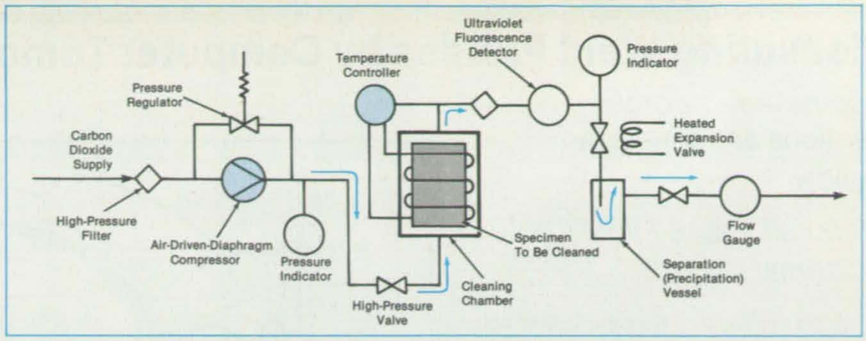

The **Laboratory-Scale Cleaning System** contains instruments that measure the effectiveness of cleaning at various pressures, temperatures, and rates of flow. The ultraviolet-fluorescence detector measures the amount of oil in the gas flow from the cleaning chamber and thus monitors the progress of the cleaning process.

Transducer-Mounting Fixture

The easy-to-use fixture holds the transducer securely.

Marshall Space Flight Center, Alabama

A transducer-mounting fixture holds a transducer securely against a stud. It projects only slightly beyond the stud after installation.

The fixture includes two halves of a cylindrical block that is hinged so that it can be opened like a clamshell. When the fixture is open, the transducer is inserted by placing its flange in a groove in one of the halves (see figure). The halves are closed, securing the transducer. The internally threaded fixture is rotated about one-quarter turn on the externally threaded stud to seat it and the transducer.

The flange, a ring of corrosion-resistant stainless steel, is bonded to the transducer package with a silicone adhesive. The flange acts as a spring, holding the transducer against the stud.

The fixture is machined from the cylindrical block as a unit. It is then cut in half by electrical-discharge machining by a wire no more than 0.010 in. (0.254 mm) in diameter. A 0.040-in. (1.02-mm) hole is drilled along the pivot axis, and a pin is inserted in the hole to form the hinge.

This work was done by Kirk W. Spiegel of Rockwell International Corp. for **Marshall Space Flight Center**. *For further information, Circle 71 on the TSP Request Card.*

Inquiries concerning rights for the commercial use of this invention should be addressed to the Patent Counsel, Marshall Space Flight Center [see page 16]. Refer to MFS-29600.

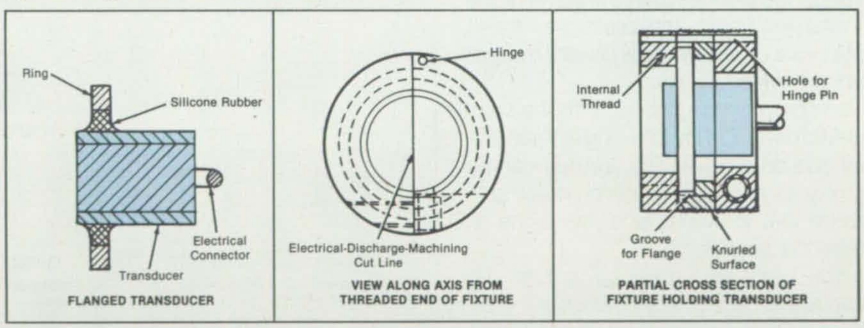

The **Flanged Transducer Fits** into the fixture when the hinged halves are open. When the halves are reclosed, the fixture is tightened onto a threaded stud until the stud makes contact with the transducer. The knurled area on the fixture aids in tightening the fixture on the stud.

Washing off Polyurethene Foam Insulation

A jet of hot water removes the material quickly and safely.

Marshall Space Flight Center, Alabama

A simple, environmentally sound technique has been found to remove polyurethene foam insulation from metal parts. The technique was developed for (but is not limited to) use during the rebuilding of the fuel system of the Space Shuttle main engine, during which the insulation must be removed for penetrant inspection of metal parts.

Previously, it was necessary to remove the insulation manually, at the risk of scratching the metal parts, thereby causing them to fail penetrant inspection. In the new technique, the insulation is sprayed by a jet of hot water at a pressure of 200 psi (1.4 MPa) and a temperature of 190 °F (88 °C) from a commercial hot-water cleaning system (for example, K.E.W. model 380 3V-103 or equivalent). The jet removes all residue of the insulation.

This work was done by Richard K. Burley and Irving Fogel of Rockwell International Corp. for **Marshall Space Flight Center**. *No further documentation is available. MFS-29578*

Measuring Weld Profiles by Computer Tomography

Accurate x-ray cross sections are generated rapidly.

Marshall Space Flight Center, Alabama

A noncontacting, nondestructive computer tomography system determines the internal and external contours of welded objects. The system makes it unnecessary to take metallurgical sections (a destructive technique) or to take silicone impressions of hidden surfaces (a technique that contaminates) to inspect them. Measurements of contours via tomography can be performed 10 times as fast as measurements via impression molds, and the tomography does not contaminate the inspected parts.

A welded part or other workpiece to be inspected is rotated, under computer control, in the fan-shaped beam from an x-ray source, as shown in the preceding article, "Viewing Welds by Computer Tomography" (MFS-29555). The x rays travel in straight lines unless they are absorbed or deflected by features in the workpiece. Detectors measure the x-ray flux passing through the workpiece about once per degree of rotation. The computer compares each reading of each detector with a calibration reading made before the workpiece was emplaced. It calculates the total mass along each of many thousands of lines through the workpiece in the plane of the fan-shaped beam and processes these data into a cross-sectional density map, or tomogram (see figure).

An operator can interact with the computer to develop a line drawing of the inside and outside profiles. The drawing can be compared with an engineering drawing to ensure that the workpiece meets the dimensional specifications.

This work was done by Antonio G. Pascua and Jagatjit Roy of Rockwell International Corp. for **Marshall Space Flight Center**. *No further documentation is available.*

Inquiries concerning rights for the commercial use of this invention should be addressed to the Patent Counsel, Marshall Space Flight Center [see page 16]. Refer to MFS-29554

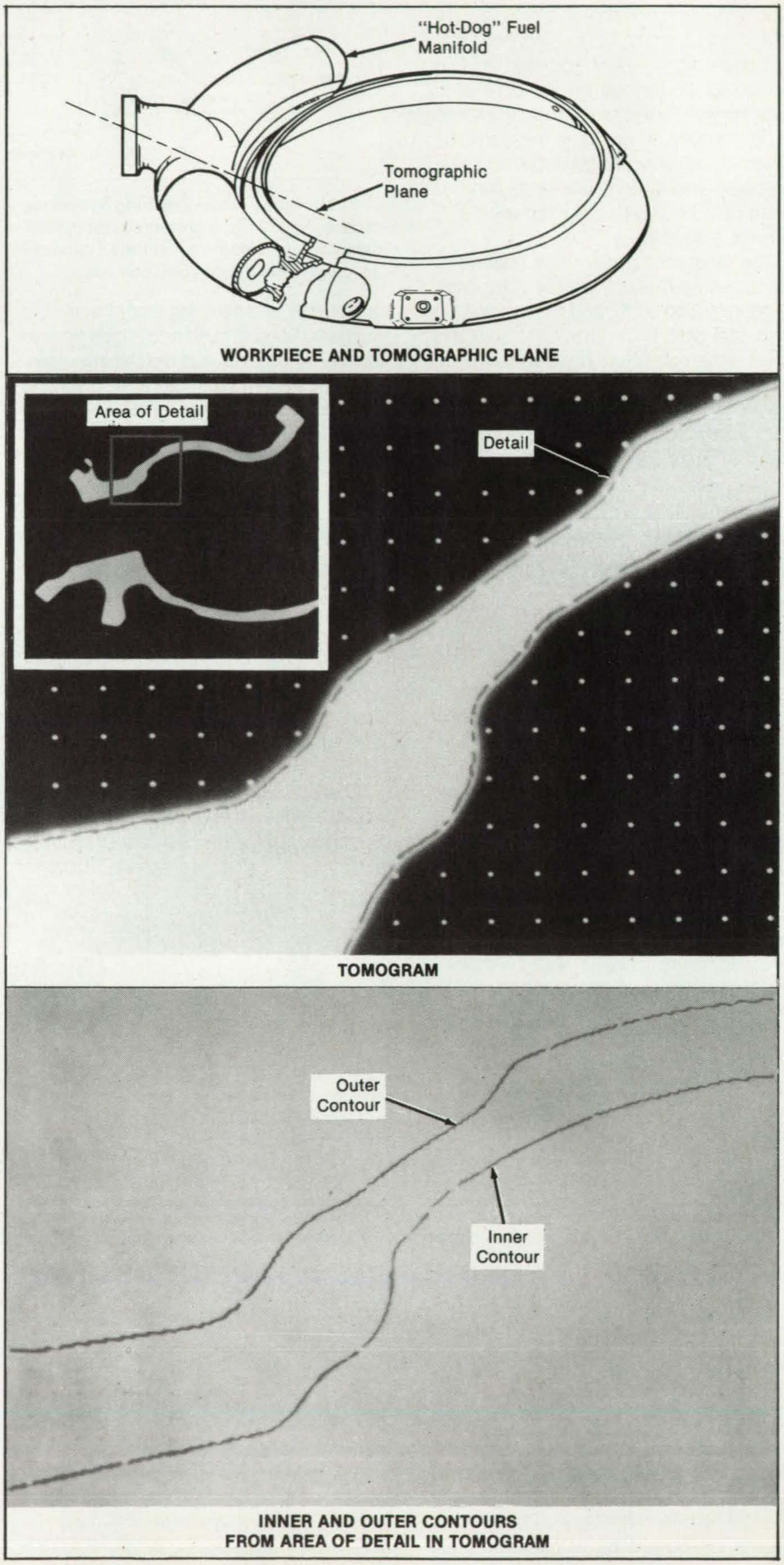

A **Cross Section of a Weld** on a manifold was made by computer tomography.

Positioning X-Ray Film Inside a Flow Splitter

A simple and inexpensive tool ensures secure placement for radiographic inspection.

Marshall Space Flight Center, Alabama

A holder places film positively and securely for x-ray inspection inside sections of tube with splitter welds. With the holder, the film can be inserted past a 90° turn in the neck to a point about 12 in. (30 cm) from the opening of the neck.

A V-shaped piece of x-ray film with an opaque cover taped on it is taped onto the scissorslike arms of the holder (see figure). The arms are squeezed together, and the holder and film are inserted into the opening. The holder is equipped with a magnet, and a magnet on the outside of the neck is used to pull the holder and film along the inside of the neck.

As the arms leave the neck and enter the larger-diameter tube beyond it, the spring action of the film opens the film and arms. The film is thus placed snugly against the welded seams in the tube. The film is exposed to x rays from an external x-ray generator, creating images of the weld(s).

This work was done by Charles Darter and Darryl Pierce of Rockwell International Corp. for **Marshall Space Flight Center**. *No further documentation is available.*
MFS-29322

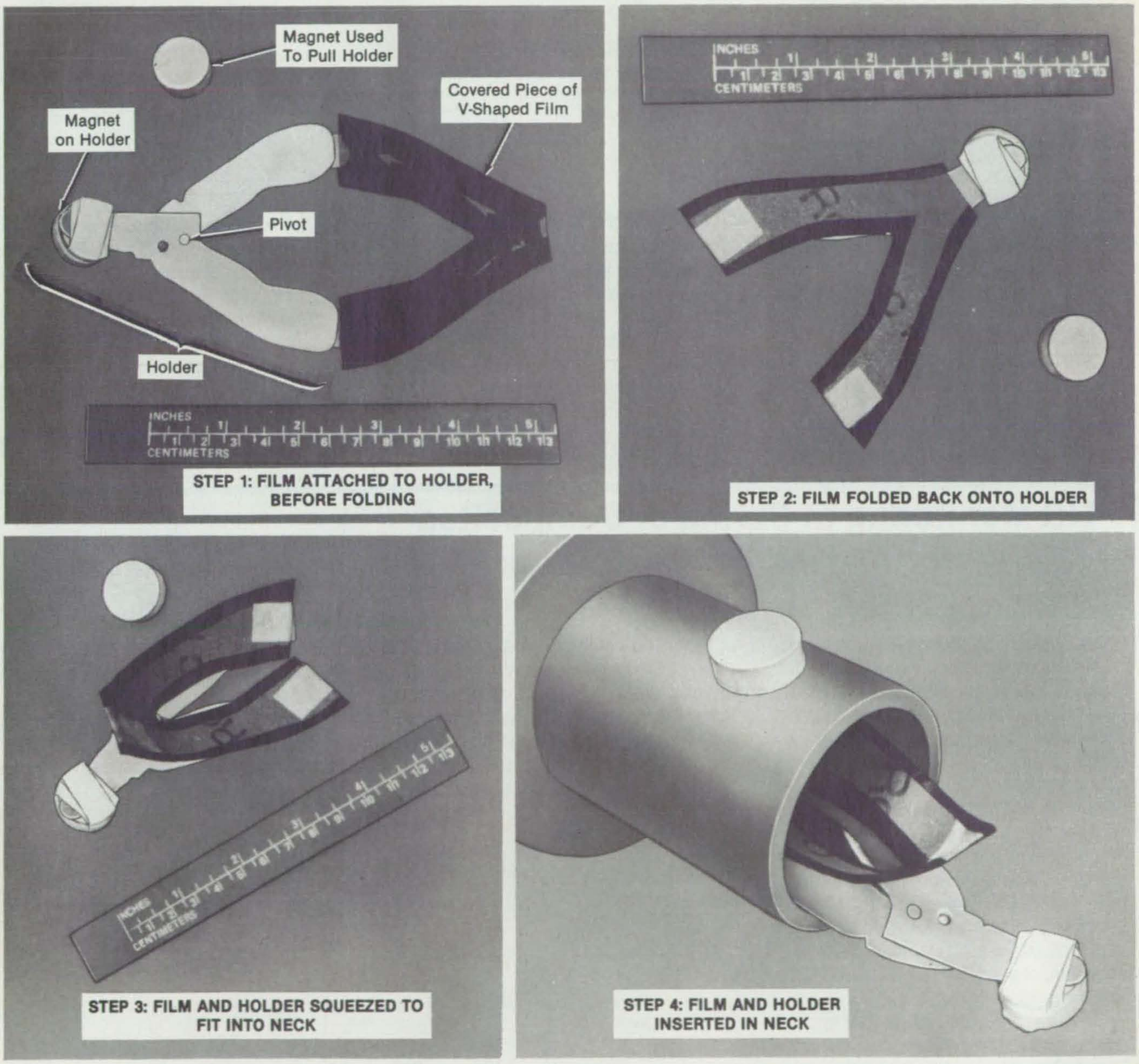

The **V-Shaped Piece of Film** fits on the arms of the holder (top). With the arms squeezed together, the holder is inserted in the opening of the neck (bottom). The arms of the holder are cut from 0.020-in. (0.51-mm) thick stock of unspecified material.

Simple Regulator for Positive-Pressure Glove Box

A capacious inflated bag absorbs transient pressure changes.

NASA's Jet Propulsion Laboratory, Pasadena, California

A weighted, inflated bag regulates the pressure in a positive-pressure glove box such as those used to manipulate samples in an atmosphere isolated from such contaminants in the open air as moisture or oxygen.

With this simple pressure regulator, sensitive materials can be manipulated in a dry or inert atmosphere without danger of overpressure when a technician inserts hands in the gloves, or of underpressure — and inward leakage of air — when the technician draws hands out of the gloves. The inflated-bag regulator can replace an elaborate system of pressure-activated valves. It is quieter, cheaper, and more reliable.

The bag, which can be a rubber raft or innertube of a truck tire, for example, is mounted over the glove box and connected to the box by a hose and valve (see figure). The bag is partially inflated and maintained at a constant positive pressure by a cover and weight resting on it.

When the box is not in use, its internal pressure extends the gloves outward. When the technician places hands and arms in the gloves and forces them into the box, gas flows from the box into the bag so that the pressure in the box does not rise excessively. When the technician finishes work and withdraws hands and arms, gas flows from the bag into the box to prevent the pressure in the box from dropping suddenly.

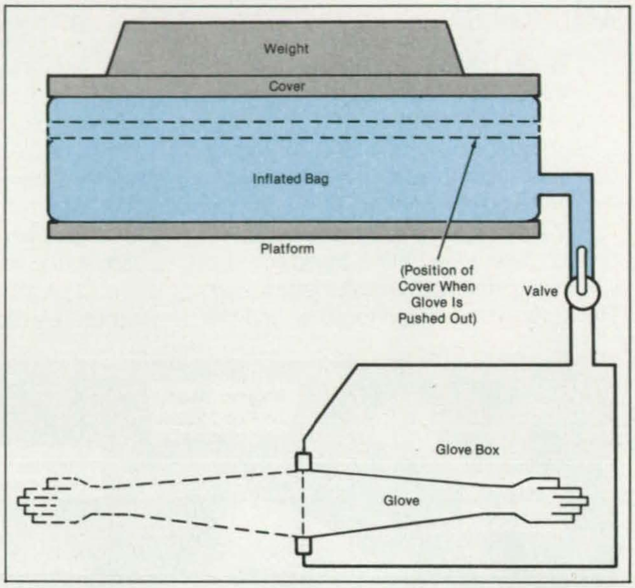

The **Weight Atop the Inflated Bag** rises and falls as gas flows into and out of the bag from the glove box. Positive pressure relative to the surroundings pushes the gloves outward when they are not being used (dashed line). To manipulate items in the box, the technician forces the gloves inside (solid line).

When the gas in the box is circulated continuously to purge it of moisture or oxygen, the bag can be included in the circuit. The bag and box would then have two connecting ducts so that both volumes were included in the purging cycle.

This work was done by Paul J. Shlichta of Caltech for **NASA's Jet Propulsion Laboratory**. *For further information, Circle 11 on the TSP Request Card.*

This invention is owned by NASA, and a patent application has been filed. Inquiries concerning nonexclusive or exclusive license for its commercial development should be addressed to the Patent Counsel, NASA's Resident Office-JPL [see page 16]. Refer to NPO-17786.

FTIR Monitoring of Curing of Composites

The FTIR spectrum is obtained with an embedded fiber optic sensor.

Langley Research Center, Hampton, Virginia

The repeatable processing and manufacture of advanced composite materials is perhaps the major obstacle to the widest possible acceptance of resin/matrix composites as materials for structural elements of aircraft. Considerable research and development efforts have been expended to improve the quality of this class of materials. Current sensor technology for monitoring the curing of composites, based primarily on dielectric or ultrasonic principles, involves the measurement of such secondary effects as dielectric losses or ultrasonic attenuation in matrix resins. The chemistry of a matrix resin is inferred from these effects.

An infrared-sensing optical fiber system has been developed to monitor principal infrared absorption bands that result from the vibrations of atoms and molecules as chemical bonds form when a resin is cured. Thus, this system monitors the resin chemistry more directly.

The optical fiber is embedded in the sample to be analyzed (see figure). A small portion of the cladding of the optical fiber is removed to make contact with the sample. Infrared radiation passes through the fiber from which the sample absorbs selected wavelengths via an attenuated reflection mechanism. The radiation that leaves the fiber thus contains optical information about the sample. Fourier transformation of this information produces an infrared spectrum.

The system has been used to obtain the Fourier transform infrared (FTIR) spectrum from a graphite fiber/polyimide matrix resin prepreg. A chalcogenide fiber that had a

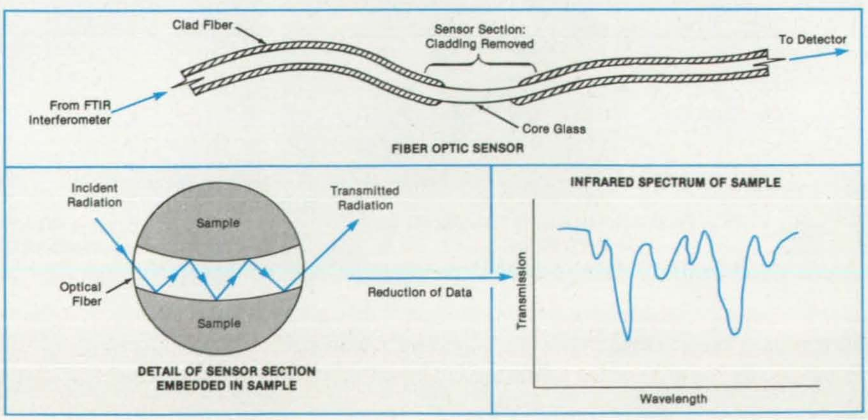

The **Embedded Fiber Optic FTIR Sensor** is used to indicate the state of cure of a thermosetting composite material.

length of 3 m and an outside diameter of 0.1 mm was used to carry the infrared beam outside an FTIR spectrometer optical bench and return it. Readily interpretable spectra were obtained during a simulated curing cycle.

By the use of sensors of this type to monitor the curing of advanced composite materials, feedback to control manufacturing processes should be possible. While this sensor was developed primarily to improve the quality of advanced composites, many additional potential applications exist because the principle of operation is applicable to all organic materials and most inorganic gases. These applications include monitoring the integrities of composite materials in service, the remote sensing of hazardous materials, and the examination of processes in industrial reactors and furnaces.

This work was done by Mark A. Druy of Foster-Miller, Inc., William A. Stevenson of IRIS Fiber Optics, Inc., and Philip R. Young of **Langley Research Center**. *For further information, Circle 158 on the TSP Request Card.* *LAR-14040*

Polishing Difficult-to-Reach Cavities

A flexible abrasive tool conforms to the cavities.

Marshall Space Flight Center, Alabama

A springy abrasive tool can be used to finish the surfaces of narrow cavities that have been made by electrical-discharge machining. This special tool is needed because such cavities are inaccessible or at least difficult to reach with most surface-finishing tools.

The tool is mounted on a vibrator on a robot arm (see figure). It is equipped with fingers that match the contour and length of the cavities to be polished. The fingers are made of polytetrafluoroethylene in which abrasive particles are embedded. As the fingers are vibrated, they remove material from the walls of the cavities.

The vibrator moves the abrasive around the cavities. The robot arm moves the vibrator around the circumferences of the cavities in an orbiting motion. As material is removed, the robot arm moves outward to maintain contact between the abrasive and the walls of the cavities.

This work was done by R. Michael Malinzak and Gary N. Booth of Rockwell International Corp. **Marshall Space Flight Center**. *For further information, Circle 77 on the TSP Request Card.* *MFS-29592*

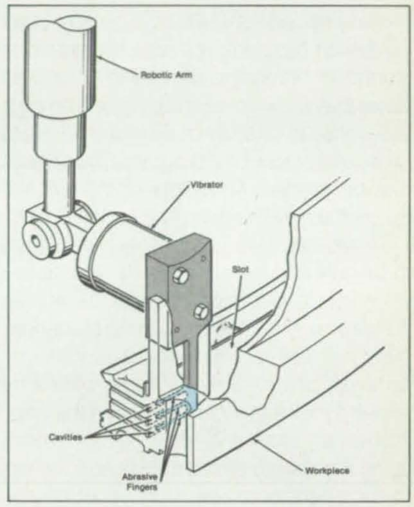

The **Robot Arm Moves the Vibrator** around the perimeters of the cavities, polishing the walls of the cavities as it does so. The procedure eliminates roughness resulting from electrical-discharge machining.

Mathematics and Information Sciences

Hardware, Techniques, and Processes
64 Scaled Ellipses for Computer-Aided Design

Books and Reports
64 Minimum-Time Slewing of Space Infrared Telescope
66 Random-Field Estimation for Dynamics of Robots
66 Locating a Planar Target From an Image

Computer Programs
40 Software for Least-Squares and Robust Estimation
41 Design-Tradeoff Model for Space Station
42 An Ada Linear-Algebra Software Package Modeled After HAL/S
44 CYBER-205 Devectorizer

Scaled Ellipses for Computer-Aided Design

A selection of rotatable ellipses helps designers draw circular features in isometric views.

Marshall Space Flight Center, Alabama

An addition to CAD-PACK, a computer-aided design program, speeds preparation of isometric drawings, particularly cutaway views that show bores and threads. The addition consists of a set of 50 scaled ellipses on detail pages of the program. The ellipses can be rotated. The sizes of the ellipses range from 1/8 to 4 in. (3.2 to 101.6 mm).

Previously, it was necessary to construct three orthographic views of a feature before edge lines could be selected for the isometric drawing — a time-consuming procedure. Now, with the set of ellipses, a user selects an ellipse of the appropriate size, rotates the ellipse as necessary, and draws on the video screen an isometric view of the feature, using the rotated ellipse (see figure). An isometric-orientation cube in the upper left corner of the screen helps the user choose the correct rotation.

The designer can, if necessary, erase the major- and minor-axis lines on the ellipse and repeat the process with succeeding elipses, until the threaded cutaway is complete.

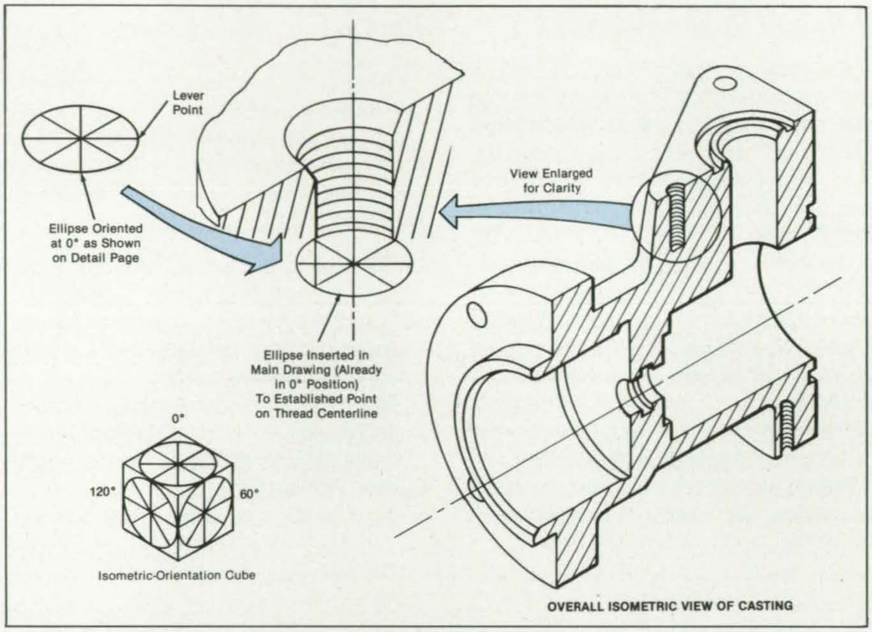

The **Designer Selects an Ellipse**, rotates it, and draws a feature (here, a threaded hole in a casting). The designer then erases reference lines on the video screen.

This work was done by Anthony J. Schembri of Rockwell International Corp. for **Marshall Space Flight Center**. *For further information, Circle 86 on the TSP Request Card. MFS-29629*

Books and Reports

These reports, studies, handbooks are available from NASA as Technical Support Packages (TSP's) when a Request Card number is cited; otherwise they are available from the National Technical Information Service.

Minimum-Time Slewing of Space Infrared Telescope

A "bang-bang" control algorithm is formulated.

A report discusses the formulation of an algorithm to be used in pointing the proposed Space Infrared Telescope Facility at various celestial objects. The control system of the telescope is required to aim and keep the telescope aimed within 0.15 arc second of an intended target. In addition, it is required to perform 120° slews in 8 min and 7.5-arc-minute nods (a nod is a small-angle slew) within 20 s. This study concentrates on the nod maneuver. The spacecraft is represented mathematically as a rigid body plus several bending modes.

Feedforward torquing is needed because the maximum torque available from the usual actuators is severely limited in comparison with the moment of inertia of the spacecraft. Rather than select an arbitrary torque profile and postpone the stabilization of higher-order modes to the end of the maneuver, this study seeks to determine the torque as a function of time that will maneuver the spacecraft and simultaneously reduce the contributions of the modes to a specified level; the most efficient use of the torque is sought by solving a minimum-time optimal-control problem. Given an initial state or estimate of the state of the spacecraft, the torque-versus-time history for slewing can then be predicted. Feedback can also be determined by constructing switching curves.

The equations of rotation and vibration are written for a flexible spacecraft with M bending modes; expressions for the open-loop control and the adjoint variables of the Hamiltonian formulation of mechanics are derived. These are integrated analytically and expressed in terms of the time-to-go to termination. The minimum-time control strategy turns out to be "bang-bang"; that is, to involve the sequential turning on, turning off, or reversal of torques (but no smooth transitions to intermediate torques) during each maneuver.

These results are applied to analyze a nod maneuver of a model with a single flexible mode. The torque-switch curves are computed for representative parameters. The first reversal or other switch of torque designed to decelerate to the final angular position can occur over a wide range of time. Subsequent switches are of the order of a half period of the flexible mode apart in time.

This work was done by N. Rajan of Sterling Software for **Ames Research Center**. *To obtain a copy of the report, "Minimum Time Slewing of the SIRTF Spacecraft," Circle 146 on the TSP Request Card.*
ARC-12155

Random-Field Estimation for Dynamics of Robots

Random field models lead to a new and faster class of robot-dynamics algorithms.

A report discusses the use of random-field mathematical models as alternatives to deterministic models of classical mechanics to describe the dynamics of robot arms. These alternative models can be used to establish a relationship between the methods of estimation theory and robot dynamics. This approach yields a new class of algorithms that perform computations typical of estimation theory to solve such fundamental problems in robotics as forward and inverse dynamics and inverse kinematics.

The mathematical development begins with a state-space model of the bodies in a multibody system (more specifically, the links in a robot arm). The inertial forces in the system are represented by a spatially distributed mean bias force with superimposed white noise. The covariance of the inertial force is set equal to the load spatial inertia. The output of the system and of this mathematical model is defined as the vector of torques exerted by external sources acting at the joints in the robot arm.

The kinetic energy of the system is then expressed in terms of the vector of joint-angle velocities and a transformed version of the spatial inertia called the "composite multibody inertia matrix." This leads to one of the central findings in the report: namely, that the covariance matrix of the output equals the composite multibody inertia matrix. This is important because, as a result, the inertia matrix can be factored and inverted by use of techniques already developed for the factoring and inversion of covariance matrices. In particular, previous work has shown that the difference equations of Kalman filtering and smoothing can be used to factor and invert recursively the covariance of the output of a linear state-space system driven by a white-noise process. In this report, it is shown that similar recursive techniques can be used to factor and invert the composite multibody inertia matrix.

The random-field models are easy to describe and are based on the assumption that all of the inertial (D'Alembert) forces in the system are represented by a spatially distributed white-noise mathematical model. This differs from the more common methods of classical mechanics, which typically require extensive derivation and manipulation of equations of motion for complex mechanical systems. By use of the spatially random models, locally specified computations that are more primitive (in the sense that they are simpler and less dependent on mathematical derivations) result in a global collective behavior of the system (as represented by the inertia matrix) equivalent to that obtained with deterministic models.

This work was done by Guillermo Rodriguez of Caltech for **NASA's Jet Propulsion Laboratory**. *To obtain a copy of the report, "Random Field Estimation Approach to Robot Dynamics," Circle 106 on the TSP Request Card.*
NPO-17788

Locating a Planar Target From an Image

Tests of two algorithms are described.

A report describes experiments to test two algorithms that are being considered for use in the automatic control of robots and remote manipulators. Typically, a solid-state video camera mounted on the end effector of the manipulator or robot would view the target, which would be part of the object to be manipulated. After suitable processing of the image in the camera to extract the target points, one of the algorithms would use the target points to determine the position and orientation of the target with respect to the camera and, therefore, with respect to the end effector. The control system of the robot or manipulator would use this information to guide the end effector toward the position and orientation for grasping the object.

Target points are selected features (e.g., boltheads and boltholes) of known shape and location, forming a convex polygon on a planar or nearly planar surface of the object to be manipulated. The preliminary analysis of the image data yields the location of perspective projection of the target points on the image plane of the sensor via moments of these features in the image. The problem to be solved by either algorithm is to compute the position and orientation of the target surface by comparing the projected image of the points defining the polygon with the image of an identical polygon undistorted by the displacement of position and orientation.

One algorithm is based on the quadrangle-projection method, which involves the use of four target points that lie at the corners of a quadrangle. In this method, the system of equations for the projection of the quadrangle on the image plane is solved, yielding explicit equations for the position and orientation vectors as functions of the locations of the target points in the image.

The other algorithm is based on the elastic-matching ("rubber-mask") approach, in which a reference image is warped to conform to the actual image. The reference image is represented by a system of pairs of equations in which each pair represents a linear combination of patterns that a point in the reference image can occupy in moving to a point in the actual image. The amount of displacement each pattern contributes to the distortion is determined by identifying the values of parameters associated with each of the distortion patterns. These values are derived by minimizing the absolute differences between corresponding reference and actual image points without violating the pattern constraints. This type of problem is easily modeled mathematically by use of the linear programming technique of goal programming.

The experiments were performed with a solid-state camera viewing a planar target from a six-degree-of-freedom robotic end effector. The rotational and translational accuracies of both algorithms were tested at various ranges representative of the sensing requirements involved in a typical telerobot target-acquisition task. Both algorithms determined the position and orientation of the target with an accuracy sufficient for consistent and efficient acquisition by a telerobot.

This work was done by Karin Cornils and Plesent W. Goode of **Langley Research Center**. *For further information, Circle 15 on the TSP Request Card.*
LAR-14128

Life Sciences

Hardware, Techniques, and Processes

67 Growing and Assembling Cells Into Tissues

Growing and Assembling Cells Into Tissues

A process and apparatus provide minimal fluid shear stress.

Lyndon B. Johnson Space Center, Houston, Texas

A laboratory process for the growth and assembly of mammalian cells into tissue-like masses has been demonstrated with hamster and rat cells. In comparison with other processes tried before, the new process is better able to provide a culture environment with reduced fluid shear stress, freedom for three-dimensional spatial orientation of particles suspended in the culture medium, and localization of particles of different or similar sedimentation properties in a similar spatial region.

In a representative version of the process, the cells are grown on carrier beads suspended in the flowing culture medium in a rotating-wall, vaned bioreactor vessel (see figure). The rate of rotation is adjusted to provide the requisite sedimentation characteristics and stirring of the medium without introducing excessive turbulence. This feature is particularly important because turbulence and the resultant fluid shear stress can damage the delicate mammalian cells and/or prevent the desired aggregation of cells.

The vessel rotates about a horizontal axis. The paths of cells, carrier beads, and tissues depend on the rate of rotation, gravitation, rates of sedimentation, dimensions of the vessel, and the flow of the culture medium. The rate of rotation can be adjusted in combination with the choice of carrier beads and their sedimentation properties in such a way that particles initially close to each other remain fairly close for relatively long times (up to several hours). The time of proximal suspension is thus extended in comparison to what it would be in a more-primitive culture vessel (e.g., a static or spinner flask or a conventional bioreactor). This promotes the growth of individual cells in proximity, allowing the expression of cellular functions at nearly tissuelike density.

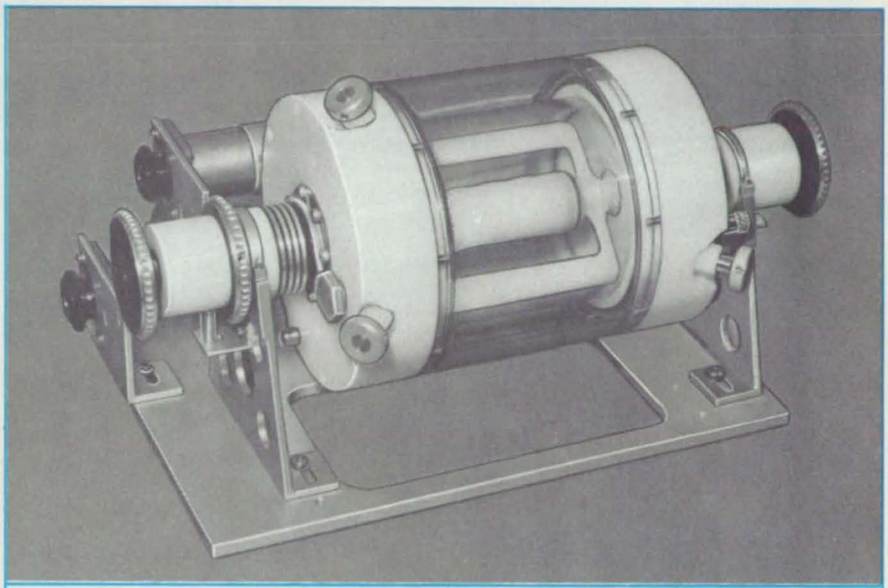

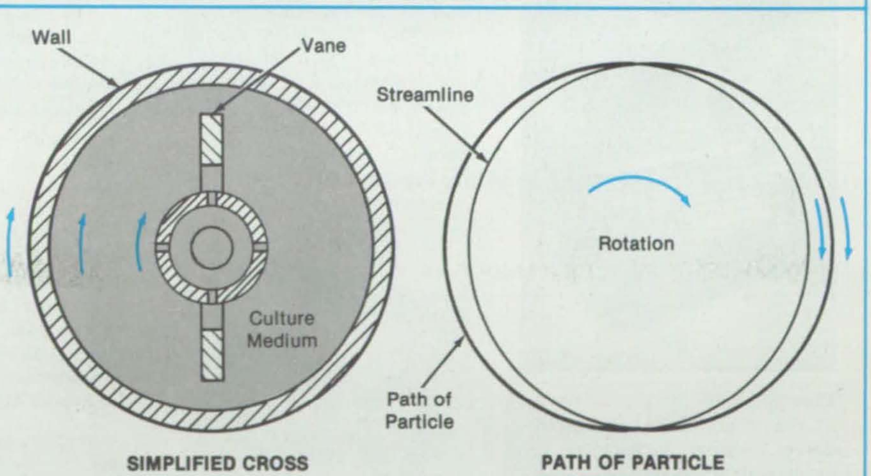

The **Rotating-Wall, Vaned Vessel** provides a low-fluid-shear environment conducive to the growth and aggregation of cells suspended on carrier beads in the growth medium.

The pH, oxygen content, nutrient contents, temperature, rate of flow, and other parameters of the culture medium are controlled as in other bioreactor systems to optimize the conditions for growth and to remove metabolic waste products. With suitable adjustments of all parameters, three-dimensional aggregates of cells can be grown. Slight but significant modifications of cell-feeding regimes and adjustments of the microenvironments of the cells are expected to enhance the controllability of sizes and structures in tissue-like masses.

This work was done by David A. Wolf of **Johnson Space Center** *and Ray P. Schwarz, Marian L. Lewis, John H. Cross, and M. Helen Huls of KRUG International.*

For further information, Circle 63 on the TSP Request Card.

This invention is owned by NASA, and a patent application has been filed. Inquiries concerning nonexclusive or exclusive license for its commercial development should be addressed to the Patent Counsel, Johnson Space Center [see page 16]. Refer to MSC-21559.

New on the Market

3D-CAM Inc., Canoga Park, CA, has developed a **stereolithography technique** which forms plastic models or parts from CAD-generated graphics in a liquid photo-polymer resin, using laser beams. Depending on prototype size and complexity, the process can take as little as a few hours. 3D-CAM's engineers can computer-design a part or prototype, then produce it using equipment from 3D Systems. Or the part can be formed, with a 24-hour turnaround, directly from the customer's design on compatible software, including ACAD, ANVIL, ARIES, AUTOSOLID, and HP ME SERIES 30.
Circle Reader Action Number 790.

ZEOS International, Ltd., St. Paul, MN, has introduced a lightweight **notebook computer** based on Intel's 80286 microprocessor. Retailing for $1995, it weighs less than seven pounds and includes one megabyte of memory, a VGA display, a 20 megabyte hard disk drive, and a 1.44 megabyte floppy drive. Other features include a snap-in, snap-out battery and an 82-key keyboard with 101-key emulation and industry-standard I/O port connectors.
Circle Reader Action Number 800.

Elmwood Sensors Inc., Pawtucket, RI, has introduced a line of **transparent resistive touchscreens** featuring custom surface treatments for commercial, industrial, and military applications. Available in flat and curved configurations, the touchscreens are made of high-quality, rugged thermoplastics or glass/thermoplastic combinations. Both analog and matrix touchscreen panels are available. Elmwood also offers contrast enhancement filters to optimize light transmission and screen definition, as well as anti-glare and abrasion-resistant coatings developed for aerospace applications.
Circle Reader Action Number 792.

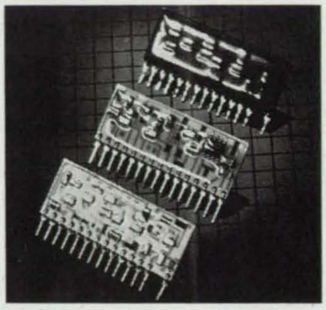

Emerson & Cuming, Inc., Woburn, MA, has developed a family of **silicone resin based, 100 percent solids conformal coatings** for use on printed circuit boards and hybrid circuitry. The UNICOAT™ coatings are able to cure at room temperature or with heat application, and can withstand operating temperatures ranging from -45° to +155° C. They are environmentally safe and do not emit acetic acid or other byproducts which can interfere with proper functioning of electrical/electronic devices or components.
Circle Reader Action Number 798.

A **voice input/output system** which provides voice recognition of 1000 words with accuracy better than 98 percent, and unlimited text-to-speech synthesis, has been introduced by Voice Dynamics Corp., Irvine, CA. MicroDyn II listens to command or data input, then responds by sending keystrokes via the serial port, and text to the onboard synthesizer for audio prompting and verification. It provides DOS compatibility for use with IBM XT, AT, 386, or PS/2 Micro Channel computers.
Circle Reader Action Number 794.

The 900A **solder system tester** from Tegam Inc., Madison, OH, checks all makes of soldering irons with 0.15 percent accuracy on temperature, one percent accuracy on 2 and 20 ohms tip to ground resistance, and one percent accuracy on AC or AC+DC volts. Its "Mach-1" sensor runs tip millivolts, tip resistance, and tip temperature in ten seconds. One switch selects all parameters; green and red lights instantly tell the user whether the iron passed or failed the test.
Circle Reader Action Number 796.

Sky Computers, Chelmsford, MA, has announced the first **desktop supercomputer for Sun's SPARCstation™**. Dubbed the SKYstation™, it accelerates existing applications without requiring source code modification, providing supercomputing performance - 65 MIPS and 12 Linpack MFLOPS computational speed - for under $10,000. Desktop applications include simulation, modeling, finite element analysis, seismic analysis, fluid dynamics, and chemistry.
Circle Reader Action Number 788.

Model 3000 Series **filters** from Krohn-Hite Corp., Avon, MA, can be modified to fit a wide range of applications without purchasing additional filter cards. Up to four filter channels have independently variable parameters. A push of a button allows selection for each channel of Butterworth, Bessel, Chebyshev, or RC responses with attenuation slopes from 6dB/octave to 48dB/octave in 6dB/octave steps. Cutoff frequencies are tunable from 0.001Hz to 200kHz.
Circle Reader Action Number 778.

The Turbolab **software package** developed by Scentech, Inc., Woburn, MA, enables a PC user to perform complex data analysis functions and generate printouts for documentation of experiments. It can read/display 80,000 points in less than one second. Portions of the curve can then be magnified for precise measurements and detailed explanations.
Circle Reader Action Number 780.

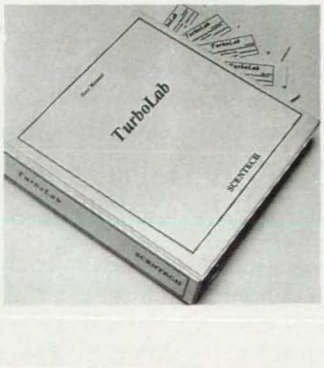

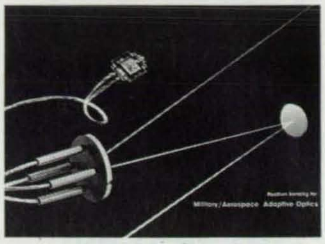

The KP-2025 **severe environment pressure sensor** from Kaman Instrumentation, Colorado Springs, CO, operates reliably from -200° to +540° C and can withstand continuous exposure to high radiation, liquid sodium, liquid nitrogen, plastics, petrochemicals, and high-temperature steam. The 0.25" diameter sensor is half the size of other miniature sensors, and can be mounted mechanically or welded to optional adapters.
Circle Reader Action Number 786.

Providing a full range of 3D capabilities, the MICRO CADAM 3D **integrated 3D software package** from CADAM, Burbank, CA, integrates the functions for working with wireframe, surfaces, and solids in a single module, eliminating the need for switching between different software products or user interfaces. MICRO CADAM 3D displays fully-shaded, high-definition images of both surfaces and solids. Users can create and save 3D "details" of a drawing; copies of collections of 3D geometry and text can be associative with the master version, immediately reflecting any changes to the master.
Circle Reader Action Number 782.

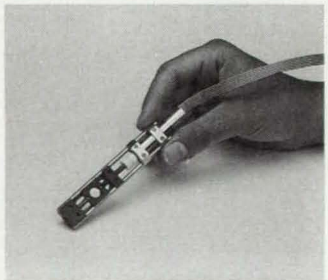

The model MM-3M **motorized micro-mini stage** from National Aperture, Inc., Windham, NH, weighs 2 ounces and measures .66" × .29" × 4.38" (stage with encoder). Standard travel is .5" with straightness and wobble within ±1 micron total deviation. Models are available with either a 16:1 gearhead, which produces a stage travel of 3.5mm/sec with an encoder of .6 micron per count, or a 64:1 gearhead, which produces a travel of 1.5mm/sec and .15 micron per count.
Circle Reader Action Number 784.

New Literature

Mack Molding Company, Arlington, VA, has published a 12-page brochure highlighting its **molding and manufacturing capabilities**. Starting with design and engineering services, the brochure describes the company's resources, from part design and processing recommendations to computer-aided design services, model building, and prototyping. Custom molding and finishing techniques are also discussed.

Circle Reader Action Number 713.

Designing with a Distributed-Power Architecture, from Interpoint, Redmond, WA, describes design considerations for **power systems that use board-mounted DC-to-DC converters** rather than larger bulk power supplies. The free guide discusses the overall organization of distributed power systems as well as the most effective approaches for EMI filtering and thermal management. One section describes test conditions for accurate measurement of different noise components and discusses optimal filter strategies for each. Another gives a step-by-step guide for calculating heat sink requirements.

Circle Reader Action Number 704.

CONAP, Inc., Olean, NY, has published a 20-page, full-color brochure which highlights its line of **polymer engineering materials**. The publication features CONAP's wide range of polyurethane and epoxy potting and encapsulating compounds for the electrical/electronics industry, and conformal coatings for military and commercial electronics applications. Also described are high-strength, abrasion-resistant tooling resins and elastomers, and a variety of epoxy and polyurethane adhesives and sealants for such applications as biomedicine and air and liquid filtration.

Circle Reader Action Number 706.

Perkin-Elmer's Physical Electronics Division, Eden Prairie, MN, has released a brochure describing the PHI *ACCESS* data system for **surface analysis.** The brochure describes the capabilities of PHI's menu-driven software package working in tandem with the 32-bit HP-Apollo UNIX workstation. It shows graphics of computer screens displaying "windowing" which facilitates the performance of tasks such as data massage, automated analysis, data reduction, and word processing.

Circle Reader Action Number 708.

Diamond Coating - A World of Opportunity, from Genasystems, Inc., Worthington, OH, describes uses of **manufactured diamond coatings** in industry. The brochure highlights two types of coatings or films: the chemical vapor deposition (CVD) diamond, and diamond-like carbon (DLC). It lists properties as well as potential applications.

Circle Reader Action Number 712.

A four-color brochure from Optical Coating Laboratory, Inc., Santa Rosa, CA, describes **thermal control mirrors and solar cell covers** which provide solar absorptance protection to stabilize temperature aboard a spacecraft and enable solar arrays to function more efficiently in solar power space applications. The publication features six product data sheets, each containing transmission and/or reflectance performance data in graph form and detailed specification information on material choices, coating and finishing options, physical properties, and spectral characteristics.

Circle Reader Action Number 710.

Rare Earth permanent magnet materials are presented in a four-page catalog from Recoma, Inc., Boonton, NJ. The catalog describes the various 1:5, 2:17, and temperature-compensated samarium cobalt grades as well as neodymium iron boron materials offered. Typical magnetic characteristics and second quadrant demagnetization curves are included covering the RECOMA®, REFEMA®, and UGISTAB® family of materials.

Circle Reader Action Number 702.

Subject Index of all 1990 Briefs

The following pages contain a cross-referenced index of all technical briefs published in NASA Tech Briefs during 1990 (Volume 14). The blue listings refer to briefs appearing in this issue. You can receive more information on these briefs by requesting the Technical Support Package (TSP) referenced at the end of the full-length article. For information on briefs featured in previous issues of volume 14, contact NASA's Scientific and Technical Information Facility (see page 16).

A

ABRASION
Weld-bead shaver
May page 80 MFS-29593

Ultrasonic abrasive removal of EDM recast
Oct page 97 MFS-29545

ACCELEROMETERS
Shaft-rotation detector
Aug page 33 MFS-29540

ACCESS CONTROL
Computer-access-code matrices
Apr page 82 NPO-17525

ACCUMULATOR
Two-phase accumulator
Apr page 68 MSC-21464

ACOUSTIC EXCITATION
Acoustic reduction of separation of flow
Sep page 78 LEW-14876

ACOUSTIC MEASUREMENT
Acoustic humidity sensor
Apr page 47 NPO-17685

ACTINOMETERS
Field-induced-gap infrared detectors
Mar page 32 NPO-17526

Diagnosis of a pressure-modulator-radiometer cell
Mar page 63 NPO-17528

ACOUSTIC SCATTERING
Acoustophoresis--a new separation concept
Jan page 38 LAR-13388

ACTUATORS
Electrostatic linear actuator
Mar page 87 NPO-17684

ADA (PROGRAMMING LANGUAGE)
Flight dynamics analysis system
June page 70 GSC-13163

An Ada linear-algebra software package modeled after HAL/S
Dec page 42 NPO-17985

ADAPTIVE CONTROL
Adaptive-control experiments on a large flexible structure
Mar page 78 NPO-17478

Method for model-reference adaptive control
June page 94 NPO-17717

Robust adaptive control in Hilbert space
June page 53 NPO-17588

Exponentially stabilizing robot control laws
Sep page 95 NPO-17587

Robust, high-performance control for robotic manipulators
Sep page 36 NPO-17785

Forward stochastic nonlinear adaptive control method
Nov page 95 NPO-17861

Principles and applications of dual adaptive control
Nov page 98 ARC-12310

ADHESION
Adhesion between particles and surfaces in a vacuum
Nov page 60 NPO-17743

ADHESIVE BONDING
Bonding elastomers to metal substrates
July page 82 LAR-13645

ADHESIVES
Epoxies bond waveguides to flanges
Mar page 40 NPO-17497

Polyimidazoles via aromatic nucleophilic displacement
Aug page 48 LAR-14145

Polyimides containing carbonyl and ether connecting groups
Dec page 35 LAR-14001

ADSORPTION
Concentrating gaseous contaminants for monitoring
Sep page 45 MSC-21424

AEROBRAKING
Aerobrakes for a manned Mars mission
July page 78 ARC-12117

AERODYNAMIC DRAG
Reducing aerodynamic drag of bluff bodies
Aug page 56 LAR-13768

Wing-design and -analysis code
Oct page 74 LAR-13995

AERODYNAMIC HEATING
Response of ceramic insulation to aerothermodynamic heating
May page 58 ARC-12156

Aerothermodynamic heating of a transatmospheric vehicle
June page 74 ARC-11854

AERODYNAMIC LOADS
Predicting unsteady aeroelastic behavior
Sep page 77 LAR-14130

AERODYNAMICS
Wing covers for aerodynamic studies
Jan page 65 ARC-12238

Flight dynamics analysis system
June page 70 GSC-13163

Code for analysis of wing-and-flap systems
Oct page 74 LAR-13994

Dye tracing of flow on forebody of airplane
Nov page 78 ARC-12237

AEROELASTICITY
Predicting unsteady aeroelastic behavior
Sep page 77 LAR-14130

AFFINITY
Affinity electrophoresis using ligands attached to polymers
June page 95 MFS-26049

AIR
Radiative processes in air excited by an ArF laser
Oct page 66 ARC-12136

AIRBORNE EQUIPMENT
Preliminary analysis of data from AVIRIS
Oct page 68 NPO-17622

AIR BREATHING ENGINES
Compact analyzer/controller for oxygen-enrichment system
June page 50 LAR-14016

AIRCRAFT CONTROL
Stochastic feedforward control technique
May page 92 LAR-13796

AIRCRAFT INSTRUMENTS
System predicts critical runway performance parameters
Nov page 40 LAR-13809

AIRCRAFT NOISE
Stowable mechanical sound suppressor
Mar page 86 LAR-14158

AIRCRAFT TIRES
Measurement of water sprays generated by airplane tires
Sep page 70 LAR-14030

AIR DUCTS
Remotely-controlled variable-orifice valve
June page 75 MFS-28369

AIR FLOW
Simulated hypersonic flows about a blunt body
July page 74 ARC-12251

AIRFOILS
Acoustic reduction of separation of flow
Sep page 78 LEW-14876

Comparison of calculations of viscous transonic flow
Oct page 85 ARC-12192

AIR PURIFICATION
Stability of a carbon-dioxide-removing resin
July page 59 ARC-12129

AIR SAMPLING
Venturi air-jet vacuum ejector for sampling air
Oct page 86 LAR-14024

AIRSPEED
Air-velocity sensor for helicopter
July page 39 LAR-13598

AIR TRAFFIC
Details of collision-avoidance study
Nov page 48 ARC-12396

Evaluation of an aircraft-collision-avoidance system
Nov page 47 ARC-11367

AIR TRAFFIC CONTROL
Algorithm schedules airplane landings
June page 92 ARC-12197

ALGEBRA
Algebraic generation of two-dimensional grids
Mar page 69 LAR-13800

ALIGNMENT
Quick check of butt-weld alignment
Mar page 69 MFS-29423

ALGORITHMS
Improved coupled fluid/structural dynamical model
Jan page 54 MFS-29439

Performances of fixed-lag phase-smoothing algorithms
Jan page 73 NPO-17202

Differential sampling for fast acquisition of frequency
Apr page 79 NPO-17358

Pipeline time- and transform-domain Reed-Solomon decoders
May page 94 NPO-17510

Algorithm for "bang-bang" control laws
July page 112 NPO-17603

Spectral analysis of linear, shift-invariant interpolants
Aug page 67 LAR-13751

Locating a planar target from an image
Dec page 66 LAR-14128

ALLOYS
Directional solidification of monotectic alloys
Sep page 61 MFS-26080

Making self-lubricating parts by powder metallurgy
Sep page 63 LEW-14902

Calculating masses, densities, and compositions of alloys
Oct page 73 LEW-14914

Heat- and oxidation-resistant electrodes
Dec page 34 NPO-17156

TAZ-8A alloy increases the thermal endurance of steel
Dec page 32 LEW-14280

ALUMINUM ARSENIDES
AlAs diffusion/Schottky barrier on GaAs
July page 30 NPO-17796

ALUMINUM COATING
Polytetrafluoroethylene-impregnated anodization for aluminum
Nov page 63 MFS-27229

ALUMINUM GRAPHITE COMPOSITES
Lightweight, thermally conductive composite material
Mar page 66 LEW-14814

AMMETERS
Small, lightweight welding-current indicator
July page 32 MFS-29622

AMORPHOUS MATERIALS
Absorption of gases by glassy polymers
Feb page 45 NPO-17636

Cell model of a disordered solid
Feb page 40 NPO-17217

AMORPHOUS SILICON
Detection of gas-phase polymerization in SiH4 and GeH4
July page 47 NPO-17779

AMPLIFIERS
32-GHz wideband maser amplifier
Mar page 38 NPO-17558

External Peltier cooler for low-noise amplifier
Nov page 26 MSC-21422

ANALOG TO DIGITAL CONVERTERS
Portable high-frequency data-acquisition system
Jan page 30 MSC-21521

Enhanced data-acquisition system
May page 36 MSC-21598

ANALYSIS (MATHEMATICS)
Hypercube-computer analysis of electromagnetic scattering
Jan page 33 NPO-17551

Spectral analysis of linear, shift-invariant interpolants
Aug page 67 LAR-13751

ANIMATION
Fast,real-time, animated displays
July page 40 LAR-14140

Collection of software for computer graphics
Aug page 52 ARC-12350

Flexible animation computer program
Sep page 68 LAR-14102

ANODES
Finding platinum-coating gaps on titanium anodes
Feb page 46 MFS-29389

ANODIC COATING
Polytetrafluoroethylene-impregnated anodization for aluminum
Nov page 63 MFS-27229

ANTENNA ARRAYS
Printed-circuit cross-slot antenna
Feb page 26 NPO-17706

Imaging antenna structure for submillimeter wavelengths
Aug page 24 NPO-17799

More about lens antenna for mobile/satellite communication
Sep page 33 NPO-17680

ANTENNA FEEDS
Array feed to compensate for distortion in antenna
Apr page 38 NPO-17667

Rain-blowing plenum for antenna feed horn
Nov page 36 NPO-17493

ANTENNA RADIATION PATTERNS
Interpolation and FFT of near-field antenna measurements
Feb page 44 NPO-17597

Automatic range changer for SWR meter
Aug page 18 NPO-17822

ANTENNAS
Algorithm for control of large antenna
Feb page 64 NPO-17482

Wideband microstrip antenna-feeding array
Mar page 26 NPO-17548

Optical detection of deformations of an antenna
May page 38 NPO-17677

Dielectric-filled paraboloidal front ends
Sep page 24 NPO-17802

Planar microstrip Yagi antennas
Sep page 18 NPO-17873

ANTIFRICTION BEARINGS
Corrosion-resistant ball bearings
Dec page 46 MSC-21319

APPROXIMATION
Truncation of images for correlation
Aug page 68 NPO-17847

ARCHITECTURE (COMPUTERS)
Master/programmable-slave computer
Oct page 50 MSC-21550

Generating semi-Markov models automatically
Nov page 71 LAR-14193

ARC JET ENGINES
Analysis of used arc-jet electrodes
Dec page 30 NPO-17575

ARC WELDING
Development of advanced welding control system
Jan page 64 MFS-26106

Camera would monitor weld-pool contours
Jan page 26 MFS-29450

Physics of variable-polarity plasma arc welding
Feb page 60 MFS-27207

Calibration fixture for welding robot
Apr page 72 MFS-29548

Internal filler-wire feed for arc welding
Apr page 75 MFS-29491

Internal wire guide for gas/tungsten-arc welding
Apr page 76 MFS-29489

Optical arc-length sensor for TIG welding
Apr page 72 MFS-29497

Monitoring both sides of a weld in progress
Sep page 84 MFS-28389

Arc reflector for welding ducts
Oct page 89 MFS-29640

ARGON LASERS
Radiative processes in air excited by an ArF laser
Oct page 66 ARC-12136

ARRAYS
Wideband microstrip antenna-feeding array
Mar page 26 NPO-17548

Optimization of array of laser retroreflectors
Dec page 31 NPO-17778

ARRIVALS
Algorithm schedules airplane landings
June page 92 ARC-12197

ARTERIES
Flows in model human femoral arteries
Jan page 76 NPO-17599

Ultrasonic imaging of deep arteries
Oct page 54 NPO-17439

ARTIFICIAL INTELLIGENCE
Automatic monitoring of complicated systems
Mar page 100 NPO-17409

Software for development of expert systems
June page 86 NPO-17536

Using expert systems for computational tasks
Nov page 96 ARC-12137

ASTROMETRY
Astrometric telescope facility for the Space Station
July page 52 ARC-11842

ASTRONOMICAL SATELLITES
Minimum-time slewing of space infrared telescope
Dec page 64 ARC-12155

ASTRONOMY
Computing orbital viewing parameters
Jan page 46 GSC-13083

ATMOSPHERIC COMPOSITION
Measuring concentration of ozone automatically
June page 60 ARC-12230

ATMOSPHERIC TURBULENCE
Noncoherent combination of optical-heterodyne outputs
Oct page 55 NPO-17693

ATOMIC CLOCKS
Linear ion trap for atomic clock
Sep page 44 NPO-17758

ATTITUDE CONTROL
Laws for stable control of orientation
Aug page 69 NPO-17790

Liquid-ring attitude-control system for spacecraft
Sep page 82 NPO-17485

Thrust-vector deflectors for spacecraft
Sep page 81 MSC-21672

AUTOCLAVING
Process for autoclaving HMW PMR-II composites
Sep page 64 LEW-14839

AUTOMATA THEORY
Probabilistic determination of motions of robots
July page 111 NPO-17738

AUTOMATIC CONTROL
Designing digital control systems with averaged measurements
May page 42 MFS-28362

Software for numerically controlled matching
May page 62 GSC-13214

Forward stochastic nonlinear adaptive control method
Nov page 95 NPO-17861

Principles and applications of dual adaptive control
Nov page 98 ARC-12310

AUXILIARY POWER SOURCES
Mobile centers for secondary power distribution
June page 28 KSC-11410

Mobile uninterruptible power supply
June page 34 KSC-11409

AVIONICS
Using expert systems for computational tasks
Nov page 96 ARC-12137

AXIAL FLOW PUMPS
Back-to-back, counterrotating turbopumps
May page 76 MFS-28349

AZIMUTH
Algorithm for control of large antenna
Feb page 64 NPO-17482

B

BACKGROUND NOISE
Low-noise, long-life, high-gain microchannel-plate glass
Aug page 47 LAR-14010

BACKSCATTERING
Viewing integrated-circuit interconnections by SEM
Sep page 18 NPO-17635

BACKUPS
Preventing contamination in electron-beam welds
Mar page 90 MFS-29428

Mobile uninterruptible power supply
June page 34 KSC-11409

BACTERIA
Indicator for pseudomonas bacteria
Oct page 101 NPO-17653

BALL BEARINGS
Vibrations caused by cracked turbopump bearing race
Apr page 71 MFS-29656

Silicon nitride balls for cryogenic bearings
July page 63 MFS-29613

Testing bearing balls for ignition in liquid oxygen
July page 75 MFS-29410

Ball-pass cage-modulation detector
Aug page 32 MFS-29539

Identifying bearing balls with radioisotopes
Nov page 91 MFS-29724

Corrosion-resistant ball bearings
Dec page 46 MSC-21319

BALLOONS
Two tethered balloon systems
Feb page 39 LAR-13837

BARS
Delamination analysis of composite curved bars
Oct page 71 ARC-12347

BEACONS
Digital controller for emergency beacon
May page 43 LEW-14857

BEAMS (RADIATION)
Beam stop for high-power lasers
Dec page 28 NPO-17465

BEARINGS
Using ruby balls as fiducial marks
Jan page 54 MFS-29394

Rolling-contact spalling in bearings
Mar page 81 MFS-27201

Ball-pass cage-modulation detector
Aug page 32 MFS-29539

Damping seals and bearings for a turbomachine
Sep page 80 MFS-28345

Computing flows in turbine end bearings
Dec page 54 MFS-29681

Corrosion-resistant ball bearings
Dec page 46 MSC-21319

New materials and treatments for turbopump bearings
Dec page 36 MFS-27238

BINARY ALLOYS
Calculating masses, densities, and compositions of alloys
Oct page 73 LEW-14914

BINARY CODES
Simplified correction of errors in Reed-Solomon codes
Jan page 68 NPO-17381

Synchronization technique for reception of coded data
Jan page 67 NPO-17037

Acquisition of spread-spectrum code
Apr page 38 NPO-17472

Simplified correlator for ranging codes
May page 36 NPO-17415

Procedure for labeling linear finite-state codes
July page 107 NPO-17774

BINARY SYSTEMS (MATERIALS)
Two-phase accumulator
Apr page 68 MSC-21464

BIOINSTRUMENTATION
Self-calibrating respiratory-flowmeter combination
June page 96 MSC-21430

BIOPROCESSING
Affinity electrophoresis using ligands attached to polymers
June page 95 MFS-26049

BIOREACTORS
Hollow-fiber clinostat
June page 96 MFS-28370

Perfusion bioreactor module
July page 113 MSC-21361

Growing and assembling cells into tissues
Dec page 67 MSC-21559

BIREFRINGENCE
Monolithic unidirectional planar ring laser
Nov page 58 LAR-14045

BIREFRINGENT FILTERS
Improved design for birefringent filter
May page 56 LAR-13887

Birefringent-filter model
July page 60 LAR-13945

BISMALEIMIDE
Ethynyl-terminated imido thioethers and derived resins
May page 59 LAR-13910

BLOCKING
Impact wire dislodges obstructions
June page 83 MFS-29513

Beam stop for high-powered lasers
Dec page 28 NPO-17465

BLOOD FLOW
Flows in model human femoral arteries
Jan page 76 NPO-17599

Computing blood flows
Oct page 83 ARC-12253

BLUFF BODIES
Reducing aerodynamic drag of bluff bodies
Aug page 56 LAR-13768

BLUNT BODIES
Simulated hypersonic flows about a blunt body
July page 74 ARC-12251

BOLTS
Spring-loaded-bolt locking device
Dec page 47 LEW-14887

BONDING
Bonding elastomers to metal substrates
July page 82 LAR-13645

BOUNDARY LAYER FLOW
Simulation of turbulent, oscillating boundary layer
July page 73 ARC-11858

Microphone detects waves in laminar boundary-layer flow
Nov page 56 NPO-17479

BOUNDARY LAYER SEPARATION
Acoustic reduction of separation of flow
Sep page 78 LEW-14876

Measurements of shock-separated turbulent boundary layers
Nov page 78 ARC-12298

BOUNDARY LAYER TRANSITION
Detecting boundary-layer transition in cold environments
Mar page 76 LAR-13830

BREATHING APPARATUS
Liquid-air breathing apparatus
Aug page 74 KSC-11431

BUCKLING
Numerical simulation of buckling in waffle panels
June page 73 MSC-21599

BUFFER STORAGE
Virtual frame buffer interface program
Apr page 59 NPO-16713

BUS CONDUCTORS
Automated power-distribution system
Oct page 48 MFS-28440

BUTT JOINTS
Rounding and aligning tubes for butt welding
Jan page 62 MFS-29363

Quick check of butt-weld alignment
Mar page 89 MFS-29423

C

CALIBRATING
Automatic calibration of manual machine tools
Jan page 61 MFS-29380

Calibration for on-machine inspections
May page 81 MFS-29523

Calibrator blocks for computerized tomography (CT)
July page 50 KSC-11397

CALORIMETERS
Isothermal calorimeter
Aug page 44 NPO-17419

CAMBERED WINGS
Wing-design and -analysis code
Oct page 74 LAR-13995

CAPACITORS
Charging/safety-interlock connection for capacitor
Dec page 20 NPO-17519

CAPILLARY TUBES
Capillary pumped loop modeler
Oct page 76 GSC-13145

CARBON DIOXIDE
Stability of a carbon-dioxide-removing resin
July page 59 ARC-12129

Cleaning with super-critical CO_2
Dec page 58 MFS-29611

CARTS
Moving large wiring-harness boards
June page 82 MFS-29510

CASCADE CONTROL
Output control using feedforward and cascade controllers
Feb page 37 NPO-17420

CATALYSTS
Enhancement of Pt/SnO_2 catalysts by addition of H_2O
July page 54 LAR-14084

CATHODES
$NbSe_3$ cathodes for Li rechargeable cells
Nov page 61 NPO-17491

Cheaper hybride-forming cathodes
Dec page 34 NPO-17927

CAVITIES
Polishing difficult-to-reach cavities
Dec page 63 MFS-29592

CAVITY RESONATORS
Generating second harmonics in nonlinear resonant cavities
May page 52 LAR-14051

1990 Annual Subject Index

CELLS (BIOLOGY)
Hollow-fiber clinostat
June page 96 MFS-28370

Perfusion bioreactor module
July page 113 MSC-21361

Emulsions containing perfluorocarbon support cell cultures
Sep page 99 MSC-21480

Growing and assembling cells into tissues
Dec page 67 MSC-21559

CENTRAL PROCESSING UNITS
Neural-network processor would allocate resources
Oct page 46 NPO-17781

CERAMIC COATINGS
Response of ceramic insulation to aerothermodynamic heating
May page 58 ARC-12156

Reducing run-in wear of ceramic-based coatings
July page 56 LEW-14834

CERAMIC MATRIX COMPOSITES
Mechanical properties of SiC/Si_3N_4 laminates
Dec page 37 LEW-14896

CERAMICS
Tribological properties of ceramics
Mar page 67 LEW-14833

Friction and wear of silicon ceramics
June page 67 LEW-14835

Heat- and oxidation-resistant electrodes
Dec page 34 NPO-17156

Optical properties of ceramic fabrics
Dec page 36 ARC-11739

CHAMBERS
Simple regulator for positive-pressure glove box
Dec page 62 NPO-17786

CHANNEL FLOW
Transport of passive scalars in a turbulent channel flow
Apr page 62 ARC-12109

CHANNELS (DATA TRANSMISSION)
Connection protocol for mobile/satellite communications
June page 91 NPO-17735

Managing mobile/satellite propagation data
July page 62 NPO-17269

CHARGE COUPLED DEVICES
Iridium film for charge-coupled device
June page 26 NPO-17327

Nitric oxide enhances charge-coupled device
June page 26 NPO-17281

Silicide Schottky barrier for back-surface-illuminated CCD
June page 26 NPO-17328

Multi-pinned-phase charge-coupled device
Aug page 22 NPO-17462

CHARTS
S-chart -- scheduling-chart program
Nov page 74 MFS-29531

CHEMICAL REACTIONS
Numerical methods for chemically reacting flows
Dec page 30 ARC-12282

CHORDS (GEOMETRY)
Exact chord length distribution for SEU calculation
Apr page 30 NPO-17657

CIRCUIT BOARDS
Connecting multiple wires to a single through hole
Mar page 92 MFS-29405

Data-acquisition board for IBM PS/2 computer
Oct page 45 MSC-21590

CIRCUIT BREAKERS
Improved thermal-switch disks protect batteries
May page 24 MSC-21428

CIRCUITS
Tester detects steady-short or intermittent-open circuits
Jan page 18 MFS-29466

Concept for generation of long Pseudorandom sequences
Mar page 50 NPO-17241

Program for engineering electrical connections
May page 62 NPO-17619

Control circuit for two stepping motors
June page 30 GSC-13202

Starting circuit for erasable programmable logic device
Aug page 20 NPO-17827

Removing dross from molten solder
Sep page 88 MFS-28406

Current-monitoring and -limiting circuit for 28-Vdc supply
Oct page 28 GSC-13310

Voltage-boosting driver for switching regulator
Nov page 26 MFS-28437

CIRCULAR WAVEGUIDES
Directional couplers for detecting circular waveguide modes
Sep page 33 NPO-17175

CLAMPS
Post clamp with attached collar
Jan page 48 LEW-14862

CLEANING
Cleaning with super-critical CO_2
Dec page 58 MFS-29611

Washing off polyurethane foam insulation
Dec page 59 MFS-29578

CMOS
Upper-bound estimates of SEU in CMOS
Apr page 26 NPO-17566

Failures of CMOS circuits irradiated at low rates
Aug page 29 NPO-17867

Effects of dose rates on radiation damage in CMOS parts
Sep page 32 NPO-17344

Failures of CMOS devices at low radiation-dose rates
Nov page 30 NPO-17868

COAL
Hydromechanical advanced coal excavator
Nov page 80 NPO-16442

COATING
Polytetrafluoroethylene-impregnated anodization for aluminum
Nov page 63 MFS-27229

New materials and treatments for turbopump bearings
Dec page 36 MFS-27238

COATINGS
Survey of infrared-absorbing coatings
Jan page 42 ARC-11767

Reducing run-in wear of ceramic-based coatings
July page 56 LEW-14834

Monitoring coating thickness during plasma spraying
Sep page 84 LEW-14919

Dielectric coating for hot-film flow sensors
Oct page 90 LAR-13678

COCKPIT SIMULATORS
General-purpose data-formatting input/output system
July page 42 LAR-13529

CODERS
Finite-state codes
Feb page 61 NPO-17285

VLSI Reed-Solomon encoder with interleaver
Feb page 28 NPO-17280

CODES
Computer-access-code matrices
Apr page 82 NPO-17525

Procedure for labeling linear finite-state codes
July page 107 NPO-17774

XTRN -- automatic code generator for C header files
Nov page 72 MSC-21298

CODING
Multiple-trellis-coded modulation
Jan page 71 NPO-17100

Pyramidal image-processing code for hexagonal grid
May page 91 ARC-12178

Bar-code system tracks test equipment
June page 42 KSC-11370

COLLISION AVOIDANCE
Details of collision-avoidance study
Nov page 48 ARC-12396

Evaluation of an aircraft-collision-avoidance system
Nov page 47 ARC-12367

COLOR TELEVISION
Real-time digital compression of television image data
Sep page 40 LEW-14945

COMBUSTION CHAMBERS
Perspective on dilution jet mixing
Mar page 83 LEW-14614

Electrodeposited nickel reinforces outlet neck
May page 80 MFS-29447

High-pressure promoted-combustion chamber
Sep page 46 MSC-21470

COMBUSTION CHEMISTRY
Two radiative/thermochemical instruments
Nov page 54 MSC-21639/40

COMBUSTION STABILITY
System detects vibrational instabilities
May page 41 MSC-21408

COMMUNICATION NETWORKS
Carrying synchronous voice data on asynchronous networks
Feb page 31 NPO-17431

Computer-access-code matrices
Apr page 82 NPO-17525

COMMUNICATION SATELLITES
Estimation of interference in satellite/ground communications
Jan page 45 NPO-17500

COMPOSITE MATERIALS
Lightweight, thermally conductive composite material
Mar page 66 LEW-14814

Making fiber-reinforced metal by rapid solidification
Mar page 94 LEW-14918

Flammabilities of graphite-reinforced composites
May page 60 ARC-12165

Polymetric additives for graphite/epoxy composites
July page 56 ARC-11427

Braided composite threaded fasteners
Oct page 94 LAR-14062

Effects of rapid crushing on composites
Oct page 84 LAR-14087

Finite-element composite-analysis program
Oct page 73 LAR-14109

COMPOSITE STRUCTURES
Preloaded composite-strut/end-fitting joint
July page 82 MFS-28339

Advanced composite pistons
Sep page 90 LAR-13926

COMPRESSED GAS
High-pressure promoted-combustion chamber
Sep page 46 MSC-21470

COMPRESSIBLE FLOW
Analysis of stepped labyrinth seals
Sep page 79 MFS-29585

COMPUTATIONAL FLUID DYNAMICS
Computational fluid dynamics for helicopters
Jan page 59 ARC-12143

Computing blood flows
Oct page 83 ARC-12253

Computing flows in turbine end bearings
Dec page 54 MFS-29681

COMPUTER AIDED DESIGN
Modification of gear teeth to reduce vibrations
May page 75 LEW-14738

Computing mass properties from AutoCAD
June page 68 GSC-13228

Computer program relayers engineering drawings
Dec page 57 MFS-28445

System-design-tradeoff model for space station
Dec page 41 NPO-17878

Scaled ellipses for computer-aided design
Dec page 64 MFS-29629

Software for drawing design details concurrently
Dec page 57 MFS-28444

COMPUTER AIDED MANUFACTURING
Method for automatic downhand welding
Jan page 65 MFS-27209

COMPUTER AIDED MAPPING
Extracting geocoded images from SAR data
Apr page 59 NPO-17418

Making mosaics of SAR imagery
Apr page 58 NPO-17586

COMPUTER AIDED TOMOGRAPHY
Calibrator blocks for computerized tomography (CT)
July page 50 KSC-11397

Viewing welds by computer tomography
July page 79 MFS-29555

Measuring weld profiles by computer tomography
Dec page 60 MFS-29554

COMPUTER ANIMATION
Flexible animation computer program
Sep page 68 LAR-14102

COMPUTER DESIGN
Bus-programmable slave card
Sep page 34 MSC-21387

Master/programmable-slave computer
Oct page 50 MSC-21550

COMPUTER GRAPHICS
Graphical display of test-flight trajectories
Feb page 28 ARC-12211

Collection of software for computer graphics
Aug page 52 ARC-12350

Displaying TeX files on graphics terminals
Aug page 51 NPO-17296

Program manipulates plots for effective display
Oct page 78 GSC-13232

Software for three-dimensional Space Shuttle imagery
Dec page 38 GSC-13246

COMPUTER NETWORKS
Communication-gateway software for NETEX, DECnet, and TCP/IP
Oct page 77 GSC-13236

Local-area-network simulator
Dec page 38 ARC-12168

COMPUTER PROGRAMS
XTRN -- automatic code generator for C header files
Nov page 72 MSC-21298

COMPUTERIZED SIMULATION
Computer animation in perception research
Jan page 76 ARC-11774

Computer simulation for multilevel optimization of design
Apr page 87 LAR-13850

Simulating a factory via software
May page 62 MFS-28398

Numerical simulation of buckling in waffle panels
June page 73 MSC-21599

Program aids simulation of neural networks
Aug page 50 MSC-21588

COMPUTER PROGRAMS
Simulating orbiting spacecraft
Feb page 49 MSC-21462

Numerical analysis of flows with FIDAP
Mar page 84 MFS-27219

Pivotal-function assessment of reliability of software
July page 107 LAR-13842

Program aids simulation of neural networks
Aug page 50 MSC-21588

COMPUTER STORAGE DEVICES
Fast, capacious disk memory device
June page 44 GSC-13196

32-bit-wide memory tolerates failures
June page 38 MSC-21566

COMPUTER NETWORKS
Remote maintenance monitoring
June page 38 KSC-11398

COMPUTER VISION
High-voltage digital-to-analog converter
July page 32 MFS-29605

CONCENTRATORS
Concentrating gaseous contaminants for monitoring
Sep page 45 MSC-21424

CONCURRENT PROCESSING
Optimal allocation of tasks in hypercube computers
Apr page 79 NPO-17215

Concurrent algorithm for particle-in-cell simulations
Sep page 95 NPO-17737

Concurrent finite-element analysis on hypercube computers
Oct page 100 NPO-17602

CONDUCTIVE HEAT TRANSFER
Pressurized-flat-interface heat exchanger
July page 68 MSC-21271

CONFIGURATION MANAGEMENT
Increasing the dexterity of redundant robots
Oct page 88 NPO-17801

CONTAINERS
Vacuum-gauge connection for shipping container
Sep page 85 MSC-21523

CONTAMINANTS
Hot wax sweeps debris from narrow passages
Mar page 89 MFS-29462

Concentrating gaseous contaminants for monitoring
Sep page 45 MSC-21424

Adhesion between particles and surfaces in a vacuum
Nov page 60 NPO-17743

CONTAMINATION
X-ray fluorescence surface-contamination detector
Apr page 52 MFS-27222

CONTROL
Autonomous-control concept for instrument pointing system
Mar page 95 NPO-17521
Control circuit for two stepping motors
June page 30 GSC-13202

Minimal-inversion feedforward-and-feedback control system
July page 111 NPO-17701

Estimability and regulability of linear systems
Aug page 35 ARC-12173

Flow-control unit for nitrogen and hydrogen gases
Aug page 54 ARC-11772

CONTROL EQUIPMENT
Hard contact with a force-reflecting teleoperator
Apr page 70 NPO-17549

CONTROLLERS
Principles and applications of dual adaptive control
Nov page 98 ARC-12310

CONTROL SYSTEMS DESIGN
Proximity sensors make robot dexterous
Oct page 50 MSC-21476

CONTROL UNITS (COMPUTERS)
Master/programmable-slave computer
Oct page 50 MSC-21550

CONTROLLERS
Disturbance-accommodating controller would aim antenna
Mar page 42 NPO-17631

Programmable direct-memory-access controller
Mar page 54 NPO-17341

Digital controller for emergency beacon
May page 43 LEW-14857

Compact analyzer/controller for oxygen-enrichment system
June page 50 LAR-14016

Multivariable PID controller for robotic manipulator
June page 93 NPO-17647

CONTROL SYSTEMS DESIGN
Designing digital control systems with averaged measurements
May page 42 MFS-28362

CONTROL THEORY
Algorithm for control of large antenna
Feb page 64 NPO-17482

Finding optimal gains in linear-quadratic control problems
Apr page 87 NPO-17011

Algorithm for "bang-bang" control laws
July page 112 NPO-17603

Laws for stable control of orientation
Aug page 69 NPO-17790

COOLING SYSTEMS
Ozone treatment for cooling towers
Aug page 60 KSC-11384

COORDINATES
Determining spatial coordinates by laser ranging
Jan page 57 NPO-17436

Algebraic generation of two-dimensional grids
Mar page 69 LAR-13800

COORDINATE TRANSFORMATIONS
Programmable remapper
June page 46 MSC-21350

Neural-network computer transforms coordinates
July page 35 NPO-17753

CORRELATORS
Simplified correlator for ranging codes
May page 36 NPO-17415

CORROSION
Electrochemical study of corrosion of painted steel
Jan page 44 MFS-27213

CORROSION RESISTANCE
Corrosion-resistant ball bearings
Dec page 46 MSC-21319

COSTS
Managing information on costs
July page 61 MFS-28361

COUPLERS
Fiber-optic coupler and dynamic-range enhancer for CARS
Nov page 52 LAR-14235

COUPLINGS
Redundant, confined-explosive severance device
Sep page 75 LAR-13582

Self-aligning coupler
Nov page 90 MSC-21459

COVERINGS
Wing covers for aerodynamic studies
Jan page 65 ARC-12238

CRACK PROPAGATION
Dissipation of energy in extension of cracks
Sep page 73 LAR-14025

CRACKS
Radial cracks would signal wearout of turbine blades
June page 72 MFS-28363

Ultrasonic monitor to determine crack-opening load
Aug page 57 LAR-13889

CREEP PROPERTIES
High-temperature creep behavior of fiber-reinforced niobium
July page 58 LEW-14831

CRUSHING
Effects of rapid crushing on composites
Oct page 84 LAR-14087

CRYOGENIC EQUIPMENT
Advanced reusable foam cryogenic insulation
Apr page 55 LAR-14014

CRYOGENIC ROCKET PROPELLANTS
Insulation for cryogenic-liquid tanks
Mar page 82 LEW-14707

CRYOGENICS
Visual-inspection probe for cryogenic chamber
Feb page 53 MSC-21444

Reinforcing liner for composite cryogenic tank
June page 66 MFS-28399

Automatic refilling system for liquid helium
July page 46 GSC-13270

Silicon nitride balls for cryogenic bearings
July page 63 MFS-29613

Vacuum-gauge connection for shipping container
Sep page 85 MSC-21523

Dielectric coating for hot-film flow sensors
Oct page 90 LAR-13678

CRYOGENIC WIND TUNNELS
Detecting boundary-layer transition in cold environments
Mar page 76 LAR-13830

CRYSTAL OSCILLATORS
Crystal oscillators operate beyond rated frequencies
Apr page 30 GSC-13171

CRYSTALS
Spectroscopic analysis of insulating crystal fibers
July page 34 LAR-13831

CUBIC EQUATIONS
Algebraic generation of two-dimensional grids
Mar page 69 LAR-13800

CULTURE TECHNIQUES
Emulsions containing perfluorocarbon support cell cultures
Sep page 99 MSC-21480

CURVE FITTING
Least-squares curve-fitting program
Aug page 53 NPO-17819

CURVES (GEOMETRY)
Program manipulates plots for effective display
Oct page 78 GSC-13232

CUTTERS
Jam-resistant cutters for emergency separation
July page 68 MSC-21474

CYBERNETICS
Programmable analog memory resistors for electronic neural networks
Feb page 18 NPO-17398

Analog delta-back-propagation neural-network circuitry
June page 28 NPO-17564

Program aids simulation of neural networks
Aug page 50 MSC-21588

Adaptive neurons for artificial neural networks
Dec page 24 NPO-17803

CYCLOTRONS
Improved multiple-species cyclotron ion source
Aug page 43 NPO-17766

D

DAMPING
Nonobstructive damping for parts vibrating in flows
Jan page 61 MFS-29572

Damping seals and bearings for a turbomachine
Sep page 80 MFS-28345

DATA ACQUISITION
Portable high-frequency data-acquisition system
Jan page 30 MSC-21521

Enhanced data-acquisition system
May page 36 MSC-21598

Data-acquisition board for IBM PS/2 computer
Oct page 45 MSC-21590

DATA COMPRESSION
Competitive parallel processing for compression of data
Feb page 32 NPO-17445

Real-time digital compression of television image data
Sep page 40 LEW-14945

DATA CONVERTERS
Monolithic optoelectronic integrated circuit
Aug page 25 LEW-14922

DATA CONVERSION ROUTINES
Peripheral equipment interchanges bytes of data
Mar page 48 MFS-29478

CYBER-205 devectorizer
Dec page 44 LAR-13810

DATA LINKS
Analyzing optical communication links
Mar page 68 NPO-17444

DATA MANAGEMENT
Cooperating expert systems for automated monitoring and diagnostics
Nov page 94 NPO-17804

Data-management software for PiFEx
Dec page 39 NPO-17463

DATA PROCESSING
Parallel architecture for robotics computation
June page 36 NPO-17629

General-purpose data-formatting input/output system
July page 42 LAR-13529

Balancing loads among parallel data processors
Aug page 67 MSC-21348

Collection of software for computer graphics
Aug page 52 ARC-12350

Test processor for PCM telemetry
Aug page 27 GSC-13291

Analyzing distributed processing for electric utilities
Dec page 38 NPO-17710

DATA PROCESSING EQUIPMENT
Integrated optoelectronic interface
Feb page 33 NPO-17650

General-purpose serial interface for remote control
Aug page 34 LAR-13739

Bus-programmable slave card
Sep page 34 MSC-21387

DATA SAMPLING
Differential sampling for fast acquisition of frequency
Apr page 79 NPO-17358

DATA SMOOTHING
Performances of fixed-lag phase-smoothing algorithms
Jan page 73 NPO-17202

DATA TRANSFER (COMPUTERS)
SCSI communication test bus
Dec page 25 MSC-21704

DATA TRANSMISSION
Synchronization technique of reception of coded data
Jan page 67 NPO-17037

DEBRIS
Hot wax sweeps debris from narrow passages
Mar page 89 MFS-29462

DECISION MAKING
Scheduling nonconsumable resources
Jan page 72 NPO-16988

DECODERS
VLSI architecture for Viterbi decoder
Jan page 28 NPO-17310

Large-constraint-length, fast Viterbi decoder
Apr page 34 NPO-17639

Pipeline time- and transform-domain Reed-Solomon decoders
May page 94 NPO-17510

DECONTAMINATION
Catalytic destruction of toxic organic compounds
Sep page 46 NPO-17669

DEEP SPACE NETWORK
More about fixed-lag smoothers for tracking carriers
Apr page 45 NPO-17389

DEFECTS
Using ruby balls as fiducial marks
Jan page 54 MFS-29394

Radial cracks would signal wearout of turbine blades
June page 72 MFS-28363

DEFLECTORS
Thrust-vector deflectors for spacecraft
Sep page 81 MSC-21672

DEFORMATION
Optical detection of deformations of an antenna
May page 38 NPO-17677

Computing deformations of rubbery materials
Sep page 47 NPO-17670

Monitoring small deformations in an instrument
Oct page 80 GSC-13271

DELAMINATING
Delamination analysis of composite curved bars
Oct page 71 ARC-12347

DEMODULATORS
Digital demodulator for advanced receiver
Mar page 44 NPO-17628

DENSITY (MASS/VOLUME)
Calculating masses, densities, and compositions of alloys
Oct page 73 LEW-14914

DEPOSITION
Probe measures fouling as in heat exchangers
Aug page 58 NPO-17322

DESIGN ANALYSIS
Computer simulation for multilevel optimization of design
Apr page 87 LAR-13850

System-design-tradeoff model for space station
Dec page 41 NPO-17878

DETONATION
Steel foil improves performance of blasting caps
Apr page 60 LAR-13832

DIAGNOSIS
Indicator for pseudomonas bacteria
Oct page 101 NPO-17653

DIAMAGNETISM
Electromagnetic Meissner-effect launcher
Apr page 64 MFS-28323

DIAMETERS
Measuring diameters of large vessels
Jan page 53 MFS-28287

DIAPHRAGMS (MECHANICS)
Pressure-measuring diaphragm transmits optical signals
Sep page 76 MFS-29535

DIELS-ALDER REACTIONS
Preparation of high-temperature reactive oligomers
June page 66 LAR-13965

DIES
Graphite-thermoplastic-pultrusion die
Feb page 59 LAR-13719

DIFFERENTIAL EQUATIONS
SINDA '85/FLUINT, Version 2.2
Sep page 68 MSC-21528

DIFFRACTION
Diffraction analysis of distorted reflector antennas
Sep page 66 NPO-16818

DIFFUSION
Perfusion bioreactor module
July page 113 MSC-21361

DIFFUSION PUMPS
Rotor/stator interaction in a diffuser pump
Aug page 60 MFS-26092

DIGITAL DATA
Peripheral equipment interchanges bytes of data
Mar page 48 MFS-29478

Balancing loads among parallel data processors
Aug page 67 MSC-21348

DIGITAL ELECTRONICS
Digital demodulator for advanced receiver
Mar page 44 NPO-17628

DIGITAL FILTERS
Reducing speckle in one-look SAR images
Feb page 70 NPO-17254

DIGITAL SYSTEMS
Concept for generation of long pseudorandom sequences
Mar page 50 NPO-17241

Operation of the X-29A digital flight control system
Apr page 45 ARC-12209

Frequency synthesizer for tracking filter
Aug page 33 MFS-29541

DIGITAL TECHNIQUES
Finite-state codes
Feb page 61 NPO-17285

DIGITAL TO ANALOG CONVERTERS
High-voltage digital-to-analog converter
July page 32 MFS-29605

DIMENSIONAL MEASUREMENT
Measuring changes in dimensions of turbine blades
Apr page 60 MFS-28338

DIODES
Header for laser diode
Apr page 16 GSC-13234

DIRECT CURRENT
Circuit regulates speed of dc motor
July page 28 MSC-21345

DIRECTIONAL COUPLERS
Directional couplers for detecting circular waveguide modes
Sep page 33 NPO-17175

DIRECTIONAL SOLIDIFICATION (CRYSTALS)
Programmable multizone furnace
July page 49 MFS-28375

Directional solidification of monotectic alloys
Sep page 61 MFS-26080

Three-zone programmable temperature controller
Nov page 44 MFS-28435

DISCONNECT DEVICES
Two-fault-tolerant release mechanism
Feb page 50 MSC-21354

DISPLAY DEVICES
Software for clear-air Doppler-radar display
Feb page 69 KSC-11427

Fast, real-time, animated displays
July page 40 LAR-14140

Helmet-mounted visual display for flight simulation
Aug page 30 ARC-12160

Human factors in the design of video displays
Aug page 34 ARC-11847

Window utility system program
Nov page 73 LAR-13993

DISTANCE MEASURING EQUIPMENT
Electronically scanned laser rangefinder
May page 46 NPO-17571

DISTRIBUTED PROCESSING
Remote maintenance monitoring
June page 38 KSC-11398

Analyzing distributed processing for electric utilities
Dec page 38 NPO-17710

DISTRIBUTING
Schedule-organizer computer program
Nov page 69 MSC-21525

Schedule-report-generator computer program
Nov page 68 MSC-21527

Schedule-tracker computer program
Nov page 70 MSC-21526

DISTRIBUTION FUNCTIONS
Cumulative Poisson distribution program
July page 62 NPO-17714

DOCUMENTATION
Documenting software automatically
Nov page 70 MSC-21297

DOMES (STRUCTURAL FORMS)
Polyhedral observation cupola
Nov page 93 MSC-21689

DOPPLER EFFECT
Doppler-shifted Raman spectroscopy measures flows
Mar page 58 LAR-14133

Double differential encoding and detection in MPSK
June page 46 NPO-17666

Compensating for Doppler shift in laser instrumentation
Aug page 31 GSC-13194

Linear ion trap for atomic clock
Sep page 44 NPO-17758

DOPPLER RADAR
Software for clear-air Doppler-radar display
Feb page 69 KSC-11427

DOWNCONVERTERS
Sampling downconverter for radio-frequency signals
May page 44 NPO-17530

DRAG
Model of orbital density of air for computing drag
Feb page 48 MSC-21154

Predictions of drag in viscous transonic flow
Nov page 76 ARC-12252

DRAG REDUCTION
Reducing aerodynamic drag of bluff bodies
Aug page 56 LAR-13768

DRAWINGS
Software for drawing design details concurrently
Dec page 57 MFS-28444

DROPS (LIQUIDS)
Convective evaporation of clusters of drops
Feb page 42 NPO-17171

Behavior of evaporating liquid drops in clusters
Sep page 61 NPO-17843

Electrostatic dispersion of drops in clusters
Oct page 67 NPO-17516

More about evaporation in clusters of drops
Oct page 67 NPO-17594

DUCTS
Borescope device takes impressions in ducts
Apr page 74 MFS-29483

Positioning x-ray film by balloon
Aug page 63 MFS-29588

Arc reflector for welding ducts
Oct page 89 MFS-29640

DYNAMICAL SYSTEMS
Organizing performance requirements for dynamic systems
Aug page 72 MSC-21235

Non-Lipschitzian dynamics for modeling neural networks
Sep page 97 NPO-17814

DYNAMIC CHARACTERISTICS
Random-field estimation for dynamics of robots
Dec page 66 NPO-17788

DYNAMIC CONTROL
Simplified dynamic control of redundant manipulators
June page 48 NPO-17593

DYNAMIC STRUCTURAL ANALYSIS
Flexible animation computer program
Sep page 68 LAR-14102

DYNODES
Multiple-dynode-layer microchannel plate
July page 33 GSC-13203

E

EARTH OBSERVATION (FROM SPACE)
Autonomous-control concept for instrument pointing system
Mar page 95 NPO-17521

EARTH OBSERVING SYSTEM (EOS)
High resolution imaging spectrometer
Mar page 52 NPO-17624

EARTH ORBITS
Computing orbital viewing parameters
Jan page 46 GSC-13083

EARTHQUAKE RESISTANT STRUCTURES
Propagation of pulse vibrations in large structures
July page 74 NPO-17559

EATING
Aerospace food tray
Feb page 72 MSC-21412

EDUCATION
Space information for educators
July page 108 MFS-27221

EJECTION
Serial escape system for aircraft crews
Apr page 65 MSC-21310

Mechanism for guided release
June page 80 NPO-17617

EJECTORS
Control-volume analysis of thrust-augmenting ejectors
Oct page 87 LEW-14877

ELASTIC PROPERTIES
Cell model of a disordered solid
Feb page 40 NPO-17217

ELASTIC WAVES
Microphone detects waves in laminar boundary-layer flow
Nov page 56 NPO-17479

ELASTOMERS
Bonding elastomers to metal substrates
July page 82 LAR-13645

ELASTOPLASTICITY
Dissipation of energy in extension of cracks
Sep page 73 LAR-14025

ELECTRICAL POWER TRANSMISSION
Automated power-distribution system
Oct page 48 MFS-28440

ELECTRICAL RESISTIVITY
Calculating the resistivity of a deposited film
Oct page 72 LEW-14389

ELECTRIC ARCS
Etching electrode prevents arcs
June page 84 MFS-29508

ELECTRIC BATTERIES
Durable bipolar plates lead/acid batteries
Apr page 22 NPO-17662

Improved thermal-switch disks protect batteries
May page 24 MSC-21428

$NbSe_3$ cathodes for Li rechargeable cells
Nov page 61 NPO-17491

ELECTRIC COILS
Adjustable induction-heating coil
Nov page 50 LEW-14963

Segmented coil fails in steps
Nov page 36 MSC-21574

ELECTRIC CONNECTORS
Connecting multiple wires to a single through hole
Mar page 92 MFS-29405

Program for engineering electrical connections
May page 62 NPO-17619

ELECTRIC FIELDS
Net photorefractive gain in gallium arsenide
Apr page 50 NPO-17626

ELECTRIC FIELD STRENGTH
Electro-optical probing of terahertz integrated circuits
Aug page 29 LEW-14956

ELECTRIC FURNACES
Programmable multizone furnace
July page 49 MFS-28375

Three-zone programmable temperature controller
Nov page 44 MFS-28435

ELECTRIC GENERATORS
Rotary Stirling-cycle engine and generator
June page 78 MSC-21530

ELECTRIC MOTORS
Balanced-bridge feedback control of motor
Mar page 52 NPO-17430

Electrostatic linear actuator
Mar page 87 NPO-17684

Control circuit for two stepping motors
June page 30 GSC-13202

Circuit regulates speed of dc motor
July page 28 MSC-21345

ELECTRIC POWER SUPPLIES
Mobile centers for secondary power distribution
June page 28 KSC-11410

Mobile uninterruptible power supply
June page 34 KSC-11409

ELECTRIC STIMULI
Implantable electrode for critical locations
Aug page 74 NPO-17264

ELECTRIC WELDING
Dummy cup helps robot-welder programmers
Jan page 62 MFS-29499

Welding-current indicator
Jan page 24 MFS-29574

Resistance-welding test fixture
July page 80 MFS-29426

Small, lightweight welding-current indicator
July page 32 MFS-29622

Controlled-pinch spot welder
Sep page 87 MFS-29606

Rolling spot welder
Sep page 86 MFS-29580

Compact pinch welder
Oct page 89 MFS-29612

ELECTRIC WIRE
Splicing wires permanently with explosives
Nov page 81 LAR-13825

ELECTROACOUSTIC TRANSDUCERS
Improved voice-coil actuators have lower copper losses
Dec page 18 MFS-26111

ELECTROCHEMICAL CELLS
Improved liquid-electrode/solid-electrolyte cell
Apr page 51 NPO-17604

Copper chloride cathode for liquid-sodium cell
Aug page 28 NPO-17640

ELECTROCHEMISTRY
Cheaper hybride-forming cathodes
Dec page 34 NPO-17927

ELECTRODE MATERIALS
Copper chloride cathode for liquid sodium cell
Aug page 28 NPO-17640

ELECTRODES
Making more efficient use of battery-plate mass
May page 34 NPO-17435

Etching electrode prevents arcs
June page 84 MFS-29508

Analysis of used arc-jet electrodes
Dec page 30 NPO-17575

Heat- and oxidation-resistant electrodes
Dec page 34 NPO-17156

Sintered fiber electrodes
Dec page 32 NPO-17213

ELECTROFORMING
Simplified models speed electroforming tests
Apr page 76 MFS-29505

ELECTROLYSIS
Electrolysis bubbles make waterflow visible
Mar page 76 LEW-14797

ELECTROLYTIC CELLS
Antireduction insulator for solid-electrolyte cell
Oct page 24 NPO-17211

ELECTROMAGNETIC SCATTERING
Hypercube-computer analysis of electromagnetic scattering
Jan page 33 NPO-17551

ELECTROMIGRATION
Thermal-interaction matrix for resistive test structure
Apr page 32 NPO-17673

ELECTRON BEAM WELDING
Preventing contamination in electron beam welds
Mar page 90 MFS-29428

Checking automated-welder programs by computer
Sep page 41 MFS-29006

ELECTRONIC MODULES
Perpendicular-force latch
Feb page 54 MSC-21406

ELECTRON MICROSCOPES
Ballistic-electron-emission microscope
Jan page 34 NPO-17384

ELECTRON MICROSCOPY
Viewing integrated-circuit interconnections by SEM
Sep page 18 NPO-17635

ELECTRO-OPTICS
Fast feature-recognizing optoelectronic system
Nov page 42 NPO-17690

ELECTROPHORESIS
Affinity electrophoresis using ligands attached to polymers
June page 95 MFS-26049

ELECTROPLATING
Finding platinum-coating gaps on titanium anodes
Feb page 46 MFS-29389

Electrodeposited nickel reinforces outlet neck
May page 80 MFS-29447

ELECTROSTATIC CHARGE
Electrostatic dispersion of drops in clusters
Oct page 67 NPO-17516

ELEVATION
Differential radar interferometry maps changes in elevation
Sep page 36 NPO-17831

ELEVATION ANGLE
Algorithm for control of large antenna
Feb page 64 NPO-17482

ELLIPSES
Scaled ellipses for computer-aided design
Dec page 64 MFS-29629

EMBRITTLEMENT
Nondestructive technique to assess embrittlement in steels
Oct page 64 LAR-13817

EMERGENCIES
Jam-resistant cutters for emergency separation
July page 68 MSC-21474

EMISSION SPECTRA
Radiative processes in air excited by an ArF laser
Oct page 66 ARC-12136

EMULSIONS
Emulsions containing perfluorocarbon support cell cultures
Sep Page 99 MSC-21480

END EFFECTORS
Increasing the dexterity of redundant robots
Oct page 88 NPO-17801

ENDOSCOPES
Magnetically-guided penetrant applicator
Feb page 58 MFS-29358

Visual-inspection probe for cryogenic chamber
Feb page 53 MSC-21444

Filter enhances fluorescent penetrant-inspecting borescope
Mar page 91 MFS-29379

Borescope device takes impressions in ducts
Apr page 74 MFS-29483

Borescope with large depth of focus
May page 64 MFS-29461

Impact wire dislodges obstructions
June page 83 MFS-29513

Borescope aids welding in confined spaces
Aug page 64 MFS-29635

Combined borescope and flushing wand
Aug page 62 MFS-29581

ENERGY ABSORPTION
Effects of rapid crushing on composites
Oct page 84 LAR-14087

ENERGY DISSIPATION
Nonobstructive damping for parts vibrating in flows
Jan page 61 MFS-29572

Dissipation of energy in extension of cracks
Sep page 73 LAR-14025

ENGINEERING DRAWINGS
Computer program relayers engineering drawings
Dec page 57 MFS-28445

Scaled ellipses for computer-aided design
Dec page 64 MFS-29629

Software for drawing design details concurrently
Dec page 57 MFS-28444

ENTRAINMENT
Hot wax sweeps debris from narrow passages
Mar page 89 MFS-29462

ENZYMES
Dry-enzyme test for gaseous chemicals
Jan page 74 NPO-17642

EPOXY RESINS
Epoxies bond waveguides to flanges
Mar page 40 NPO-17497

ERROR CORRECTING CODES
Simplified correction of errors in Reed-Solomon codes
Jan page 68 NPO-17381

Asymmetrical memory circuit would resist soft errors
Jan page 23 NPO-17394

Finite-state codes
Feb page 61 NPO-17285

ERROR CORRECTING DEVICES
32-bit-wide memory tolerates failures
June page 38 MSC-21566

ERROR SIGNALS
Frequency-tracking-error detector
Aug page 32 MFS-29538

ESCAPE ROCKETS
Array of rocket for multicrewmember evacuation
Apr page 64 MSC-21332

ESCAPE SYSTEMS
Serial escape system for aircraft crews
Apr page 65 MSC-21310

Safe-egress pole for vehicle in motion
July page 72 MSC-21461

ESTIMATING
Estimability and regulability of linear systems
Aug page 35 ARC-12173

Trigonometric polynomials for estimation of spectra
Nov page 94 NPO-17885

ETALON
Calculating performances of Fabry-Perot etalons
Sep page 66 LAR-14055

ETCHANTS
Prepenetrant etchant for Incoloy* 903 weld overlays
Apr page 78 MFS-29576

Milder etchant for penetrant inspection
Sep page 63 MFS-29645

ETCHING
Etching electrode prevents arcs
June page 84 MFS-29508

ETHYL ALCOHOL
Dry-enzyme test for gaseous chemicals
Jan page 74 NPO-17642

EULER EQUATIONS OF MOTION
Laws for stable control of orientation
Aug page 69 NPO-17790

EVACUATING (TRANSPORTATION)
Safe-egress pole for vehicle in motion
July page 72 MSC-21461

EVACUATION (TRANSPORTATION)
Array of rockets for multicrewmember evacuation
Apr page 64 MSC-21332

EVAPORATION
Convective evaporation of clusters of drops
Feb page 42 NPO-17171

Behavior of evaporating liquid drops in clusters
Sep page 61 NPO-17843

Electrostatic dispersion of drops in clusters
Oct page 67 NPO-17516

More about evaporation in clusters of drops
Oct page 67 NPO-17594

EXCAVATION
Hydromechanical advanced coal excavator
Nov page 80 NPO-16442

EXPERT SYSTEMS
Automatic monitoring of complicated systems
Mar page 100 NPO-17409

Software model of software-development process
Mar page 100 NPO-17424

Software for development of expert systems
June page 86 NPO-17536

Cooperating expert systems for automated monitoring and diagnostics
Nov page 94 NPO-17804

Using expert systems for computational tasks
Nov page 96 ARC-12137

EXPLOSIVE DEVICES
Redundant, confined-explosive severance device
Sep page 75 LAR-13582

EXPLOSIVE WELDING
Splicing wires permanently with explosives
Nov page 81 LAR-13825

EXTRASOLAR PLANETS
Astrometric telescope facility for the Space Station
July page 52 ARC-11842

F

FABRICS
Integrated process for insertion and beatup of fill yarns
Oct page 92 LAR-14046

Optical properties of ceramic fabrics
Dec page 36 ARC-11739

FABRY-PEROT INTERFEROMETERS
Calculating performances of Fabry-Perot etalons
Sep page 66 LAR-14055

FAILURE
Averaging sampled sensor outputs to detect failures
Aug page 70 MFS-29719

Segmented coil fails in steps
Nov page 36 MSC-21574

F-18 AIRCRAFT
Dye tracing of flow on forebody of airplane
Nov page 78 ARC-12237

FAIRINGS
Improved hub fairings for helicopters
May page 69 ARC-12288

FAR FIELDS
Time-resolved measurements of laser far-field patterns
Oct page 55 GSC-13338

FAR INFRARED RADIATION
Optically-tuned far-infrared device
May page 30 NPO-17160

FASTENERS
Braided composite threaded fasteners
Oct page 94 LAR-14062

Self-aligning coupler
Nov page 90 MSC-21459

Rotary ball locking mechanism
Dec page 56 MSC-21396

FAST FOURIER TRANSFORMATIONS
Interpolation and FFT of near-field antenna measurements
Feb page 44 NPO-17597

FAULT TOLERANCE
Generating semi-Markov models automatically
Nov page 71 LAR-14193

FEATURE IDENTIFICATION AND LOCATION EXPER
Fast feature-recognizing optoelectronic system
Nov page 42 NPO-17690

FEEDBACK CONTROL
Balanced-bridge feedback control of motor
Mar page 52 NPO-17430

Recursive construction of Jacobian matrix and its time derivative for robot arm
Apr page 89 NPO-17364

Designing digital control systems with averaged measurements
May page 42 MFS-28362

Flux-feedback magnetic-suspension actuator
July page 44 LAR-13785

Minimal-inversion feedforward-and-feedback control system
July page 111 NPO-17701

FEEDFORWARD CONTROL
Output control using feedforward and cascade controllers
Feb page 37 NPO-17420

Stochastic feedforward control technique
May page 92 LAR-13796

or the nission-unique lectronics hey call Motorola.

Aotorola space lectronics will be on oard the futuristic latforms of tomorrow.

xciting! Unpredictable! pace City? Factory? esort Hotel? Or Corporate Headquarters? takes visionary systems rchitects to turn ideas nto reality. Motorola's xpertise in space ommunications has set he stage for our future in pace electronics.

visionary electronics on our space platform is of rime interest, call the ioneers in space ommunications and lectronics: 602/732-3015 r write Motorola GEG, .O. Box 2606, cottsdale, AZ 85252.

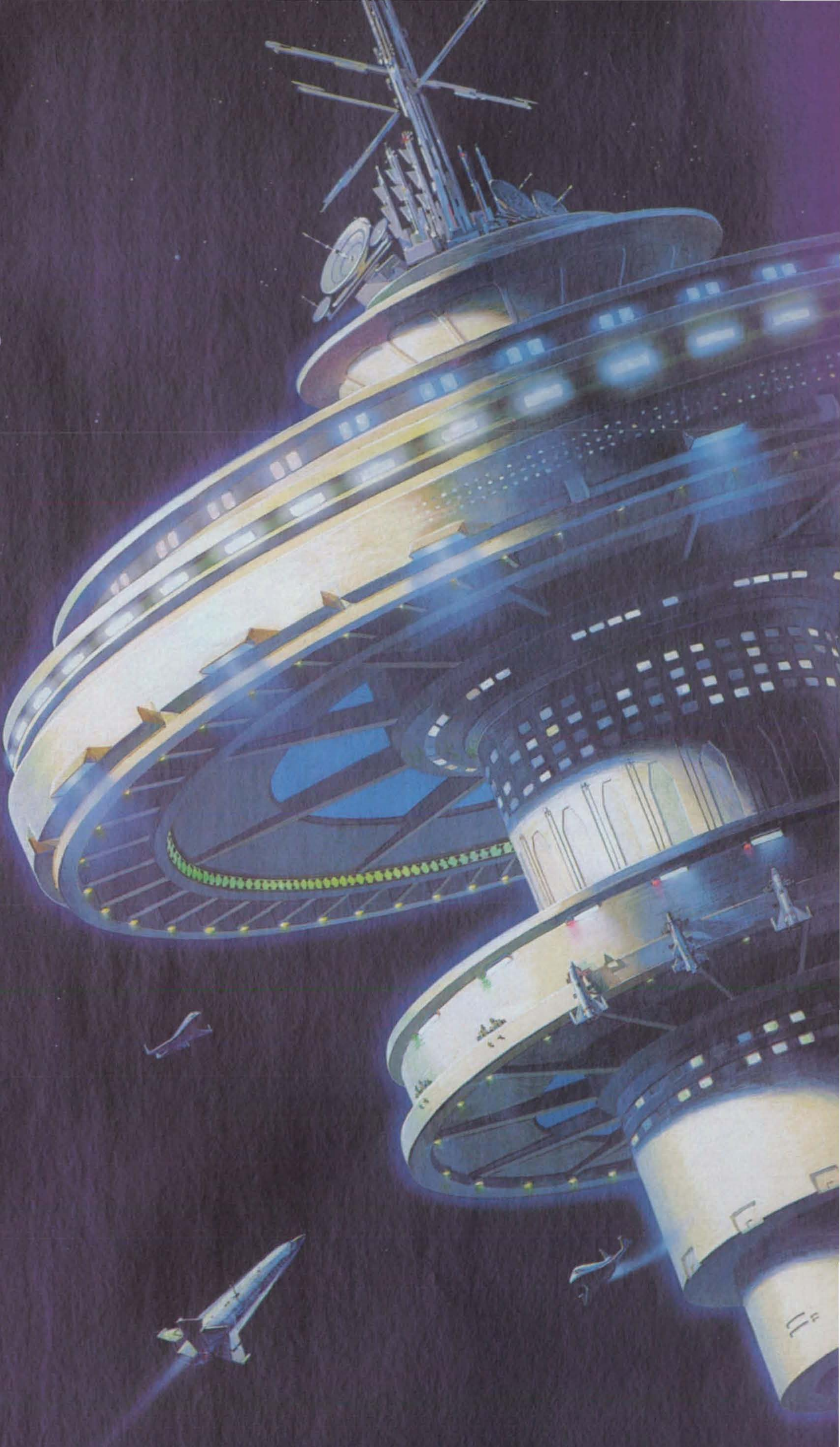

ircle Reader Action No. 655

MOTOROLA INC.

FEED SYSTEMS
Feeder system for particle-size analyzer
Apr page 61 MFS-28326

FIBER COMPOSITES
Graphite-thermoplastic-pultrusion die
Feb page 59 LAR-13719

Fiber-reinforced superalloys for rocket engines
July page 58 LEW-14871

High-temperature creep behavior of fiber-reinforced niobium
July page 58 LEW-14831

High-temperature polyimide resin
July page 54 LEW-14923

Advanced composite pistons
Sep page 90 LAR-13926

Microstructure of a SiC/(Ti/V/Cr/Sn/Al) composite
Nov page 61 LEW-14868

FIBER OPTICS
Interferometric fiber-optic gyroscope
Apr page 22 NPO-17515

Borescope with large depth of focus
May page 64 MFS-29461

Phase-compensating system for fiber-optic holography
June page 34 LEW-14864

Fiber-optic frequency-transfer link
July page 43 NPO-17703

Two-way optical data link on one fiber
Oct Page 31 NPO-17884

Fiber-optic coupler and dynamic-range enhancer for CARS
Nov page 52 LAR-14235

FIBERS
Spectroscopic analysis of insulating crystal fibers
July page 34 LAR-13831

FIELD EFFECT TRANSISTORS
Calculating second-order effects in MOSFET's
Jan page 22 NPO-17395

Gallium arsenide domino circuit
Mar page 36 NPO-17417

Recovering energy from a rapidly switched gate
May page 20 NPO-17221

GTO/FET cascode three-terminal switch
July page 18 NPO-17865

Porous-floating-gate field-effect transistor
July page 18 NPO-17532

MCI/MOSFET switch
Sep page 26 NPO-18001

Current-monitoring and -limiting circuit for 28-Vdc supply
Oct page 28 GSC-13310

FILE MAINTENANCE (COMPUTERS)
XTRN -- automatic code generator for C header files
Nov page 72 MSC-21298

FINANCIAL MANAGEMENT
Managing information on costs
July page 61 MFS-28361

FINITE ELEMENT METHOD
Assignment of finite elements to parallel processors
Feb page 61 NPO-17371

Numerical analysis of flows with FIDAP
Mar page 84 MFS-27219

Combining thermal and structural analyses
Mar page 84 LEW-14741

Improved stress analysis of multicomponent rotors
Apr page 67 LEW-14838

Computing deformations of rubbery materials
Sep page 47 NPO-17670

Concurrent finite-element analysis on hypercube computers
Oct page 100 NPO-17602

Finite-element composite-analysis program
Oct page 73 LAR-14109

FITTINGS
Simple, internally adjustable valve
Sep page 76 MFS-29463

Mechanized fluid connector and assembly tool
Oct page 79 MSC-21434

FIXTURES
Resistance-welding test fixture
July page 80 MFS-29426

Transducer-mounting fixture
Dec page 59 MFS-29600

FLAMMABILITY
Flammabilities of graphite-reinforced composites
May page 60 ARC-12165

FLEXIBLE BODIES
Adaptive-control experiments on a large flexible structure
Mar page 78 NPO-17478

Experiments on active members in large space structures
Oct page 81 NPO-17623

FLIGHT CREWS
Array of rockets for multicrewmember evacuation
Apr page 65 MSC-21332

Serial escape system for aircraft crews
Apr page 65 MSC-21310

FLIGHT CONTROL
Operation of the X-29A digital flight-control system
Apr page 45 ARC-12209

FLIGHT INSTRUMENTS
Air-velocity sensor for helicopter
July page 39 LAR-13598

FLIGHT MECHANICS
Flight dynamics analysis system
June page 70 GSC-13163

FLIGHT SIMULATION
Fast, real-time, animated displays
July page 40 LAR-14140

Improved insert for variable mach number
July page 63 LAR-13548

Helmet-mounted visual display for flight simulation
Aug page 30 ARC-12160

Details of collision-avoidance study
Nov page 48 ARC-12396

Evaluation of an aircraft-collision-avoidance system
Nov page 47 ARC-12367

FLIGHT TESTS
Graphical display of test-flight trajectories
Feb page 28 ARC-12211

FLOODS
Making topographical maps from SAR and flood-gauge data
Sep page 44 GSC-13212

FLOW CHARACTERISTICS
Numerical analysis of flows with FIDAP
Mar page 84 MFS-27219

FLOW DISTRIBUTION
Flows in model human femoral arteries
Jan page 76 NPO-17599

FLOW EQUATIONS
Upwind algorithm for parabolized Navier-Stokes equations
May page 73 ARC-12146

Simulation of unsteady, viscous, incompressible flow
July page 67 ARC-12277

SINDA '85/FLUINT, Version 2.2
Sep page 68 MSC-21528

FLOW MEASUREMENT
Doppler-shifted Raman spectroscopy measures flows
Mar page 58 LAR-14133

Frequency-domain signal processor for laser velocimeter
May page 45 LAR-13552

FLOWMETERS
Self-calibrating respiratory-flowmeter combination
June page 96 MSC-21430

Dielectric coating for hot-film flow sensors
Oct page 90 LAR-13678

FLOW REGULATORS
Liquid-flow controller responds to pressure
Mar page 72 MFS-28329

Liquid-flow controller with preset break pressure
Mar page 73 MFS-28330

Liquid-flow controller with trickle preflow
Mar page 74 MFS-28331

Flow-control unit for nitrogen and hydrogen gases
Aug page 54 ARC-11772

Controlling gas-flow mass ratios
Dec page 26 MSC-21542

FLOW THEORY
Control-volume analysis of thrust-augmenting ejectors
Oct page 87 LEW-14877

FLOW VELOCITY
Multiple-inlet/single-outlet orifice plate
May page 67 MFS-29407

Processing laser-velocimetric data by vector scanning
Oct page 98 LEW-14925

FLOW VISUALIZATION
Electrolysis bubbles make waterflow visible
Mar page 76 LEW-14797

Schlieren system for flow studies in round glass pipes
Oct page 58 LAR-13944

Dye tracing of flow on forebody of airplane
Nov page 78 ARC-12237

FLUID FLOW
Improved coupled fluid/structural dynamical model
Jan page 54 MFS-29439

Fixed-position isolation
May page 71 NPO-17707

Combination of techniques for computing incompressible flow
June page 71 ARC-12257

Simulation of turbulent, oscillating boundary layer
July page 73 ARC-11858

Numerical methods for chemically reacting flows
Dec page 30 ARC-12282

FLUORESCENCE
Filter enhances fluorescent-penetrant-inspecting borescope
Mar page 91 MFS-29379

FLUSHING
Combined borescope and flushing wand
Aug page 62 MFS-29581

FLUTTER ANALYSIS
Computation of flutter in turbomachinery
Feb page 56 LEW-14742

FLUX (RATE)
Heat-flux-measuring facility
Aug page 42 LEW-14917

Simplified calculation of solar fluxes in solar receivers
Sep page 68 NPO-17732

FOAMS
Advanced reusable foam cryogenic insulation
Apr page 55 LAR-14014

FORMAT
Displaying TeX files on graphics terminals
Aug page 51 NPO-17296

FORMING TECHNIQUES
Simplified models speed electroforming tests
Apr page 76 MFS-29505

FORTRAN
CYBER-205 devectorizer
Dec page 44 LAR-13810

FOULING
Probe measures fouling as in heat exchangers
Aug page 58 NPO-17322

FOURIER ANALYSIS
Fourier analysis of vibrations of round structures
Mar page 74 MFS-29334

FRAMES (DATA PROCESSING)
Virtual frame buffer interface program
Apr page 59 NPO-16713

FREQUENCY DISCRIMINATORS
Frequency-tracking-error detector
Aug page 32 MFS-29538

FREQUENCY MEASUREMENT
Differential sampling for fast acquisition of frequency
Apr page 79 NPO-17358

FREQUENCY MULTIPLIERS
Generating second harmonics in nonlinear resonant cavities
May page 52 LAR-14051

Millimeter-wave quantum-well frequency multipliers
Sep page 28 NPO-17584

FREQUENCY SHIFT
Compensating for Doppler shift in laser instrumentation
Aug page 31 GSC-13194

FREQUENCY STABILITY
Fiber-optic frequency-transfer link
July page 43 NPO-17703

FREQUENCY SYNTHESIZERS
Frequency synthesizer for tracking filter
Aug page 33 MFS-29541

FRICTION
Friction and wear of silicon ceramics
June page 67 LEW-14835

FROZEN FOODS
Sensor detects overheating of perishable material
May page 95 NPO-17585

FUEL CELLS
Sintered fiber electrodes
Dec page 32 NPO-17213

FUEL FLOW REGULATORS
Liquid-flow controller responds to pressure
Mar page 72 MFS-28329

Liquid-flow controller with trickle preflow
Mar page 74 MFS-28331

FUEL PUMPS
Back-to-back, counterrotating turbopumps
May page 76 MFS-28349

FUEL SPRAYS
Liquid-flow controller with preset break pressure
Mar page 73 MFS-28330

Electrostatic dispersion of drops in clusters
Oct page 67 NPO-17516

More about evaporation in clusters of drops
Oct page 67 NPO-17594

FUMES
Photochemical degradation of organic-solvent fumes
June page 61 MFS-29596

FUNCTIONS (MATHEMATICS)
Cumulative Poisson distribution program
July page 62 NPO-17714

FURNACES
Programmable multizone furnace
July page 49 MFS-28375

G

GAIN (AMPLIFICATION)
Net photorefractive gain in gallium arsenide
Apr page 50 NPO-17626

GALLIUM ARSENIDES
Gallium arsenide domino circuit
Mar page 36 NPO-17417

Net photorefractive gain in gallium arsenide
Apr page 50 NPO-17626

Optical modulation via the photorefractive effect
May page 48 NPO-17460

Matrix•vector multiplication in thin photorefractive crystal
June page 62 NPO-17455

AlAs diffusion/Schottky barrier on GaAs
July page 30 NPO-17796

GaAlAs traveling-wave electro-optical modulators
July page 24 LEW-14866

GAPS
Measuring gaps in O-ring seals
Feb page 52 MFS-28332

GARMENTS
Microprocessor control for liquid-cooled garment
Oct page 52 MSC-21359

GAS DETECTORS
Silicon detectors for helium liquid and vapor
Aug page 44 GSC-13281

GASES
Absorption of gases by glassy polymers
Feb page 45 NPO-17636

GAS ANALYSIS
Concentrating gaseous contaminants for monitoring
Sep page 45 MSC-21424

GAS FLOW
Flow-control unit for nitrogen and hydrogen gases
Aug page 54 ARC-11772

Controlling gas-flow mass ratios
Dec page 26 MSC-21542

GAS-METAL INTERACTIONS
Fast quenching for hydrogen-embrittlement tests
June page 60 MFS-29549

GAS TUNGSTEN ARC WELDING
Calibration fixture for welding robot
Apr page 72 MFS-29548

Internal filler-wire feed for arc welding
Apr page 75 MFS-29491

Internal wire guide for gas/tungsten-arc welding
Apr page 76 MFS-29489

Optical arc-length sensor for TIG welding
Apr page 72 MFS-29497

Borescope aids welding in confined spaces
Aug page 64 MFS-29635

Characterization of robot work cell
Nov page 92 MFS-29731

GAS TURBINE ENGINES
Perspective on dilution jet mixing
Mar page 83 LEW-14614

GATES (CIRCUITS)
Recovering energy from a rapidly switched gate
May page 20 NPO-17221

GEAR TEETH
Modification of gear teeth to reduce vibrations
May page 75 LEW-14738

GERMANIDES
Ge/Si integrated circuit for infrared imaging
Mar page 28 NPO-17397

GLASS
Cell model of a disordered solid
Feb page 40 NPO-17217

Low-noise, long-life, high-gain microchannel-plate glass
Aug page 47 LAR-14010

GLASS LASERS
Monolithic unidirectional nonplanar ring laser
Nov page 58 LAR-14146

GLOBAL POSITIONING SYSTEM
Testing microwave landing systems with satellite navigation
Apr page 36 KSC-11451

Tests of a differential global positioning system
Oct page 56 ARC-12313

GRAPHITE-EPOXY COMPOSITES
Flammabilities of graphite-reinforced composites
May page 60 ARC-12165

Reinforcing liner for composite cryogenic tank
June page 66 MFS-28399

Polymeric additives for graphite/epoxy composites
July page 56 ARC-11427

GRAPHITE-POLYIMIDE COMPOSITES
Process for autoclaving HMW PMR-II composites
Sep page 64 LEW-14839

GRATINGS (SPECTRA)
Integrated grating spectrometer
Apr page 49 NPO-17733

GRAY SCALE
Optical pseudocolor encoding of gray-scale image
Oct page 59 NPO-17764

GREASES
Second vapor-level sensor for vapor degreaser
May page 82 MFS-29493

GRINDING MACHINES
Automatic tension adjuster for flexible-shaft grinder
Mar page 93 MFS-29351

GRINDING (MATERIAL REMOVAL)
Weld-bead shaver
May Page 80 MFS-29593

Removing burrs in confined spaces
July page 81 MFS-29392

Grinding away microfissures
Aug page 62 MFS-29566

Polishing difficult-to-reach cavities
Dec page 63 MFS-29592

GUARDS (SHIELDS)
Mechanism for guided release
June page 80 NPO-17617

GYROSCOPES
Interferometric fiber-optic gyroscope
Apr page 22 NPO-17515

H

HALL EFFECT
Flux-feedback magnetic-suspension actuator
July page 44 LAR-13785

HAL/S
An Ada linear-algebra software package modeled after HAL/S
Dec page 42 NPO-17985

HARMONICS
Compounds generate optical second harmonics
June page 56 NPO-17731

HARNESSES
Moving large wiring-harness boards
June page 82 MFS-29510

HEAT EXCHANGERS
Pressurized-flat-interface heat exchanger
July page 68 MSC-21271

HEAT FLUX
Heat-flux-measuring facility
Aug page 42 LEW-14917

Probe measures fouling as in heat exchangers
Aug page 58 NPO-17322

Measuring response of propellant to oscillatory heat flux
Oct page 59 NPO-17428

HEAT MEASUREMENT
Isothermal calorimeter
Aug page 44 NPO-17419

HEAT PIPES
Capillary pumped loop modeler
Oct page 76 GSC-13145

HEAT RADIATORS
Prototype V-groove radiator heat shield
Apr page 55 NPO-17744

HEAT RESISTANT ALLOYS
Fiber-reinforced superalloys for rocket engines
July page 58 LEW-14871

HEAT SHIELDING
Heat shield and axial retainer for turbopump blade
Dec page 53 MFS-28417

HEAT TRANSFER
Systems improved numerical fluids analysis code
Nov page 64 GSC-13231

Trap for noncondensable gas in heat-transfer fluid
Dec page 48 MSC-21389

HELICAL WINDINGS
Electrostatic linear actuator
Mar page 87 NPO-17684

HELICOPTERS
Computational fluid dynamics for helicopters
Jan page 59 ARC-12143

Improved hub fairings for helicopters
May page 69 ARC-12288

Air-velocity sensor for helicopter
July page 39 LAR-13598

Tests of a differential global positioning system
Oct page 56 ARC-12313

HELIUM
Static pressure-assisted seal for helium
Mar page 70 MFS-29429

HELMETS
Helmet-mounted visual display for flight simulation
Aug page 30 ARC-12160

HERMETIC SEALS
O-ring-testing fixture
Dec page 46 MFS-28376

HETERODYNING
Noncoherent combination of optical-heterodyne outputs
Oct page 55 NPO-17693

HEURISTIC METHODS
Probabilistic determination of motions of robots
July page 111 NPO-17738

HIGH CURRENT
Welding-current indicator
Jan page 24 MFS-29574

HIGH POWER LASERS
Beam stop for high-power lasers
Dec page 28 NPO-17465

HIGH PRESSURE OXYGEN
High-pressure promoted-combustion chamber
Sep page 46 MSC-21470

HIGH TEMPERATURE SUPERCONDUCTORS
$YBa_2Cu_3O_x$ superconductors doped with AgO
Mar page 66 MFS-26078

HILBERT SPACE
Robust adaptive control in Hilbert space
June page 53 NPO-17588

HINGES
Precise hinge has low friction
Sep page 71 NPO-17749

HOLDERS
Post clamp with attached collar
Jan page 48 LEW-14862

Positioning x-ray film inside a flow splitter
Dec page 61 MFS-29322

HOLOGRAPHY
Phase-compensating system for fiber-optic holography
June page 34 LEW-14864

Holographic reticle
Sep page 89 MFS-29597

HONEYCOMB STRUCTURES
Crash-resistant shield
June page 71 NPO-17616

Making lightweight structures by vapor deposition
Nov page 81 LAR-14059

HOT-WIRE ANEMOMETERS
Further studies of hot-wire anemometry
Dec page 31 MFS-12104

HOT-WIRE FLOWMETERS
Dielectric coating for hot-film flow sensors
Oct page 90 LAR-13678

HUBS
Improved hub fairings for helicopters
May page 69 ARC-12288

HULLS (STRUCTURES)
Preventing ventilation on sailboard skegs
Nov page 75 LAR-14008

HUMAN FACTORS ENGINEERING
Human factors in the design of video displays
Aug page 34 ARC-11847

HYDROGEN EMBRITTLEMENT
Fast quenching for hydrogen-embrittlement tests
June page 60 MFS-29549

HYDROPLANES (SURFACES)
Preventing ventilation on sailboard skegs
Nov page 75 LAR-14008

HYGROMETERS
Acoustic humidity sensor
Apr page 47 NPO-17685

HYPERBOLIC DIFFERENTIAL EQUATIONS
Numerical methods for chemically reacting flows
Dec page 30 ARC-12282

HYPERCUBE MULTIPROCESSORS
Concurrent finite-element analysis on hypercube computers
Oct page 100 NPO-17602

HYPERSONIC FLOW
Simulated hypersonic flows about a blunt body
July page 74 ARC-12251

HYPERSONIC WIND TUNNELS
Compact analyzer/controller for oxygen-enrichment system
June page 50 LAR-14016

I

IDENTIFYING
Identifying bearing balls with radioisotopes
Nov page 91 MFS-29724

IMAGE CORRELATORS
Truncation of images for correlation
Aug page 68 NPO-17847

IMAGE ENHANCEMENT
Enhancement of penetrant-inspection images
Oct page 97 MFS-29496

IMAGE PROCESSING
Computer assembles mosaics of satellite-SAR imagery
Apr page 42 NPO-17683

Determining sense of motion in robotic vision
Apr page 84 NPO-17552

Virtual frame buffer interface program
Apr page 59 NPO-16713

Processor would find best paths on map
May page 40 NPO-17716

Pyramidal image-processing code for hexagonal grid
May page 91 ARC-12178

Programmable remapper
June page 46 MSC-21350

Multiple-dynode-layer microchannel plate
July page 33 GSC-13203

Optical pseudocolor encoding of gray-scale image
Oct page 59 NPO-17764

IMAGERY
Software for three-dimensional Space Shuttle imagery
Dec page 38 GSC-13246

IMAGING RADAR
Phase calibration of radar polarimetric data
Sep page 91 NPO-17844

IMAGING SPECTROMETERS
High-resolution imaging spectrometer
Mar page 52 NPO-17624

Calibration of airborne visible/IR imaging spectrometer
June page 63 NPO-17582

Preliminary analysis of data from AVIRIS
Oct page 68 NPO-17622

IMAGING TECHNIQUES
Ultrasonic imaging of deep arteries
Oct page 54 NPO-17439

IMPACT RESISTANCE
Crash-resistant shield
June page 71 NPO-17616

IMPINGEMENT
Computing impingements of rocket exhausts
Sep page 67 MSC-21419

IMPLANTED ELECTRODES (BIOLOGY)
Implantable electrode for critical locations
Aug page 74 NPO-17264

INCOMPRESSIBLE FLOW
Combination of techniques for computing incompressible flow
June page 71 ARC-12257

Simulation of unsteady, viscous, incompressible flow
July page 67 ARC-12277

INCONEL (TRADEMARK)
Welding and cutting a nickel alloy by laser
Mar page 93 MFS-27208

Milder etchant for penetrant inspection
Sep page 63 MFS-29645

Treating nickel alloy for sonic quality
Sep page 85 MFS-29594

INDUCTION HEATING
Adjustable induction-heating coil
Nov page 50 LEW-14963

INDUSTRIAL PLANTS
Simulating a factory via software
May page 62 MFS-28398

INFORMATION DISSEMINATION
Space information for educators
July page 108 MFS-27221

INFORMATION MANAGEMENT
Managing information on costs
July page 61 MFS-28361

INFRARED DETECTORS
Anomalous polarization may improve infrared detectors
Jan page 22 NPO-17450

Field-induced-gap infrared detectors
Mar page 32 NPO-17526

Tunable-quantum-well infrared detector
Mar page 34 NPO-17361

Layered internal-photoemission sensor
May page 32 NPO-17751

Superlattice long-wavelength infrared sensors
May page 18 NPO-17713

Self-aligned guard rings for Schottky-barrier diodes
Aug page 20 NPO-17734

INFRARED IMAGERY
Ge/Si integrated circuit for infrared imaging
Mar page 28 NPO-17397

INFRARED RADIATION
Optically-tuned far-infrared device
May page 30 NPO-17160

INFRARED SPECTROMETERS
Compact, broadband infrared spectrometer
Jan page 38 NPO-17562

Calibration of airborne visible/IR imaging spectrometer
June page 63 NPO-17582

INFRARED SPECTROSCOPY
FTIR monitoring of curing of composites
Dec page 62 LAR-14040

INFRARED TELESCOPES
Survey of infrared-absorbing coatings
Jan page 42 ARC-11767

INPUT/OUTPUT ROUTINES
General-purpose data-formatting input/output system
July page 42 LAR-13529

INSPECTION
Using ruby balls as fiducial marks
Jan page 54 MFS-29394

Magnetically-guided penetrant applicator
Feb page 58 MFS-29358

Visual-inspection probe for cryogenic chamber
Feb page 53 MSC-21444

Calibration for on-machine inspections
May page 81 MFS-29523

Inspecting the full circumferences of tubes
May page 64 MFS-29221

Milder etchant for penetrant inspection
Sep page 63 MFS-29645

Enhancement of penetrant-inspection images
Oct page 97 MFS-29496

Atomized water as couplant for ultrasonic imaging
Dec page 47 MFS-28442

INSTRUMENT ORIENTATION
Autonomous-control concept for instrument pointing system
Mar page 95 NPO-17521

INSULATION
Insulation for cryogenic-liquid tanks
Mar page 82 LEW-14707

Advanced reusable foam cryogenic insulation
Apr page 55 LAR-14014

Response of ceramic insulation to aerothermodynamic heating
May page 58 ARC-12156

Washing off polyurethane foam insulation
Dec page 59 MFS-29578

INSULATORS
Antireduction insulator for solid-electrolyte cell
Oct page 24 NPO-17211

INTEGRATED CIRCUITS
Generating weighted test patterns for VLSI chips
Jan page 30 NPO-17514

VLSI architecture for Viterbi decoder
Jan page 28 NPO-17310

VLSI Reed-Solomon encoder with interleaver
Feb page 28 NPO-17280

Integrated optoelectronic interface
Feb page 33 NPO-17650

Forward bias inhibits single-event upsets
Apr page 28 NPO-17573

Optoelectronic integrated circuits for neural networks
May page 28 NPO-17652

Electro-optical probing of terahertz integrated circuits
Aug page 29 LEW-14956

Imaging antenna structure for submillimeter wavelengths
Aug page 24 NPO-17799

Monolithic optoelectronic integrated circuit
Aug page 25 LEW-14922

Starting circuit for erasable programmable logic device
Aug page 20 NPO-17827

Viewing integrated-circuit interconnections by SEM
Sep page 18 NPO-17635

Failures of CMOS devices at low radiation-dose rates
Nov page 30 NPO-17868

INTERFACES
SCSI communication test bus
Dec page 25 MSC-21704

INTERFEROMETRY
Interferometric measurement of residual stress
Feb page 51 NPO-17440

Interferometric fiber-optic gyroscope
Apr page 22 NPO-17515

Differential radar interferometry maps changes in elevation
Sep page 36 NPO-17831

Two-wavelength optical-path-difference mapping
Nov page 55 NPO-17725

INTERPLANETARY TRANSFER ORBITS
Aerobrakes for a manned Mars mission
July page 78 ARC-12117

INTERPOLATION
Spectral analysis of linear, shift-invariant interpolants
Aug page 67 LAR-13751

INTERPROCESSOR COMMUNICATION
Communication-gateway software for NETEX, DECnet, and TCP/IP
Oct page 77 GSC-13236

INVISCID FLOW
Flux Jacobian matrices for equilibrium real gas
Dec page 28 ARC-12409

ION CURRENTS
Nonvolatile ionic two-terminal memory device
May page 20 NPO-17621

ION EXCHANGE RESINS
Stability of a carbon-dioxide-removing resin
July page 59 ARC-12129

IONIZATION
High-sensitivity ionization trace-species detector
Feb page 38 NPO-17596

ION SOURCES
Improved multiple species cyclotron ion source
Aug page 43 NPO-17766

ION TRAPS (INSTRUMENTATION)
Linear ion trap for atomic clock
Sep page 44 NPO-17758

IONIZING RADIATION
Effects of dose rates on radiation damage in CMOS parts
Sep page 32 NPO-17344

IRIDIUM
Iridium film for charge-coupled device
June page 26 NPO-17327

IRRADIANCE
Calculating irradiance for photosynthesis in the ocean
Mar page 64 NPO-17645

ISOLATORS
Fixed-position isolation valve
May page 71 NPO-17707

ITERATION
Newton/Poisson-distribution program
Aug page 53 NPO-17715

ITERATIVE SOLUTION
Computation of flutter in turbomachinery
Feb page 56 LEW-14742

J

JACOBO MATRIX METHOD
Flux Jacobian matrices for equilibrium real gas
Dec page 28 ARC-12409

JET MIXING FLOW
Perspective on dilution jet mixing
Mar page 83 LEW-14614

JET ENGINES
Stowable mechanical sound suppressor
Mar page 86 LAR-14158

JIGS
Jig for stereoscopic photography
Mar page 70 MSC-21397

JOINTS (JUNCTIONS)
Static pressure-assisted seal for helium
Mar page 70 MFS-29429

Compliant joints for robots
May page 70 GSC-13127

Preloaded composite-strut/end-fitting joint
July page 82 MFS-28339

Offset joint for segmented pressure vessel
Sep page 70 MFS-28365

Redundant, confined-explosive severance device
Sep page 75 LAR-13582

Removing dross from molten solder
Sep page 88 MFS-28406

Low-thermal-stress structural joints for dissimilar materials
Nov page 75 LAR-14138

Self-aligning coupler
Nov page 90 MSC-21459

K

KLYSTRONS
High-efficiency klystron for television transmitters
Sep page 30 LEW-14926

KRYPTON ISOTOPES
Improved multiple-species cyclotron ion source
Aug page 43 NPO-17766

L

LABORATORIES
Nano-G laboratory
June page 63 GSC-13197

LABYRINTH SEALS
Analysis of stepped labyrinth seals
Sep page 79 MFS-29585

LAMINATES
Process for autoclaving HMW PMR-II composite
Sep page 64 LEW-14839

LANDING
Algorithm schedules airplane landings
June page 92 ARC-12197

LANDING INSTRUMENTS
System predicts critical runway performance parameters
Nov page 40 LAR-13809

LAND MOBILE SATELLITE SERVICE
Connection protocol for mobile/satellite communications
June page 91 NPO-17735

Managing mobile/satellite propagation data
July page 62 NPO-17269

More about lens antenna for mobile/satellite communication
Sep page 33 NPO-17680

Study of adaptive-array signal processing
Oct page 57 NPO-17492

Data-management software for PiFEx
Dec page 39 NPO-17463

LARGE SPACE STRUCTURES
Experiments on active members in large space structures
Oct page 81 NPO-17623

LASER ANEMOMETERS
Processing laser-velocimetric data by vector scanning
Oct page 98 LEW-14925

LASER APPLICATIONS
Header for laser diode
Apr page 16 GSC-13234

Integrated electro-optical laser-beam scanners
May page 26 MSC-21498

Laser Schlieren system detects sounds of leaks
Aug page 45 NPO-17009

LASER DOPPLER VELOCIMETERS
Laser Doppler and range systems for spacecraft
Feb page 36 NPO-17486

Frequency-domain signal processor for laser velocimeter
May page 45 LAR-13552

Laser velocimetry in low-speed wind tunnels
Sep page 42 ARC-11564

LASER GUIDANCE
Compensating for Doppler shift in laser instrumentation
Aug page 31 GSC-13194

LASER INTERFEROMETRY
Automatic calibration of manual machine tools
Jan page 61 MFS-29380

Interferometric measurement of residual stress
Feb page 51 NPO-17440

LASER RANGE FINDERS
Electronically scanned laser rangefinder
May page 46 NPO-17571

LASER RANGER/TRACKER
Determining spatial coordinates by laser ranging
Jan page 57 NPO-17436

LASERS
Improved design for birefringent filter
May page 56 LAR-13887

Annular-Bragg-grating surface-emitting laser
Oct page 20 NPO-17912

Unstable-resonator distributed-Bragg-reflector laser
Oct page 20 NPO-17906

Monolithic unidirectional nonplanar ring laser
Nov page 58 LAR-14146

Monolithic unidirectional planar ring laser
Nov page 58 LAR-14045

LATCHES
Perpendicular-force latch
Feb page 54 MSC-21406

Simulating a massive, mobile structure
Sep page 72 MSC-21482

LAUNCHERS
Electromagnetic Meissner-effect launcher
Apr page 64 MFS-28323

LEAD ACID BATTERIES
Durable bipolar plates lead/acid batteries
Apr page 22 NPO-17662

Making more efficient use of battery-plate mass
May page 34 NPO-17435

LEADING EDGE FLAPS
Code for analysis of wing-and-flap systems
Oct page 74 LAR-13994

LEAKAGE
Pressure gauges monitor leakage past seals
Feb page 50 MSC-21385

Laser Schlieren system detects sounds of leaks
Aug page 45 NPO-17009

Sealing nitrogen tetroxide leaks
Nov page 89 MSC-21600

LEARNING MACHINES
Method for model-reference adaptive control
June page 94 NPO-17717

LEAST SQUARES METHOD
Least-squares curve-fitting program
Aug page 53 NPO-17819

Software for least-squares and robust estimation
Dec page 40 MFS-26108

LENS ANTENNA
More about lens antenna for mobile/satellite communication
Sep page 33 NPO-17680

LEVERS
Four-wheel vehicle suspension system
Aug page 55 NPO-17407

LIGHT EMITTING DIODES
Two-way optical data link on one fiber
Oct page 31 NPO-17884

LIGHT MODULATION
Optical modulation via the photorefractive effect
May page 48 NPO-17460

Improved photovoltaic-driven quantum light modulator
Aug page 26 NPO-17357

Multi-quantum-well spatial light modulators on Si substrates
Nov page 32 NPO-17651

LIGHTNING
Determining polarities of distant lightning strokes
June page 56 MFS-26102

LIGHT VALVES
Binary operation of a liquid-crystal light valve
Oct page 24 NPO-17614

LIGNIN
Lignin sensor based on flash-pyrolysis mass spectrometry
Mar page 62 NPO-17592

LINEARIZATION
Exact linearization for control of robots
Sep page 97 NPO-17363

LINEAR POLARIZATION
KD_2PO_4 polarization modulator with large field of view
Nov page 54 MFS-28418

LINEAR SYSTEMS
Estimability and regulability of linear systems
Aug page 35 ARC-12173

LININGS
Reinforcing liner for composite tank
June page 66 MFS-28399

LINKAGES
Perpendicular-force latch
Feb page 54 MSC-21406

LIPSCHITZ CONDITIONS
Non-Lipschitzian dynamics for modeling neural networks
Sep page 97 NPO-17814

LITHIUM SULFUR BATTERIES
$NbSe_3$ cathodes for Li rechargeable cells
Nov page 61 NPO-17491

LIQUID AIR
Liquid-air breathing apparatus
Aug page 74 KSC-11431

LIQUID CRYSTALS
Binary operation of a liquid-crystal light valve
Oct page 24 NPO-17614

LIQUID FUELS
Convective evaporation of clusters of drops
Feb page 42 NPO-17171

LIQUID HELIUM
Automatic refilling system for liquid helium
July page 46 GSC-13270

Equations for isocaloric fountain-effect pumps
July page 52 ARC-11850

Silicon detectors for helium liquid and vapor
Aug page 44 GSC-13281

LIQUID HELIUM 2
Temperature rises in pumps for superfluid helium
July page 51 ARC-12264

LIQUID OXYGEN
Testing bearing balls for ignition in liquid oxygen
July page 75 MFS-29410

LIQUID SODIUM
Copper chloride cathode for liquid-sodium cell
Aug page 28 NPO-17640

LOADS (FORCES)
Ultrasonic monitor to determine crack-opening load
Aug page 57 LAR-13889

Balancing loads among robotic-manipulator arms
Sep page 98 NPO-17649

LOCAL AREA NETWORKS
Carrying synchronous voice data on asynchronous networks
Feb page 31 NPO-17431

Local-area-network simulator
Dec page 38 ARC-12168

LOCKING
Charging/safety-interlock connection for capacitor
Dec page 20 NPO-17519

Rotary ball locking mechanism
Dec page 56 MSC-21396

LOCKS (FASTENERS)
Spring-loaded-bolt locking device
Dec page 47 LEW-14887

LOGIC CIRCUITS
Gallium arsenide domino circuit
Mar page 36 NPO-17417

Quantized-gray-scale electronic synapses
Apr page 21 NPO-17579

Analog delta-back-propagation neural-network circuitry
June page 28 NPO-17564

Neural-network computer transforms coordinates
July page 35 NPO-17753

Program aids simulation of neural networks
Aug page 50 MSC-21588

Starting circuit for erasable programmable logic device
Aug page 20 NPO-17827

Adaptive neurons for artificial neural networks
Dec page 24 NPO-17803

Neural network solves "traveling-salesman" problem
Dec page 22 NPO-17807

LOGISTICS MANAGEMENT
Bar-code system tracks test equipment
June page 42 KSC-11370

LOUD SPEAKERS
Improved voice-coil actuators have lower copper losses
Dec page 18 MFS-26111

LOW SPEED WIND TUNNELS
Laser velocimetry in low-speed wind tunnels
Sep page 42 ARC-11564

M

MACHINE TOOLS
Automatic calibration of manual machine tools
Jan page 61 MFS-29380

Calibration for on-machine inspections
May page 81 MFS-29523

MACHINING
Software for numerically controlled machining
May page 62 GSC-13214

Removing burrs in confined spaces
July page 81 MFS-29392

Ultrasonic abrasive removal of EDM recast
Oct page 97 MFS-29545

Numerically controlled machining wind-tunnel models
Dec page 58 LAR-14004

MAGNETIC DISKS
Fast, capacious disk memory device
June page 44 GSC-13196

MAGNETIC MATERIALS
Filling porous microspheres with magnetic material
Feb page 47 NPO-17044

Enhanced data-acquisition system
May page 36 MSC-21598

MAGNETIC RECORDING
Enhanced data-acquisition system
May page 36 MSC-21598

MAGNETIC SUSPENSION
Heteropolar magnetic suspension
June page 75 MFS-26096

Flux-feedback magnetic-suspension actuator
July page 44 LAR-13785

MAGNETOACOUSTICS
Nondestructive technique to assess embrittlement in steels
Oct page 64 LAR-13817

MAINTENANCE
Remote maintenance monitoring
June page 38 KSC-11398

MANAGEMENT ANALYSIS
Analyzing distributed processing for electric utilities
Dec page 38 NPO-17710

MANAGEMENT PLANNING
Software model of software-development process
Mar page 100 NPO-17424

MANIPULATORS
Robot hand would adapt to contours
Mar page 86 NPO-16766

Hard contact with a force-reflecting teleoperator
Apr page 70 NPO-17549

Recursive construction of Jacobian matrix and its time derivative for robot arm
Apr page 89 NPO-17364

Compliant joints for robots
May page 70 GSC-13127

Multivariable PID controller for robotic manipulator
June page 93 NPO-17647

Robust, high-performance control for robotic manipulators
Sep page 36 NPO-17785

Improved "smart" robot hand
Nov page 38 NPO-17917

MANNED MARS MISSION
Aerobrakes for a manned Mars mission
July page 78 ARC-12117

MANUFACTURING
Simulating a factory via software
May page 62 MFS-28398

MAPPING
Extracting geocoded images from SAR data
Apr page 59 NPO-17418

Programmable remapper
June page 46 MSC-21350

Differential radar interferometry maps changes in elevation
Sep page 36 NPO-17831

MAPS
Processor would find best paths on map
May page 40 NPO-17716

MARKOV CHAINS
Markov chains for testing redundant software
Mar page 101 LAR-13812

MARKOV PROCESSES
Generating semi-Markov models automatically
Nov page 71 LAR-14193

MARS OBSERVER
Prototype V-groove radiator heat shield
Apr page 55 NPO-17744

MASERS
32-GHz wideband maser amplifier
Mar page 38 NPO-17558

MASS DISTRIBUTION
Computing mass properties from AutoCAD
June page 68 GSC-13228

MASS RATIOS
Controlling gas-flow mass ratios
Dec page 26 MSC-21542

MASS SPECTROMETERS
High-sensitivity ionization trace-species detector
Feb page 38 NPO-17596

Lignin sensor based on flash-pyrolysis mass spectrometry
Mar page 62 NPO-17592

MATHEMATICAL MODELS
Calculating second-order effects in MOSFET's
Jan page 22 NPO-17395

More about multiple-boundary-condition testing
Jan page 58 NPO-17574

MATRICES (MATHEMATICS)
Matrix•vector multiplication in thin photorefractive crystal
June page 62 NPO-17455

MATRICES (CIRCUITS)
Switching matrix for optical signals
Sep page 22 KSC-11392

MATRIX MATERIALS
Tough, microcracking-resistant, high-temperature polymer
June page 64 LAR-13925

High-temperature polyimide resin
July page 54 LEW-14923

LARC-I-TPI: a new thermoplastic polyimide
July page 55 LAR-14101

Microstructure of a SiC/(Ti/V/Cr/Sn/Al) composite
Nov page 61 LEW-14868

MEASURING INSTRUMENTS
Measuring diameters of large vessels
Jan page 53 MFS-28287

Printed-circuit tape measures for x-ray inspections
Feb page 58 MFS-28388

Shape gauge measures surfaces
Feb page 52 MFS-28284

Radial profilometry
Sep page 74 MFS-26101

Two radiative/thermochemical instruments
Nov page 54 MSC-21639/40

MECHANICAL DEVICES
Double-swivel mechanism for reliable release
July page 64 MSC-21436

MECHANICAL PROPERTIES
Superplastically formed titanium hat-stiffened panels
Jan page 63 LAR-13814

MEMORY (COMPUTERS)
Programmable analog memory resistors for electronic neural networks
Feb page 18 NPO-17398

Programmable direct-memory-access controller
Mar page 54 NPO-17341

Molecular electronic shift registers
May page 55 NPO-17606

Nonvolatile ionic two-terminal memory device
May page 20 NPO-17621

Fast, capacious disk memory device
June page 44 GSC-13196

Porous-floating-gate field-effect transistor
July page 18 NPO-17532

METAL FATIGUE
Thermal-transient testing of turbine blades
May page 68 MFS-29416

METAL FILMS
Iridium film for charge-coupled device
June page 26 NPO-17327

METAL FOILS
Steel foil improves performance of blasting caps
Apr page 60 LAR-13832

METAL HYDRIDES
Cheaper hydride-forming cathodes
Dec page 34 NPO-17927

METAL JOINTS
Noncontact ultrasonic vibration of weld puddles
Nov page 91 MFS-29715

METAL OXIDES
Computer simulation of cyclic oxidation
Apr page 48 LEW-14890

METAL OXIDE SEMICONDUCTORS
Calculating second-order effects in MOSFET's
Jan page 22 NPO-17395

Upper-bound estimates of SEU in CMOS
Apr page 26 NPO-17566

Failures of CMOS circuits irradiated at low rates
Aug page 29 NPO-17867

METAL GRINDING
Automatic tension adjuster for flexible-shaft grinder
Mar page 93 MFS-29351

METAL MATRIX COMPOSITES
Making fiber-reinforced metal by rapid solidification
Mar page 94 LEW-14918

METAL OXIDE SEMICONDUCTORS
Calculating second-order effects in MOSFET's
Jan page 22 NPO-17395

METAL SURFACES
Bonding elastomers to metal substrates
July page 82 LAR-13645

METEOROLOGICAL BALLOONS
Two tethered balloon systems
Feb page 39 LAR-13837

MICROCHANNEL PLATES
Multiple-dynode-layer microchannel plate
July page 33 GSC-13203

Low-noise, long-life, high-gain microchannel-plate glass
Aug page 47 LAR-14010

MICROCRACKS
Grinding away microfissures
Aug page 62 MFS-29566

MICROMECHANICS
Tribological properties of ceramics
Mar page 67 LEW-14833

MICROPARTICLES
Filling porous microspheres with magnetic material
Feb page 47 NPO-17044

MICROPHONES
Microphone detects waves in laminar boundary-layer flow
Nov page 56 NPO-17479

MICROPROCESSORS
Bus-programmable slave card
Sep page 34 MSC-21387

Microprocessor control for liquid-cooled garment
Oct page 52 MSC-21359

MICROSCOPES
Ballistic-electron-emission microscope
Jan page 34 NPO-17384

MICROSTRIP ANTENNAS
Wideband microstrip antenna-feeding array
Mar page 26 NPO-17548

Planar microstrip Yagi antennas
Sep page 18 NPO-17873

MICROWAVE AMPLIFIERS
32-GHz wideband maser amplifier
Mar page 38 NPO-17558

External Peltier cooler for low-noise amplifier
Nov page 26 MSC-21422

MICROWAVE ANTENNAS
Optical detection of deformations of an antenna
May page 38 NPO-17677

Planar microstrip Yagi antennas
Sep page 18 NPO-17873

MICROWAVE LANDING SYSTEMS
Testing microwave landing systems with satellite navigation
Apr page 36 KSC-11451

MICROWAVE RADIOMETERS
Multibeam 1.4-GHz pushbroom microwave radiometer
July page 38 LAR-14023

MICROWAVE TRANSMISSION
Trellis-coded MDPSK system with Doppler correction
Apr page 40 KSC-17644

MILLIMETER WAVES
Millimeter-wave quantum-well frequency multipliers
Sep page 28 NPO-17584

MINING
Hydromechanical advanced coal excavator
Nov page 80 NPO-16442

MOBILE COMMUNICATION SYSTEMS
Trellis-coded MDPSK system with Doppler correction
Apr page 40 KSC-17644

More about lens antenna for mobile/satellite communication
Sep page 33 NPO-17680

Data-management software for PiFEx
Dec page 39 NPO-17463

MODAL RESPONSE
Characteristic-wave approach complements modal analysis
May page 72 NPO-17741

MODEL REFERENCE ADAPTIVE CONTROL
Method for model-reference adaptive control
June page 94 NPO-17717

MODELS
Simplified models speed electroforming tests
Apr page 76 MFS-29505

Computer program relayers engineering drawings
Dec page 57 MFS-28445

MODULATION
Multiple-trellis-coded modulation
Jan page 71 NPO-17100

Selecting modulation indices for telemetry and ranging
June page 54 NPO-17535

MODULATORS
KD_2PO_4 polarization modulator with large field of view
Nov page 54 MFS-28418

MOIRE EFFECTS
Laser Schlieren system detects sounds of leaks
Aug page 45 NPO-17009

MOISTURE CONTENT
Acoustic humidity sensor
Apr page 47 NPO-17685

MOLDS
Borescope device takes impressions in ducts
Apr page 74 MFS-29483

MONITORS
Automatic monitoring of complicated systems
Mar page 100 NPO-17409

Monitoring both sides of a weld in progress
Sep page 84 MFS-28389

Cooperating expert systems for automated monitoring and diagnostics
Nov page 94 NPO-17804

MONOTECTIC ALLOYS
Directional solidification of monotectic alloys
Sep page 61 MFS-26080

MOSAICS
Making mosaics of SAR imagery
Apr page 58 NPO-17586

MOTION SIMULATION
Computer animation in perception research
Jan page 76 ARC-11774

MOTORS
Balanced-bridge feedback control of motor
Mar page 52 NPO-17430

MULTISPECTRAL RESOURCE SAMPLER
Terrestrial-imaging spectroscopy
Mar page 65 NPO-17432

Processing of multispectral data for identification of rocks
Apr page 53 NPO-17581

MUSCLES
Implantable electrode for critical locations
Aug page 74 NPO-17264

Mathematical model of nerve/muscle interaction
Aug page 73 NPO-17816

N

NASA PROGRAMS
Space information for educators
July page 108 MFS-27221

NAVIER-STOKES EQUATION
Upwind algorithm for parabolized Navier-Stokes equations
May page 73 ARC-12146

Combination of techniques for computing incompressible flow
June page 71 ARC-12257

Simulation of unsteady, viscous, incompressible flow
July page 67 ARC-12277

Computing blood flows
Oct page 83 ARC-12253

Simulation of three-dimensional supersonic flows
Oct page 82 ARC-12235

NAVIGATION
Tests of a differential global positioning system
Oct page 56 ARC-12313

NEAR FIELDS
Interpolation and FFT of near-field antenna measurements
Feb page 44 NPO-17597

NEODYMIUM LASER
Monolithic unidirectional nonplanar ring laser
Nov page 58 LAR-14146

NERVES
Mathematical model of nerve/muscle interaction
Aug page 73 NPO-17816

NETWORK CONTROL
Communication-gateway software for NETEX, DECnet, and TCP/IP
Oct page 77 GSC-13236

NEURAL NETS
Programmable analog memory resistors for electronic neural networks
Feb page 18 NPO-17398

Quantized-gray-scale electronic synapses
Apr page 21 NPO-17579

Nonvolatile ionic two-terminal memory device
May page 20 NPO-17621

Optoelectronic integrated circuits for neural networks
May page 28 NPO-17652

Analog delta-back-propagation neural-network circuitry
June page 28 NPO-17564

Neural-network computer transforms coordinates
July page 35 NPO-17753

Porous-floating-gate field-effect transistor
July page 18 NPO-17532

Program aids simulation of neural networks
Aug page 50 MSC-21588

Non-Lipschitzian dynamics for modeling neural networks
Sep page 97 NPO-17814

Neural-network processor would allocate resources
Oct page 46 NPO-17781

Adaptive neurons for artificial neural networks
Dec page 24 NPO-17803

Neural network solves "traveling-salesman" problem
Dec page 22 NPO-17807

NEWTON METHODS
Newton/Poisson-distribution program
Aug page 53 NPO-17715

NICKEL ALLOYS
Welding and cutting a nickel alloy by laser
Mar page 93 MFS-27208

Treating nickel alloy for sonic quality
Sep page 85 MFS-29594

TAZ-8A alloy increases the thermal endurance of steel
Dec page 32 LEW-14280

NICKEL PLATE
Electrodeposited nickel reinforces outlet neck
May page 80 MFS-29447

NIOBIUM ALLOYS
High-temperature creep behavior of fiber-reinforced niobium
July page 58 LEW-14831

NITRIC OXIDE
Nitric oxide enhances charge-coupled device
June page 26 NPO-17281

NITROGEN COMPOUNDS
Polyimidazoles via aromatic nucleophilic displacement
Aug page 48 LAR-14145

Polyimides containing carbonyl and ether connecting groups
Dec page 35 LAR-14001

NITROGEN TETROXIDE
Sealing nitrogen tetroxide leaks
Nov page 89 MSC-21600

NOISE SPECTRA
Predicting noise from wind turbines
Mar page 68 LAR-13984

NOISE REDUCTION
Stowable mechanical sound suppressor
Mar page 86 LAR-14158

NONCONDENSABLE GASES
Trap for noncondensable gas in heat-transfer fluid
Dec page 48 MSC-21389

NONDESTRUCTIVE TESTS
Ballistic-electron-emission microscope
Jan page 34 NPO-17384

Nondestructive technique to assess embrittlement in steels
Oct page 64 LAR-13817

Atomized water as couplant for ultrasonic imaging
Dec page 47 MFS-28442

NONFLAMMABLE MATERIALS
Isomeric trisaryloxycyclotriphosphazene polymer precursors
Jan page 42 LAR-13819

NONLINEAR FILTERS
Performances of fixed-lag phase-smoothing algorithms
Jan page 73 NPO-17202

NONLINEAR OPTICS
Compounds generate optical second harmonics
June page 56 NPO-17731

NUMERICAL ANALYSIS
Assignment of finite elements to parallel processors
Feb page 61 NPO-17371

Finite-element composite-analysis program
Oct page 73 LAR-14109

NUMERICAL CONTROL
Numerical models for control of robots
Apr page 88 MFS-28360

Software for numerically controlled machining
May page 62 GSC-13214

Numerically controlled machining of wind-tunnel models
Dec page 58 LAR-14004

O

OCEANS
Calculating irradiance for photosynthesis in the ocean
Mar page 64 NPO-17645

OPTICAL COMMUNICATION
Analyzing optical communication links
Mar page 68 NPO-17444

Header for laser diode
Apr page 16 GSC-13234

Fiber-optic frequency-transfer link
July page 43 NPO-17703

Switching matrix for optical signals
Sep page 22 KSC-11392

OPTICAL DATA PROCESSING
Optical pseudocolor encoding of gray-scale image
Oct page 59 NPO-17764

OPTICAL EQUIPMENT
Post clamp with attached collar
Jan page 48 LEW-14862

Borescope with large depth of focus
May page 64 MFS-29461

Inspecting the full circumferences of tubes
May page 64 MFS-29221

OPTICAL FILTERS
Filter enhances fluorescent-penetrant-inspecting borescope
Mar page 91 MFS-29379

Improved design for birefringent filter
May page 56 LAR-13887

Birefringent-filter model
July page 60 LAR-13945

Calculating performances of Fabry-Perot etalons
Sep page 66 LAR-14055

OPTICAL GYROSCOPES
Interferometric fiber-optic gyroscope
Apr page 22 NPO-17515

OPTICAL HETERODYNING
Noncoherent combination of optical-heterodyne outputs
Oct page 55 NPO-17693

OPTICAL MEASUREMENT
Measuring monodisperse small particles en masse
Dec page 45 LAR-14152

OPTICAL MEASURING INSTRUMENTS
Compact, broadband infrared spectrometer
Jan page 38 NPO-17562

OPTICAL PATHS
Two-wavelength optical-path-difference mapping
Nov page 55 NPO-17725

OPTICAL PROPERTIES
Optical properties of ceramic fabrics
Dec page 36 ARC-11739

OPTICAL SCANNERS
Integrated electro-optical laser-beam scanners
May page 26 MSC-21498

OPTIMIZATION
Computer simulation for multilevel optimization of design
Apr page 87 LAR-13850

Software for least-squares and robust estimation
Dec page 40 MFS-26108

OPTOELECTRONIC DEVICES
Integrated optoelectronic interface
Feb page 33 NPO-17650

Optoelectronic integrated circuits for neural networks
May page 28 NPO-17652

Matrix•vector multiplication in thin photorefractive crystal
June page 62 NPO-17455

GaAlAs traveling-wave electro-optical modulators
July page 24 LEW-14866

Electro-optical probing of terahertz integrated circuits
Aug page 29 LEW-14956

Monolithic optoelectronic integrated circuit
Aug page 25 LEW-14922

Active limiters for photodetectors
Sep page 38 NPO-17654

Radial profilometry
Sep page 74 MFS-26101

Two-way optical data link on one fiber
Oct page 31 NPO-17884

Fast feature-recognizing optoelectronic system
Nov page 42 NPO-17690

ORBITAL MECHANICS
Model of orbital density of air for computing drag
Feb page 48 MSC-21154

ORGANIC COMPOUNDS
Compounds generate optical second harmonics
June page 56 NPO-17731

ORGANIZING
Schedule-organizer computer program
Nov page 69 MSC-21525

Schedule-report-generator computer program
Nov page 68 MSC-21527

Schedule-tracker computer program
Nov page 70 MSC-21526

ORIFICES
Multiple-inlet/single-outlet orifice plate
May page 67 MFS-29407

Simple, internally adjustable valve
Sep page 76 MFS-29463

O RING SEALS
Measuring gaps in O-ring seals
Feb page 52 MFS-28332

O-ring-testing fixture
Dec page 46 MFS-28376

OSCILLATORS
Crystal oscillators operate beyond rated frequencies
Apr page 30 GSC-13171

Tunable quantum-well submillimeter-wave oscillators
July page 26 NPO-17754

OUTPUT
Output control of using feedforward and cascade controllers
Feb page 37 NPO-17420

OXIDATION
Computer simulation of cyclic oxidation
Apr page 48 LEW-14890

Catalytic destruction of toxic organic compounds
Sep page 46 NPO-17669

OXYGEN
Compact analyzer/controller for oxygen-enrichment system
June page 50 LAR-14016

OXYGEN PLASMA
Chamber for testing polymers in oxygen plasma
Aug page 46 MFS-28368

OZONE
Measuring concentration of ozone automatically
June page 60 ARC-12230

Ozone treatment for cooling towers
Aug page 60 KSC-11384

P

PANELS
Numerical simulation of buckling in waffle panels
June page 73 MSC-21599

PARABOLIC ANTENNAS
An optimal design for steerable dish antenna with BWG
Mar page 33 NPO-17429

Disturbance-accommodating controller would aim antenna
Mar page 42 NPO-17631

Array feed to compensate for distortion in antenna
Apr page 38 NPO-17667

Dielectric-filled paraboloidal front ends
Sep page 24 NPO-17802

PARABOLIC REFLECTORS
Two-wavelength optical-path-difference mapping
Nov page 55 NPO-17725

PARALLEL PROCESSING (COMPUTERS)
Hypercube-computer analysis of electromagnetic scattering
Jan page 33 NPO-17551

Assignment of finite elements to parallel processors
Feb page 61 NPO-17371

Competitive parallel processing for compression of data
Feb page 32 NPO-17445

Optimal allocation of tasks in hypercube computers
Apr page 79 NPO-17215

Parallel architecture for robotics computation
June page 36 NPO-17629

Balancing loads among parallel data processors
Aug page 67 MSC-21348

PARTICLE IN CELL TECHNIQUE
Concurrent algorithm for particle-in-cell simulations
Sep page 95 NPO-17737

PARTICLES
Measuring monodisperse small particles en masse
Dec page 45 LAR-14152

PARTICLE SIZE DISTRIBUTION
Feeder system for particle-size analyzer
Apr page 61 MFS-28326

PARTICULATES
Adhesion between particles and surfaces in a vacuum
Nov page 60 NPO-17743

PCM TELEMETRY
Test processor for PCM telemetry
Aug page 27 GSC-13291

PELTIER EFFECTS
External Peltier cooler for low-noise amplifier
Nov page 26 MSC-21422

PENETRANTS
Magnetically-guided penetrant applicator
Feb page 58 MFS-29358

Prepenetrant etchant for Incoloy* 903 weld overlays
Apr page 78 MFS-29576

Milder etchant for penetrant inspection
Sep page 63 MFS-29645

Enhancement of penetrant-inspection images
Oct page 97 MFS-29496

PERFLUORO COMPOUNDS
Emulsions containing perfluorocarbon support cell cultures
Sep page 99 MSC-21480

PERFORMANCE PREDICTION
Pivotal-function assessment of reliability of software
July page 107 LAR-13842

Organizing performance requirements for dynamic systems
Aug page 72 MSC-21235

PERIPHERAL EQUIPMENT (COMPUTERS)
Peripheral equipment interchanges bytes of data
Mar page 48 MFS-29478

PERMITTIVITY
Additives lower dielectric constants of polyimides
Aug page 49 LAR-13902

PERSONAL COMPUTERS
Data-acquisition board for IBM PS/2 computer
Oct page 45 MSC-21590

PHASE CONTROL
Phase-compensating system for fiber-optic holography
June page 34 LEW-14864

PHASED ARRAYS
Printed-circuit cross-slot antenna
Feb page 26 NPO-17706

PHASE ERROR
Phase calibration of radar polarimetric data
Sep page 91 NPO-17844

PHASE SHIFT KEYING
Multiple-trellis-coded modulation
Jan page 71 NPO-17100

Trellis-coded MDPSK system with Doppler correction
Apr page 40 NPO-17644
Double differential encoding and detection in MPSK
June page 46 NPO-17666

PHOSPHAZENE
Isomeric trisaryloxycyclotriphosphazene polymer precursors
Jan page 42 LAR-13819

PHOTOCHEMICAL REACTIONS
Photochemical degradation of organic-solvent fumes
June page 61 MFS-29596

PHOTOCONDUCTIVITY
Binary operation of a liquid-crystal light valve
Oct page 24 NPO-17614

PHOTOCONDUCTORS
Detection of gas-phase polymerization in SiH_4 and GeH_4
July page 47 NPO-17779

PHOTOELECTRIC EMISSION
Layered internal-photoemission sensor
May page 32 NPO-17751

PHOTOGRAPHIC FILM
Positioning x-ray film with string and magnets
May page 78 MFS-29448

PHOTOMETERS
Nitric oxide enhances charge-coupled device
June page 26 NPO-17281

Active limiters for photodetectors
Sep page 38 NPO-17654

PHOTOSYNTHESIS
Calculating irradiance for photosynthesis in the ocean
Mar page 64 NPO-17645

PHOTOVOLTAIC EFFECT
Improved photovoltaic-driven quantum light
Aug page 26 NPO-17357

PHYSICAL EXERCISE
Programmable cadence timer
July page 42 MSC-21551

PIEZOELECTRIC TRANSDUCERS
Piezoelectric pushers suppress vibrations
Aug page 59 LEW-14927

PINS
Double-swivel mechanism for reliable release
July page 64 MSC-21436

PINTLES
Liquid-flow controller with preset break pressure
Mar page 73 MFS-28330

Liquid-flow controller with trickle preflow
Mar page 74 MFS-28331

PIPE FLOW
Schlieren system for flow studies in round glass pipes
Oct page 58 LAR-13944

PIPELINING (COMPUTERS)
Simplified correction of errors in Reed-Solomon codes
Jan page 68 NPO-17381

Pipeline time- and transform-domain Reed-Solomon decoders
May page 94 NPO-17510

PIPES (TUBES)
Rounding and aligning tubes for butt welding
Jan page 62 MFS-29363
Inspecting the full circumferences of tubes
May page 64 MFS-29221

Mechanized fluid connector and assembly tool
Oct page 79 MSC-21434

PISTON ENGINES
High-temperature materials for Stirling engines
Apr page 56 LEW-14836

PISTONS
Advanced composite pistons
Sep page 90 LAR-13926

PLASMA CHEMISTRY
Chamber for testing polymers in oxygen plasma
Aug page 46 MFS-28368

PLASMA PHYSICS
Concurrent algorithm for particle-in-cell simulations
Sep page 95 NPO-17737

PLASMA SPRAYING
Monitoring coating thickness during plasma spraying
Sep page 84 LEW-14919

PLAN POSITION INDICATORS
Software for clear-air Doppler-radar display
Feb page 69 KSC-11427

PLANETARY ATMOSPHERES
Survey of gas-correlation spectroradiometry
Feb page 43 NPO-17345

PLASMA ARC WELDING
Development of advanced welding control system
Jan page 64 MFS-26106

Physics of variable-polarity plasma arc welding
Feb page 60 MFS-27207

PLATES (STRUCTURAL MEMBERS)
Multiple-inlet/single-outlet orifice plate
May page 67 MFS-29407

PLATINUM BLACK
Enhancement of Pt/SnO_2 catalysts by addition of H_2O
July page 54 LAR-14084

PLOTTING
Program manipulates plots for effective display
Oct page 78 GSC-13232

PLUGGING
Sealing nitrogen tetroxide leaks
Nov page 89 MSC-21600

PLUMES
Computing impingements of rocket exhausts
Sep page 67 MSC-21419

PLY ORIENTATION
Angle-ply weaving
Oct page 91 LAR-14048

PNEUMATIC EQUIPMENT
Automatic tension adjuster for flexible-shaft grinder
Mar page 93 MFS-29351

Spot-welding gun with adjustable pneumatic spring
June page 81 MFS-29569

POISSON DENSITY FUNCTIONS
Cumulative Poisson distribution program
July page 62 NPO-17714

Newton/Poisson-distribution program
Aug page 53 NPO-17715

POLARIMETRY
Classification of radar scatters via polarimetric data
May page 54 NPO-17373

Phase calibration of radar polarimetric data
Sep page 91 NPO-17844

POLARITY
Determining polarities of distant lightning strokes
June page 56 MFS-26102

POLARIZATION (WAVES)
Anomalous polarization may improve infrared detectors
Jan page 22 NPO-17450

POLARIZED ELECTROMAGNETIC RADIATION
KD_2PO_4 polarization modulator with large field of view
Nov page 54 MFS-28418

POLARIZED LIGHT
Optical modulation via the photorefractive effect
May page 48 NPO-17460

POLISHING
Grinding away microfissures
Aug page 62 MFS-29566

Polishing difficult-to-reach cavities
Dec page 63 MFS-29692

POLYIMIDE RESINS
Ethynyl-terminated imidothioethers and derived resins
May page 59 LAR-13910

Tough, microcracking-resistant, high-temperature polymer
June page 64 LAR-13925

High-temperature polyimide resin
July page 54 LEW-14923

LARC-I-TPI: a new thermoplastic polyimide
July page 55 LAR-14101

POLYIMIDES
Preparation of high-temperature reactive oligomers
June page 66 LAR-13965

Additives lower dielectric constants of polyimides
Aug page 49 LAR-13902

Polymides containing carbonyl and ether connecting groups
Dec page 35 LAR-14001

POLYMER CHEMISTRY
Polyimidazoles via aromatic nucleophilic displacement
Aug page 48 LAR-14145

POLYMERIZATION
FTIR monitoring of curing of composites
Dec page 62 LAR-14040

POLYMERS
Absorption of gases by glassy polymers
Feb page 45 NPO-17636

Chamber for testing polymers in oxygen plasma
Aug page 46 MFS-28368

POLYNOMIALS
Least-squares curve-fitting program
Aug page 53 NPO-17819

Trigonometric polynomials for estimation of spectra
Nov page 94 NPO-17885

POLYURETHANE FOAM
Washing off polyurethane foam insulation
Dec page 59 MFS-29578

POROUS MATERIALS
Predicting pressure drop in porous materials
Jan page 56 LAR-14105

POSITION INDICATOR
Printed-circuit tape measures for x-ray inspections
Feb page 58 MFS-28388

POSITIONING DEVICES (MACHINERY)
Jig for steroscopic photography
Mar page 70 MSC-21397

POWDER METALLURGY
Making self-lubricating parts by powder metallurgy
Sep page 63 LEW-14902

POWER SUPPLY CIRCUITS
Current-monitoring and -limiting circuit for 28-Vdc supply
Oct page 28 GSC-13310

Preventing simultaneous conduction in switching transistors
Nov page 34 NPO-17775

Charging/safety-interlock connection for capacitor
Dec page 20 NPO-17519

PREFORMS
Angle-ply weaving
Oct page 91 LAR-14048

PRESERVING
Sensor detects overheating of perishable material
May page 95 NPO-17585

PRESSURE GAUGES
Pressure gauges monitor leakage past seals
Feb page 50 MSC-21385

PRESSURE GRADIENTS
Predicting pressure drop in porous materials
Jan page 56 LAR-14105

PRESSURE MEASUREMENT
Pressure-measuring diaphragm transmits optical signals
Sep page 76 MFS-29535

PRESSURE MODULATOR RADIOMETERS
Diagnosis of a pressure-modulator-radiometer cell
Mar page 63 NPO-17528

PRESSURE REGULATORS
Simple regulator for positive-pressure glove box
Dec page 62 NPO-17786

PRESSURE VESSELS
Wrapped wire detects rupture of pressure vessel
Apr page 66 MSC-21449

Offset joint for segmented pressure vessel
Sep page 70 MFS-28365

PRIMERS (EXPLOSIVES)
Steel foil improves performance of blasting caps
Apr page 60 LAR-13832

PRINTED CIRCUITS
Printed-circuit cross-slot antenna
Feb page 26 NPO-17706

Connecting multiple wires to a single through hole
Mar page 92 MFS-29405

PRINTOUTS
Displaying TeX files on graphics terminals
Aug page 51 NPO-17296

PROCESS CONTROL (INDUSTRY)
Markov chains for testing redundant software
Mar page 101 LAR-13812

PROFILOMETERS
Radial profilometry
Sep page 74 MFS-26101

PROGRAMMING LANGUAGES
An Ada linear-algebra software package modeled after HAL/S
Dec page 42 NPO-17985

PROJECT MANAGEMENT
S-chart -- scheduling-chart program
Nov page 74 MFS-29531

PROPELLANT COMBUSTION
Measuring response of propellant to oscillatory heat flux
Oct page 59 NPO-17428

PROPELLANT SPRAYS
Liquid-flow controller responds to pressure
Mar page 72 MFS-28329

PROTECTIVE COATINGS
Electrochemical study of corrosion of painted steel
Jan page 44 MFS-27213

PSEUDOMONAS
Indicator for psuedomonas bacteria
Oct page 101 NPO-17653

PSEUDORANDOM SEQUENCES
Concept for generation of long Pseudorandom sequences
Mar page 50 NPO-17241

PULSE COMMUNICATION
Carrying synchronous voice data on asynchronous networks
Feb page 31 NPO-17431

Connection protocol for mobile/satellite communications
June page 91 NPO-17735

Two-way optical data link on one fiber
Oct page 31 NPO-17884

PULSED LASERS
Time-resolved measurements of laser far-field patterns
Oct page 55 GSC-13338

PULSE POSITION MODULATION
Analyzing optical communication links
Mar page 68 NPO-17444

PULTRUSION
Graphite-thermoplastic-pultrusion die
Feb page 59 LAR-13719

PUMPS
Equations for isocaloric fountain-effect pumps
July page 52 ARC-11850

Temperature rises in pumps for superfluid helium
July page 51 ARC-12264

PUSHBROOM SENSOR MODE
Multibeam 1.4-GHz pushbroom microwave radiometer
July page 38 LAR-14023

PYROLYSIS
Lignin sensor based on flash-pyrolysis mass spectrometry
Mar page 62 NPO-17592

Pyrolysis products of dimethyldichlorosilane
May page 61 ARC-12169

Two-radiative/thermochemical instruments
Nov page 54 MSC-21639/40

PYROTECHNICS
Two-fault-tolerant release mechanism
Feb page 50 MSC-21354

Jam-resistant cutters for emergency separation
July page 68 MSC-21474

Q

QUADRATIC EQUATIONS
Finding optimal gains in linear-quadratic control problems
Apr page 87 NPO-17011

QUALITATIVE ANALYSIS
Dry-enzyme test for gaseous chemicals
Jan page 74 NPO-17642

QUANTUM WELLS
Anomalous polarization may improve infrared detectors
Jan page 22 NPO-17450

Tunable-quantum-well infrared detector
Mar page 34 NPO-17361

Tunable quantum-well submillimeter-wave oscillators
July page 26 NPO-17754

Improved photovoltaic-driven quantum light modulator
Aug page 26 NPO-17357

Millimeter-wave quantum-well frequency multipliers
Sep page 28 NPO-17584

Multi-quantum-well spatial light modulators on Si substrates
Nov page 32 NPO-17651

QUENCHING (COOLING)
Fast quenching for hydrogen-embrittlement tests
June page 60 MFS-29549

R

RADAR ANTENNAS
Diffraction analysis of distorted reflector antennas
Sep page 66 NPO-16818

RADAR CORNER REFLECTORS
Cheap corner reflectors for radar
May page 30 NPO-17658

RADAR IMAGERY
Differential radar interferometry maps changes in elevation
Sep page 36 NPO-17831

RADAR SCATTERING
Classification of radar scatterers via polarimetric data
May page 54 NPO-17732

RADIANT FLUX DENSITY
Simplified calculation of solar fluxes in solar receivers
Sep page 68 NPO-17344

Time-resolved measurements of laser far-field patterns
Oct page 55 GSC-13338

RADIANT HEATING
Measuring irradiance over large areas
Aug page 42 NPO-17810

RADIATION ABSORPTION
Survey of infrared-absorbing coatings
Jan page 42 ARC-11767

RADIATION DAMAGE
Failures of CMOS circuits irradiated at low rates
Aug page 29 NPO-17822

Effects of dose rates on radiation damage in CMOS parts
Sep page 32 NPO-17344

Failures of CMOS devices at low radiation-dose rates
Nov page 30 NPO-17868

RADIATION DETECTORS
Prototype V-groove radiator heat shield
Apr page 55 NPO-17744

RADIATION EFFECTS
Exact chord-length distribution for SEU calculation
Apr page 30 NPO-17657

Forward bias inhibits single-event upsets
Apr page 28 NPO-17573

Temperature dependence of single-event effects
Oct page 70 NPO-17870

RADIATION MEASURING INSTRUMENTS
Tunable-quantum-well infrared detector
Mar page 34 NPO-17361

RADIATION SOURCES
Optically-tuned far-infrared device
May page 30 NPO-17160

RADIOACTIVE ISOTOPES
Identifying bearing balls with radioisotopes
Nov page 91 MFS-29724

RADIO ANTENNAS
An optimal design for steerable dish antenna with BWG
Mar page 33 NPO-17429

RADIO BEACONS
Digital controller for emergency beacon
May page 43 LEW-14857

RADIO COMMUNICATION
Mechanically-steered, mobile satellite-tracking antenna
Feb page 24 NPO-17607

Sampling downconverter for radio-frequency signals
May page 44 NPO-17530

Managing mobile/satellite propagation data
July page 62 NPO-17269

RADIO FREQUENCY INTERFERENCE
Estimation of interference in satellite/ground communications
Jan page 45 NPO-17500

Study of adaptive-array signal processing
Oct page 57 NPO-17492

RADIOGRAPHY
Positioning x-ray film with string and magnets
May page 78 MFS-29448

Improved radiography of wooden parts
July page 47 LAR-13724

Positioning x-ray film by balloon
Aug page 63 MFS-29588

Positioning x-ray film inside a flow splitter
Dec page 61 MFS-29322

RADIOMETERS
Diagnosis of a pressure-modulator-radiometer cell
Mar page 63 NPO-17528

Field-induced-gap infrared detectors
Mar page 32 NPO-17526

RADIO TRANSMISSION
Acquisition of spread-spectrum code
Apr page 38 NPO-17472

RADOMES
Rain-blowing plenum for antenna feed horn
Nov page 36 NPO-17493

RAINDROPS
Rain-blowing plenum for antenna feed horn
Nov page 36 NPO-17493

RAMAN SPECTROSCOPY
Doppler-shifted Raman spectroscopy
Mar page 58 LAR-14133

Fiber-optic coupler and dynamic-range enhancer for CARS
Nov page 52 LAR-14235

RANDOM ACCESS MEMORY
Asymmetrical memory circuit would resist soft errors
Jan page 23 NPO-17394

32-bit-wide memory tolerates failures
June page 38 MSC-21566

RANGEFINDING
Determining spatial coordinates by laser ranging
Jan page 57 NPO-17436

Laser Doppler and range systems for spacecraft
Feb page 36 NPO-17486

Simplified correlator for ranging codes
May page 36 NPO-17415

Selecting modulation indices for telemetry and ranging
June page 54 NPO-17535

RAPID QUENCHING (METALLURGY)
Making fiber-reinforced metal by rapid solidification
Mar page 94 LEW-14918

REACTION KINETICS
Computer simulation of cyclic oxidation
Apr page 48 LEW-14890

REACTION WHEELS
Inertia-wheel vibration-damping system
June page 76 GSC-13077

REAL GASES
Flux Jacobian matrices for equilibrium real gas
Dec page 28 ARC-12409

RECEIVERS
Digital demodulator for advanced receiver
Mar page 44 NPO-17628

REDUCED GRAVITY
Design of robots for outer space
May page 76 NPO-17113

Nano-G laboratory
June page 63 GSC-13197

Hollow-fiber clinostat
June page 96 MFS-28370

REFILLING
Automatic refilling system for liquid helium
July page 46 GSC-13270

REFLECTING TELESCOPES
Wide-field, two stage optical system
Jan page 34 NPO-17392

Compact sunshade for telescope antenna
June page 58 NPO-17674

REFLECTOR ANTENNAS
Disturbance-accommodating controller would aim antenna
Mar page 42 NPO-17631

Array feed to compensate for distortion in antenna
Apr page 38 NPO-17667

Diffraction analysis of distorted reflector antennas
Sep page 66 NPO-16818

REFLECTORS
Controlling shape and vibration of antennas
Apr page 43 NPO-17598

REFRACTORY MATERIALS
High-temperature materials for Stirling engines
Apr page 56 LEW-14836

Mechanical properties of SiC/Si_3N_4 laminates
Dec page 37 LEW-14896

REGISTERS (COMPUTERS)
Molecular electronic shift registers
May page 55 NPO-17606

RELEASING
Two-fault-tolerant release mechanism
Feb page 50 MSC-21354

Mechanism for guided release
June page 80 NPO-17617

Double-swivel mechanism for reliable release
July page 64 GSC-21436

RELIABILITY ANALYSIS
Pivotal-function assessment of reliability of software
July page 107 LAR-13842

RELIEF MAPS
Making topographical maps from SAR and flood-gauge data
Sep page 44 GSC-13212

REMOTE CONTROL
Numerical models for control of robots
Apr page 88 MFS-28360

Remotely-controlled variable-orifice valve
June page 75 MFS-28369

Switching x-ray tubes remotely
July page 24 MFS-29357

General-purpose serial interface for remote control
Aug page 34 LAR-13739

REMOTE HANDLING
Random-field estimation for dynamics of robots
Dec page 66 NPO-17788

REMOTE MANIPULATOR SYSTEM
Simplified dynamic control of redundant manipulators
June page 48 NPO-17593

Balancing loads among robotic-manipulator arms
Sep page 98 NPO-17649

Exact linearization for control of robots
Sep page 97 NPO-17363

Exponentially stabilizing robot control laws
Sep page 95 NPO-17587

Robust, high-performance control for robotic manipulators
Sep page 36 NPO-17785

Proximity sensors make robot dexterous
Oct page 50 MSC-21476

Test bed for telerobots
Nov page 46 NPO-17898

Locating a planar target from an image
Dec page 66 LAR-14128

REMOTE SENSING
Survey of gas-correlation spectroradiometry
Feb page 43 NPO-17345

High-resolution imaging spectrometer
Mar page 52 NPO-17624

Terrestrial-imaging spectroscopy
Mar page 65 NPO-17432

Processing of multispectral data for identification of rocks
Apr page 53 NPO-17581

Calibration of airborne visible/IR imaging spectrometer
June page 63 NPO-17582

Multibeam 1.4-GHz pushbroom microwave radiometer
July page 38 LAR-14023

Preliminary analysis of data from AVIRIS
Oct page 68 NPO-17622

REMOTE SENSORS
Averaging sampled sensor outputs to detect failures
Aug page 70 MFS-29719

REQUIREMENTS
Organizing performance requirements for dynamic systems
Aug page 72 MSC-21235

RESCUE OPERATIONS
Liquid-air breathing apparatus
Aug page 74 KSC-11431

RESIDUAL STRESS
Interferometric measurement of residual stress
Feb page 51 NPO-17440

RESIN MATRIX COMPOSITES
Polymeric additives for graphite/epoxy composites
July page 56 ARC-11427

FTIR monitoring of curing of composites
Dec page 62 LAR-14040

RESINS
Tough, microcracking-resistant, high-temperature polymer
June page 64 LAR-13925

RESISTANCE HEATING
Thermal-interaction matrix for resistive test structure
Apr page 32 NPO-17673

RESOURCE ALLOCATION
Scheduling nonconsumable resources
Jan page 72 NPO-16988

Neural-network processor would allocate resources
Oct page 46 NPO-17781

RESPIROMETERS
Self-calibrating respiratory-flowmeter combination
June page 96 MSC-21430

RETICLES
Holographic reticle
Sep page 89 MFS-29597

RETRACTABLE EQUIPMENT
Shock-absorbing, retractable docking mechanism
Aug page 61 MSC-21327

RETROREFLECTORS
Cheap corner reflectors for radar
May page 30 NPO-17658

Optimization of array of laser retroreflectors
Dec page 31 NPO-17778

RHYTHM
Programmable cadence timer
July page 42 MSC-21551

RING LASERS
Monolithic unidirectional nonplanar ring laser
Nov page 58 LAR-14146

Monolithic unidirectional planar ring laser
Nov page 58 LAR-14045

ROBOT EXHAUST
Computing impingements of rocket exhausts
Sep page 67 MSC-21419

ROBOTICS
Camera would monitor weld-pool contours
Jan page 26 MFS-29450

Dummy cup helps robot-welder programmers
Jan page 62 MFS-29499

Method for automatic downhand welding
Jan page 65 MFS-27209

Determining sense of motion in robotic vision
Apr page 84 NPO-17552

Recursive construction of Jacobian matrix and its time derivative for robot arm
Apr page 89 NPO-17364

Compliant joints for robots
May page 70 GSC-13127

Multivariable PID controller for robotic manipulator
June page 93 NPO-17647

Parallel architecture for robotics computation
June page 36 NPO-17629

Simplified dynamic control of redundant manipulators
June page 48 NPO-17593

High-voltage digital-to-analog converter
July page 32 MFS-29605

Balancing loads among robotic-manipulator arms
Sep page 98 NPO-17649

Checking automated-welder programs by computer
Sep page 41 MFS-29006

Exponentially stabilizing robot control laws
Sep page 95 NPO-17587

Proximity sensors make robot dexterous
Oct page 50 MSC-21476

Improved "smart" robot hand
Nov page 38 NPO-17917

Test bed for telerobots
Nov page 46 NPO-17898

Zoom vision system for robotic welding
Nov page 82 MFS-29712

ROBOTS
Robot hand would adapt to contours
Mar page 86 NPO-16766

Numerical models for control of robots
Apr page 88 MFS-28360

Design of robots for outer space
May page 76 NPO-17113

Probabilistic determination of motions of robots
July page 111 NPO-17738

Dual-head robotic welder
Sep page 87 MFS-29610

Exact linearization for control of robots
Sep page 97 NPO-17363

Increasing the dexterity of redundant robots
Oct page 88 NPO-17801

Characterization of robot work cell
Nov page 92 MFS-29731

Agile walking robot
Dec page 52 NPO-17874

Random-field estimation for dynamics of robot
Dec page 66 NPO-17788

Rolling robot
Dec page 52 NPO-17842

Rugged walking robot
Dec page 53 NPO-17825

ROBUSTNESS (MATHEMATICS)
Robust adaptive control in Hilbert space
June page 53 NPO-17588

Software for least-squares and robust estimation
Dec page 40 MFS-26108

ROCKET ENGINES
System detects vibrational instabilities
May page 41 MSC-21408

Analysis of used arc-jet electrodes
Dec page 30 NPO-17575

Contoller gas-flow mass ratio
Dec page 26 MSC-21542

ROCKET EXHAUST
Computing impingements of rocket exhausts
Sep page 67 MSC-21419

ROCKS
Processing of multispectral data for identification of rocks
Apr page 53 NPO-17581

ROLLER BEARINGS
Rolling-contact spalling in bearings
Mar page 81 MFS-27201

Securing bearing races to turbopump shafts
June page 79 MFS-28384

ROTARY ENGINES
Rotary Stirling-cycle engine and generator
June page 78 MSC-21530

ROTARY WING AIRCRAFT
Civil applications for new V/STOL and STOL aircraft
Sep page 81 ARC-12175

ROTARY WINGS
Computational fluid dynamics for helicopters
Jan page 59 ARC-12143

ROTATING SHAFTS
Ball-pass cage-modulation detector
Aug page 32 MFS-29539

Shaft adapter for data coupler
Oct page 80 LAR-13805

ROTATION
Shaft-rotation detector
Aug page 33 MFS-29540

ROTOR BLADES (TURBOMACHINERY)
Heat shield and axial retainer for turbopump blade
Dec page 53 MFS-28417

ROTORS
Improved stress analysis of multicomponent rotors
Apr page 67 LEW-14838

Rubbing between rotors and stators
July page 76 MFS-27226

Rotor/stator interaction in a diffuser pump
Aug page 60 MFS-26092

Precise hinge has low friction
Sep page 71 NPO-17749

ROVING VEHICLES
Stabilizing wheels for rover vehicle
May page 74 NPO-17495

Rolling robot
Dec page 52 NPO-17842

RUBBER
Computing deformations of rubbery materials
Sep page 47 NPO-17670

RUNWAYS
System predicts critical runway performance parameters
Nov page 40 LAR-13809

RUPTURING
Wrapped wire detects rupture of pressure vessel
Apr page 66 MSC-21449

S

SAMPLING
Sampling downconverter for radio-frequency signals
May page 44 NPO-17530

Averaging sampled sensor outputs to detect failures
Aug page 70 MFS-29719

SAPPHIRE
Pressure-measuring diaphragm transmits optical signals
Sep page 76 MFS-29535

SATELLITE ATTITUDE CONTROL
Liquid-ring attitude-control system for spacecraft
Sep page 82 NPO-17485

SATELLITE-BORNE RADAR
Computer assembles mosaics of satellite-SAR imagery
Apr page 42 NPO-17683

SATELLITE NAVIGATION SYSTEMS
Testing microwave landing systems with satellite navigation
Apr page 36 KSC-11451

SATELLITE TRACKING
Mechanically-steered, mobile satellite-tracking antenna
Feb page 24 NPO-17607

SCALARS
Transport of passive scalars in a turbulent channel flow
Apr page 62 ARC-12109

SCANNERS
Electronically scanned laser rangefinder
May page 46 NPO-17571

Integrated electro-optical laser-beam scanners
May page 26 MSC-21498

SCATTERING
Computing scattering matrices for circular waveguides
Sep page 65 NPO-17245

SCHEDULES
Schedule-organizer computer program
Nov page 69 MSC-21525

Schedule-report-generator computer program
Nov page 68 MSC-21527

Schedule-tracker computer program
Nov page 70 MSC-21526

SCHEDULING
Scheduling nonconsumable resources
Jan page 72 NPO-16988

Optimal allocation of tasks in hypercube computers
Apr page 79 NPO-17215

S-chart -- scheduling-chart program
Nov page 74 MFS-29531

SCHLIEREN PHOTOGRAPHY
Schlieren system for flow studies in round glass pipes
Oct page 58 LAR-13944

SCHMIDT TELESCOPES
Wide-field, two-stage optical system
Jan page 34 NPO-17392

Compact, broadband infrared spectrometer
Jan page 38 NPO-17562

SCHOTTKY DIODES
Ge/Si integrated circuit for infrared imaging
Mar page 28 NPO-17397

Silicide Schottky barrier for back-surface-illuminated CCD
June page 26 NPO-17328

AlAs diffusion/Schottky barrier on GaAs
July page 30 NPO-17796

Self-aligned guard rings for Schottky-barrier diodes
Aug page 20 NPO-17734

SEALING
Sealing nitrogen tetroxide leaks
Nov page 89 MSC-21600

SEALS (STOPPERS)
Measuring gaps in O-ring seals
Feb page 52 MFS-28332

Pressure gauges monitor leakage past seals
Feb page 50 MSC-21385

Static pressure-assisted seal for helium
Mar page 70 MFS-29429

Squeezing salvages oversize seals
May page 79 MFS-29527

SELF LUBRICATING MATERIALS
Reducing run-in wear of ceramic-based coatings
July page 56 LEW-14834

Making self-lubricating parts by powder metallurgy
Sep page 63 LEW-14902

SEMICONDUCTOR DEVICES
Multi-pinned-phase charge-coupled device
Aug page 22 NPO-17462

Silicon detectors for helium liquid and vapor
Aug page 44 GSC-13281

1990 Annual Subject Index

SEMICONDUCTOR DIODES
Self-aligned guard rings for Schottky-barrier diodes
Aug page 20 NPO-17734

SEMICONDUCTOR LASERS
Annular-Bragg-grating surface-emitting laser
Oct page 20 NPO-17912

Unstable-resonator distributed-Bragg-reflector laser
Oct page 20 NPO-17906

SENSORS
Second vapor-level sensor for vapor degreaser
May page 82 MFS-29493

SEPARATED FLOW
Measurements of shock-separated turbulent boundary layers
Nov page 78 ARC-12298

SEPARATORS
Acoustophoresis--a new separation concept
Jan page 38 LAR-13388

SERVOCONTROL
Improved "smart" robot hand
Nov page 38 NPO-17917

SERVOMECHANISMS
Design of robots for outer space
May page 76 NPO-17113

SHADES
Compact sunshade for telescope antenna
June page 58 NPO-17674

SHAFTS (MACHINE ELEMENTS)
Securing bearing races to turbopump shafts
June page 79 MFS-28384

Shaft-rotation detector
Aug page 33 MFS-29540

Shaft adapter for data coupler
Oct page 80 LAR-13805

Rotary ball locking mechanism
Dec page 56 MSC-21396

SHAPES
Shape gauge measures surfaces
Feb page 52 MFS-28284

SHELLS (STRUCTURAL FORMS)
Dual-head robotic welder
Sep page 87 MFS-29610

SHIELDING
Crash-resistant shield
June page 71 NPO-17616

SHIFT REGISTERS
Molecular electronic shift registers
May page 55 NPO-17606

Procedure for labeling linear finite-state codes
July page 107 NPO-17774

SHIP HULLS
Preventing ventilation on sailboard skegs
Nov page 75 LAR-14008

SHORT CIRCUITS
Tester detects steady-short or intermittent-open circuits
Jan page 18 MFS-29466

Segmented coil fails in steps
Nov page 36 MSC-21574

SHORT TAKEOFF AIRCRAFT
Civil applications for new V/STOL and STOL aircraft
Sep page 81 ARC-12175

SHUTTERS
Active limiters for photodetectors
Sep page 38 NPO-17654

SIGNAL ANALYSIS
Noise-contamination detector
Apr page 79 MFS-29537

SIGNAL ENCODING
Double differential encoding and detection in MPSK
June page 46 NPO-17666

SIGNAL PROCESSING
Frequency-domain signal processor for laser velocimeter
May page 45 LAR-13552

Study of adaptive-array signal processing
Oct page 57 NPO-17492

SILANES
Pyrolysis products of dimethyldichlorosilane
May page 61 ARC-12169

Rewaterproofing chemical for use with silicones
Aug page 47 MSC-21569

SILICIDES
Layered internal-photoemission sensor
May page 32 NPO-17751

SILICON
Multi-quantum-well spatial light modulators on Si substrates
Nov page 32 NPO-17651

SILICON ALLOYS
Improved analysis of heat-pulse data
July page 48 NPO-17729

SILICON CARBIDES
Calculating the resistivity of a deposited film
Oct page 72 LEW-14389

Making lightweight structures by vapor deposition
Nov page 81 LAR-14059

Microstructure of a SiC/(Ti/V/Cr/Sn/Al) composite
Nov page 61 LEW-14868

SILICON COMPOUNDS
Friction and wear of silicon ceramics
June page 67 LEW-14835

SILICON NITRIDES
Silicon nitride balls for cryogenic bearings
July page 63 MFS-29613

Mechanical properties of SiC/Si_3N_4 laminates
Dec page 37 LEW-14896

SILICON RADIATION DETECTORS
Integrated grating spectrometer
Apr page 49 NPO-17733

Superlattice long-wavelength infrared sensors
May page 18 NPO-17713

SILICONES
Rewaterproofing chemical for use with silicones
Aug page 47 MSC-21569

SILVER OXIDES
$YBa_2Cu_3O_x$ superconductors doped with AgO
Mar page 66 MFS-26078

SIMULATION
Simulating orbiting spacecraft
Feb page 49 MSC-21462

Mathematical model of nerve/muscle interaction
Aug page 73 NPO-17816

Simulating a massive, mobile structure
Sep page 72 MSC-21482

SINE WAVES
Noise-contamination detector
Apr page 34 MFS-29537

SINGLE-EVENT UPSETS
Asymmetrical memory circuit would resist soft errors
Jan page 23 NPO-17394

Exact chord-length distribution for SEU calculation
Apr page 30 NPO-17657

Forward bias inhibits single-event upsets
Apr page 28 NPO-17573

Upper-bound estimates of SEU in CMOS
Apr page 26 NPO-17566

Temperature dependence of single-event effects
Oct page 70 NPO-17870

SINTERING
Sintered fiber electrodes
Dec page 32 NPO-17213

SIZE DETERMINATION
Feeder system for particle-size analyzer
Apr page 61 MFS-28326

Measuring monodisperse small particles en masse
Dec page 45 LAR-14152

SIZING (SHAPING)
Squeezing salvages oversive seals
May page 79 MFS-29527

SLEWING
Minimum-time slewing of space infrared telescope
Dec page 64 ARC-12155

S MATRIX THEORY
Computing scattering matrices for circular waveguides
Sep page 65 NPO-17245

SMOOTHING
More about fixed-lag smoothers for tracking carriers
Apr page 45 NPO-17389

SOFTWARE (COMPUTERS)
Markov chains for testing redundant software
Mar page 101 LAR-13812

SOFTWARE ENGINEERING
Software model of software-development process
Mar page 100 NPO-17424

SOFTWARE TOOLS
Software for development of expert systems
June page 86 NPO-17536

Documenting software automatically
Nov page 70 MSC-21297

Window utility system program
Nov page 73 LAR-13993

Local-area-network simulator
Dec page 38 ARC-12168

SOLAR CONNECTORS
Simplified calculation of solar fluxes in solar receivers
Sep page 68 NPO-17732

SOLDERING
Removing dross from molten solder
Sep page 88 MFS-28406

SOLID ELECTROLYTES
Improved liquid-electrode/solid-electrolyte cell
Apr page 51 NPO-17604

Antireduction insulator for solid-electrolyte cell
Oct page 24 NPO-17211

SOLID PROPELLANT COMBUSTION
Measuring response of propellant to oscillatory heat flux
Oct page 59 NPO-17428

SOLID PROPELLANT ROCKET ENGINES
Offset joint for segmented pressure vessel
Sep page 70 MFS-28365

SOLID STATE DEVICES
Portable high-frequency data-acquisition system
Jan page 30 MSC-21521

Silicide Schottky barrier for back-surface-illuminated CCD
June page 26 NPO-17328

Multi-pinned-phase charge-coupled device
Aug page 22 NPO-17462

SOLID STATE LASERS
Generating second harmonics in nonlinear resonant cavities
May page 52 LAR-14051

Birefringent-filter model
July page 60 LAR-13945

SOUND TRANSDUCERS
Laser Schlieren system detects sounds of leaks
Aug page 45 NPO-17009

Improved voice-coil actuators have lower copper losses
Dec page 18 MFS-26111

SORPTION
Absorption of gases by glassy polymers
Feb page 45 NPO-17636

SPACEBORNE ASTRONOMY
Computing orbital viewing parameters
Jan page 46 GSC-13083

SPACEBORNE TELESCOPES
Astrometric telescope facility for the Space Station
July page 52 ARC-11842

SPACECRAFT
Nano-G laboratory
June page 63 GSC-13197

SPACECRAFT ANTENNAS
Controlling shape and vibration of antennas
Apr page 43 NPO-17598

SPACECRAFT CONTROL
Liquid-ring attitude-control system for spacecraft
Sep page 82 NPO-17485

SPACECRAFT DOCKING
Shock-absorbing, retractable docking mechanism
Aug page 61 MSC-21327

SPACECRAFT DOCKING MODULES
Shock absorbing, retractable docking mechanism
Aug page 61 MSC-21327

SPACECRAFT ORBITS
Simulating orbiting spacecraft
Feb page 49 MSC-21462

SPACECRAFT STRUCTURES
Simulating a massive, mobile structure
Sep page 72 MSC-21482

SPACECRAFT TRACKING
Laser doppler and range systems for spacecraft
Feb page 36 NPO-17486

SPACE DENSITY
Model of orbital density of air for computing drag
Feb page 48 MSC-21154

SPACE FLIGHT FEEDING
Aerospace food tray
Feb page 72 MSC-21412

SPACE INFRARED TELESCOPE FACILITY
Minimum-time slewing of space infrared telescope
Dec page 64 ARC-12155

SPACE SHUTTLES
Safe-egress pole for vehicle in motion
July page 72 MSC-21461

Software for three-dimensional Space Shuttle imagery
Dec page 38 GSC-13246

Design-tradeoff model for space station
Dec page 41 NPO-17878

SPACE STATIONS
System-design-tradeoff model for space station
Dec page 41 NPO-17878

SPACE STATION STRUCTURES
Polyhedral observation cupola
Nov page 93 MSC-21689

SPALLING
Rolling-contact spalling in bearings
Mar page 81 MFS-27201

SPARK MACHINING
Ultrasonic abrasive removal of EDM recast
Oct page 97 MFS-29545

SPECIFIC HEAT
Improved analysis of heat-pulse data
July page 48 NPO-17729

SPECKLE PATTERNS
Reducing speckle in one-look SAR images
Feb page 70 NPO-17254

SPECTRA
Trigonometric polynomials for estimation of spectra
Nov page 94 NPO-17885

SPECTROMETERS
Integrated grating spectrometer
Apr page 49 NPO-17733

SPECTRORADIOMETERS
Survey of gas-correlation spectroradiometry
Feb page 43 NPO-17345

SPECTROSCOPIC ANALYSIS
Spectroscopic analysis of insulating crystal fibers
July page 34 LAR-13831

SPECTROSCOPY
Terrestrial-imaging spectroscopy
Mar page 65 NPO-17432

SPHERES
Filling porous microspheres with magnetic material
Feb page 47 NPO-17044

SPLICING
Splicing wires permanently with explosives
Nov page 81 LAR-13825

SPOT WELDS
Spot-welding gun with adjustable pneumatic spring
June page 81 MFS-29569

Controlled-pinch spot welder
Sep page 87 MFS-29606

Rolling spot welder
Sep page 86 MFS-29580

Compact pinch welder
Oct page 89 MFS-29612

SPRAY CHARACTERISTICS
Behavior of evaporating liquid drops in clusters
Sep page 61 NPO-17843

SPRAY INGESTION
Measurement of water sprays generated by airplane tires
Sep page 70 LAR-14030

SPREAD SPECTRUM TRANSMISSION
Acquisition of spread-spectrum code
Apr page 38 NPO-17472

SPRINGS (ELASTIC)
Spring-loaded-bolt locking device
Dec page 47 LEW-14887

SQUARE WAVES
High-voltage square-wave generator
Oct page 26 NPO-17772

STABILITY AUGMENTATION
Stabilizing wheels for rover vehicle
May page 74 NPO-17495

STANDING WAVE RATIOS
Automatic range changer for SWR meter
Aug page 18 NPO-17822

STATORS
Rubbing between rotors and stators
July page 76 MFS-27226

Rotor/stator interaction in diffuser pump
Aug page 60 MFS-26092

Precise hinge has low friction
Sep page 71 NPO-17749

STEELS
Electrochemical study of corrosion of painted steel
Jan page 44 MFS-27213

MARKETPLACE To Advertise—Call (212) 490-3999

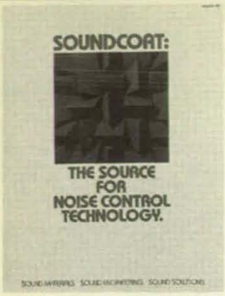

NOISE CONTROL MATERIALS

Soundcoat's Bulletin 900 illustrates and describes Soundcoat's complete line of noise and vibration control materials. In addition to showing which materials are used to solve specific problems (electronic, aircraft, vehicular, heavy equipment, etc.), the brochure explains how Soundcoat's two state-of-the-art acoustic laboratories locate and define noise problems in either pre- or post-production stages of any design. Ask for Bulletin 900.

THE SOUNDCOAT COMPANY, INC.
Deer Park, NY / Santa Ana, CA

Circle Reader Action No.438

FREE! 130 Page Catalog

"Optics for Industry"

Free 130 page product catalog from Rolyn, world's largest supplier of "Off-the-Shelf" optics. 24-hour delivery of simple or compound lenses, filters, prisms, mirrors, beamsplitters, reticles, objectives, eyepieces plus thousands of other stock items. Rolyn also supplies custom products and coatings in prototype or production quantities. **ROLYN OPTICS Co.,** 706 Arrowgrand Circle, Covina, CA 91722-2199, (818)915- 5707, FAX (818)915-1379

Circle Reader Action No.551

Quality Precision Assemblies & Components

SINCE 1962 • Custom • Stock
At Sterling we're equipped to handle your entire assembly project starting with the creative engineering phase.

Call for FREE brochure.

Sterling Instrument
2101 Jericho Turnpike,
New Hyde Park, NY 11040
Phone: (516) 328-3300
Fax: (516) 326-8827

For OEM Application Circle No. 391 For In-House Use Circle No. 556

Free Standing Wire Grid Polarizers

For Spectroscopy at Millimeter and Sub-millimeter wavelength

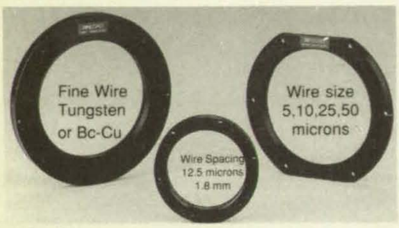

Applications
- . FAR-IR Wavelength Polarization
- . Interferometer Beam Divider
- . Variable Reflector
- . Coupling Device for Long Wavelength Lasers
- . Suitable for High Vacuum and Cryogenic Conditions

Custom design available

Another quality product from SPECAC

SPECAC ANALYTICAL INC.
301 Commerce Drive Tel (203) 366-5112
Fairfield, CT 06430 Fax (203) 384-1524
A Cambridge Electronics Industries (CEI) Company

Circle Reader Action No. 621

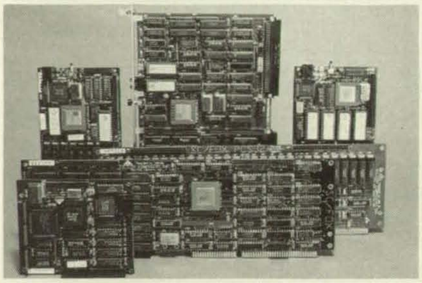

SC/FOX™ Embedded-System Computers

SC/FOX VME SBC (Single Board Computer) 18 MIPS, 60 MIPS burst, general-purpose, slot-1 Master/Slave System Controller. Up to 640 K bytes 0-ws memory, 1 SCSI, 1 ptr, 2 serial ports. Uses 16-bit Harris RTX 2000.

SC/FOX PCS (Parallel Coprocessor System) 15 MIPS, 50 MIPS burst, general purpose PC/AT/386 plug-in board, 32K to 1M byte 0-ws static memory, multiple PCS operation, SCSI option. Uses Harris RTX 2000.

SC/FOX SBC (Single Board Computer) 18 MIPS, 60 MIPS burst, Standalone operation, Eurocard size, 1 ptr, 1 serial port, up to 512K bytes O-ws memory, 2 50-pin user connectors, SCSI option. Uses Harris RTX 2000.

SC/FOX PCS32 (Parallel Coprocessor System 32) 15 MIPS to 70 MIPS, general-purpose PC/AT/386 32-bit plug-in board with 64K to 1M byte 0-ws static memory. Uses 32-bit SC32 Forth microprocessor.

Ideal for embedded real-time control, data acquisition, or high-speed processing. Forth software included, C optional. OEM pricing.

SILICON COMPOSERS INC *(415) 322-8763*
208 California Ave., Palo Alto, CA 94306

Circle Reader Action No. 679

Tachion-I™

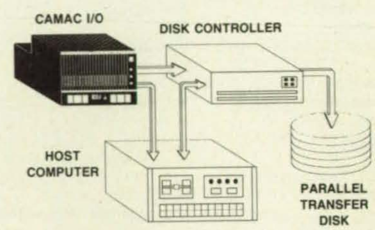

The new high-speed CAMAC data acquisition and recording system with:

- up to 15.2 Mbyte/sec throughput to disk
- data storage from 200 Mbytes to 56 Gbytes
- up to 1280 analog channels per subsystem
- sampling rates to 2 MHz per channel
- all-digital recording for repeatable accuracy
- real-time monitoring of selected channels
- interfaces for ARINC-429 and MIL-STD-1553

Call us today!

KineticSystems Corporation
11 Maryknoll Drive, Lockport, Illinois 60441 (815) 838 0005

Circle Reader Action No. 334

HI TEMP MATERIALS

CONTINUOUS USE TO 4000°F

EPOXIES
CERAMICS
ADHESIVES
INSULATION
CASTABLES
MACHINABLES
ENCAPSULANTS

Includes Complete Technical And Application Data For All Your Hi Temp Needs

COTRONICS CORP
3379 Shore Pkway. Brooklyn, N. Y.11235
718-646-7996 FAX 718-646-3028

Circle ReaderAction No.409

How to Protect Your Computer

And Make It Last Longer

FREE money-saving literature is offered by the world's largest manufacturer of single-phase uninterruptible power systems. Learn how to get complete protection from power line problems with advanced, on-line UPS ranging in size from 500 VA through 18 KVA.

Best Power Technology, Inc.
P.O. Box 280, Necedah, WI 54646
Toll-Free 800-356-5794, ext. 2205
(U.S.A. & Canada)
Telephone (608) 565-7200, ext. 2205

Circle Reader Action No. 306

Imagine a lightweight metal foil with a mesh-like, single-unit structure that eliminates the unraveling and contact resistance of woven mesh.

Imagine it with superior EMI/RFI/ESD shielding, electrical and heat transfer properties.

Imagine it wrapping, laminating, contracting, expanding.

Now imagine how you'd use it.

Call 203/481-4277 for a free sample of MicroGrid®.

DELKER
CORPORATION
Branford, CT 06405

Circle Reader Action No. 316

Nondestructive technique to assess embrittlement in steels
Oct page 64 LAR-13817

TAZ-8A alloy increases the thermal endurance of steel
Dec page 32 LEW-14280

STEERABLE ANTENNAS
Mechanically-steered, mobile satellite-tracking antenna
Feb page 24 NPO-17607

An optimal design for steerable dish antenna with BWG
Mar page 33 NPO-17429

STEPPING MOTORS
Control circuit for two stepping motors
June page 30 GSC-13202

STEREO-PHOTOGRAPHY
Jig for stereoscopic photography
Mar page 70 MSC-21397

STIMULATED EMISSION DEVICES
Annular-Bragg-grating surface-emitting laser
Oct page 20 NPO-17912

Unstable-resonator distributed-Bragg-reflector laser
Oct page 20 NPO-17906

STIRLING ENGINES
High-temperature materials for Stirling engines
Apr page 56 LEW-14836

Rotary Stirling-cycle engine and generator
June page 78 MSC-21530

STOCHASTIC PROCESSES
Stochastic feedforward control technique
May page 92 LAR-13796

Forward stochastic nonlinear adaptive control method
Nov page 95 NPO-17861

STORAGE BATTERIES
Durable bipolar plates lead/acid batteries
Apr page 22 NPO-17662

Improved liquid-electrode/solid-electrolyte cell
Apr page 51 NPO-17604

Making more efficient use of battery-plate mass
May page 34 NPO-17435

STRESS ANALYSIS
Improved stress analysis of multicomponent rotors
Apr page 67 LEW-14838

STRESSES
Delamination analysis of composite curved bars
Oct page 71 ARC-12347

STRESS MEASUREMENT
Treating nickel alloy for sonic quality
Sep page 85 MFS-29594

STRATOSPHERE
Measuring concentration of ozone automatically
June page 60 ARC-12230

STRUCTURAL ANALYSIS
Combining thermal and structural analyses
Mar page 84 LEW-14741

Computing mass properties from AutoCAD
June page 68 GSC-13077

STRUCTURAL MEMBERS
Low-thermal-stress structural joints for dissimilar materials
Nov page 75 LAR-14138

STRUCTURAL VIBRATION
More about multiple-boundary-condition testing
Jan page 58 NPO-17574

Improved coupled fluid/structural dynamical model
Jan page 54 MFS-29439

Fourier analysis of vibrations of round structures
Mar page 74 MFS-29334

Vibrational responses of structures to impulses
Mar page 80 NPO-17343

Characteristic-wave approach complements modal analysis
May page 72 NPO-17741

Inertia-wheel vibration-damping system
June page 76 GSC-13077

Propagation of pulse vibrations in large structures
July page 74 NPO-17559

Passive damping of vibrations in truss structures
Nov page 79 NPO-17609

STRUTS
Preloaded composite-strut/end-fitting joint
July page 82 MFS-28339

SUBMILLIMETER WAVES
Tunable quantum-well submillimeter-wave oscillators
July page 26 NPO-17754

Imaging antenna structure for submillimeter wavelengths
Aug page 24 NPO-17799

Dielectric-filled paraboloidal front ends
Sep page 24 NPO-17802

SUBSONIC FLUTTER
Predicting unsteady aeroelastic behavior
Sep page 77 LAR-14130

SUITS
Microprocessor control for liquid-cooled garment
Oct page 52 MSC-21359

SUPERCONDUCTIVITY
Electromagnetic Meissner-effect launcher
Apr page 64 MFS-28323

SUPERCONDUCTORS
$YBa_2Cu_3O_x$ superconductors doped with AgO
Mar page 66 MFS-26078

SUPERCRITICAL FLUIDS
Cleaning with super-critical CO_2
Dec page 58 MFS-29611

SUPERFLUIDITY
Temperature rises in pumps for superfluid helium
July page 51 ARC-12264

SUPERLATTICES
Superlattice long-wavelength infrared sensors
May page 18 NPO-17713

SUPERPLASTICITY
Superplastically formed titanium hat-stiffened panels
Jan page 63 LAR-13814

SUPERSONIC BOUNDARY LAYERS
Further studies of hot-wire anemometry
Dec page 31 ARC-12104

SUPERSONIC FLOW
Upwind algorithm for parabolized Navier-Stokes equations
May page 73 ARC-12146

Simulation of three-dimensional supersonic flows
Oct page 82 ARC-12235

SUPERSONIC WIND TUNNELS
Improved insert for variable mach number
July page 63 LAR-13548

SUPPORTS
Transducer-mounting fixture
Dec page 59 MFS-29600

SURFACE DEFECTS
X-ray fluorescence surface-contamination detector
Apr page 52 MFS-27222

SURFACE FINISHING
Removing burrs in confined spaces
July page 81 MFS-29392

SURFACE PROPERTIES
Shape gauge measures surfaces
Feb page 52 MFS-28284

Holographic reticle
Sep page 89 MFS-29597

SURFACE VEHICLES
Four-wheel vehicle suspension system
Aug page 55 NPO-17407

Agile walking robot
Dec page 52 NPO-17874

Rolling robot
Dec page 52 NPO-17842

Rugged walking robot
Dec page 53 NPO-17825

SUSPENDING (HANGING)
Heteropolar magnetic suspension
June page 75 MFS-26096

SUSPENSION SYSTEMS (VEHICLES)
Articulated suspension without springs
Jan page 60 NPO-17354

Four-wheel vehicle suspension system
Aug page 55 NPO-17407

SWITCHES
Improved thermal-switch disks protect batteries
May page 24 MSC-21428

SWITCHING
Algorithm for "bang-bang" control laws
July page 112 NPO-17603

SWITCHING CIRCUITS
Recovering energy from a rapidly switched gate
May page 20 NPO-17221

GTO/FET cascode three-terminal switch
July page 18 NPO-17865

Switching x-ray tubes remotely
July page 24 MFS-29357

MCI/MOSFET switch
Sep page 26 NPO-18001

Switching matrix for optical signals
Sep page 22 KSC-11392

Automated power-distribution system
Oct page 48 MFS-28440

High-voltage square-wave generator
Oct page 26 NPO-17772

Low-inductance wiring for parallel switching transistors
Oct page 30 MFS-28387

Preventing simultaneous conduction in switching transistors
Nov page 34 NPO-17775

Voltage-boosting driver for switching regulator
Nov page 26 MFS-28437

SYNAPSES
Quantized-gray-scale electronic synapses
Apr page 21 NPO-17579

SYNCHRONISM
Synchronization technique for reception of coded data
Jan page 67 NPO-17037

SYNTHETIC APERTURE RADAR
Reducing speckle in one-look SAR images
Feb page 70 NPO-17254

Computer assembles mosaics of satellite-SAR imagery
Apr page 42 NPO-17683

Extracting geocoded images from SAR data
Apr page 59 NPO-17418

Making mosaics of SAR imagery
Apr page 58 NPO-17586

Classification of radar scatterers via polarimetric data
May page 54 NPO-17373

Differential radar interferometry maps changes in elevation
Sep page 36 NPO-17831

Making topographical maps from SAR and flood-gauge data
Sep page 44 GSC-13212

SYSTEMS ANALYSIS
Finding optimal gains in linear-quadratic control problems
Apr page 87 NPO-17011

Minimal-inversion feedforward-and-feedback control system
July page 111 NPO-17701

T

TAIL ROTORS
Shaft adapter for data coupler
Oct page 80 LAR-13805

TAKEOFF
System predicts critical runway performance parameters
Nov page 40 LAR-13809

TANKS (CONTAINERS)
Measuring diameters of large vessels
Jan page 53 MFS-28287

Reinforcing liner for composite cryogenic tank
June page 66 MFS-28399

TAPE RECORDERS
Circuit regulates speed of dc motor
July page 28 MSC-21345

TARGET ACQUISITION
Locating a planar target from an image
Dec page 66 LAR-14128

TECHNICAL WRITING
Documenting software automatically
Nov page 70 MSC-21297

TELECOMMUNICATION
Estimation of interference in satellite/ground communications
Jan page 45 NPO-17500

Competitive parallel processing for compression of data
Feb page 32 NPO-17445

SCSI communication test bus
Dec page 25 MSC-21704

TELEMETRY
Selecting modulation indices for telemetry and ranging
June page 54 NPO-17535

Test processor for PCM telemetry
Aug page 27 GSC-13291

TELEOPERATORS
Robot hand would adapt to contours
Mar page 86 NPO-16766

Hard contact with a force-reflecting teleoperator
Apr page 70 NPO-17549

TELESCOPES
Wide-field, two-stage optical system
Jan page 34 NPO-17392

Compact sunshade for telescope antenna
June page 58 NPO-17674

Monitoring small deformations in an instrument
Oct page 80 GSC-13271

TELEVISION CAMERAS
General-purpose serial interface for remote control
Aug page 34 LAR-13739

TELEVISION TRANSMISSION
High-efficiency klystron for television transmitters
Sep page 30 LEW-14926

Real-time digital compression of television image data
Sep page 40 LEW-14945

TEMPERATURE CONTROL
Capillary pumped loop modeler
Oct page 76 GSC-13145

Microprocessor control for liquid-cooled garment
Oct page 52 MSC-21359

Three-zone programmable temperature controller
Nov page 44 MFS-28435

TEMPERATURE DISTRIBUTION
Measuring irradiance over large areas
Aug page 42 NPO-17810

TEMPERATURE EFFECTS
Temperature dependence of single-event effects
Oct page 70 NPO-17870

TEMPERATURE GRADIENTS
Systems improved numerical fluids analysis code
Nov page 64 GSC-13231

TEMPERATURE MEASUREMENT
Sensor detects overheating of perishable material
May page 95 NPO-17585

TEST CHAMBERS
Simple regulator for positive-pressure glove box
Dec page 62 NPO-17786

TEST EQUIPMENT
Tester detects steady-short or intermittent-open circuits
Jan page 18 MFS-29466

Bar-code system tracks test equipment
June page 42 KSC-11370

Adjustable induction-heating coil
Nov page 50 LEW-14963

O-ring-testing fixture
Dec page 46 MFS-28376

TEST FACILITIES
Test bed for telerobots
Nov page 46 NPO-17898

TEST PATTERN GENERATORS
Generating weighted test patterns for VLSI chips
Jan page 30 NPO-17514

TETHERED BALLOONS
Two tethered balloon systems
Feb page 39 LAR-13837

THERMAL ANALYSIS
Combining thermal and structural analyses
Mar page 84 LEW-14741

SINDA '85/FLUINT, Version 2.2
Sep page 68 MSC-21528

Systems improved numerical fluids analysis code
Nov page 64 GSC-13231

THERMAL CONDUCTIVITY
Pressurized-flat-interface heat exchanger
July page 68 MSC-21271

THERMAL CONDUCTORS
Lightweight, thermally conductive composite material
Mar page 66 LEW-14814

THERMAL DIFFUSIVITY
Improved analysis of heat-pulse data
July page 48 NPO-17729

THERMAL FATIGUE
Thermal-transient testing of turbine blades
May page 68 MFS-29416

THERMAL MAPPING
Measuring irradiance over large areas
Aug page 42 NPO-17810

THERMAL PROTECTION
Insulation for cryogenic-liquid tanks
Mar page 82 LEW-14707

Aerothermodynamic heating of a transatmospheric vehicle
June page 74 ARC-11854

THERMAL STRESSES
Low-thermal-stress structural joints for dissimilar materials
Nov page 75 LAR-14138

THERMOELECTRIC COOLING
External Peltier cooler for low-noise amplifier
Nov page 26 MSC-21422

THERMOHYDRAULICS
Equations for isocaloric fountain-effect pumps
July page 52 ARC-11850

THERMOMIGRATION
Thermal-interaction matrix for resistive test structure
Apr page 32 NPO-17673

THERMOPLASTIC RESINS
Isomeric trisaryloxycyclotriphosphazene polymer precursors
Jan page 42 LAR-13819

LARC-I-TPI: a new thermoplastic polyimide
July page 55 LAR-14101

THICKNESS
Measuring changes in dimensions of turbine blades
Apr page 60 MFS-28338

Monitoring coating thickness during plasma spraying
Sep page 84 LEW-14919

THIN FILMS
Preparation of high-temperature reactive oligomers
June page 66 LAR-13965

Additives lower dielectric constants of polyimides
Aug page 49 LAR-13902

Calculating the resistivity of a deposited film
Oct page 72 LEW-14389

THIOPLASTICS
Ethynyl-terminated imido thioethers and derived resins
May page 59 LAR-13910

THREADS
Braided composite threaded fasteners
Oct page 94 LAR-14062

THREE DIMENSIONAL FLOW
Electrolysis bubbles make waterflow visible
Mar page 76 LEW-14797

Simulation of three-dimensional supersonic flows
Oct page 82 ARC-12235

THRUST AUGMENTATION
Control-volume analysis of thrust-augmenting ejectors
Oct page 87 LEW-14877

THRUST VECTOR CONTROL
Thrust-vector deflectors for spacecraft
Sep page 81 MSC-21672

THUNDERSTORMS
Determining polarities of distant lightning strokes
June page 56 MFS-26102

THYRISTORS
GTO/FET cascode three-terminal switch
July page 18 NPO-17865

MCI/MOSFET switch
Sep page 26 NPO-18001

TIMING DEVICES
Programmable cadence timer
July page 42 MSC-21551

TIN OXIDES
Enhancement of Pt/SnO_2 catalysts by addition of H_2O
July page 54 LAR-14084

TIRES
Measurement of water sprays generated by airplane tires
Sep page 70 LAR-14030

TISSUES (BIOLOGY)
Growing and assembling cells into tissues
Dec page 67 MSC-21559

TITANIUM
Superplastically formed titanium hat-stiffened panels
Jan page 63 LAR-13814

Finding platinum-coating gaps on titanium anodes
Feb page 46 MFS-29389

Microstructure of a SiC/(Ti/V/Cr/Sn/Al) composite
Nov page 61 LEW-14868

TOMOGRAPHY
Calibrator blocks for computerized tomography (CT)
July page 50 KSC-11397

Viewing welds by computer tomography
July page 79 MFS-29555

TOOLING
Characterization of robot work cell
Nov page 92 MFS-29731

TOOLS
Squeezing salvages oversize seals
May page 79 MFS-29527

Impact wire dislodges obstructions
June page 83 MFS-29513

Combined borescope and flushing wand
Aug page 62 MFS-29581

Mechanized fluid connector and assembly tool
Oct page 79 MSC-21434

TOPEX
Optimization of array of laser retroreflectors
Dec page 31 NPO-17778

TRACE CONTAMINANTS
High-sensitivity ionization trace-species detector
Feb page 38 NPO-17596

TRACKING FILTERS
More about fixed-lag smoothers for tracking carriers
Apr page 45 NPO-17389

Frequency synthesizer for tracking filter
Aug page 33 MFS-29541

TRAILING EDGE FLAPS
Code for analysis of wing-and-flap systems
Oct page 74 LAR-13994

TRAJECTORIES
Graphical display of test-flight trajectories
Feb page 28 ARC-12211

TRANSDUCERS
Transducer-mounting fixture
Dec page 59 MFS-29600

TRANSATMOSPHERIC VEHICLES
Aerothermodynamic heating of a transatmospheric vehicle
June page 74 ARC-11854

TRANSFORMERS
Mobile centers for secondary power distribution
June page 28 KSC-11410

TRANSISTORS
Low-inductance wiring for parallel switching transistors
Oct page 30 MFS-28387

Preventing simultaneous conduction in switching transistors
Nov page 34 NPO-17775

TRANSIENT RESPONSE
Vibrational responses of structures to impulses
Mar page 80 NPO-17343

TRANSONIC FLOW
Comparison of calculations of viscous transonic flow
Oct page 85 ARC-12192

Predictions of drag in viscous transonic flow
Nov page 76 ARC-12252

TRANSONIC WIND TUNNELS
Detecting boundary-layer transition in cold environments
Mar page 76 LAR-13830

TRAPS
Trap for noncondensable gas in heat-transfer fluid
Dec page 48 MSC-21389

TRAVELING SALESMAN PROBLEM
Processor would find best paths on map
May page 40 NPO-17716

Neural network solves "traveling-salesman" problem
Dec page 22 NPO-17807

TRAVELING WAVE MODULATION
GaAlAs traveling-wave electro-optical modulators
July page 24 LEW-14866

TRAYS
Aerospace food tray
Feb page 72 MSC-21412

TRIBOLOGY
Tribological properties of ceramics
Mar page 67 LEW-14833

TRUSSES
Passive damping of vibrations in truss structures
Nov page 79 NPO-17609

TURBINE BLADES
Measuring changes in dimensions of turbine blades
Apr page 60 MFS-28338

Thermal-transient testing of turbine blades
May page 68 MFS-29416

Radial cracks would signal wearout of turbine blades
June page 72 MFS-28363

Fiber-reinforced superalloys for rocket engines
July page 58 LEW-14871

TURBINE ENGINES
Heat-flux-measuring facility
Aug page 42 LEW-14917

TURBINE PUMPS
Fourier analysis of vibrations of round structures
Mar page 74 MFS-29334

Vibrations caused by cracked turbopump bearing race
Apr page 71 MFS-29656

Back-to-back, counterrotating turbopumps
May page 76 MFS-28349

Testing bearing balls for ignition in liquid oxygen
July page 75 MFS-29410

Computing flows in turbine end bearings
Dec page 54 MFS-29681

Heat shield and axial retainer for turbopump blade
Dec page 53 MFS-28417

New materials and treatments for turbopump bearings
Dec page 36 MFS-27238

TURBINES
Predicting noise from wind turbines
Mar page 68 LAR-13984

TURBOMACHINERY
Computation of flutter in turbomachinery
Feb page 56 LEW-14742

Rubbing between rotors and stators
July page 76 MFS-27226

Piezoelectric pushers suppress vibrations
Aug page 59 LEW-14927

Analysis of stepped labyrinth seals
Sep page 79 MFS-29585

Damping seals and bearings for a turbomachine
Sep page 80 MFS-28345

TUBOSHAFTS
Securing bearing races to turbopump shafts
June page 79 MFS-28384

TURBULENT BOUNDARY LAYER
Simulation of turbulent, oscillating boundary layer
July page 73 ARC-11858

Measurements of shock-separated turbulent boundary layers
Nov page 78 ARC-12298

Further studies of hot-wire anemometry
Dec page 31 ARC-12104

TURBULENT FLOW
Transport of passive scalars in a turbulent channel flow
Apr page 62 ARC-12109

U

ULTRAHIGH FREQUENCIES
High-efficiency klystron for television transmitters
Sep page 30 LEW-14926

ULTRASONICS
Acoustophoresis--a new separation concept
Jan page 38 LAR-13388

ULTRASONIC AGITATION
Noncontact ultrasonic vibration of weld puddles
Nov page 91 MFS-29715

ULTRASONIC FLAW DETECTION
Atomized water as couplant for ultrasonic imaging
Dec page 47 MFS-28442

ULTRASONIC SCANNERS
Ultrasonic imaging of deep arteries
Oct page 54 NPO-17439

ULTRASONIC TESTS
Ultrasonic monitor to determine crack-opening load
Aug page 57 LAR-13889

UNDERCARRIAGES
Articulated suspension without springs
Jan page 60 NPO-17354

V

VACUUM GAGES
Vacuum-gauge connection for shipping container
Sep page 85 MSC-21523

VACUUM PUMPS
Venturi air-jet vacuum ejector for sampling air
Oct page 86 LAR-14024

VALVES
Fixed-position isolation valve
May page 71 NPO-17707

Remotely-controlled variable-orifice valve
June page 75 MFS-28369

Simple, internally adjustable valve
Sep page 76 MFS-29463

VAPOR DEPOSITION
Pyrolysis products of dimethyldichlorosilane
May page 61 ARC-12169

Detection of gas-phase polymerization in SiH_4 and GeH_4
July page 47 NPO-17779

Making lightweight structures by vapor deposition
Nov page 81 LAR-14059

VAPOR PRESSURE
Isothermal calorimeter
Aug page 44 NPO-17419

VAPORS
Second vapor-level sensor for vapor degreaser
May page 82 MFS-29493

VAX COMPUTERS
Window utility system program
Nov page 73 LAR-13993

VECTORS (MATHEMATICS)
Processing laser-velocimetric data by vector scag
Oct page 98 LEW-14925

CYBER-205 devectorizer
Dec page 44 LAR-13810

VEHICLE WHEELS
Articulated suspension without springs
Jan page 60 NPO-17354

Stabilizing wheels for rover vehicle
May page 74 NPO-17495

VENTING
Predicting pressure drop in porous materials
Jan page 56 LAR-14105

VENTURI TUBES
Venturi air-jet vacuum ejector for sampling air
Oct page 86 LAR-14024

VERTICAL TAKEOFF AIRCRAFT
Civil applications for new V/STOL and STOL aircraft
Sep page 81 ARC-12175

VERY LARGE SCALE INTEGRATION
Generating weighted test patterns for VLSI chips
Jan page 30 NPO-17514

VLSI architecture for Viterbi decoder
Jan page 28 NPO-17310

VLSI Reed-Solomon encoder with interleaver
Feb page 28 NPO-17280

Programmable direct-memory-access controller
Mar page 54 NPO-17341

Large-constraint-length, fast Viterbi decoder
Apr page 34 NPO-17639

VIBRATION
Vibrational responses of structures to impulses
Mar page 80 NPO-17343

Vibrations caused by cracked turbopump bearing race
Apr page 71 MFS-29656

Modification of gear teeth to reduce vibrations
May page 75 LEW-14738

VIBRATION DAMPING
Nonobstructive damping for parts vibrating in flows
Jan page 61 MFS-29572

Adaptive-control experiments on a large flexible structure
Mar page 78 NPO-17478

Controlling shape and vibration of antennas
Apr page 43 NPO-17598

Propagation of pulse vibrations in large structures
July page 74 NPO-17559

Piezoelectric pushers suppress vibrations
Aug page 59 LEW-14927

Experiments on active members in large space structures
Oct page 81 NPO-17623

Passive damping of vibrations in truss structures
Nov page 79 NPO-17609

VIBRATION ISOLATORS
Heteropolar magnetic suspension
June page 75 MFS-26096

Inertia-wheel vibration-damping system
June page 76 GSC-13077

VIBRATION MEASUREMENT
System detects vibrational instabilities
May page 41 MSC-21408

Frequency-tracking-error detector
Aug page 32 MFS-29538

VIBRATION MODE
Characteristic-wave approach complements modal analysis
May page 72 NPO-17741

VIBRATION TESTS
More about multiple-boundary-condition testing
Jan page 58 NPO-17574

VIDEO DATA
Truncation of images for correlation
Aug page 68 NPO-17847

VIDEO DISKS
Fast, capacious disk memory device
June page 44 GSC-13196

VIDEO EQUIPMENT
Human factors in the design of video displays
Aug page 34 ARC-11847

VIEWING
Zoom vision system for robotic welding
Nov page 82 MFS-29712

VISCOUS FLOW
Comparison of calculations of viscous transonic flow
Oct page 85 ARC-12192

Predictions of drag in viscous transonic flow
Nov page 76 ARC-12252

VISION
Determining sense of motion in robotic vision
Apr page 84 NPO-17552

Pyramidal image-processing code for hexagonal grid
May page 91 ARC-12178

VISUAL OBSERVATION
Polyhedral observation cupola
Nov page 93 MSC-21689

VISUAL PERCEPTION
Computer animation in perception research
Jan page 76 ARC-11774

VITERBI DECODERS
Large-constraint-length, fast Viterbi decoder
Apr page 34 NPO-17639

VOLTAGE AMPLIFIERS
Crystal oscillators operate beyond rated frequencies
Apr page 30 GSC-13171

VOLTAGE REGULATORS
Voltage-boosting driver for switching regulator
Nov page 26 MFS-28437

W

WALKING MACHINES
Agile walking robot
Dec page 52 NPO-17874

Rugged walking robot
Dec page 53 NPO-17825

WASTE DISPOSAL
Catalytic destruction of toxic organic compounds
Sep page 46 NPO-17669

WASTE HEAT
Two-phase accumulator
Apr page 68 MSC-21464

WASTES
Photochemical degradation of organic-solvent fumes
June page 61 MFS-29596

WATER PROOFING
Rewaterproofing chemical for use with silicones
Aug page 47 MSC-21569

WATER TREATMENT
Ozone treatment for cooling towers
Aug page 60 KSC-11384

WAVE GENERATION
High-voltage square-wave generator
Oct page 26 NPO-17772

WAVEGUIDES
Epoxies bond waveguides to flanges
Mar page 40 NPO-17497

Computing scattering matrices for circular waveguides
Sep page 65 NPO-17245

Directional couplers for detecting circular waveguide modes
Sep page 33 NPO-17175

WEAR
Ball-pass cage-modulation detector
Aug page 32 MFS-29539

WEAR INHIBITORS
Reducing run-in wear of ceramic-based coatings
July page 56 LEW-14834

WEAR RESISTANCE
Friction and wear of silicon ceramics
June page 67 LEW-14835

WEAVING
Angle-ply weaving
Oct page 91 LAR-14048

Integrated process for insertion and beatup of fill yarns
Oct page 92 LAR-14046

WELDED JOINTS
Quick check of butt-weld alignment
Mar page 89 MFS-29423

Prepenetrant etchant for Incoloy* 903 weld overlays
Apr page 78 MFS-29576

Weld bead shaver
May page 80 MFS-29593

Spot-welding gun with adjustable pneumatic spring
June page 81 MFS-29569

Controlled-pinch spot welder
Sep page 87 MFS-29606

WELDING
Camera would monitor weld-pool contours
Jan page 26 MFS-29450

Development of advanced welding control system
Jan page 64 MFS-26106

Dummy cup helps robot-welder programmers
Jan page 62 MFS-29499

Method for automatic downhand welding
Jan page 65 MFS-27209

Rounding and aligning tubes for butt welding
Jan page 62 MFS-29363

Welding-current indicator
Jan page 24 MFS-29574

Physics of variable-polarity plasma arc welding
Feb page 60 MFS-27207

Preventing contamination in electron-beam welds
Mar page 90 MFS-29428

Welding and cutting a nickel alloy by laser
Mar page 93 MFS-27208

Calibration fixture for welding robot
Apr page 72 MFS-29548

Internal filler-wire feed for arc welding
Apr page 75 MFS-29491

Internal wire guide for gas/tungsten-arc welding
Apr page 76 MFS-29489

Optical arc-length sensor for TIG welding
Apr page 72 MFS-29497

Resistance-welding test fixture
July page 80 MFS-29426

Small, lightweight welding-current indicator
July page 32 MFS-29622

Viewing welds by computer tomography
July page 79 MFS-29555

Borescope aids welding in confined spaces
Aug page 64 MFS-29635

Checking automated-welder programs by computer
Sep page 41 MFS-29006

Dual-head robotic welder
Sep page 87 MFS-29610

Monitoring both sides of a weld in progress
Sep page 84 MFS-28389

Rolling spot welder
Sep page 86 MFS-29580

Arc reflector for welding ducts
Oct page 89 MFS-29640

Compact pinch welder
Oct page 89 MFS-29612

Noncontact ultrasonic vibration of weld puddles
Nov page 91 MFS-29715

Zoom vision system for robotic welding
Nov page 82 MFS-29712

WELD TESTS
Measuring weld profiles by computer tomography
Dec page 60 MFS-29554

WHITE NOISE
Noise-contamination detector
Apr page 34 MFS-29537

WIND TUNNEL MODELS
Numerically contolled machining of wind-tunnel models
Dec page 58 LAR-14004

WIND TUNNELS
Improved insert for variable mach number
July page 63 LAR-13548

WIND TURBINES
Predicting noise from wind turbines
Mar page 68 LAR-13984

WING FLAPS
Code for analysis of wing-and-flap systems
Oct page 74 LAR-13994

WINGS
Wing covers for aerodynamic studies
Jan page 65 ARC-12238

Wing-design and -analysis code
Oct page 74 LAR-13995

WING TUNNELS
Laser velocimetry in low-speed wind tunnels
Sep page 42 ARC-11564

WIRE
Wrapped wire detects rupture of pressure vessel
Apr page 66 MSC-21449

WIRE CLOTH
Cheap corner reflectors for radar
May page 30 NPO-17658

WIRING
Program for engineering electrical connections
May page 62 NPO-17619

Moving large wiring-harness boards
June page 82 MFS-29510

Low-inductance wiring for parallel switching transistors
Oct page 30 MFS-28387

WOOD
Improved radiography of wooden parts
July page 47 LAR-13724

X

X-RAY ANALYSIS
Measuring weld profiles by computer tomography
Dec page 60 MFS-29554

X-RAY FLUORESCENCE
X-ray fluorescence surface-contamination detector
Apr page 52 MFS-27222

X-RAY INSPECTION
Printed-circuit tape measures for x-ray inspections
Feb page 58 MFS-28388

Positioning x-ray film with string and magnets
May page 78 MFS-29448

Improved radiography of wooden parts
July page 47 LAR-13724

Positioning x-ray film by balloon
Aug page 63 MFS-29588

Positioning x-ray film inside a flow splitter
Dec page 61 MFS-29322

X-RAY TELESCOPES
Monitoring small deformations in an instrument
Oct page 80 GSC-13271

X-RAY TUBES
Switching x-ray tubes remotely
July page 24 MFS-29357

X-29 AIRCRAFT
Operation of the X-29A digital flight-control system
Apr page 45 ARC-12209

Y

YARNS
Integrated process for insertion and beatup of fill yarns
Oct page 92 LAR-14046

Advertiser's Index

3-D Visions .... (RAC669)* 70
Advanced Materials Laboratory, Inc. (RAC 447) 95
Aerotech, Inc. .... (RAC 375) 63
Algor Interactive Systems, Inc. (RAC 361) 77
Allied Signal .... (RAC 418) COV III
Amco Engineering Co. .... (RAC 500) 12
Ametek, Thermox Instruments Division .... (RAC 337). 85
ANA Brass Fittings .... (RAC 515) 91
Anritsu America, Inc. ...... (RAC 507) 15
Azonic, Inc. .... (RAC 478) 85
Balzers..................(RAC 403-405) COV II, 27
Best Power Technology .. (RAC 306) 94
BMDP Statistical Software, Inc. (RAC 533) 3
Boeing 4-5
Burr-Brown Corporation .. (RAC 313) 77
Cherokee Data Systems (RAC 608) 90
Cole Parmer Instrument Co. (RAC 638) 49-51
Contemporary Cybernetics Group (RAC 411) 2
Cotronics Corporation .... (RAC 409) 94
Covox, Inc. .... (RAC 380) 95
Cyber Research, Inc. ...... (RAC 371) 95
Delker Corporation .... (RAC 316) 94
Designatronics .... (RAC 391) 94
Dolphin Scientific, Inc ...... (RAC 510) 26
Electro Mechanical Systems, Inc. (RAC 518) 21
Electro-Flex Heat, Inc. .... (RAC 486) 69
Electronic Decisions Incorporated (RAC 378) 23
ERIM .... (RAC 475) 98
F.W. Bell, Inc .... (RAC 513) 74
Fluoramics, Inc ....(RAC 364,365) 1,76
Gould Recording Systems (RAC 483) 7,9
Hardigg Industries, Inc. .... (RAC 492) 25
Hitachi Denshi .... (RAC 441) 81
Hyperception.....................(RAC 445) COV IV
Inco Specialty Powder Products (RAC 452) 55
Information Development Incorporated (RAC 383) 66
International Light Inc. .... (RAC 645) 72
KineticSystems Corporation (RAC 334) 94
Laboratory Technologies Corporation (RAC 423) 33
Lake Shore Cryotronics, Inc..(RAC 578) .. 75
MACSYMA/SYMBOLICS (RAC 524) 65
MathSoft, Inc. .... (RAC 682) 13
Minco Products, Inc. .... (RAC 308) 99
Mitchell & Gauthier Associates (RAC 527) 40
Motorola, Inc. .... (RAC 655) 79
National Instruments .... (RAC 681) 96
Nicolet Instruments .... (RAC 696) 19
National Institute of Standards and Technology .... (RAC 539) 69
National Technical Systems..(RAC 358). .. 39
Numerical Algorithms Group.(RAC 477) 88
Omation .... (RAC 338) 39
Patton & Patton .... (RAC 499) 97
Photovolt .... (RAC 562) 41
Primavera Systems, Inc... (RAC 663) 73
RemGrit Corporation ...... (RAC 320) 37
RG Hansen & Associates (RAC 688) 86
RGB Spectrum .... (RAC 467) 8
Rolyn Optics Co. .... (RAC 551) 94
Silicon Composers Inc. .... (RAC 679) 94
Soft Warehouse, Inc. ...... (RAC 374) 14
SoMat Corporation .... (RAC 419) 91
Sony Data Recording ...... (RAC 580) 17
The Soundcoat Company (RAC 438) 94
Specac Analytical, Inc. .... (RAC 621) 94
Spectra Physics .... (RAC 618) 71
Spinoffs .... (RAC 366) 75
Stat-Ease Inc. .... (RAC 393) 76
Structural Research and Analysis Corp. .... (RAC 676) 87
Sweatshirts 99
Technology 2001 .... (RAC 589) 95
Teledyne Gurley .... (RAC 620) 100
The Mathworks Inc. .... (RAC 503) 29
Tiodize .... (RAC 422) 36
TransEra Corporation ...... (RAC 473) 43
Tri Metrix, Inc. .... (RAC 616) 92
US Technology Corporation (RAC 582) 95
Watlow .... (RAC 416) 42

***RAC** stands for **Reader Action Card.** For further information on these advertisers, please circle the RAC number on the Reader Action Card elsewhere in this issue. This index has been compiled as a service to our readers and advertisers. Every precaution is taken to ensure its accuracy, but the publisher assumes no liability for errors or ommisions.

Circle Reader Action No. 620

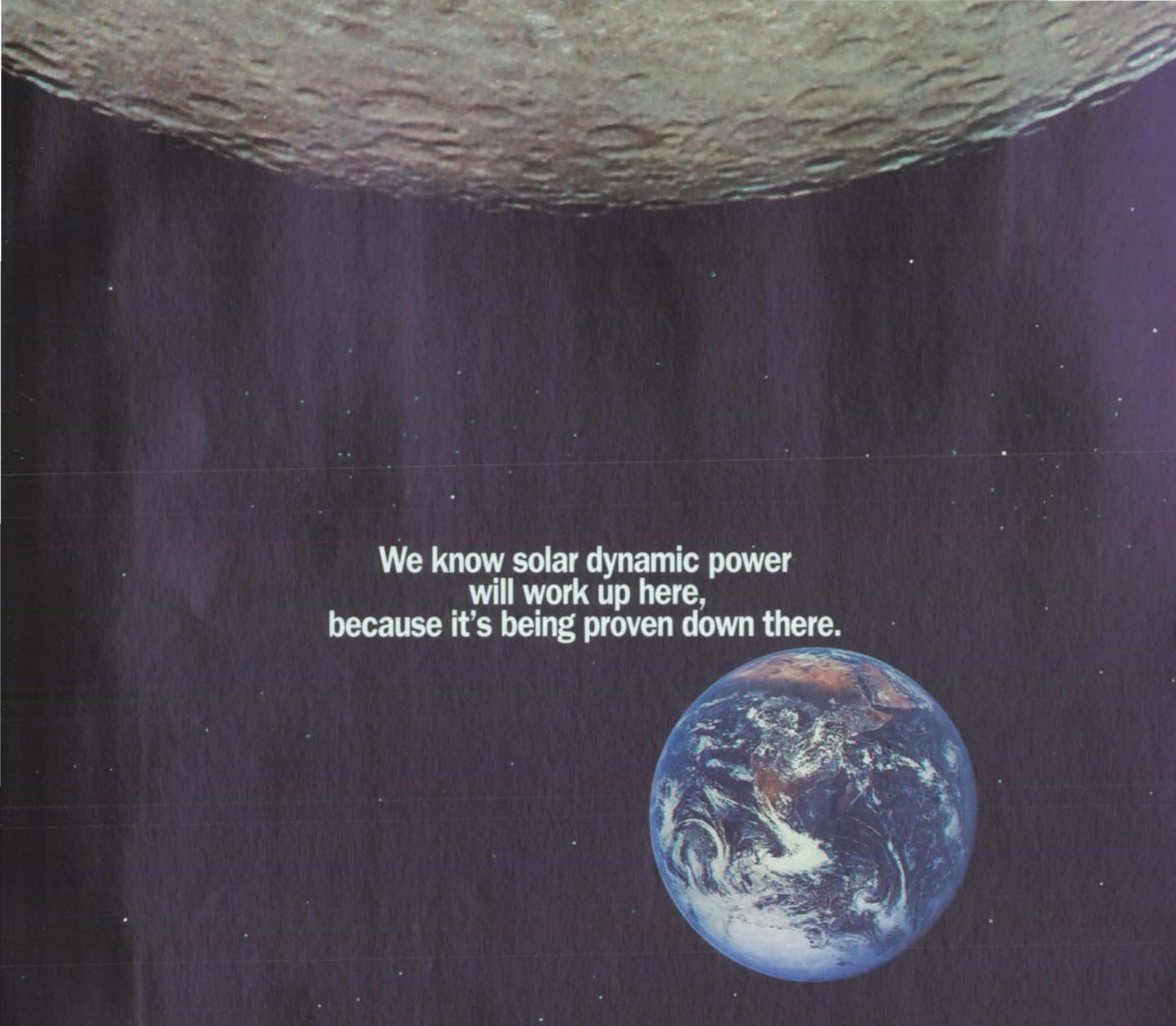
We know solar dynamic power
will work up here,
because it's being proven down there.